THE ASTROPHYSICAL JOURNAL SUPPLEMENT SERIES, 80:531–644, 1992 June

AN X-RAY CATALOG AND ATLAS OF GALAXIES

G. FABBIANO,[1] D.-W. KIM,[1] AND G. TRINCHIERI[1,2]
Received 1991 May 20; accepted 1991 September 4

ABSTRACT

We present an X-ray catalog and atlas of galaxies observed with the *Einstein Observatory* imaging instruments (IPC and HRI). The catalog comprises 493 galaxies, including targets of pointed observations, and RSA or RC2 galaxies serendipitously included in *Einstein* fields. A total of 450 of these galaxies were imaged well within the instrumental fields, resulting in 238 detections and 212 3 σ upper limits. The other galaxies were either at the edge of the visible field of view or confused with other X-ray sources. For these we also give a rough measure of their X-ray emission. The atlas shows X-ray contour maps of detected galaxies superposed on optical photographs and gives azimuthally averaged surface brightness profiles of galaxies detected with high signal-to-noise ratio.

Subject headings: atlases — catalogs — Galaxy: structure — X-rays: galaxies

1. INTRODUCTION

The *Einstein Observatory* (Giacconi et al. 1979) has given us for the first time the capability to study galaxies in the soft X-ray band (0.2–3.5 keV). The focusing optics of the *Einstein* mirror combined with the imaging capabilities and sensitivity of its instruments has led to the detection of the X-ray emission of normal galaxies at least as far as the Virgo Cluster and in some cases has given us detailed information on the morphology of the X-ray emission and on its spectral characterists. These results suggest that the X-ray emission of normal spiral galaxies in the *Einstein* band is dominated by the integrated output of evolved stellar sources, such as supernova remnants and close accreting binaries with a compact stellar remnant. Bright E and S0 galaxies are dominated by the emission of a hot interstellar medium, and a similar gaseous emission is associated with starburst nuclei (see Fabbiano 1989 for a review).

Although many of the *Einstein* observations of galaxies have been published, including the nearest best studied objects, there are many observations in the *Einstein* data bank that have never been published. These include both galaxies observed as the field target, and galaxies included serendipitously in fields pointed at other astrophysical objects. Moreover, slightly different analysis techniques have been used in different papers, resulting in a certain nonuniformity of the reported fluxes. For these reasons, we have undertaken a systematic analysis of all the galaxies observed as part of the *Einstein* mission with either the Imaging Proportional Counter (IPC) or the High Resolution Imager (HRI). We have also searched for X-ray emission from galaxies included in either A Revised Shapley-Ames Catalog of Bright Galaxies (Sandage & Tamman 1981, hereafter RSA) or the Second Revised Catalog of Bright Galaxies (de Vaucouleurs, de Vaucoulers, & Corwin 1976, hereafter RC2) that might have been included in the *Einstein* field of view of observations of unrelated targets. This search, combined with the target galaxies, has resulted in 493 galaxies observed in X-rays with *Einstein.* By comparison, only data relative to less than 200 galaxies have been previously reported (Fabbiano 1989 and references therein).

In this paper we report the selection criteria and observation parameters (§ 2), and we describe the data analysis techniques (§ 3). We give X-ray fluxes or upper limits for all these galaxies, together with detailed analysis of separate components for complex objects (§ 4). For the detected galaxies, we present X-ray surface brightness contours overlaid onto optical images, and when appropriate we give X-ray surface brightness profiles (§ 5). We then discuss our results in comparison with published work (§ 6). In a companion paper (Kim, Fabbiano, & Trinchieri 1992a, hereafter Paper II), we report the results of a systematic spectral analysis of this sample. Average spectral properties of different types of galaxies and their implications for the emission mechanisms are discussed in Kim, Fabbiano, & Trinchieri (1992b, hereafter Paper III).

2. THE SAMPLE

The galaxies used for this work (see Table 1 of the catalog, located after the text of this paper) include all the bright galaxies targets of *Einstein* observations, and all other galaxies in RSA or RC2 serendipitously included in *Einstein* fields. Galaxies of all morphological types, normal galaxies, starburst galaxies and mergers, and also galaxies with active nuclei (e.g., Seyfert galaxies) are included. In the latter, the X-ray emission is typically dominated by a pointlike nuclear source. Galaxies at the center of rich clusters (e.g., M87, NGC 1275), where the X-ray emission is clearly dominated by the hot intracluster medium (e.g., Fabricant, Lecar, & Gorenstein 1980), are excluded from this catalog. Also excluded are NGC 4476 and NGC 4478; these two galaxies are in a region of the sky which is totally dominated in X-rays by the gaseous halo of M87. Early-type galaxies in groups are, however, included, even if the group potential could account for a larger gaseous halo and brighter X-ray sources (e.g., Kriss, Cioffi, & Canizares 1983). Galaxies in clusters are also included, when the X-ray emission is clearly associated with the individual galaxy. In Table 1 we do not list the *Einstein* observations of M31, M32, LMC, and SMC, although their X-ray fluxes are included in Table 3.

[1] Harvard-Smithsonian Center for Astrophysics, 60 Garden Street, Cambridge, MA 02138.
[2] Postal address: Osservatorio Astrofisico di Arcetri, Largo Enrico Fermi 5, I-50125 Firenze, Italy.

These Local Group galaxies were targets of multiple *Einstein* observations, which have been analyzed in detail elsewhere (see notes to Table 3).

Including the former four galaxies, our sample consists of 493 galaxies, 489 of which are listed in Table 1. Of the 493 galaxies, 148 were observed in more than one occasion; 478 were observed with the IPC and 69 with the HRI; and 54 were observed with both instruments.

3. DATA ANALYSIS

The aim of this project is to extract X-ray fluxes or upper limits for typically extended objects, and to produce isointensity contour maps and surface brightness profiles. We have followed data analysis methods described in previous papers on the X-ray observations of galaxies (e.g., Trinchieri, Fabbiano, & Canizares 1986, hereafter TFC; Fabbiano & Trinchieri 1987, hereafter FT), which we summarize below. Some galaxies were observed in more than one *Einstein* pointing. In all cases we have analyzed each observation individually. For galaxies observed with the same instrument more than once, we have also merged together and used for our analysis all the different observations in which the galaxy is well within the instrumental field of view. We have excluded from this merging procedure observations in which the galaxies are partially obscured either by the edge of the field (for both HRI and IPC observations), or by the IPC window support structure (the ribs).

3.1. *IPC Data*

3.1.1. *Background Subtraction*

We have used the latest reprocessing of the IPC data in all cases (Rev 1B; Harnden et al. 1984). This reprocessing produced background maps in three standard energy bands for each observation: 0.2–0.8 keV (soft); 0.8–3.5 keV (hard); and 0.2–3.5 keV (broad). The IPC field background has a characteristic radial dependence, and it is important to subtract it carefully from the images when extracting the parameters of extended X-ray sources. The Rev 1B processing tailors the background maps to each field, after subtracting bright sources. However, in some cases where an extended source is present, the background level may be slightly overestimated. To avoid this problem, we have compared radial surface brightness profiles of each field in the three energy bands, binned about the field center, with the corresponding background profile, and we have renormalized the background if necessary. The background field was then subtracted from the galaxy field. Figure 1 illustrates this procedure using the observation of NGC 1399 (sequence number I1887) as an example.

3.1.2. *Contour Maps*

Iso-intensity contour maps of the X-ray intensity were then produced from the background-subtracted fields. For all the fields newly analyzed for this work, the data were smoothed with $\sigma = 35''$ Gaussians, and contours were plotted so that the lowest level corresponded to a 2 σ enhancement over the background level. Subsequent contours correspond to 3, 4, 5, and 6 σ; above this, some levels are skipped in strong sources to avoid contour crowding. The 35″ Gaussian smoothing function was chosen after experimenting with a range of Gaussians, as the one that gave the best compromise between retaining detail and enhancing low surface brightness features. Contour maps were made for all the three bands and inspected for significant differences. In the atlas (§ 5), we show overlays of contour maps for detected galaxies onto optical photographs, typically from the POSS plates, or ESO plates for southern galaxies. We only show the broad-band maps, unless differences were found between soft and hard maps, or a galaxy was detected either more clearly or solely in the soft or hard band. For some bright galaxies, we show contour maps from our previously published papers. Details on the smoothing functions used for these galaxies and references are given in the atlas.

The IPC point response function (Mauche & Gorenstein 1986), for an average instrumental gain, and a relatively hard X-ray emission, such as may be found in spiral galaxies (e.g. FT; Paper II) corresponds to a Gaussian of $\sigma \sim 45''$, for the broad band, when convolved with a 35″ Gaussian. If the emission has a characteristic temperature of $\sim$1 keV, as in early-type galaxies (Forman, Jones, & Tucker 1985, hereafter FJT; TFC), the IPC point response function, convolved with a 35″ Gaussian, corresponds to $\sigma \sim 55''$.

3.1.3. *Surface Brightness Profiles*

Background-subtracted radial surface brightness profiles were also produced by binning the data in circular annuli 30″ wide, centered on the galaxy X-ray centroid or on the optical nucleus in the case of complex emission where there is no identifiable X-ray centroid. Parts of the image including sources not clearly related to the galaxy under analysis were not included in the data used to produce these profiles. This was done by excluding circles centered on these extraneous sources, including all emission above background. Surface brightness profiles for detected galaxies are given in the atlas (§ 5). Most of the galaxies are not so extended that the profiles would be affected by the radial dependence of the telescope vignetting. We have applied this correction to the two most extreme cases (NGC 1399 and NGC 5128), and we find that within the errors the corrected and uncorrected profiles do not differ appreciably.

3.1.4. *Count Rate Extraction*

Contour maps and radial profiles were used as a guide for the extraction of the source counts. As discussed in § 3.1.3, parts of the image including extraneous sources were excluded. Typically, in the case of bright large galaxies, the source counts were extracted from the images using circles centered on the X-ray centroid and with a radius estimated from the surface brightness profiles. The radius was adjusted to maximize the signal-to-noise ratio of the detection: too large a radius would not increase the detected counts while increasing the noise; too small a radius would not include all the source counts. The background counts were then estimated from the appropriate template, normalized as discussed in § 3.1.1. above, and subtracted. Count rates were then derived by dividing the net source counts by the live exposure time and applying a correction to take into account telescope vignetting (Harnden et al. 1984). In the case of the very extended NGC 1399 and NGC 5128, we have used a radially variable vignetting correction.

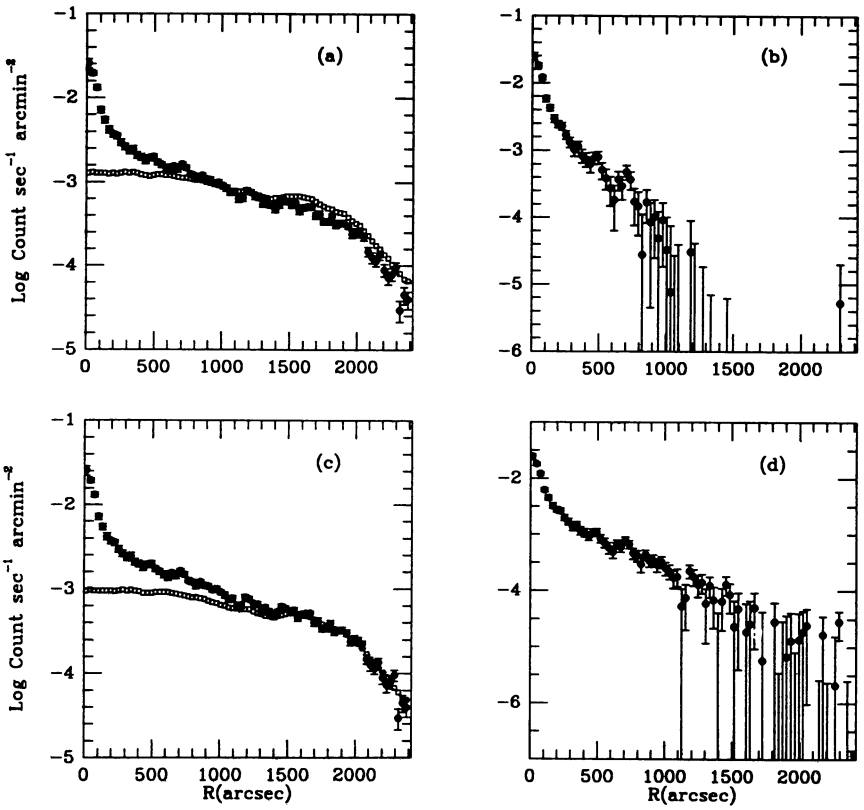

FIG. 1.—Background subtraction in IPC fields. *Upper quadrants:* Radial profiles of image centered on field center (*filled squares*) and background template with standard Rev1 B processing normalization (*open squares; left*), and resulting subtracted profile (*right*). *Lower quadrants:* Same as above, but with renormalized background template.

We find that this produces a significant difference only in NGC 1399. If the X-ray emission was due to different identifiable components, the count rate was estimated for each individual component. In these cases the total galaxy count rate would be the sum of these individual parts.

Our criterion for detection was that of a signal-to-noise ratio of 3 σ above the background. If a galaxy signal to noise fell below this threshold, we have estimated 3 σ upper limits to the count rate. These were derived by extracting the counts from an area of the image corresponding to an ellipse with axes and position angles describing the optical image of the galaxy (from RC2 and, if not available there, from the Principal Galaxy Catalogue; PGC, Paturel et al. 1989). If the galaxy major or minor axis was smaller than 3′, a radius of 3′ was used. This radius would include ~90% of the counts from a pointlike source in the IPC. Count rates and upper limits are given in the catalog (§ 4) together with the count extraction parameters (Tables 3A, 3B, and 4). In some cases, it is not clear if the emission is associated with the galaxy, or it is due to a background or foreground source. In these cases, we have flagged the count rates and added explanatory comments. In a few cases, the galaxy fell within the IPC field of view but partially outside the area commonly used for the IPC images. In these cases we have "unmasked" the image. This procedure allows one to extend the useful field of view to include the outermost regions outside the ribs. These regions are normally excluded because of a much larger field background.

For sources marginally below the detection threshold (between 2.5 and 3 σ) we also list separately the "measured" count rate (see the catalog, Table 5). We list count rates for sources partially obscured by the IPC support structure ("ribs") in Table 6. These should be considered as lower limits to the emitted value. In a few cases (Table 7), the galaxy was confused with a nearby strong and/or extended X-ray source, which did not permit a proper extraction of the source counts.

If the contour map showed different components of the X-ray emission, count rates were estimated for each component individually. Details are given in the catalog (Table 8).

3.1.5. *Flux and Luminosity*

The corrected count rates were converted into 0.2–4.0 keV fluxes and luminosities. The conversion to flux was done using a conversion factor (see the *Einstein* Revised Users Manual, RUM, Harris 1984), corresponding to an emission bremsstrahlung spectrum with kT = 5 keV and the galaxy line of sight N_H from Table 1 for spiral and irregular galaxies. A "Raymond" thermal spectrum with kT = 1 keV and the line of sight N_H were used for elliptical and S0 galaxies. This choice of spectral parameters is justified by the average spectral properties of spiral and elliptical galaxies, although in some individual cases a different choice of spectral parameters may be more appropriate (TFC; FT; Paper II; Paper III). Fluxes were converted to luminosities by using distances estimated from Tully (1988), or if these were not available from the CfA redshift survey data (J. Huchra 1990, private communication), using Virgocentric

flow corrections as in Knapp, Turner, & Cunniffe (1985). A Hubble constant of 50 km s^{-1} Mpc^{-1} was assumed throughout.

3.1.6. *Source Extent*

We have parameterized the angular extent of the X-ray emission by comparing the azimuthally averaged radial distributions of counts with the instrumental point response functions (PRF). To maximize our sensitivity in the case of faint IPC sources, we have compared the measured ratio of net counts in two circles of 90″ and 180″ radii centered on the source centroid or on the optical nucleus for cases of complex emission, with the expected ratio for a Gaussian distribution of counts convolved with the IPC PRF. A Gaussian represents well the IPC point response function. The σ of the IPC PRF varies between 30″ and 55″, depending on the energy of the incoming photons and on the instrumental gain (Mauche & Gorenstein 1986). Figure 2 shows radial profiles obtained by convolving two-dimensional Gaussians of σ ranging from 20″ to 500″ with the IPC PRF. We used the PRF appropriate for 0.3 keV and to 4.5 keV energies of the incoming photons, respectively. Using these templates, we have then calculated the expected ratio of counts within 0″–90″ and 0″–180″ circles. These ratios are plotted as a function of the σ of the "source" Gaussian in Figure 3. This ratio-σ relationship was then used to derive an equivalent Gaussian σ from the IPC radial profiles. Even if a Gaussian is not in general a good representation of the radial count distribution for a galaxy (see later), this method allows us to discriminate between pointlike and extended sources and to give a rough parameterization of the source extent. The results of this analysis are listed in the catalog (Table 9).

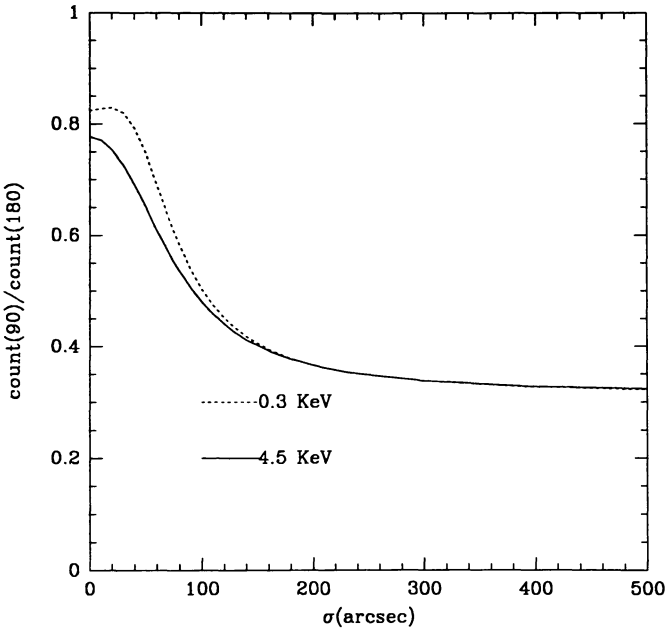

FIG. 3.—Ratio of IPC source counts within two circles of 90″ and 180″ centered on the source centroid vs. the corresponding source Gaussian sigma (see text). The two curves correspond to different photon energies.

3.2. *HRI Data*

We have followed similar techniques to those used for the IPC data analysis, with the following differences.

3.2.1. *Background Subtraction*

No HRI background template is necessary, because the HRI background does not have a radial dependence (see the HRI radial profiles in the atlas). The background was evaluated locally from annuli surrounding the source. Unless otherwise noted (catalog, Table 3), background counts were extracted from the 200″–300″ region around the field center.

3.2.2. *Contour Maps*

The HRI point response function is smaller than that of the IPC (~4″ versus 30″–55″ σ for the IPC; RUM; Mauche & Gorenstein 1986). We have produced maps with different Gaussian smoothing functions, with σ ranging from 4″ to 16″, and we show those that reveal more features. Contour levels were chosen as for the IPC maps.

3.2.3. *Surface Brightness Profiles*

Bin width is 10″.

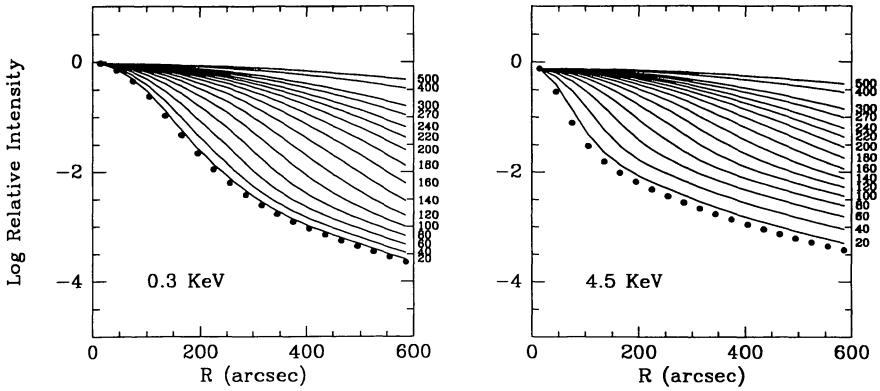

FIG. 2.—Radial profiles obtained by convolving two-dimensional Gaussians with the IPC PRF and then binning the resulting images in radial annuli. The σ of the Gaussians (in arcsec) is indicated on each curve. The dots represent the radial profile of the IPC PRF for different energies of incoming photons and standard detector gain. Profiles obtained using the IPC PRF for 0.3 keV are shown on the left. Profiles obtained using the IPC PRF for 4.5 keV are shown on the right.

3.2.4. *Count Rates*

Count rates were derived using the same method as in the IPC case, except that the background was estimated locally around the source. Except for the galaxies listed below, the field background was estimated from annuli of 200″ and 300″ inner and outer radii. The exceptions are NGC 3079: 70″–120″; NGC 4291, NGC 5548 (sequence number 8315): 100″–200″; NGC 4151: 150″–250″; NGC 4156: 100″–240″; NGC 5128 (sequence number 475): 120″–200″; NGC 2992, NGC 5195, NGC 5128 (sequence number 4495): 300″–400″.

In the case of individual sources detected within a galaxy, counts were extracted from circles surrounding the centroid position found by the HRI standard processing "Detect" algorithm (RUM).

3.2.5. *Flux and Luminosity*

Count rates were converted to X-ray fluxes in the 0.5–4.0 keV band using the appropriate HRI response (see RUM), and luminosities were derived as explained above for the IPC data. Figure 4 shows a comparison between IPC and HRI fluxes for galaxies observed with both instruments. The fluxes are in reasonable agreement, within a factor of 2 or less, except for two galaxies (NGC 4406 and NGC 4472) which have extended surface brightness distributions, and for which the HRI underestimates the total flux. For another two galaxies with bright active nuclei (NGC 315 and NGC 1566), the discrepancies may be due to time variability. NGC 5128 also has extended emission (Feigelson et al. 1981). These discrepancies persist under all reasonable spectral assumptions used to estimate the flux.

3.2.6. *Source Extent*

We followed a similar method to that used for IPC sources. Figure 5 shows the radial profiles of the convolution of the HRI PRF with two-dimensional Gaussians with σ ranging from 3″ to 180″. Figure 6 shows two ratio-σ relationships for circles of different sizes. These give a way of discriminating between source extents ranging from a few to ~100″. These curves were then used to derive equivalent source Gaussian σ as done for the IPC. The results of this analysis are listed in the catalog (Table 10).

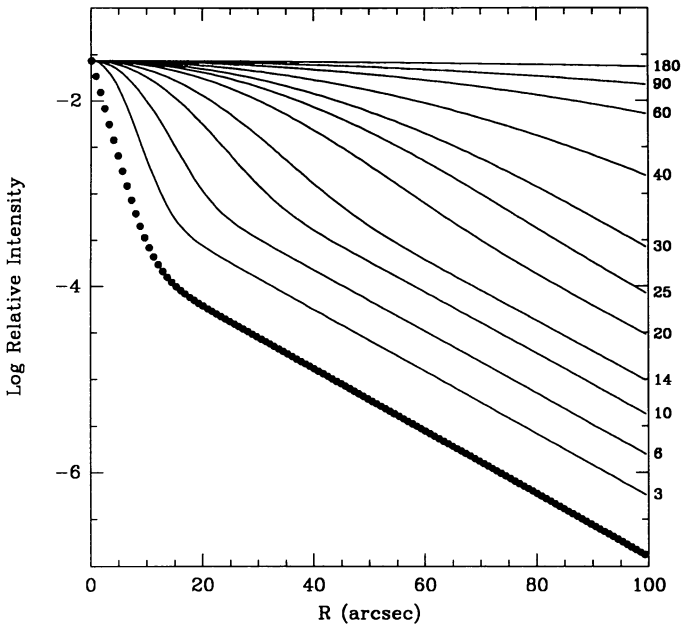

FIG. 5.—Radial profiles obtained by convolving two-dimensional Gaussians with the HRI PRF and then binning the resulting images in radial annuli. The σ of the Gaussians (in arcsec) is indicated on each curve. The dots represent the radial profile of the HRI PRF.

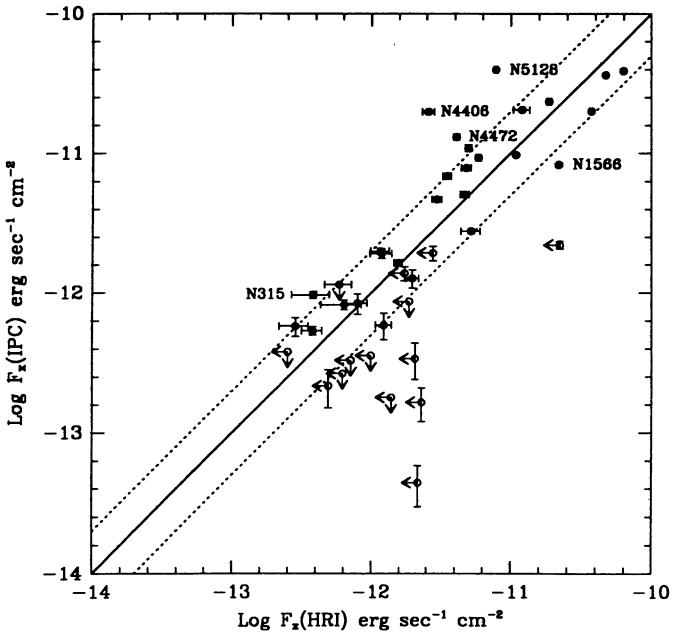

FIG. 4.—Comparison of IPC and HRI fluxes for galaxies observed with both instruments (see text).

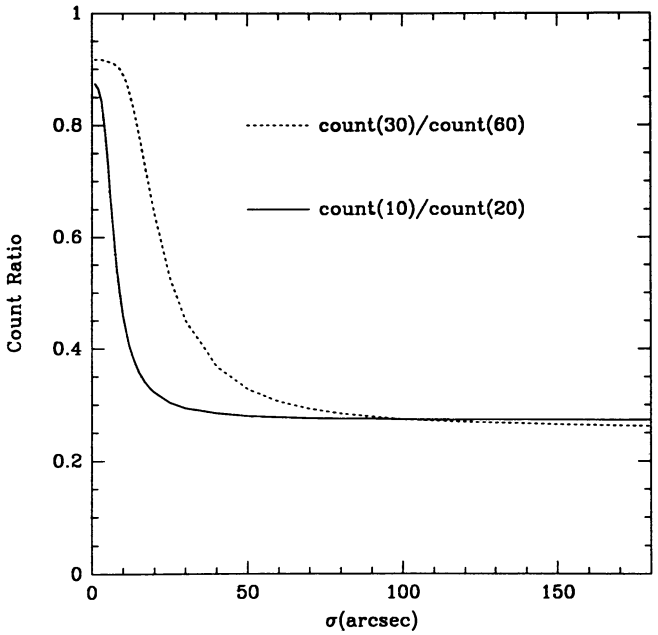

FIG. 6.—Ratio of HRI source counts within two circles centered on the source centroid vs. the corresponding source Gaussian σ (see text). The two curves correspond to different choices of radii, as indicated.

4. THE CATALOG

The catalog contains all the tabular information described in §§ 2 and 3. The entries in Tables 1–11 are detailed below. All tables except Table 2 appear after the text and the figures.

Table 1 lists all the individual observations of galaxies included in this X-ray catalog. Included are the following: galaxy name. An "AGN" following the name identifies galaxies where the X-ray emission is likely to be dominated by an active nucleus. A "VIR" following the name identifies galaxies belonging to the Virgo Cluster; 1950 coordinates from RSA, RC2, or PCG; line-of-sight equivalent hydrogen column (N_H; from Stark et al. 1992); *Einstein* instrument, where "I" identifies IPC observations and "H" identifies HRI observations; *Einstein* sequence number; year of the beginning of the observation (add 1900); day of the beginning of the observation in the given year; time in the image; angular offset of the optical center of the galaxy from the center of the instrumental field. All multiple observations for the same galaxies are listed separately. Not included in Table 1 are the *Einstein* observations of M31, M32, LMC, and SMC, for which we use data from the literature. Table 1 has 716 entries, for a total of 489 galaxies.

Table 2 lists the renormalization factors for the IPC background for all the observations where the background was renormalized.

Tables 3A and 3B list the results of our analysis for E+S0 and S+Irr galaxies, respectively. The reason for tabulating these results separately is that the X-ray emission of early- and late-type galaxies may be dominated by different components (see Fabbiano 1989; Kim et al. 1992a and b). For each entry are given the following: galaxy name; *Einstein* sequence number, where 99999 is used for values obtained from merged fields; B magnitude, where we list B_T^0 from RSA when available, or otherwise the analogous quantity from the RC2. If neither were available, we used PGC; morphological parameter T derived with RC2 prescription by using the morphological classification of RSA, RC2, or PGC, in this order of priority; position used for the extraction of the X-ray counts. If a position is not given, as in the case of nondetections, we used the optical position from Table 1; radius used for the X-ray counts extraction in arcsec; net source counts corrected for vignetting or 3 σ upper limit; statistical error on the counts; corrected count rate in units of counts per 1000 s; detected (0.2–4.0 keV) flux or upper limit. A Raymond spectrum with solar abundances and kT = 1 keV was used for Table 3A, a thermal bremsstrahlung spectrum with kT = 5 keV was used for Table 3B. In both cases low-energy cutoffs to the spectra were calculated using the N_H listed in Table 1; distance; and X-ray luminosity. Average count rates, fluxes, and luminosities are given for galaxies observed in more than one *Einstein* field. We have not analyzed the observations of the LMC, SMC, and M31. These galaxies occupy more than one *Einstein* pointing and have been studied in detail elsewhere. For these galaxies and for M32, which was observed in the M31 fields, we list the published total fluxes, and we refer to the appropriate publications for details on individual X-ray sources and on the spatial distribution of the X-ray emission. We list 81 detections and 80 upper limits in Table 3A and 157 detections and 132 upper limits in Table 3B.

TABLE 2

BACKGROUND RESCALING FACTORS FOR IPC OBSERVATIONS

Sequence	Factor	Sequence	Factor
278	1.192	5256	1.095
304	1.072	5766	1.030
352	1.090	5777	1.090
353	1.120	5803	1.077
427	1.069	5807	1.090
477	1.138	6339	1.060
1841	1.070	6643	1.100
1880	1.040	6645	1.190
1887	1.341	6653	1.303
1896	1.171	6667	1.124
1900	1.063	7028	1.066
2092	1.099	7030	1.054
2133	1.087	7034	1.089
2138	1.053	7039	1.048
3556	1.130	7046	1.080
3927	1.053	7061	1.021
3932	1.070	7766	1.151
4128	1.373	7951	1.080
4308	1.185	10226	1.060
4311	1.229	10456	1.120
5254	1.140		

Table 4 lists the results of each single observation for galaxies covered by multiple fields. For each entry are given the following: galaxy name; *Einstein* sequence number; time in the image; position used for count extraction; radius used for the extraction of source counts; count rate; statistical error; and a statement of variability between observations. If a given galaxy was detected in the merged data, we list count rates and statistical errors also in the case of nondetection in single observations. These data are not included in Table 5 (see below). NGC 1566, NGC 2992, NGC 3227, NGC 3516, and NGC 7582 are all found to vary; the X-ray emission of these galaxies is dominated by a bright active nuclear source. NGC 315, NGC 5506, and NGC 7469 could also be variable; these galaxies also host active nuclei. Maccacaro, Garilli, & Mereghetti (1987) found variability in the IPC observations of NGC 1566, NGC 3516, NGC 5506, and NGC 7582. However, they did not report any variability in NGC 315 or NGC 2992. In NGC 315 we find variability at the 3 σ level, even when we compare the counts within 3′ circles rather than the total detected source counts. The former comparison is more relevant for a variability study, in the assumption that what varies is a pointlike nuclear source. In the case of NGC 2992, Maccacaro et al. (1987) did not use the entire *Einstein* data set for their analysis. NGC 3227 and NGC 7469 are not included in the sample of Maccacaro et al. (1987).

Table 5 lists marginal detections, with signal to noise between 2.5 and 3 σ. The format is the same as for Table 3. Marginal detections of individual observations of galaxies detected in merged fields are included in Table 4.

Table 6 lists individual observations of galaxies partially obscured by the IPC ribs. For these galaxies the count rate underestimates the "emitted" flux. The format is the same as for Tables 3A, 3B, and 5. For some of these galaxies there are observations clear of the ribs, which are listed in Tables 3A and 3B. These entries are flagged. We leave blank the entries for NGC 3031, NGC 3034, NGC 5128, NGC 7320, and NGC 7331. These galaxies were also detected in other IPC fields well within the ribs. Data are given in Table 3.

Table 7 lists galaxies confused with a nearby source. For each galaxy are given the *Einstein* sequence number, the nearby strong and/or extended source, and a qualitative estimate of the galaxy being detected in X-rays.

Table 8A lists the results on separate components detected in some spiral galaxies; Table 8B gives references for similar published data. For each galaxy listed in Table 8A are given the following: source number in increasing RA order; RA and decl. of each detected source. The IPC positional error is typically of the order of 45″. The HRI positions are accurate at the ~5″ level; sequence number, with I and H identifying IPC and HRI observations, respectively; morphological type; radius used for count extraction; net source counts; statistical error; count rate in units of counts per 1000 s; source flux (0.2–4.0 keV) for the same spectral parameters used to estimate the integrated galaxy flux; distance; source X-ray luminosity.

Table 9 lists the results of our analysis of source extent for galaxies detected with at least 100 IPC counts. E and S0 galaxies, spirals, and AGNs are listed separately. For each galaxy are given the following: name; sequence number; morphological type; signal-to-noise ratio of the detection; radius used for total count extraction; ratio of net counts within 0″–90″ and 0″–180″ from centroid; statistical error on the ratio (1 standard deviation); source equivalent Gaussian σ for 0.3 keV photon energy. The ±1 standard deviation uncertainty is given in parentheses; source equivalent Gaussian σ for 4.5 keV photon energy. The ±1 standard deviation uncertainty is given in parentheses.

Table 10 lists the results of our analysis of source extent for galaxies detected with at least 150 HRI counts. E and S0 galaxies, spirals, and AGNs are listed separately. For each galaxy are given the following: name; sequence number; morphological type; signal-to-noise ratio of the detection; radius used for total count extraction; ratio of net counts within 0″–10″ and 0″–20″ from centroid; statistical error on the ratio (1 standard deviation); source equivalent Gaussian σ for this ratio. The ±1 standard deviation uncertainty is given in parentheses. Ratio of net counts within 0″–30″ and 0″–60″ from centroid; statistical error on the ratio (1 standard deviation); source equivalent Gaussian σ for this ratio. The ±1 standard deviation uncertainty is given in parentheses.

Table 11 lists alternate names for some of the galaxies in our catalog and gives references and comments on individual objects.

5. THE ATLAS

The atlas consists of the X-ray contour maps for detected galaxies overlaid onto optical (POSS or ESO) plates, and of radial surface brightness profiles.

5.1. *Iso-Intensity Contour Maps*

We show the X-ray contour maps in RA order in Figure 7 located after the text. As discussed in § 2, the IPC data were smoothed with a 35″ Gaussian, resulting in an effective beam of 45″–55″ for source kT = 5–1 keV. Table 12 gives a list of smoothing functions and number of pixels over which the image was averaged for each HRI field (each HRI pixel is 0.″5). For galaxies observed with both instruments we show first the IPC map, followed by the HRI map. The IPC maps are generally from the broad-band image (see § 3). For a few galaxies, maps in different energy bands are also shown.

TABLE 12

SMOOTHING PARAMETERS FOR HRI MAPS

Name	σ	Pixels	Name	σ	Pixels
I4329	8″	8	N4438	8	8
I4329A ...	8	8	N4449	5	8
N0253	8	8	N4472	6	[a]
N0315	6	4	N4579	8	8
N0628	8	8	N4631	8	8
M0985 ...	8	8	N4636	6	[a]
N2403	6	6	N4649	6	[a]
N3031	6	6	N4736	10	8
N3034	6	6	N5194	8	8
N3690	8	8	N5236	8	8
N3718	5	4	N5350	10	8
N4151	5	4	N5353	10	8
N4156	5	4	N5354	10	8
N4258	16	16	N5548	5	4
N4321	6	4	N6814	8	8
N4374	8	8	N6822	8	8
N4406	16	16	N7469	6	4
N4435	8	8			

[a] See text in § 5.

Also, as mentioned in § 2, we have used or adapted previously published contour maps for the galaxies below:

NGC 253.—IPC map (B) from Fabbiano (1988a); data were smoothed with 25″ Gaussian to retain information on individual point sources. HRI map adapted from Fabbiano & Trinchieri (1984); data smoothed with 7″ Gaussian; insert shows higher resolution contour map of nuclear region and gaseous plume smoothed with 2″ Gaussian. Fluxes of the individual sources detected and marked on the figures are given in the above papers.

M33 (NGC 598).—IPC map (B) from merged image containing all IPC observations (Trinchieri, Fabbiano, & Peres 1988); data smoothed with 35″ Gaussian.

NGC 628.—IPC map (B) smoothed with 45″ Gaussian (FT).

NGC 720.—IPC map (B) smoothed with 30″ Gaussian (TFC).

NGC 1313.—IPC map (B) smoothed with 35″ Gaussian (FT).

NGC 1395.—IPC map (B) smoothed with 40″ Gaussian (TFC).

NGC 1559.—IPC map (B) smoothed with 25″ Gaussian (FT).

NGC 1672.—IPC map (B) smoothed with 35″ Gaussian (FT).

NGC 2403.—IPC map (B) smoothed with 30″ Gaussian (FT).

NGC 2903.—IPC map (B) smoothed with 30″ Gaussian (FT).

M81 (NGC 3031).—IPC map (B) smoothed with 35″ Gaussian. HRI smoothed with 10″ Gaussian. Individual sources detected in these images are indicated with numbers in the maps. Fluxes and details on the analysis can be found in Fabbiano (1988b).

M82 (NGC 3034).—IPC (B) smoothed with 35″ Gaussian (Fabbiano 1988a).

NGC 4382.—IPC map (B) smoothed with 40″ Gaussian (TFC).

NGC 4472.—IPC map (B) smoothed with 40″ Gaussian. HRI map smoothed with 6″ Gaussian (TFC).

NGC 4631.—IPC map (B) smoothed with 45″ Gaussian (FT).

NGC 4636.—IPC map (B) smoothed with 30″ Gaussian. HRI map smoothed with 6″ Gaussian (TFC).

NGC 4649.—HRI map smoothed with 6″ Gaussian (TFC).

NGC 5253.—IPC map (B) smoothed with 45″ Gaussian (FT).

M101 (NGC 5457).—IPC (B) from merged image containing all the IPC observations. Data smoothed with 32″ Gaussian (Trinchieri, Fabbiano, & Romaine 1990).

IC 2574.—IPC map H smoothed with 45″ Gaussian (FT).

NGC 6744.—IPC map (B) smoothed with 30″ Gaussian (FT).

NGC 6946.—IPC maps (B) smoothed with 30″ Gaussian (FT). (*a*) Sequence I442; (*b*) Sequence I10314—this map shows X-ray emission from SN 1980K (Canizares, Kriss, & Feigelson 1982).

5.2. *Surface Brightness Profiles*

IPC radial surface brightness profiles are shown in Figure 8 for E and S0 galaxies, Figure 9 for spiral galaxies, and Figure 10 for AGNs. These galaxies were all detected with at least 100 net IPC counts. For each galaxy we show the radial profile from the raw image with the normalized background profile, and the background subtracted profile compared with the IPC PRF. We plot two PRFs, appropriate for incoming photon energy of 0.3 keV and 4.5 keV, respectively (Mauche & Gorenstein 1986). HRI radial surface brightness profiles are shown in Figures 11, 12, and 13 for E and S0, S, and AGNs, respectively. These galaxies were all detected with at least 150 net HRI counts. Here again we show the radial profile from the raw image and the background subtracted profile compared with the HRI PRF. As with Figure 7, Figures 8–13 are located after the text.

6. COMPARISONS WITH PREVIOUS WORK AND NEW RESULTS

6.1. *Fluxes*

We have compared our results with those of published papers, both to check the correctness of our results and to estimate the effect of variations in flux determination for samples of galaxies that have been used in statistical analyses. The methods used for the background subtraction and counts extraction in this paper are the same as those used in previous analysis papers by some of the present authors. Therefore it is not surprising that the results compare well with those of FT and TFC. Three other papers publish the results of the analysis of substantial lists of galaxies observed with *Einstein.* One is a paper based on the results of the *Einstein* Medium Survey (Maccacaro et al. 1987; the final Medium Survey source list can be found in Gioia et al. 1990). Very extended sources (e.g., M31) were excluded from this work. However, no effort was made to address carefully the count extraction in the case of less extended sources, which were considered pointlike and for which the count extraction relied on the standard IPC Rev 1B processing. The other two papers are the one by Long and Van Speybroeck (1983, hereafter LVS), which presents a sample of galaxies later used for many statistical studies (e.g., Fabbiano & Trinchieri 1985; Trinchieri & Fabbiano 1985); and the paper by Forman, Jones, & Tucker (1985, hereafter FJT), which presents a sample of early-type galaxies. The later work of Canizares, Fabbiano, & Trinchieri (1987, hereafter CFT) was based on the FJT fluxes.

Figure 14 (*left*) shows a comparison between our count rates and those of Maccacaro et al. (1987). While we are in very good agreement for the X-ray luminous AGNs, in many cases our count rates for normal galaxies tend to be larger. The source of this discrepancy is readily understood when we plot the ratios of the different count rates for given galaxies versus the ratios of counts that we extract in a 90″ circle centered on the X-ray centroid to the total galaxy counts (Fig. 14 [*right*]). The latter is a measure of the angular extent of the X-ray surface brightness. Figure 14 (*right*) shows a clear trend of systematically higher counts estimates in our analysis for spatially extended galaxies. As explained above, Maccacaro et al. (1987) did not do a careful extraction in the case of extended sources.

Figures 15 and 16 show the comparisons of our results with those of LVS and FJT. On average, our count rates compare well with those of LVS, although there is some scatter. This scatter is typically within a factor of 2, and it is probably due to the different count extraction methods. LVS used a local background subtraction and included all excess counts from a circle comparable to the optical radius. We have checked the three galaxies for which our and LVS estimates differ most (NGC

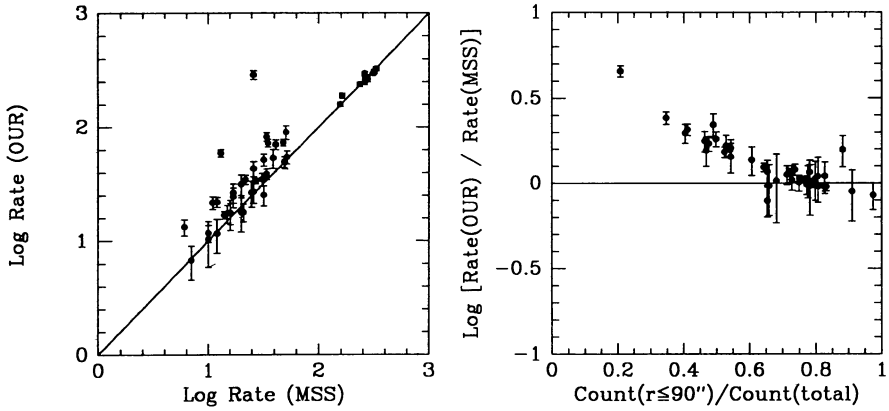

FIG. 14.—*Left:* Comparison of the count rates of this paper (OUR) with those of Maccacaro, Garilli, & Mereghetti (1987; MSS). *Right:* Ratio of count rates plotted vs. the ratio of the counts detected in 90″ circles vs. the total galaxy counts. It is clear that the discrepancies are due to extended X-ray sources.

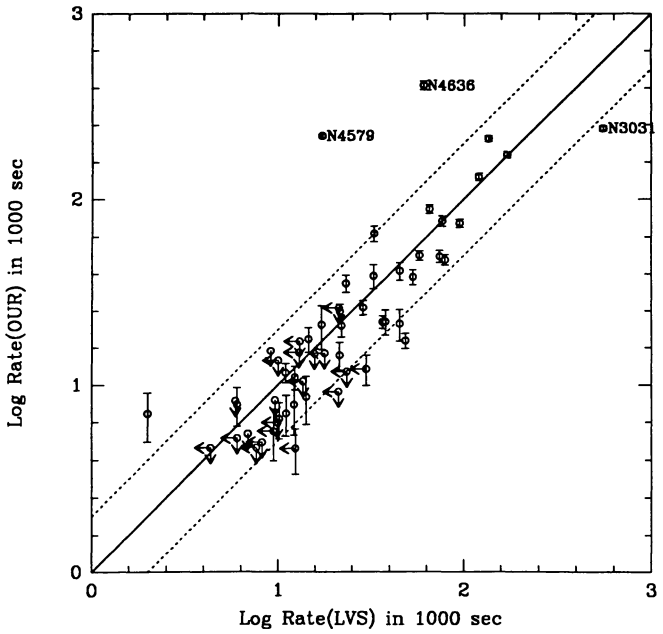

FIG. 15.—Comparison of the count rates of this paper (OUR) with those of LVS. The dotted lines indicate factors of 2 variation in the flux relative to the solid line, which indicates equality of the two count rate determinations.

3031, NGC 4636, and NGC 4579), and we have not found errors in our count extraction. The LVS flux of NGC 3031 (M81) might have included a strong source 13′ east of this galaxy (see Fabbiano 1988a).

FJT do not publish count rates. We have derived X-ray fluxes from their published luminosities and distances. Although the scatter is comparable with that of Figure 15, Figure 16 shows that there is a systematic difference between our fluxes and those in FJT, which may be due to different assumptions on the count rate to flux conversion. For one galaxy, NGC 5128, our estimate is considerably larger, but this is due mainly to the fact that the contribution from the nuclear source was subtracted in FJT.

6.2. *X-Ray–Optical Correlations*

The scatter due to different count extractions is in any case considerably smaller than the scatter in the correlations between X-ray and other wavebands discussed in the literature (e.g., Fabbiano, Gioia, & Trinchieri 1987, 1989; see Fabbiano 1989 for other references). Figure 17 shows scatter diagrams of the X-ray and optical luminosities for "normal" galaxies and AGNs from the data of Tables 3A and 3B. The same equal X-ray–to–B ratio line is drawn on all the diagrams in Figure 17. Using this line as a reference, one can see that the E and S0 sample follows a steeper relationship than the spiral sample, in agreement with published results. AGNs tend to be more X-ray–luminous than normal galaxies. No substantial differences are seen between field and Virgo galaxies.

Figure 18 shows scatter diagrams of the X-ray (0.2–4.0 keV) fluxes versus the B apparent magnitude. These graphs that can be used to "predict" the X-ray emission of a normal galaxy, given its apparent magnitude. However, it is important to keep in mind that, even in the case of spiral galaxies, there is a factor of ~10 scatter on each side of the "average." The envelope for spiral galaxies is given by the relationships

$$\log (f_X) = -(2/5)B - 9$$

and

$$\log (f_X) = -(2/5)B - 7 .$$

We have performed a regression analysis of the X-ray–optical correlations of elliptical and spiral galaxies with the Schmitt (1985) censored regression analysis method, using the software of Feigelson and Isobe. The best-fit regression lines are shown superposed on the scatter plots for the two samples in Figure 19, and are given below:

$$\log [L_X(\text{ellipticals})] = 1.8 \log (L_B) + 21.5$$

$$\log [L_B(\text{ellipticals})] = 0.3 \log (L_X) - 2.6$$

and

$$\log [L_X(\text{spirals})] = 1.0 \log (L_B) + 29.3$$

$$\log [L_B(\text{spirals})] = 0.4 \log (L_X) - 6.7 ,$$

where L_X is in ergs s^{-1} and L_B is in $L_\odot$.

These fits are in agreement with the reported steep relationship for elliptical galaxies (e.g., Fabbiano et al. 1989) but suggest the possibility of a steeper relationship for the spiral sample than previously found (e.g., Fabbiano et al. 1987). The

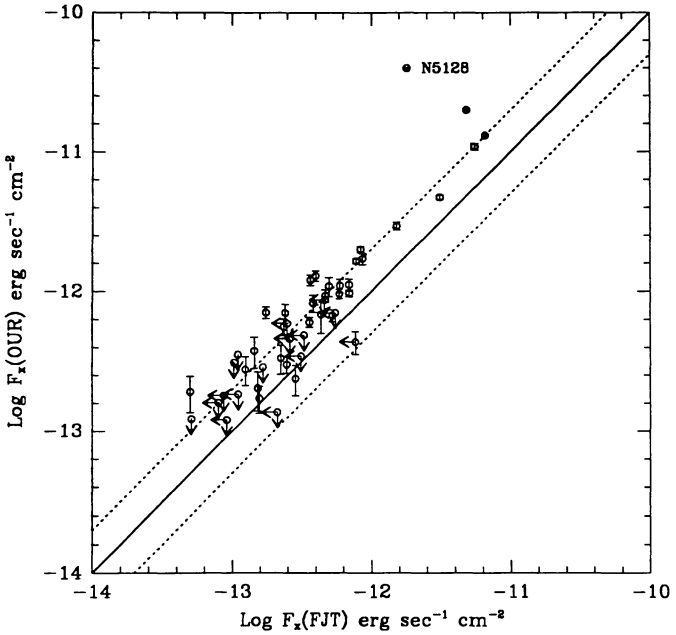

FIG. 16.—Comparison of the count rates of this paper (OUR) with count rates derived from CFT and FJT (see text). The dotted lines indicate factors of 2 variation in the flux relative to the solid line, which indicates equality of the two count rate determinations.

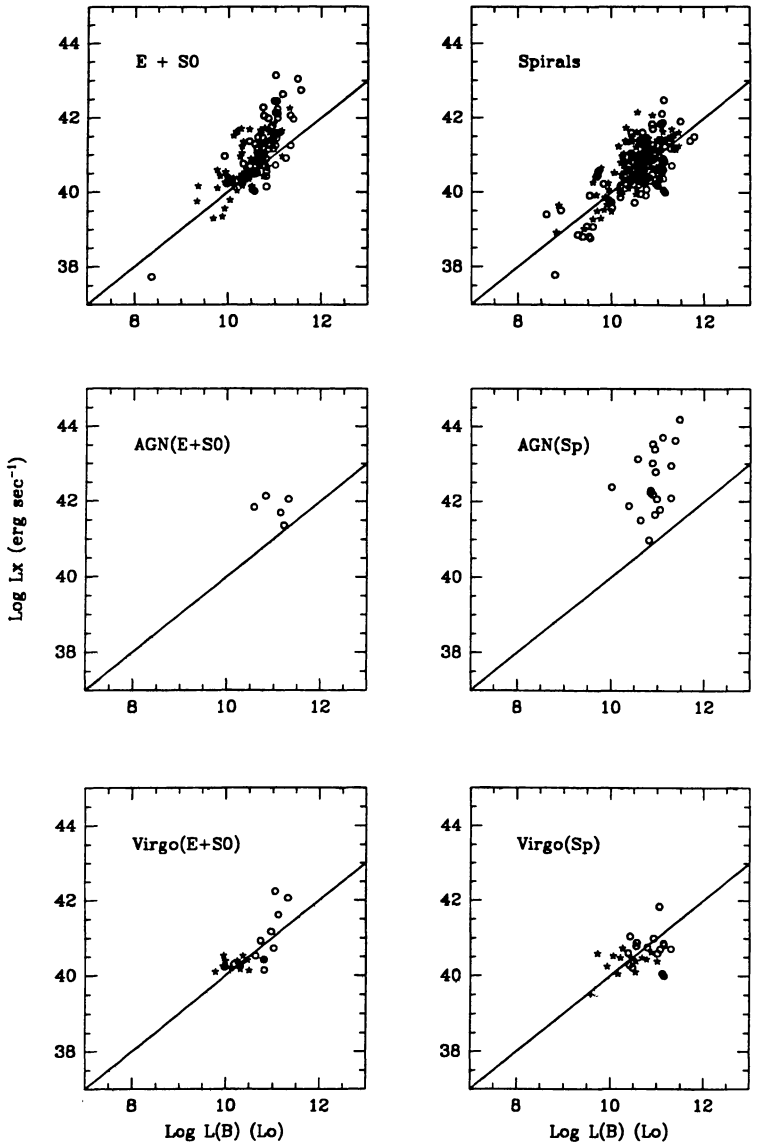

FIG. 17.—X-ray vs. optical (B) luminosities for galaxies in this catalog. Circles and stars represent detections and upper limits, respectively. The diagonal lines are lines of constant X-ray–optical ratio and are drawn to help compare different subsamples.

main difference between this and the previous analyses is in the sample analyzed. The present sample is larger, but also contains a far larger percentage of upper limits than the smaller samples analyzed previously. This results in a larger discrepancy between the two regression lines.

We will examine multiwavelength correlations in detail in a forthcoming paper.

6.3. *Individual Sources/Components in Galaxies*

As shown in Table 8, the luminosities of the individual sources/clumps detected in some galaxies are quite high, and often in excess of the Eddington limit for 1 $M_\odot$ accreting object ($\sim 1.3 \times 10^{38}$ ergs s^{-1}). The presence of these bright sources is puzzling. Very luminous sources are discussed in FT and Fabbiano (1989).

6.4. *Source Extent*

Our results confirm the conclusion that the X-ray emission of normal galaxies is spatially extended (see Fabbiano 1989), while AGNs tend to be dominated by a strong pointlike source. Figure 20 shows plots of the ratios of net IPC source counts from two circles of different radii, both centered on the source centroid, versus the maximum radius used for the source count extraction. The latter depends both on source extent and intensity. AGNs in the IPC tend to have similar ratios, compatible with the instrumental PRF. Normal galaxies instead (both early- and late-type) tend to have smaller ratios, consistent with extended X-ray emission (see also Table 9). Extended emission is also evident in the HRI images of normal galaxies (Fig. 21 and Table 10). Moreover, in the HRI there is evidence of extended components in a number of AGNs, in addition to

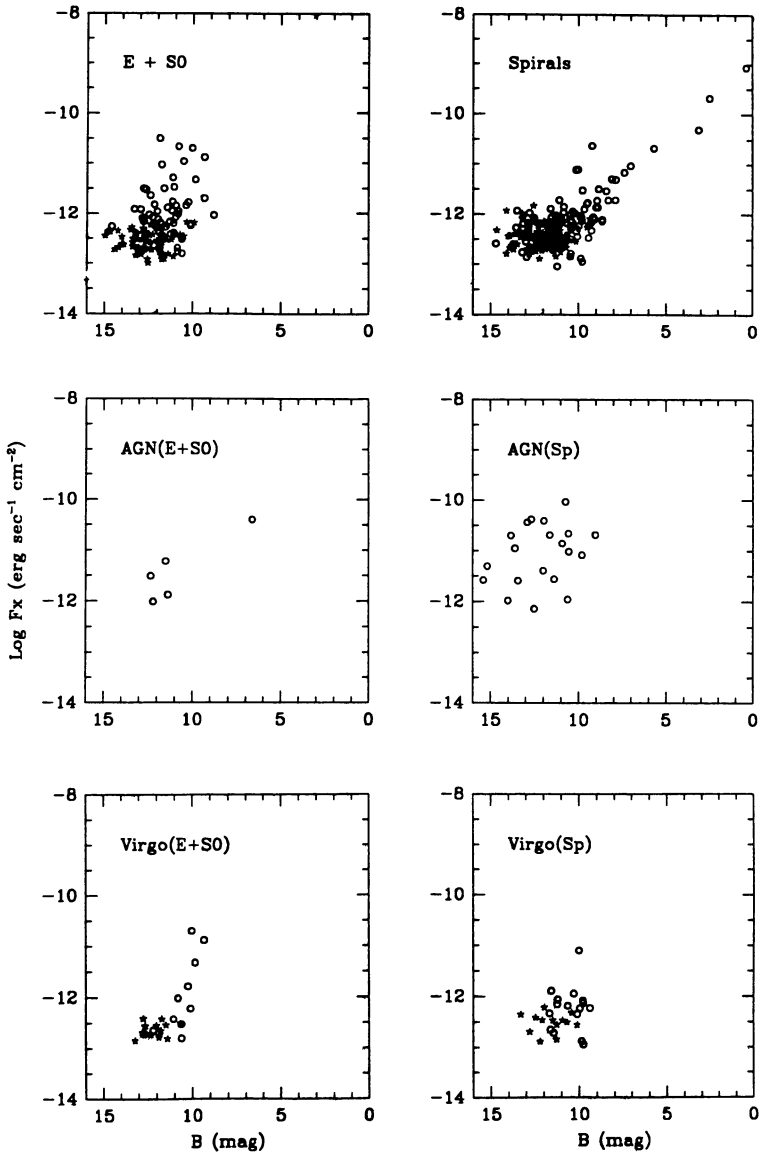

FIG. 18.—X-ray fluxes vs. apparent magnitude. Circles and stars represent detections and upper limits, respectively.

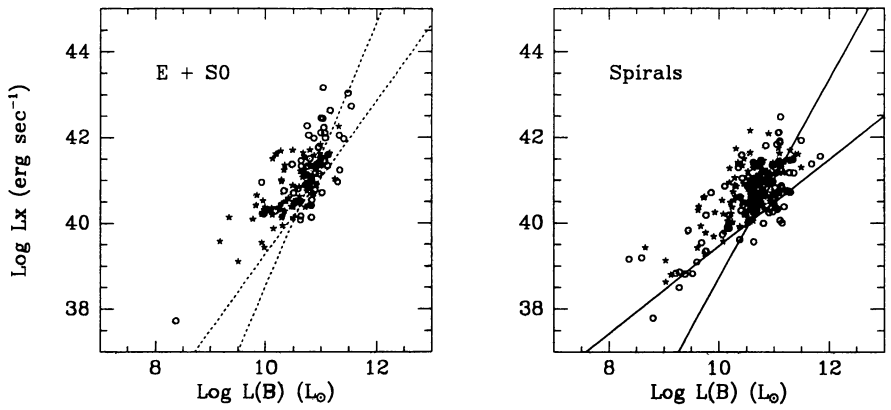

FIG. 19.—X-ray vs. *B* luminosities for elliptical and spiral galaxies with best-fit detection and limits regression lines (see text)

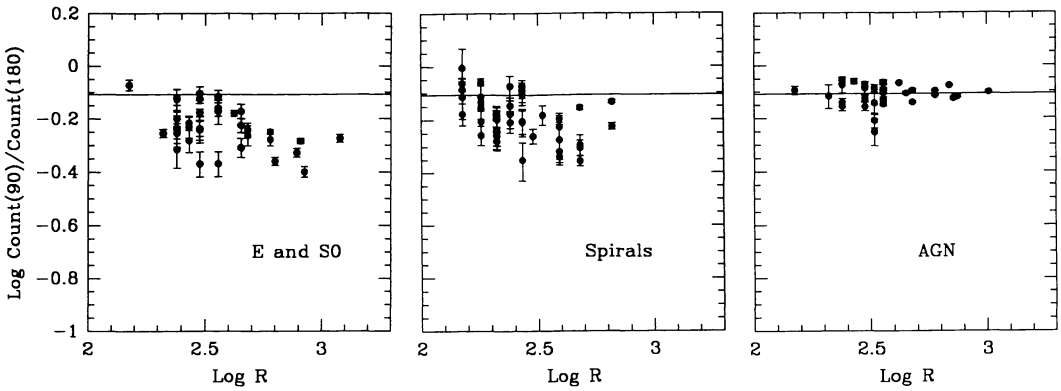

FIG. 20.—Plots of the ratios of net source counts from IPC images in two circles vs. the maximum radius used for the source count extraction (which depends both on source extent and intensity). The horizontal line is the average ratio obtained for AGNs (i.e., represents the ratio equivalent to the PRF).

the central strong pointlike source. We discuss these features in § 6.5.

Although we have used Gaussians to parameterize the extent of the X-ray emission, Gaussians are not a good representation of the X-ray surface brightness distribution. Even disregarding asymmetries in the spatial distribution of the X-ray emission (see the atlas), it has been shown in a few cases that the X-ray emission of elliptical galaxies tends to follow that of the optical light (TFC). It is well known that the latter follows a power-law rather than a Gaussian distribution. In bright spirals, except for cases where the X-ray emission is dominated by a few strong X-ray sources, the X-ray surface brightness tends to follow the optical exponential disk (Trinchieri, Fabbiano, & Palumbo 1985; Palumbo et al. 1985; FT; see Fabbiano 1989). Figure 22 demonstrates that on average the radial distribution of the X-ray surface brightness of galaxies is flatter than a

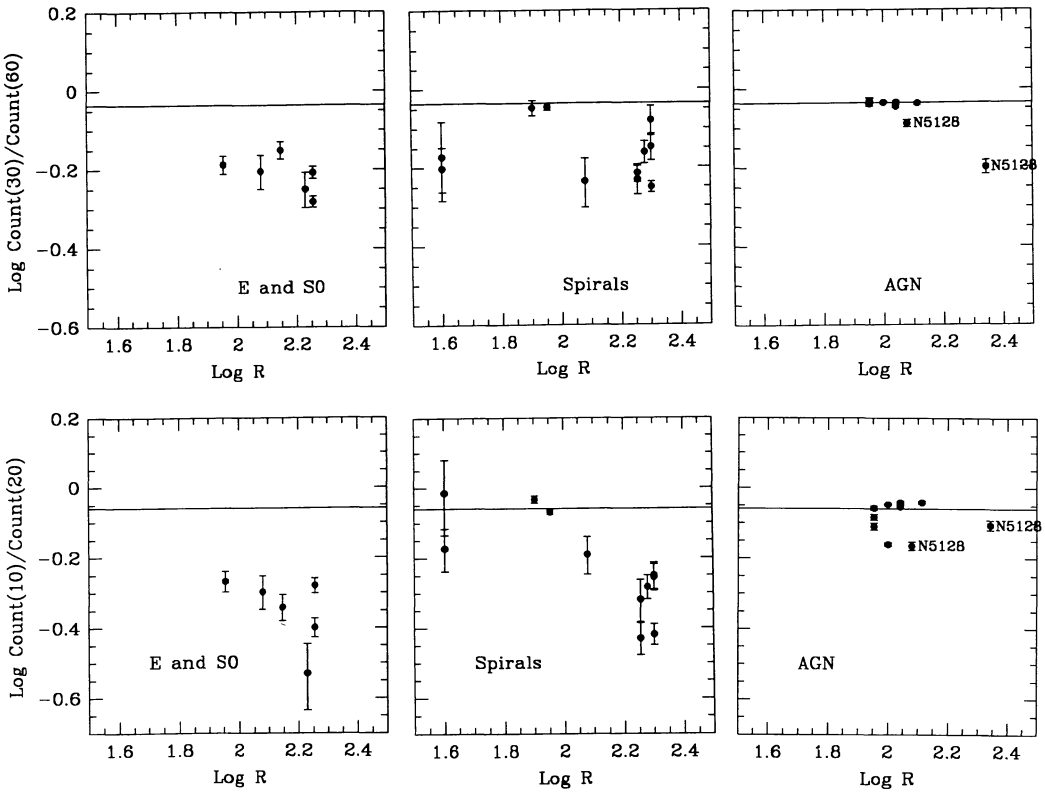

FIG. 21.—Plots of the ratios of net source counts from HRI images in two circles vs. the maximum radius used for the source count extraction (which depends both on source extent and intensity). The horizontal line is the average ratio obtained for AGNs (i.e., represents the ratio equivalent to the PRF).

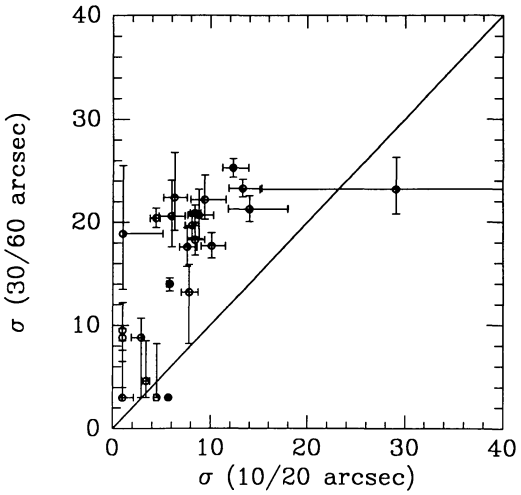

FIG. 22.—The equivalent Gaussian σ derived from the ratio of counts in different size circles for HRI sources. The distribution of points shows that the radial distribution of the X-ray surface brightness is less steep than a Gaussian.

Gaussian distribution. The equivalent Gaussian σ derived from the ratio of circles with larger radii are systematically larger than those derived from the ratio of smaller circles. It is clear that a more sophisticated analysis is needed to study in detail the spatial distribution of the X-ray surface brightness. This will be the subject of a future paper, where we will fit de Vaucoulers or King profiles to early-type galaxies, and exponentials to late-type galaxies. Care will be taken to subtract strong nuclear pointlike sources and the resulting profiles will be compared with optical data when available.

Other caveats with our analysis are that (1) we have searched only for global extent, disregarding asymmetries in the X-ray surface brightness distribution, and (2) we have not used the IPC PRF best suited to the spectral properties of each galaxy. This makes us relatively insensitive to small-scale asymmetric extent. As an example, a comparison of the IPC surface brightness of M82 (NGC 3034) in different azimuthal sectors has shown the presence of a halo elongated along the minor axis (Fabbiano 1988a). Moreover, a comparison of these profiles with the PRF appropriate for 1.5 keV X-rays (similar to that suggested by the spectral parameters of the nuclear region of M82) has shown extent in both minor and major axis directions. In the present analysis, we detect an indication of extent only when we compare the azimuthally averaged profile with the 4.5 keV PRF (Table 9).

6.5. *Extended Emission in Active Galactic Nuclei*

Table 9 shows that the equivalent Gaussian σ of all AGNs except NGC 4261 (3C 270) is compatible with that of the IPC PRF for soft photon energies. NGC 4261 is an E galaxy, and the contour map also suggests the possibility of extended emission (Fig. 7). Its X-ray luminosity (Table 3A) is well in the range of normal early-type galaxies, suggesting that the nuclear source is not dominant in the X-rays. There are marginal indications of extent in some cases when the 4.5 keV PRF is used. As mentioned above, the HRI azimuthally averaged surface brightness profiles of AGNs show extended emission components in a few cases. The most obvious case is NGC 5128 (Cen A), where extent is also suggested by the IPC radial profile at large radii. This extended emission is due to an X-ray jet and a galaxy halo (Feigelson et al. 1981). Other AGNs with an emission component extending past the central 60″ are NGC 1566 and NGC 5548. In these two galaxies, the X-ray radial profiles (Fig. 13) are systematically higher than the expected HRI PRF distribution at large radii. We can exclude that this is due to the effect of mirror scattering from a very hard point source. NGC 4151, which has a harder distribution of incoming photons (Paper II), does not look extended at large radii. Extended asymmetric emission in a 1′ scale has been reported by Elvis et al. (1990) in NGC 1566. These authors also found similar features in the HRI data of NGC 2992 and NGC 4151. Our analysis is not sensitive to azimuthal asymmetries in the photon distribution. However, we are sensitive to extended emission at larger radii from the source centroid from those considered by Elvis et al. (1990). The luminosities of these extended components, after subtracting the central point sources are $\sim 5 \times 10^{40}$ ergs s^{-1} and $\sim 10^{42}$ ergs s^{-1} in NGC 1566 and NGC 5548, respectively. We will not speculate on the nature of these components. We believe that we need to confirm their existence with *ROSAT* observations.

Two of the observations of AGNs (H6395 of NGC 4151 and H8315 of NGC 5548) differ from the HRI PRF at the innermost radii (see Table 10 and Fig. 13). We believe that this might be due to some problem with the aspect solution. The problem with NGC 5548 had been noticed by Elvis et al. (1990) who excluded this observation from their analysis. In both cases, however, we have a second observation that is consistent with the HRI PRF at the inner radii. Also, both sets of observations for each galaxy give consistent radial profiles at larger radii.

7. CONCLUSIONS

This catalog represents a summary of the *Einstein* X-ray observations of galaxies and may help in planning future X-ray observations. The tabular information included in this paper will shortly be available as part of the on-line *Einstein* data products (reachable with "einline"). We plan to keep this data base alive and growing by adding to it the results of the forthcoming *ROSAT* observations of galaxies.

We thank Susan Hazelton, Elizabeth Bohlen, Linda Kim, Chris Fassnacht, and Archan Basu for help in the data analysis and Harvey Tananbaum and Dan Harris for comments on the manuscript. This work was supported by NASA contract NAS8-30751 and Smithsonian Institution Scholarly Studies grant S910. G.T. acknowledges financial support by the Italian ASI.

REFERENCES

Biermann, P., & Kronberg, P. P. 1983, ApJ, 268, L69
Biermann, P., Kronberg, P. P., & Madore, B. F. 1982, ApJ, 256, L37
Bregman, J. N., & Glassgold, A. E. 1982, ApJ, 263, 564
Canizares, C. R., Donahue, M., Trinchieri, G., Stewart, G., & McGlynn, T. 1986, ApJ, 304, 312
Canizares, C. R., Fabbiano, G., & Trinchieri, G. 1987, ApJ, 312, 503 (CFT)
Canizares, C. R., Kriss, G. A., & Feigelson, E. D. 1982, ApJ, 253, L17
de Vaucouleurs, G., de Vaucouleurs, A., & Corwin, H. G. 1976, Second Reference Catalogue of Bright Galaxies (Austin: Univ. of Texas Press) (RC2)
Dressel, L., & Wilson, A. 1985, ApJ, 291, 668
Elvis, M., Fassnacht, C., Wilson, A. S., & Briel, U. 1990, ApJ, 361, 459
Elvis, M., & Van Speybroeck, L. 1982, ApJ, 257, L51
Fabbiano, G. 1988a, ApJ, 330, 672
———. 1988b, ApJ, 325, 544
———. 1989, ARA&A, 27, 87
Fabbiano, G., Feigelson, E., & Zamorani, G. 1982, ApJ, 256, 397
Fabbiano, G., Gioia, I. M., & Trinchieri, G. 1988, ApJ, 324, 749
———. 1989, ApJ, 347, 127
Fabbiano, G., Heckman, T., & Keel, W. C. 1990, ApJ, 355, 442
Fabbiano, G., & Trinchieri, G. 1983, ApJ, 266, L5
———. 1984, ApJ, 286, 491
———. 1985, ApJ, 296, 430
———. 1987, ApJ, 315, 46 (FT)
Fabbiano, G., Trinchieri, G., & Macdonald, A. 1984, ApJ, 284, 65
Fabbiano, G., Trinchieri, G., & Van Speybroeck, L. 1987, ApJ, 316, 127
Fabricant, D., Lecar, M., & Gorenstein, P. 1980, ApJ, 241, 552
Feigelson, E., Schreier, E., Delvaille, J., Giacconi, R., Grindlay, J., & Lightman, A. 1981, ApJ, 251, 31
Forman, W., Jones, C., & Tucker, W. 1985, ApJ, 293, 102 (FJT)
Forman, W., Schwarz, J., Jones, C., Liller, W., & Fabian, A. 1979, ApJ, 234, L27
Giacconi, R., et al. 1979, ApJ, 230, 540
Gioia, I. M., Maccacaro, T., Schild, R. E., Wolter, A., Stocke, J. T., Morris, S. L., & Henry, J. P. 1990, ApJS, 72, 567
Harnden, F. R., Jr., Fabricant, D. G., Harris, D. E., & Schwarz, J. 1984, Scientific Specification of the Data Analysis System for the *Einstein Observatory (HEAO2)* IPC (Internal SAO Special Report 393)
Harris, D. E. 1984, Einstein Observatory—Revised User's Manual (RUM)
Killeen, N. E. B., & Bicknell, G. V. 1988, ApJ, 324, 198
Killeen, N. E. B., Bicknell, G. V., & Carter, D. 1986, ApJ, 309, 45
Kim, D.-W., Fabbiano, G., & Trinchieri, G. 1992a, ApJS, 80, 645 (Paper II)
———. 1992b, ApJ, in press (Paper III)
Knapp, G. R., Turner, E. L., & Cunniffe, P. E. 1985, AJ, 90, 454
Kotanyi, C., van Gorkom, J. H., & Ekers, R. D. 1983, ApJ, 273, L7
Kriss, G. A., Cioffi, D. F., & Canizares, C. R. 1983, ApJ, 272, 439
Kronberg, P. P., Biermann, P., & Schwab, F. R. 1985, ApJ, 291, 693
Long, K. S., D'Odorico, S., Charles, P. A., & Dopita, M. A. 1981, ApJ, 246, L61
Long, K. S., & Van Speybroeck, L. P. 1983, in Accretion Driven X-Ray Sources, ed. W. Lewin & E. P. J. van den Heuvel (Cambridge: Cambridge Univ. Press), 117 (LVS)
Maccacaro, T., Garilli, B., & Mereghetti, S. 1987, AJ, 93, 1484
Maccacaro, T., & Perola, G. C. 1981, ApJ, 246, L11
Maccacaro, T., Perola, G. C., & Elvis, M. 1982, ApJ, 257, 47
Markert, T. H., & Rallis, A. D. 1983, ApJ, 275, 571
Mauche, C. W., & Gorenstein, P. 1986, ApJ, 302, 371
McCammon, D., & Sanders, W. T. 1984, ApJ, 287, 167
McKechnie, S. P., et al. 1984, in X-Ray Astronomy '84, ed. M. Oda & R. Giacconi (Tokyo: Inst. Space Aeronaut. Sci.), 373
Nulsen, P. E. J., Stewart, G. C., & Fabian, A. C. 1984, MNRAS, 208, 185
Palumbo, G. G. C., Maccacaro, T., Panagia, N., Vettolani, G., & Zamorani, G. 1981, ApJ, 247, 484
Palumbo, G. G. C., Fabbiano, G., Fransson, C., & Trinchieri, G. 1985, ApJ, 298, 259
Paturel, G., Fouque, P., Bottinelli, L., & Gouguenheim, L. 1989, Catalogue of Principal Galaxies (Lyon: Observatoire de Lyon) (PGC)
Peres, G., Reale, F., Collura, A., & Fabbiano, G. 1989, ApJ, 336, 140
Sandage, A. R., & Tammann, G. A. 1981, Revised Shapley-Ames Catalogue of Galaxies (Washington: Carnegie Institution of Washington) (RSA)
Schaaf, R., Pietsch, W., Biermann, P. L., Kronberg, P. P., & Schmutzler, T. 1989, ApJ, 336, 722
Schmitt, J. H. M. M. 1985, ApJ, 293, 178
Schreier, E. J., Feigelson, E., Delvaille, J., Giacconi, R., Grindlay, J., Schwartz, D. A., & Fabian, A. C. 1979, ApJ, 234, L39
Stark, A. A., et al. 1992, ApJS, 79, 77
Trinchieri, G., & Fabbiano, G. 1985, ApJ, 296, 447
———. 1991, ApJ, 382, 82
Trinchieri, G., Fabbiano, G., & Palumbo, G. G. C. 1985, ApJ, 290, 96
Trinchieri, G., Fabbiano, G., & Canizares, C. R. 1986, ApJ, 310, 637 (TFC)
Trinchieri, G., Fabbiano, G., & Peres, G. 1988, ApJ, 325, 531
Trinchieri, G., Fabbiano, G., & Romaine, S. 1990, ApJ, 356, 110
Tully, B. R. 1988, Nearby Galaxies Catalog (New York: Cambridge Univ. Press)
Van Speybroeck, L., & Bechtold, J. 1981, in X-Ray Astronomy with the *Einstein* Satellite, ed. R. Giacconi (Dordrecht: Reidel), 153
Van Speybroeck, L., Epstein, A., Forman, W., Giacconi, R., & Jones, C. 1979 ApJ, 234, L45
Watson, M. G., Stanger, V., & Griffiths, R. E. 1984, ApJ, 286, 144
Weedman, D. W., Feldman, F. R. Balzano, V. A., Ramsey, L. W., Sramek, R. A., & Wu, C.-C. 1981, ApJ, 248, 105

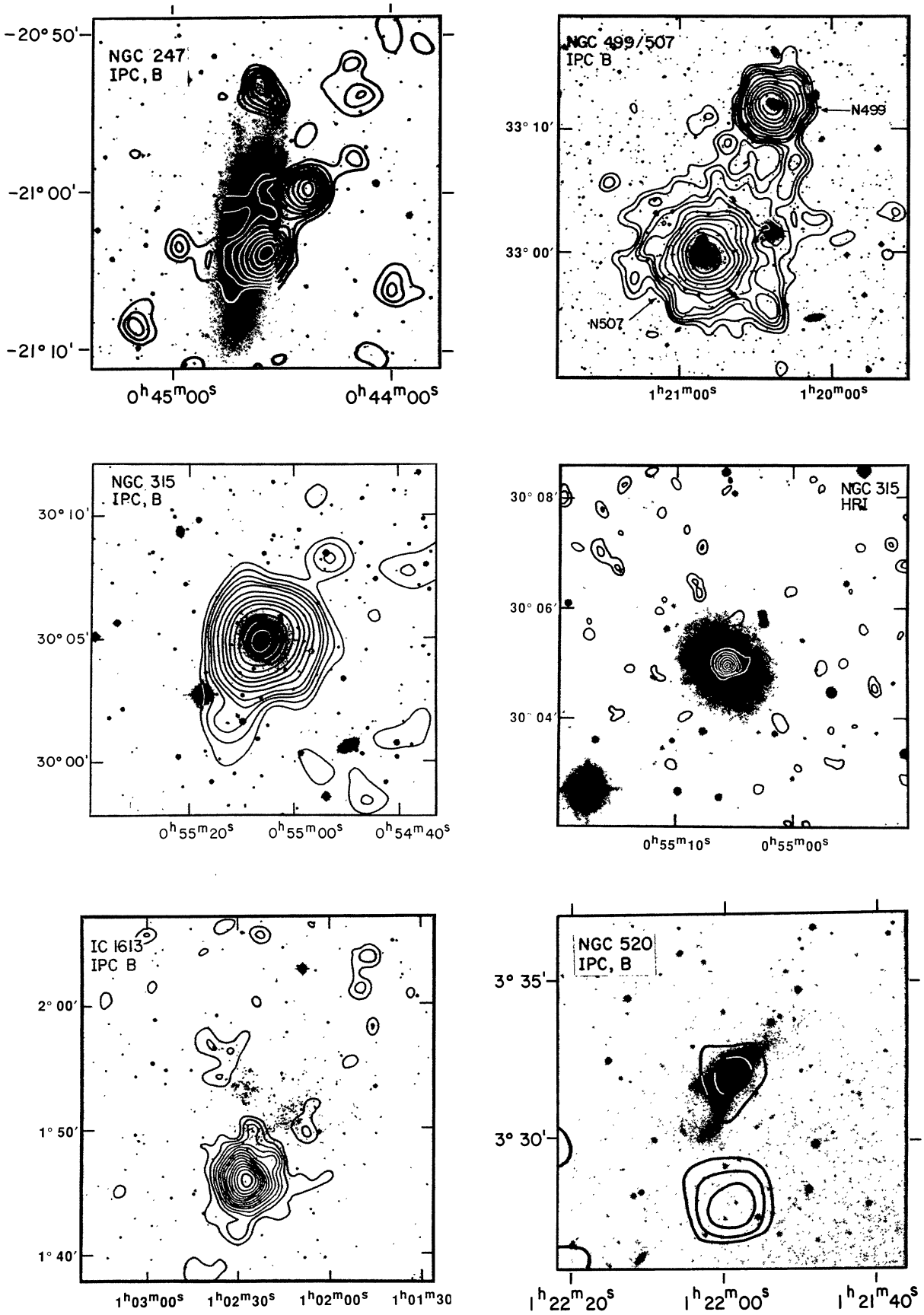

FIG. 7.—Isointensity contour maps of the X-ray emission of detected galaxies superposed onto optical plates. Galaxies are ordered by increasing RA. The galaxy name(s) and the *Einstein* sequence number are given for each overlay. The energy band used for the IPC contour maps is also indicated (S, H, or B; see text). For galaxies observed with both instruments, we give the IPC map first, and then the HRI map. The lowest contour level corresponds to a 2 σ enhancement over the background level. Subsequent contours correspond to 3, 4, 5, and 6 σ. Above this, contours may be skipped in strong sources to avoid crowding. A straight solid line represents the edge of the X-ray field of view. Dashed lines indicate the boundaries of the IPC ribs.

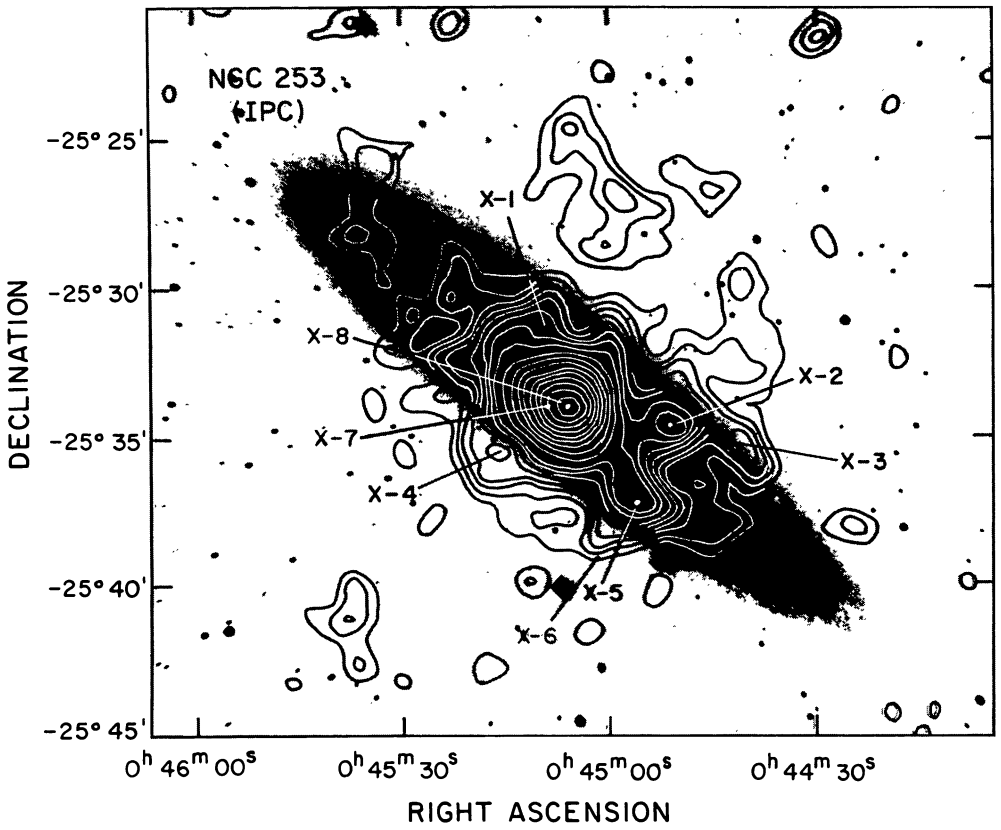

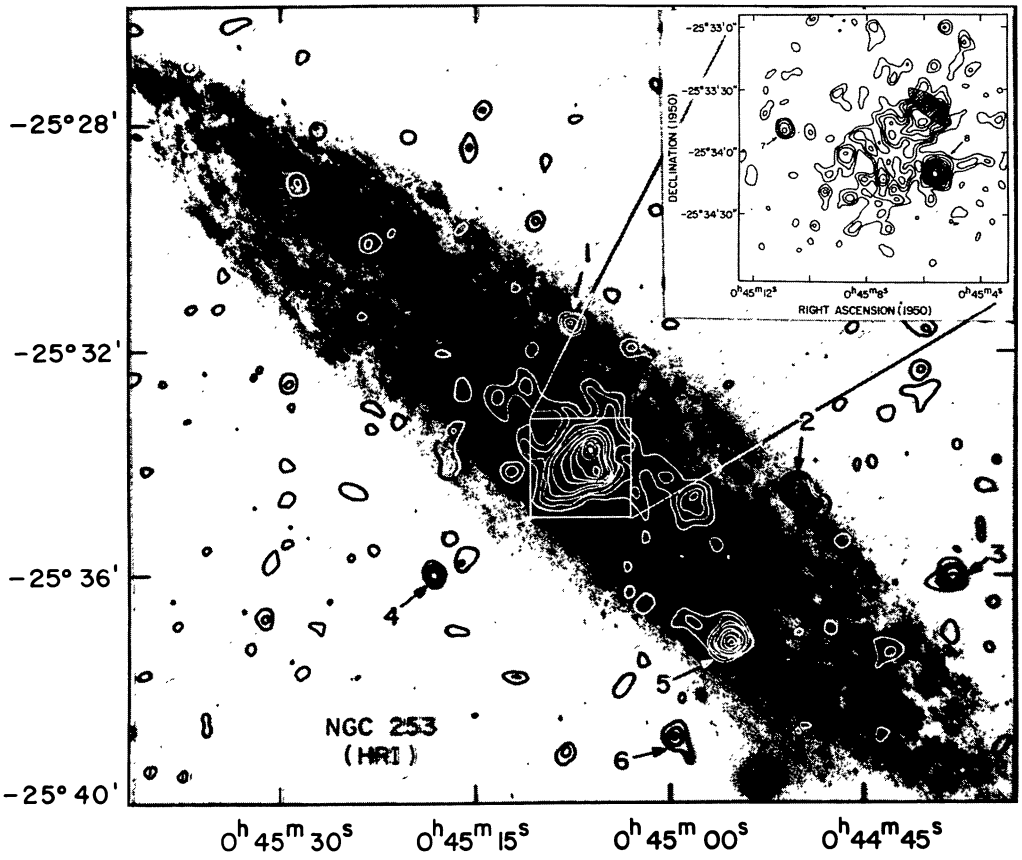

FIG. 7—*Continued*

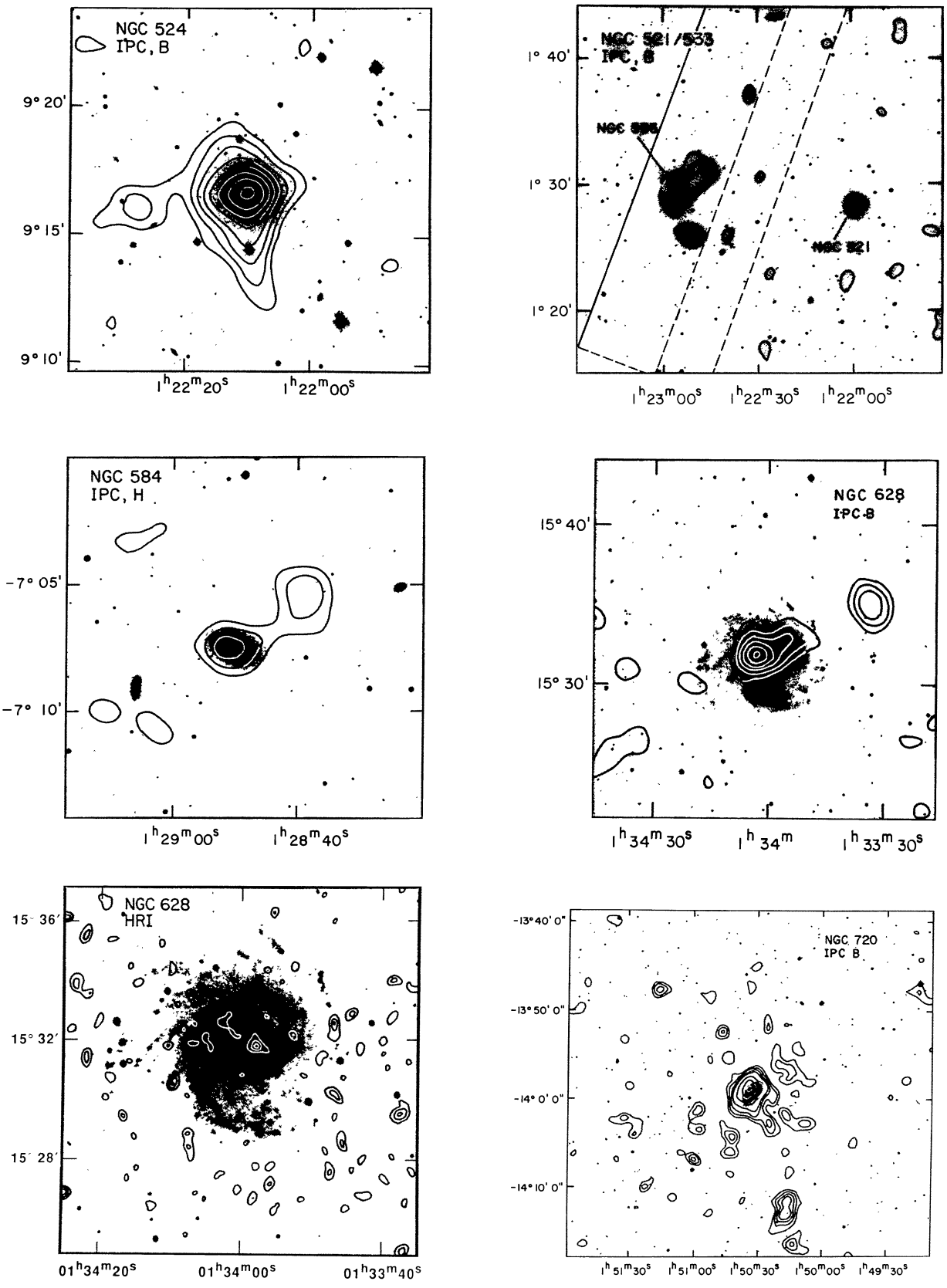

FIG. 7—*Continued*

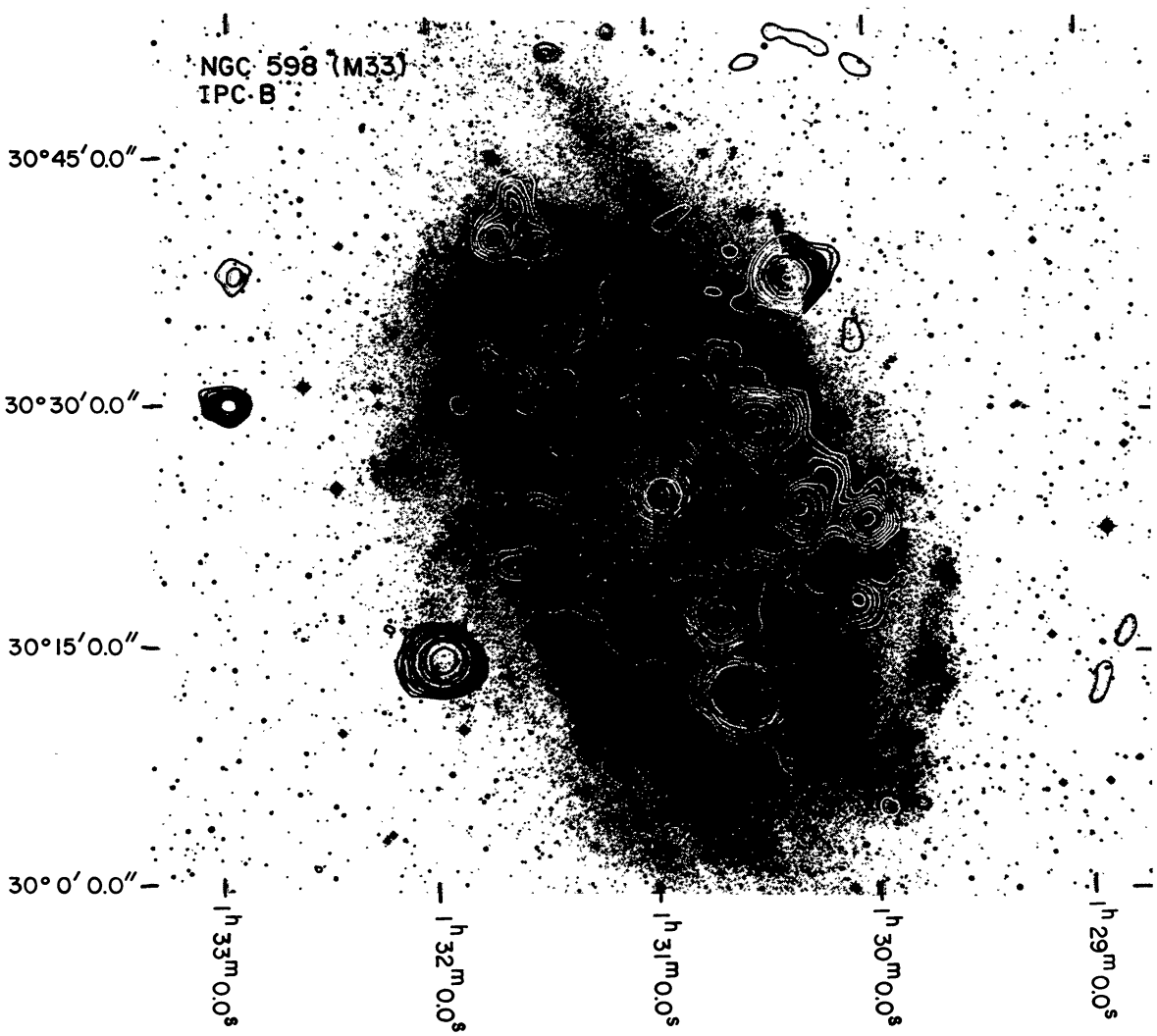

FIG. 7—*Continued*

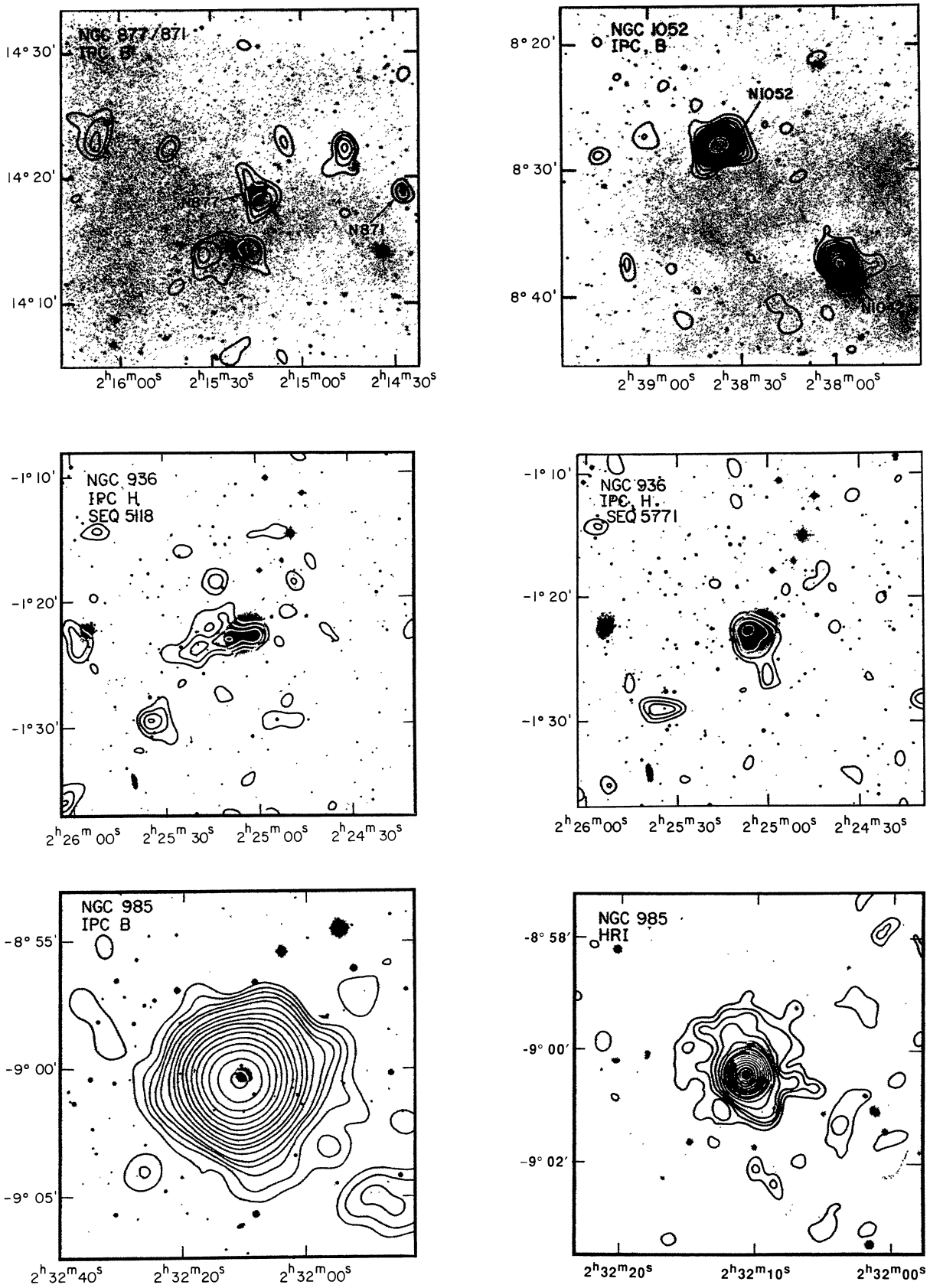

FIG. 7—*Continued*

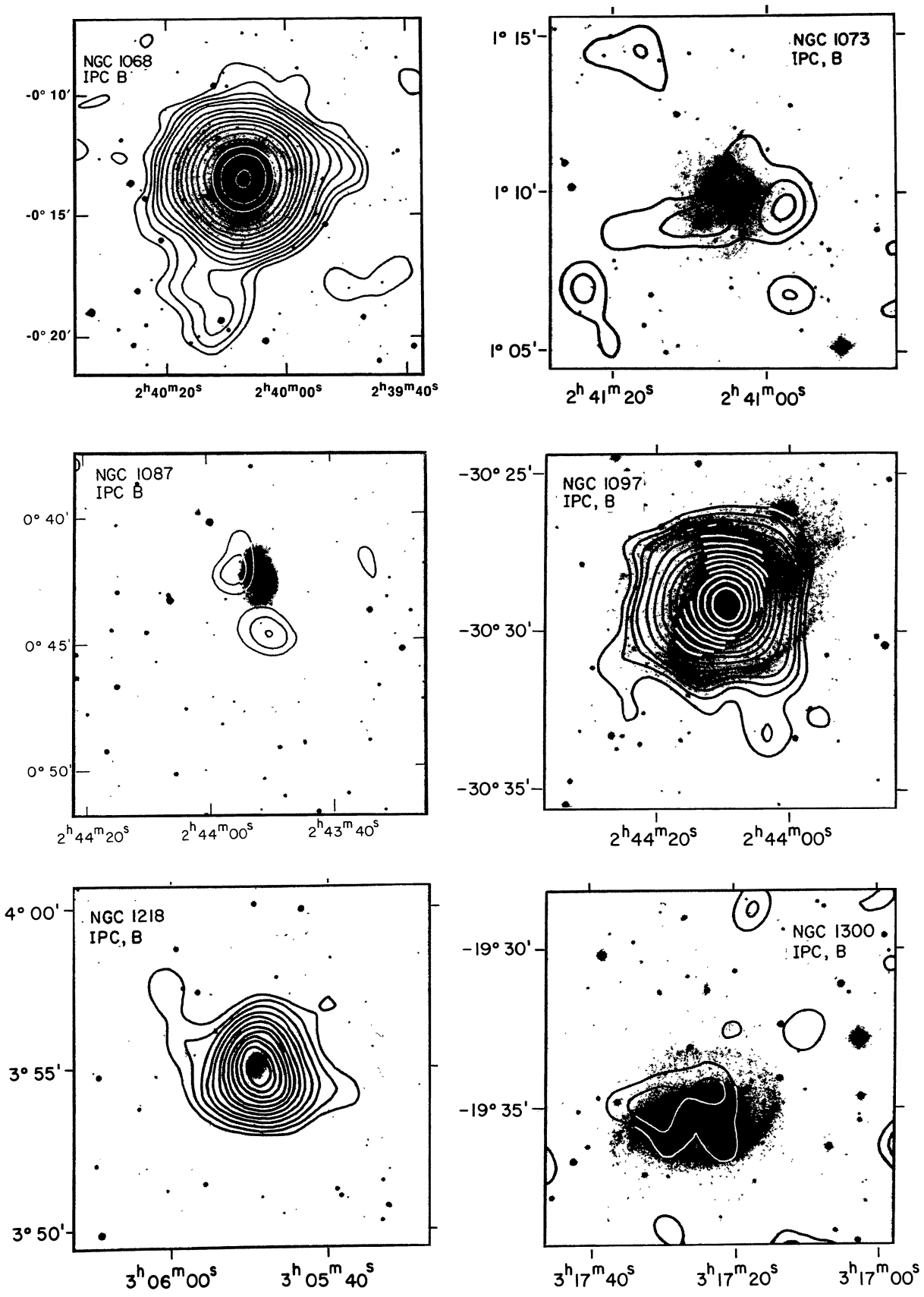

FIG. 7—*Continued*

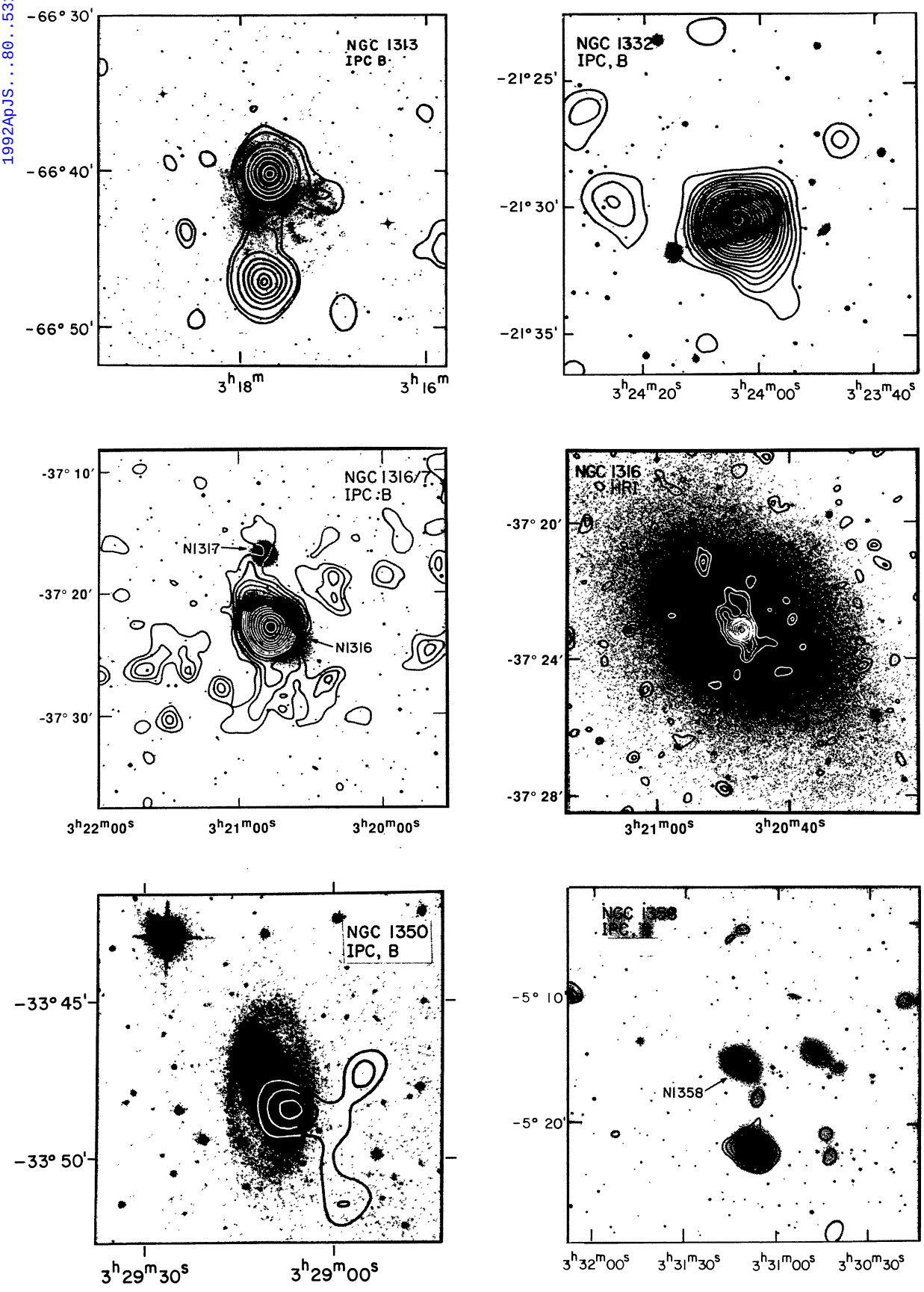

FIG. 7—*Continued*

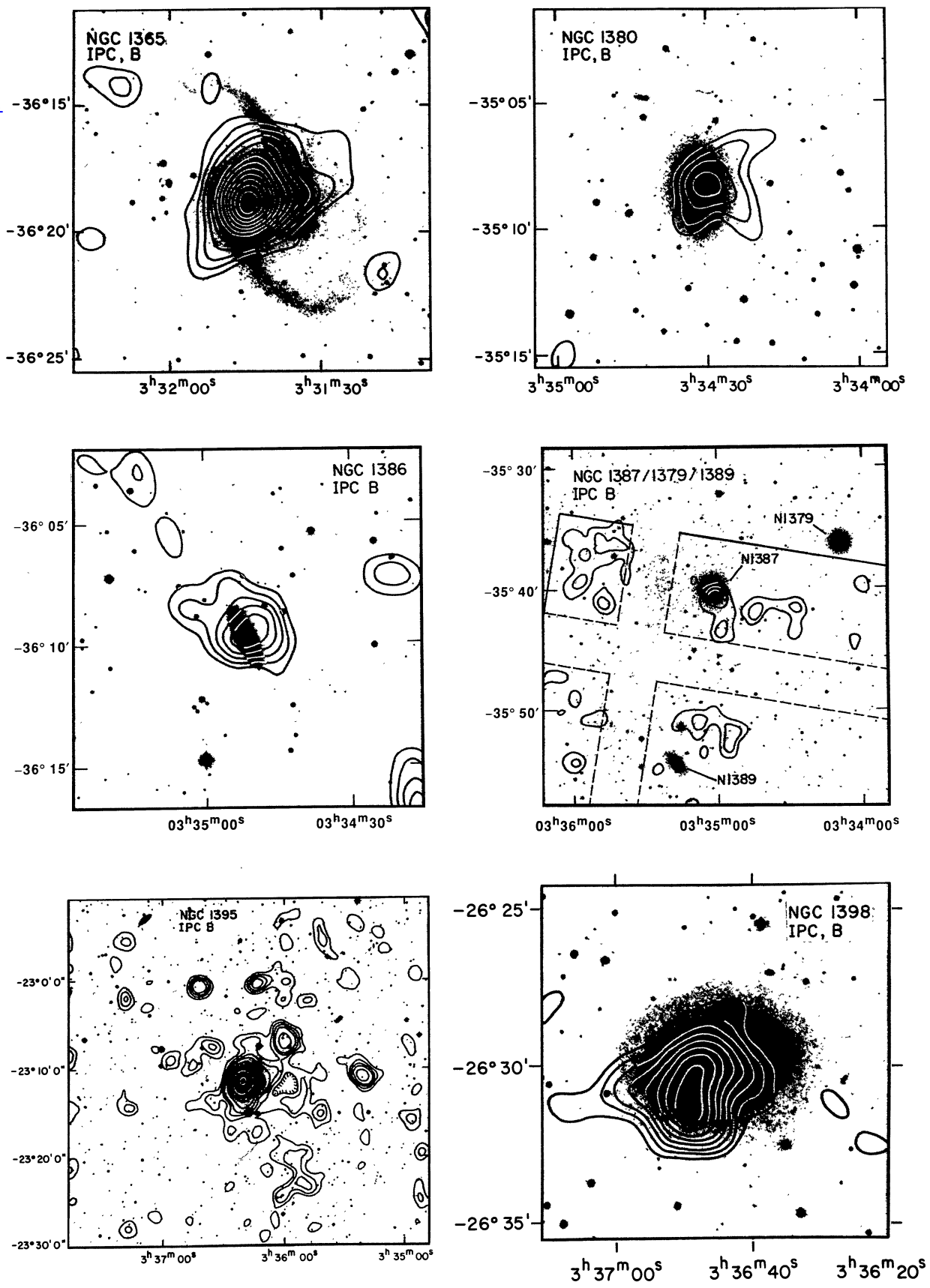

FIG. 7—*Continued*

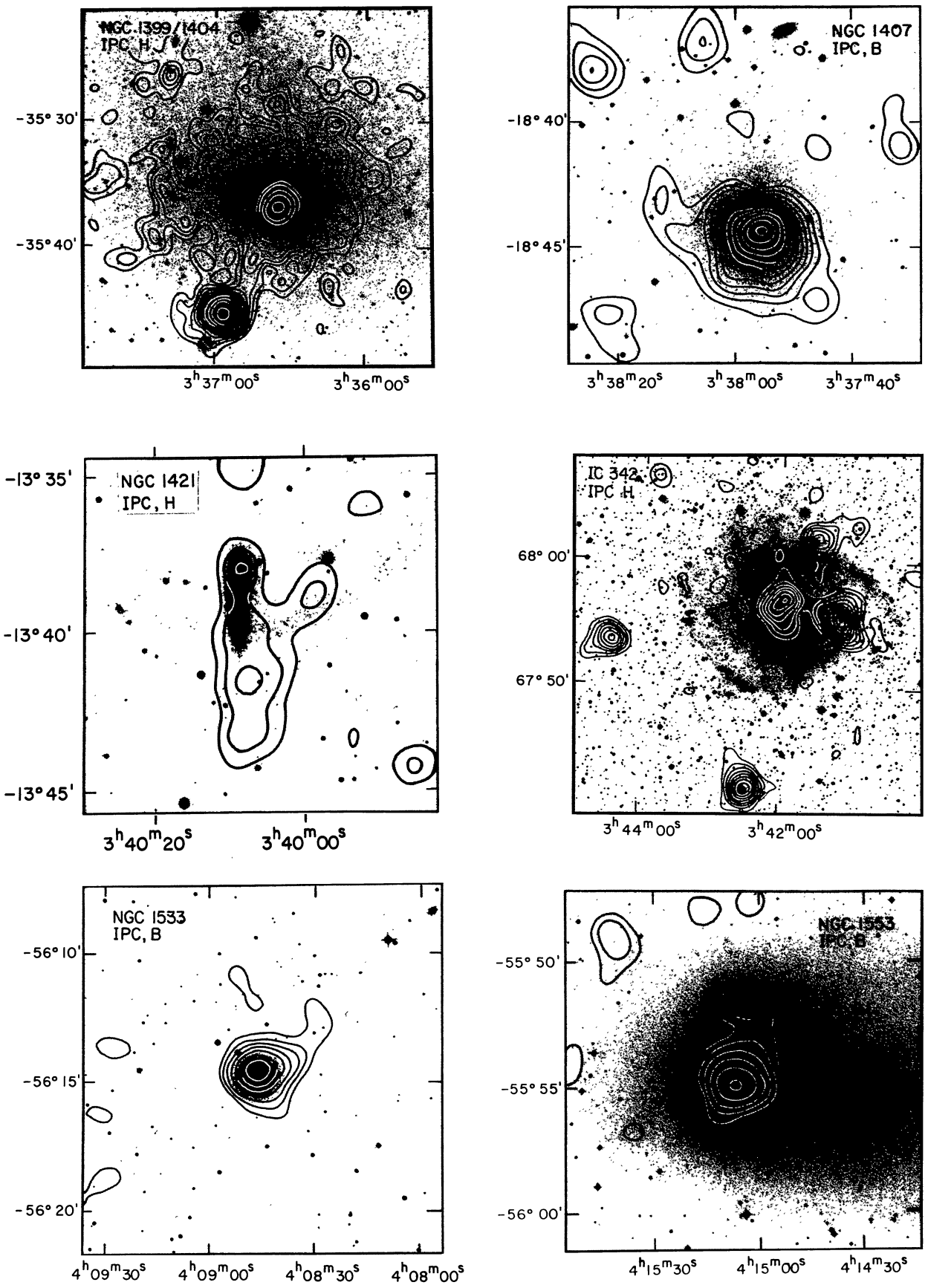

FIG. 7—*Continued*

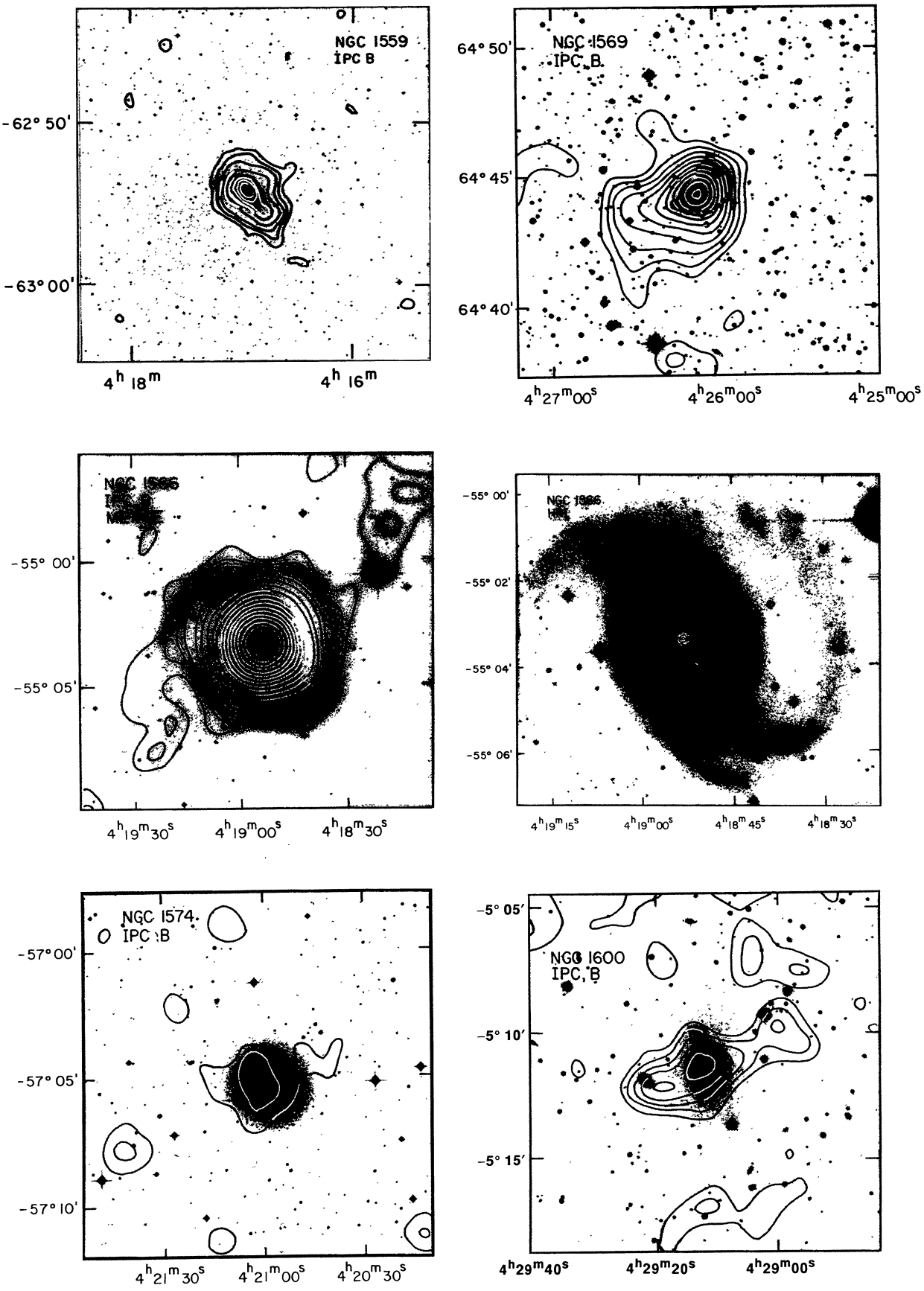

FIG. 7—*Continued*

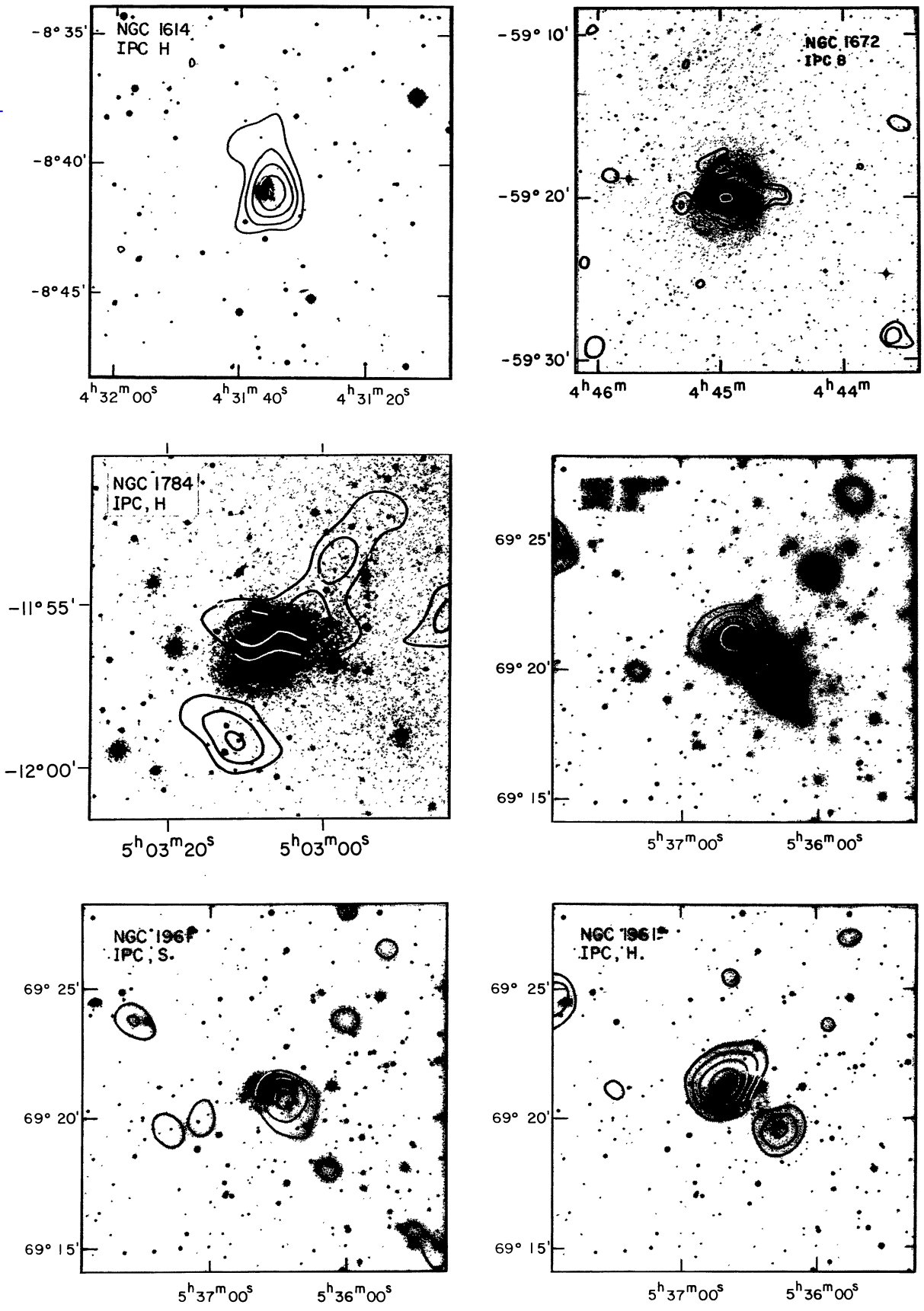

FIG. 7—*Continued*

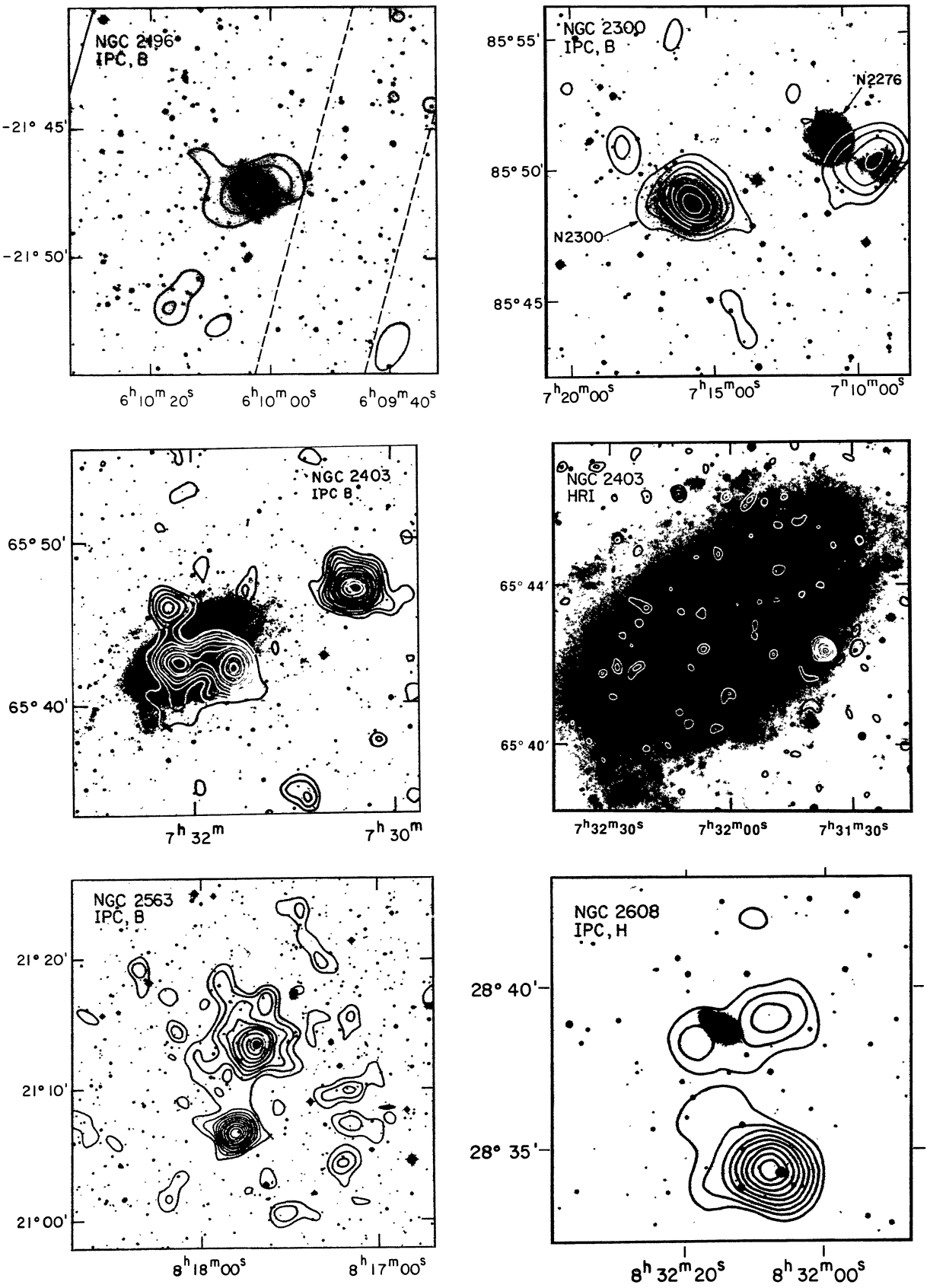

FIG. 7—*Continued*

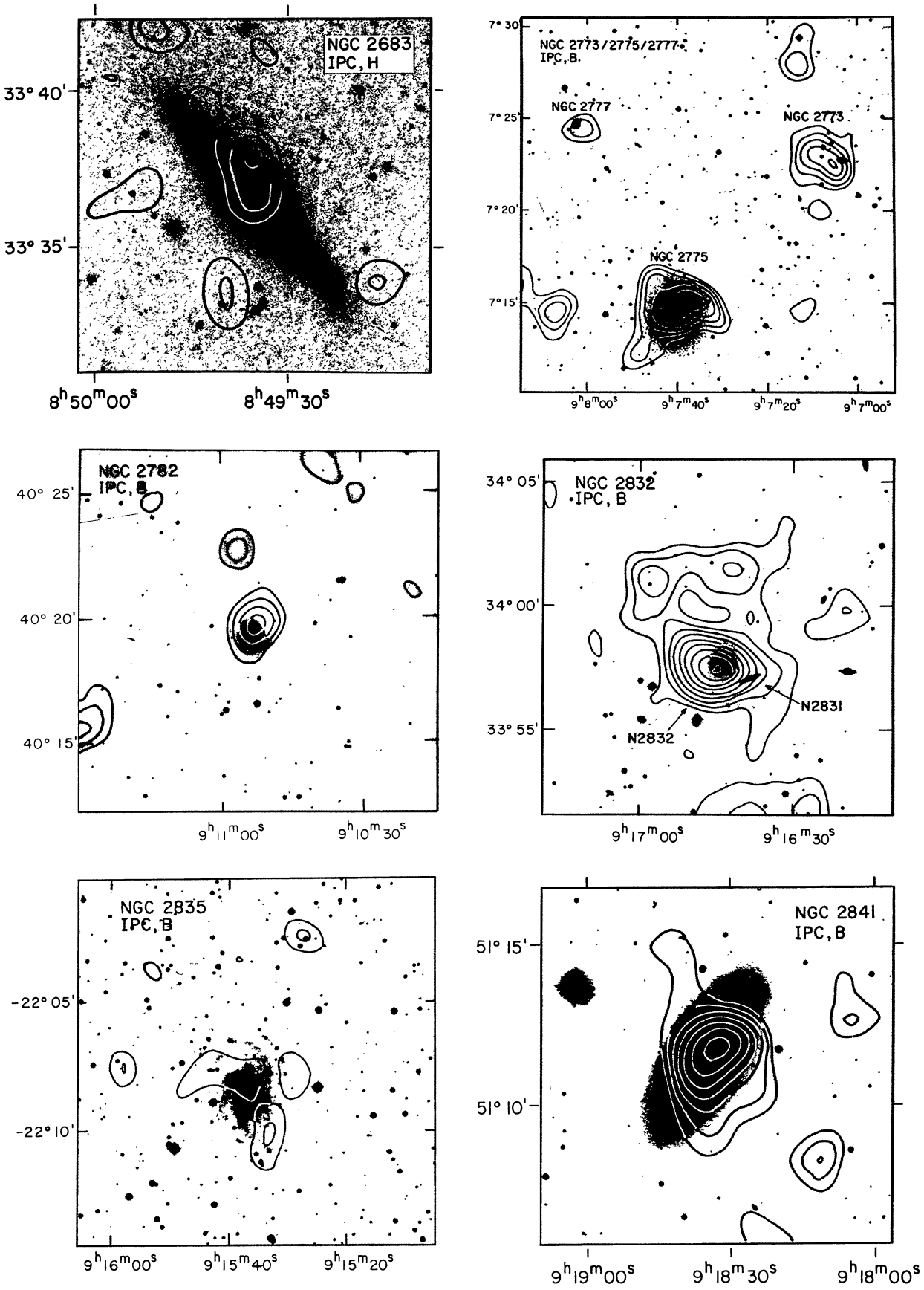

FIG. 7—*Continued*

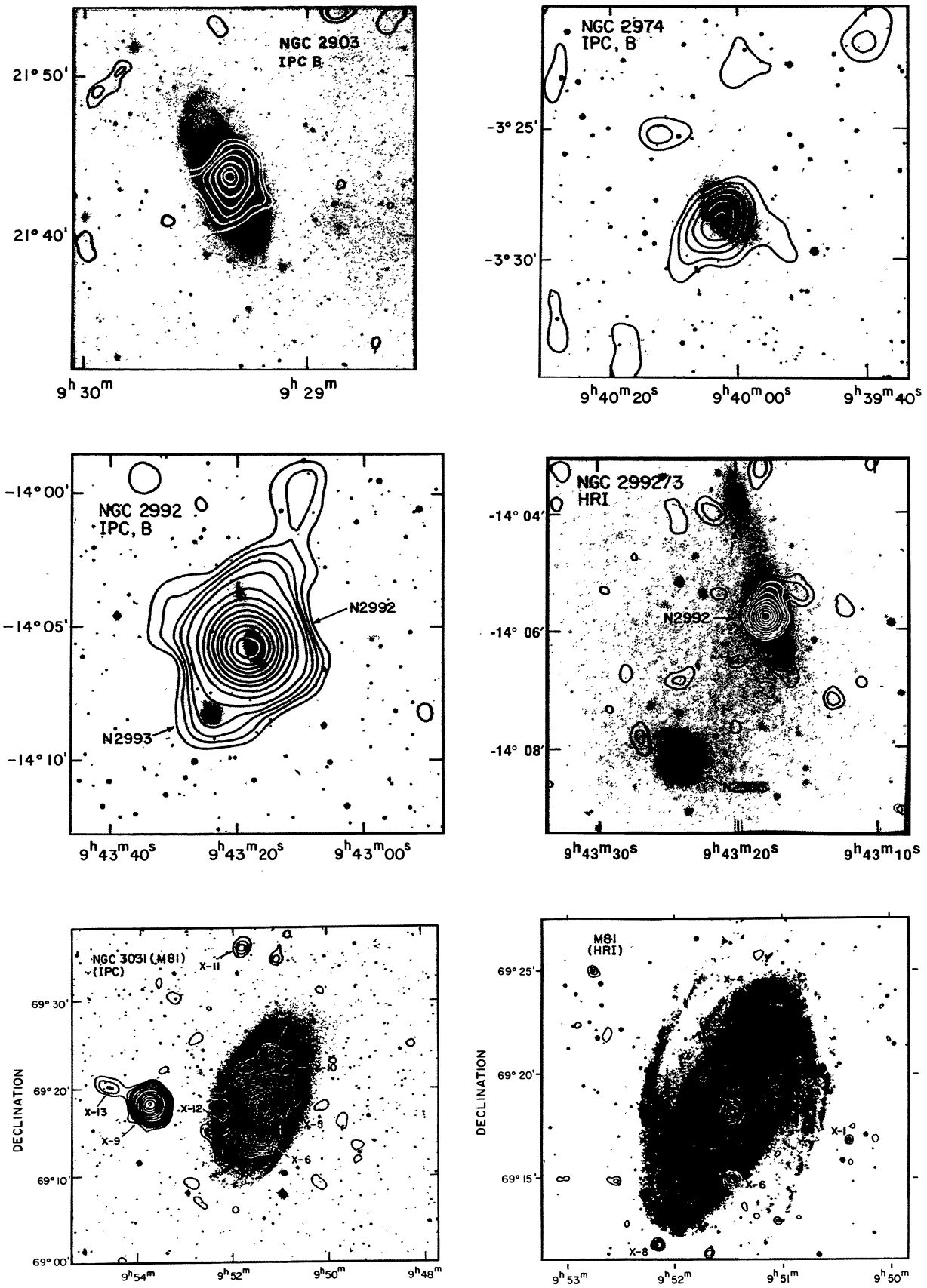

FIG. 7—*Continued*

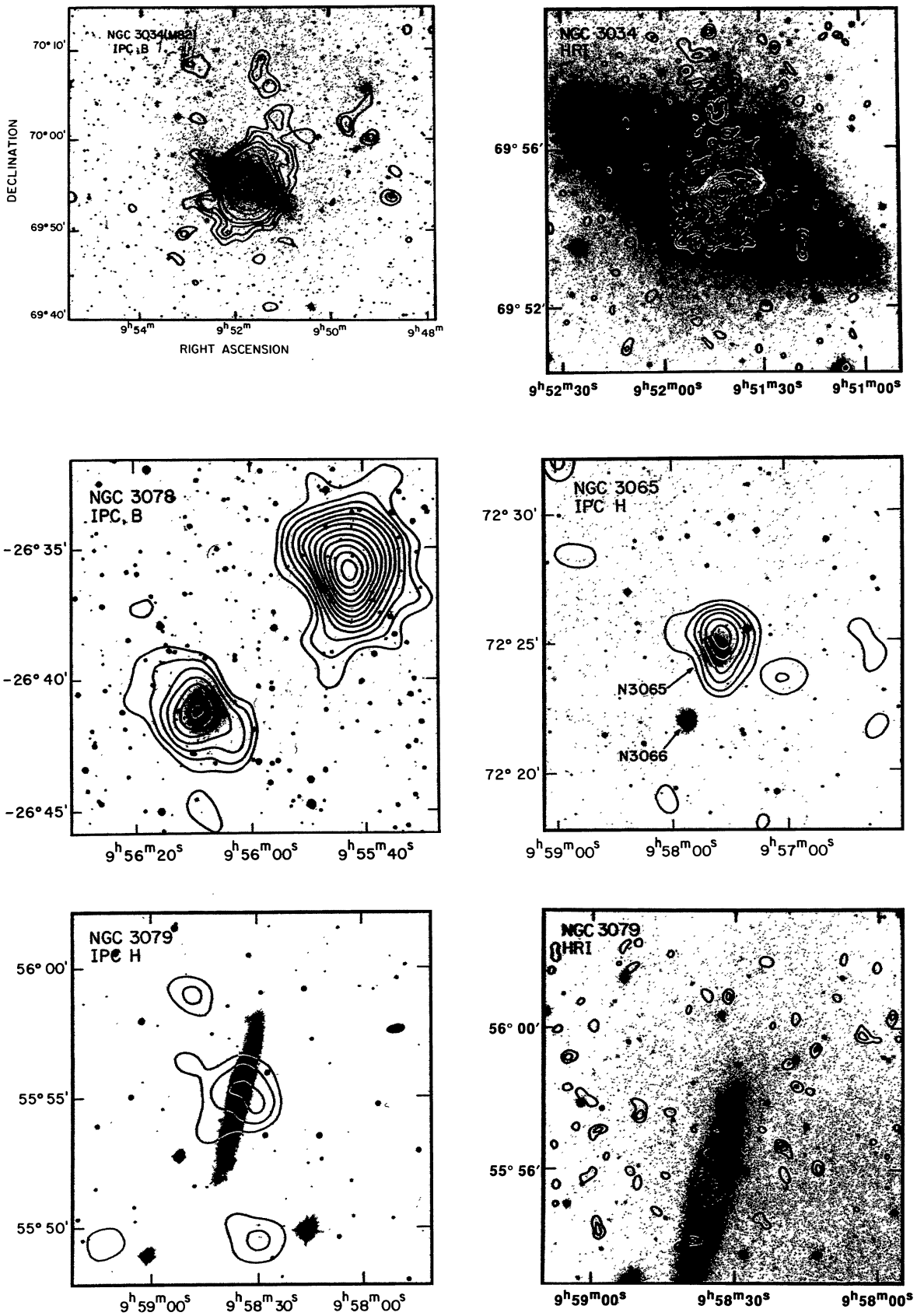

FIG. 7—*Continued*

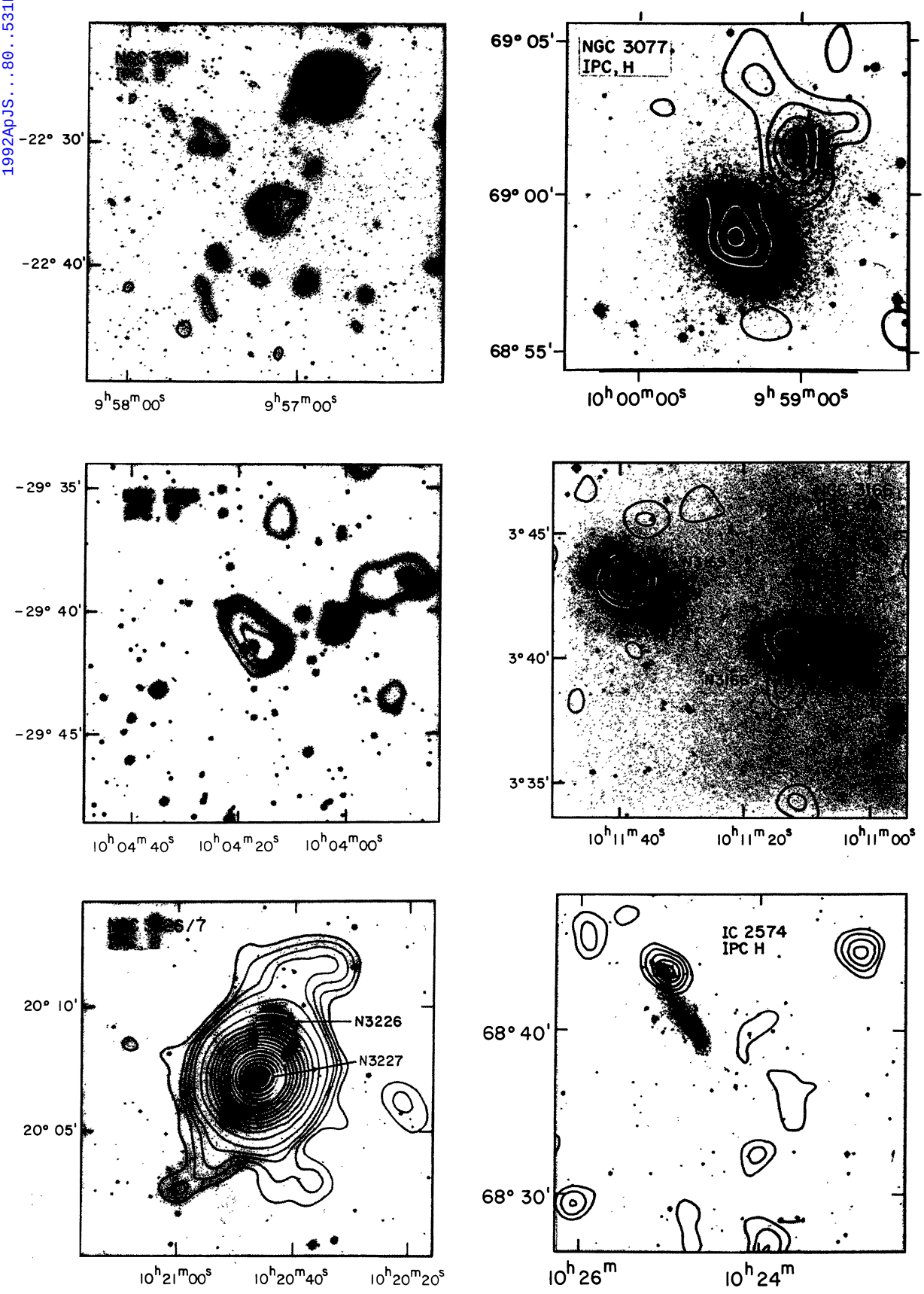

FIG. 7—*Continued*

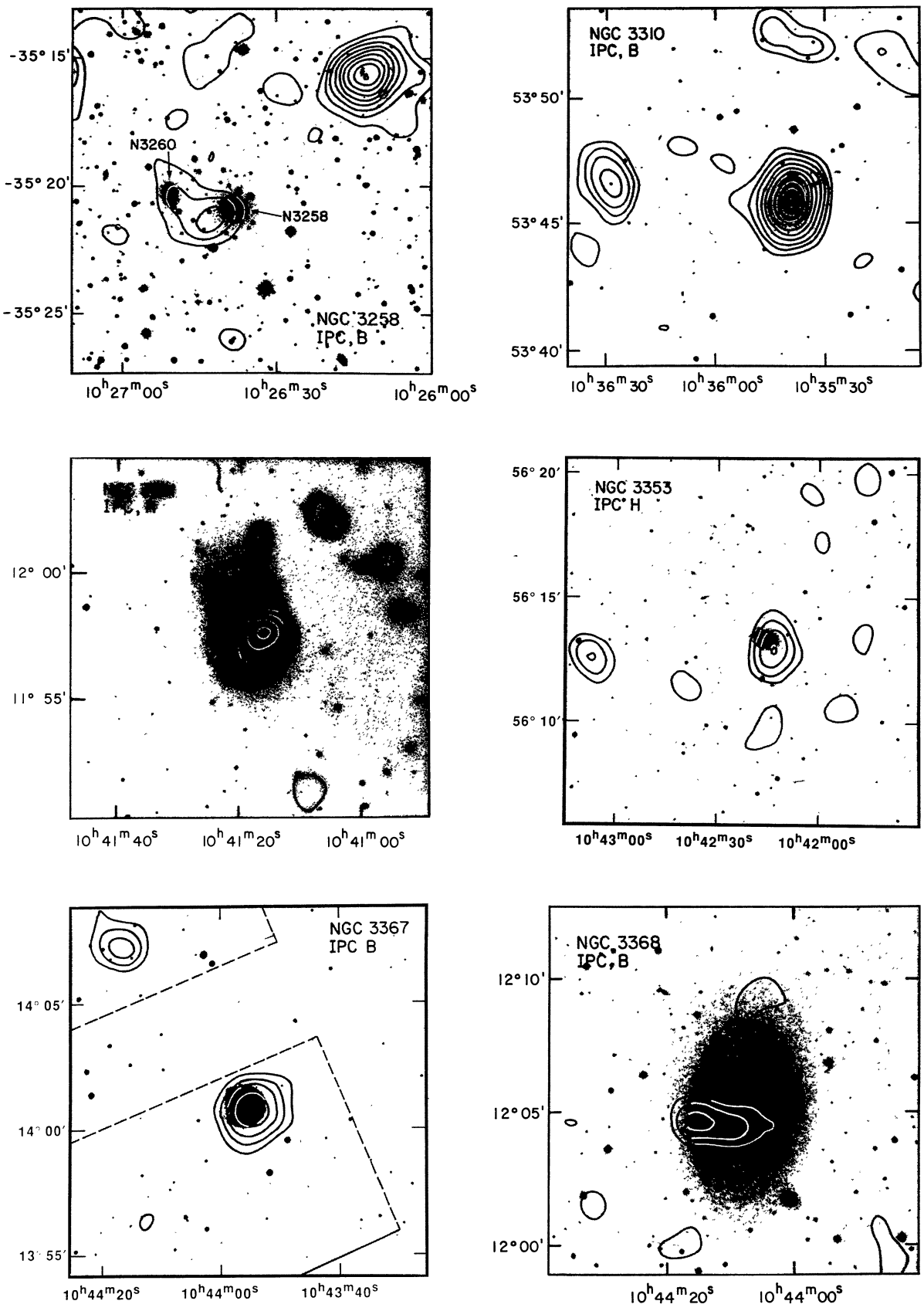

FIG. 7—*Continued*

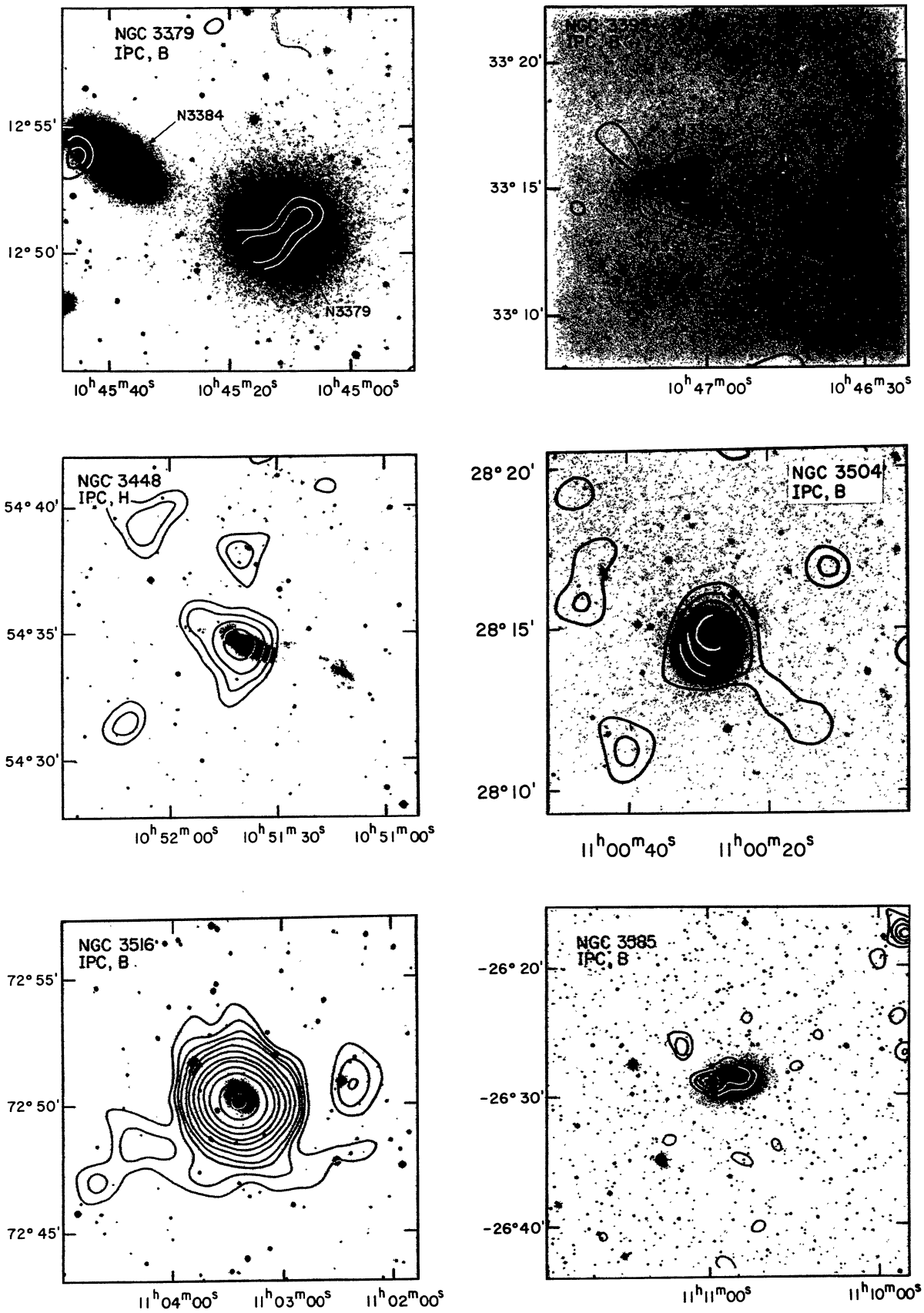

FIG. 7—*Continued*

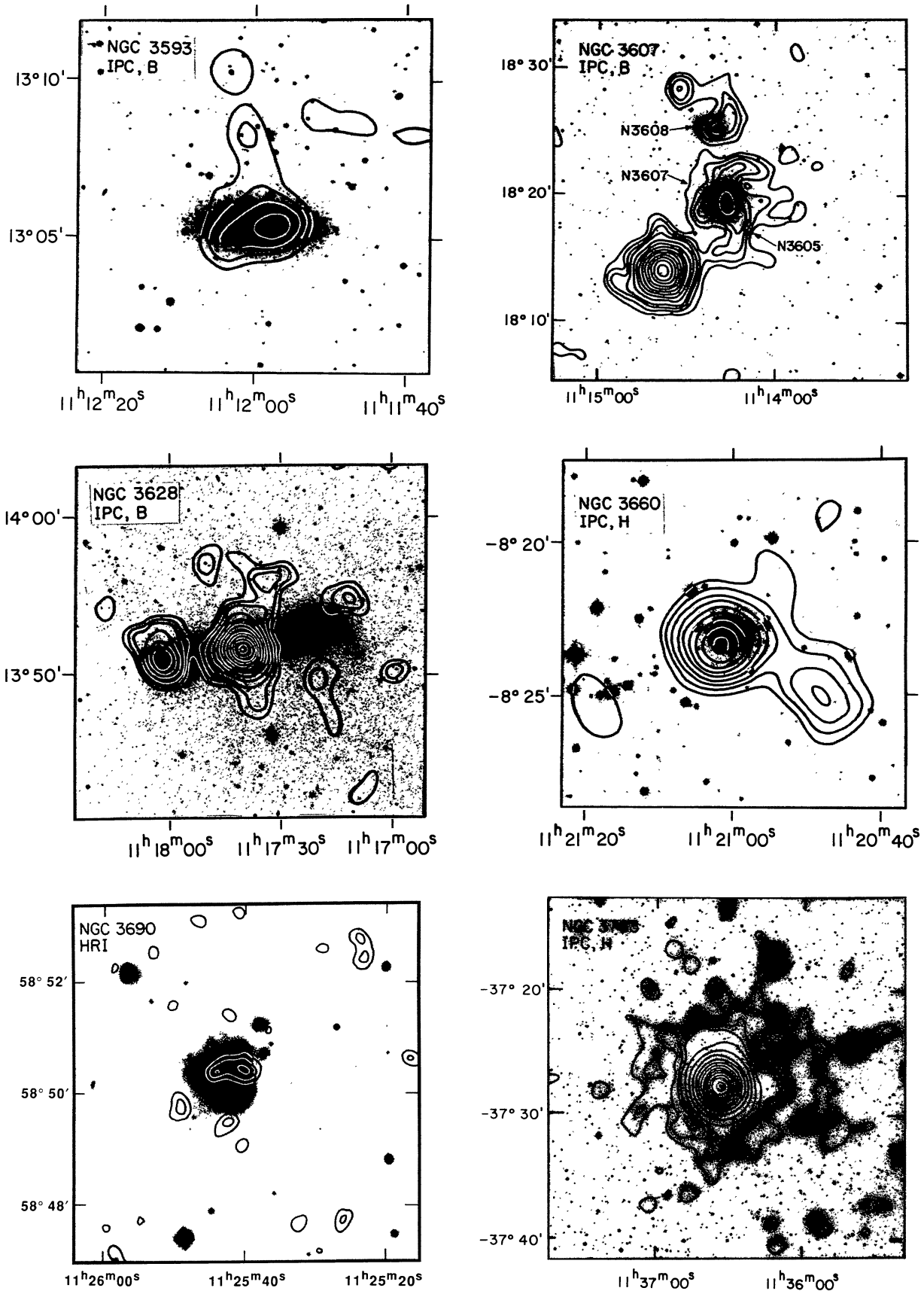

FIG. 7—*Continued*

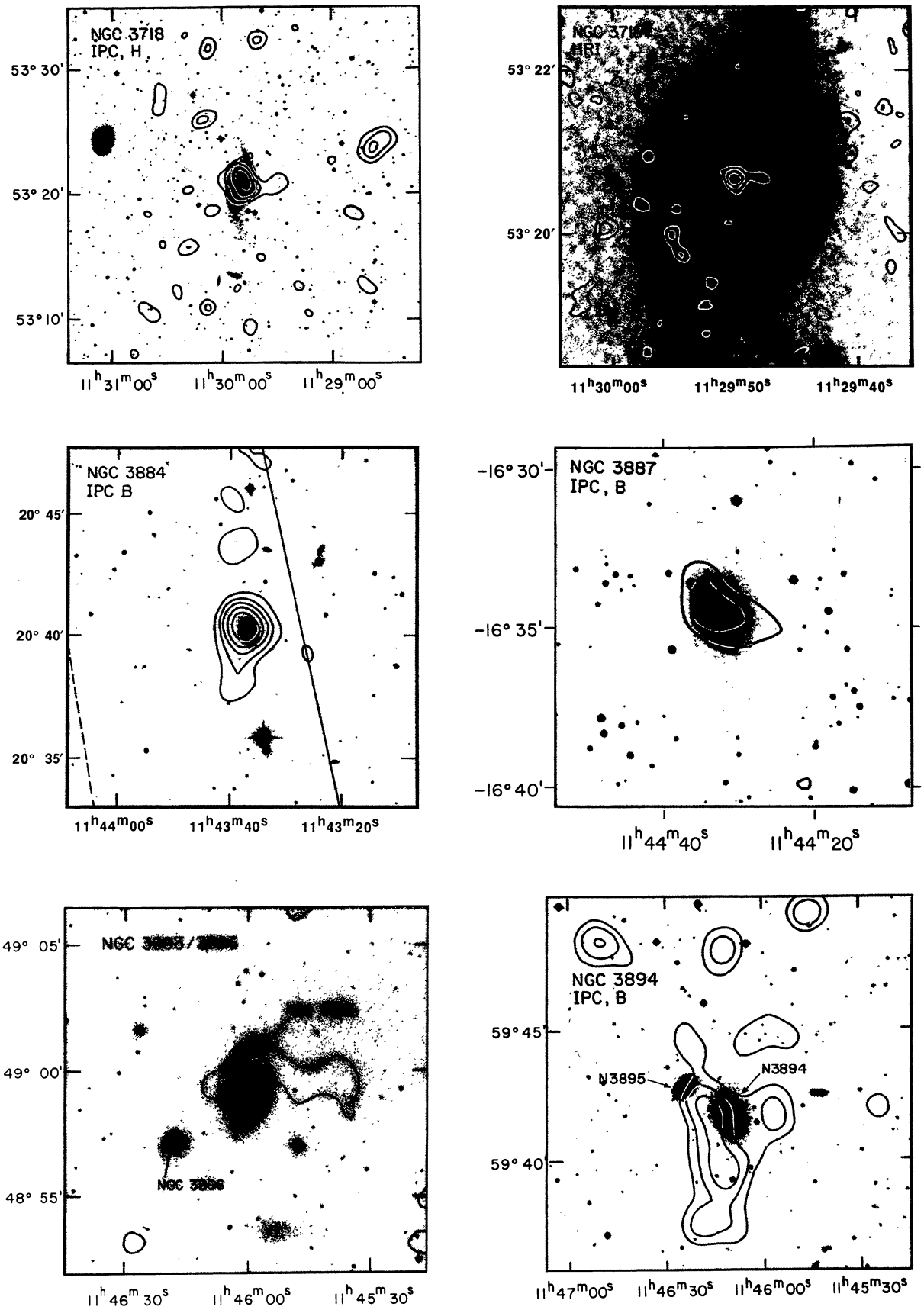

FIG. 7—*Continued*

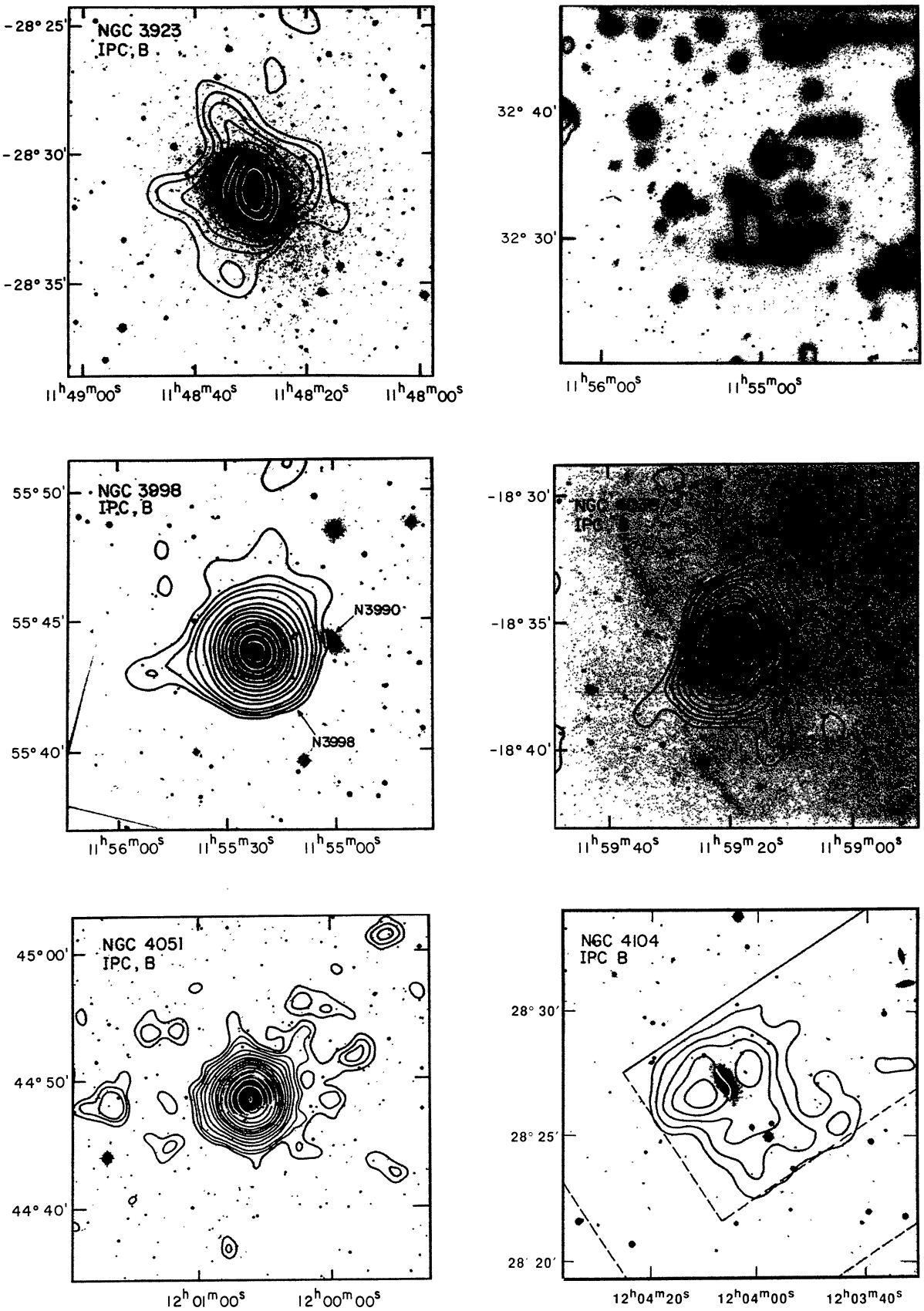

FIG. 7—*Continued*

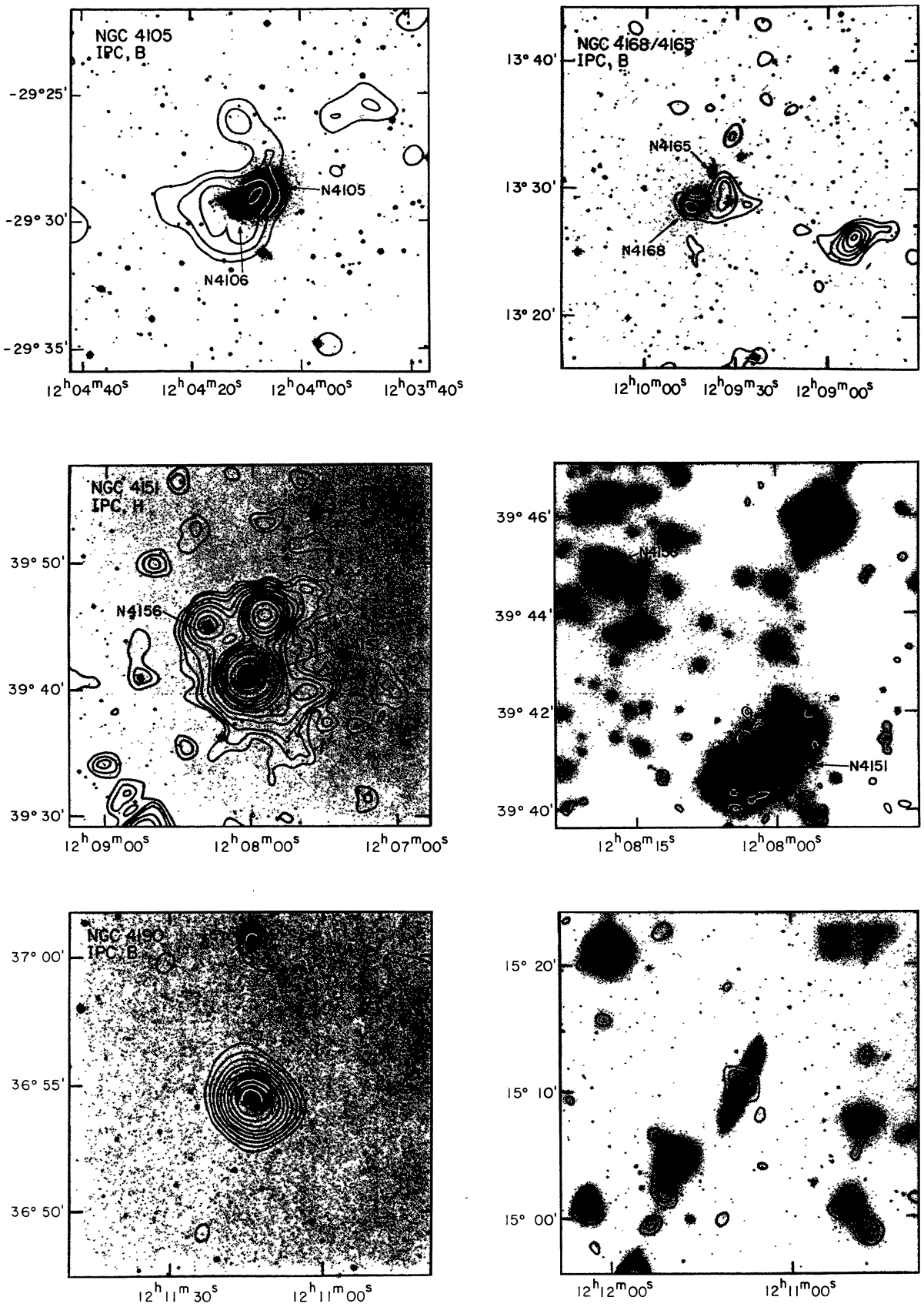

FIG. 7—*Continued*

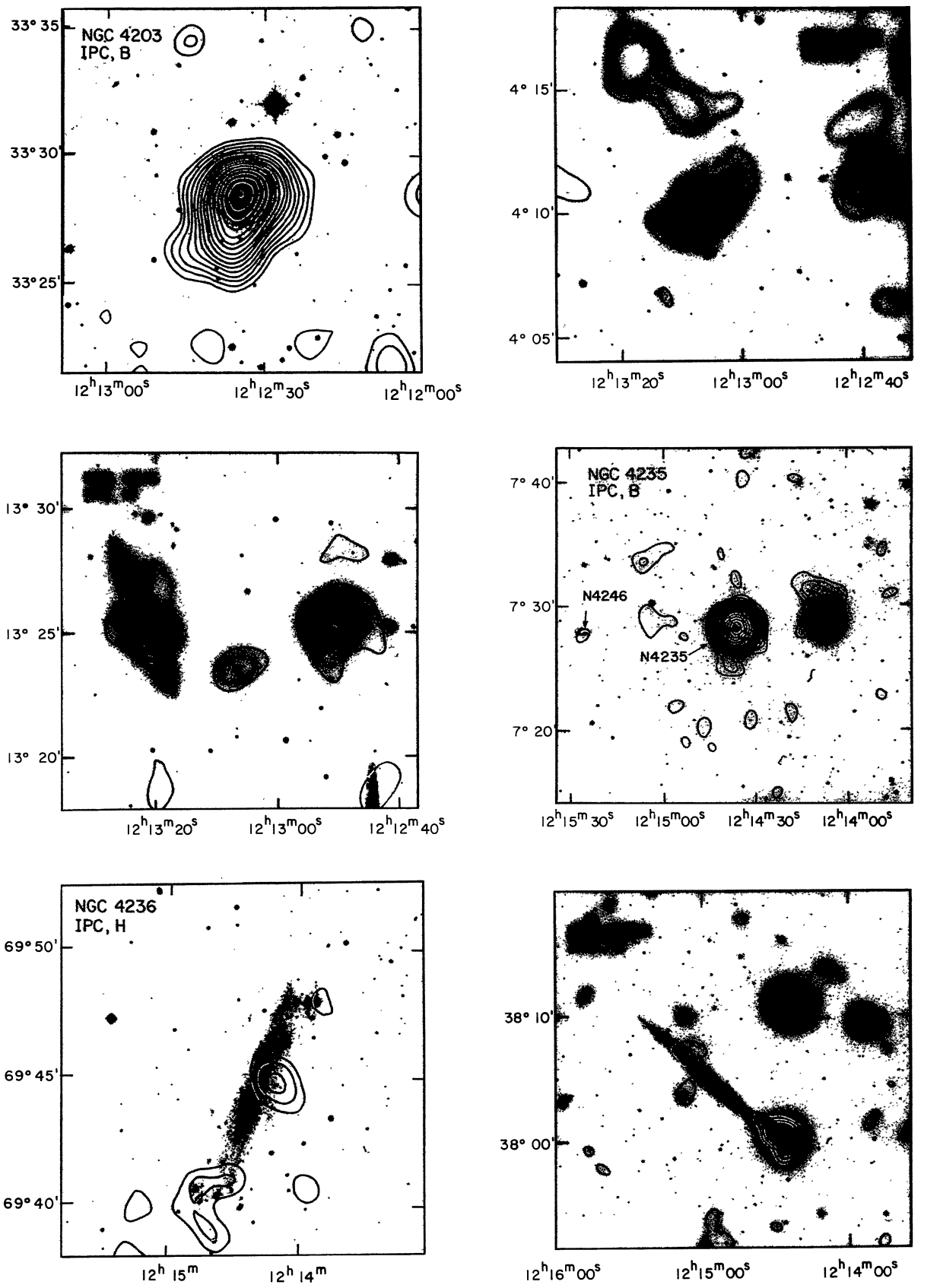

FIG. 7—*Continued*

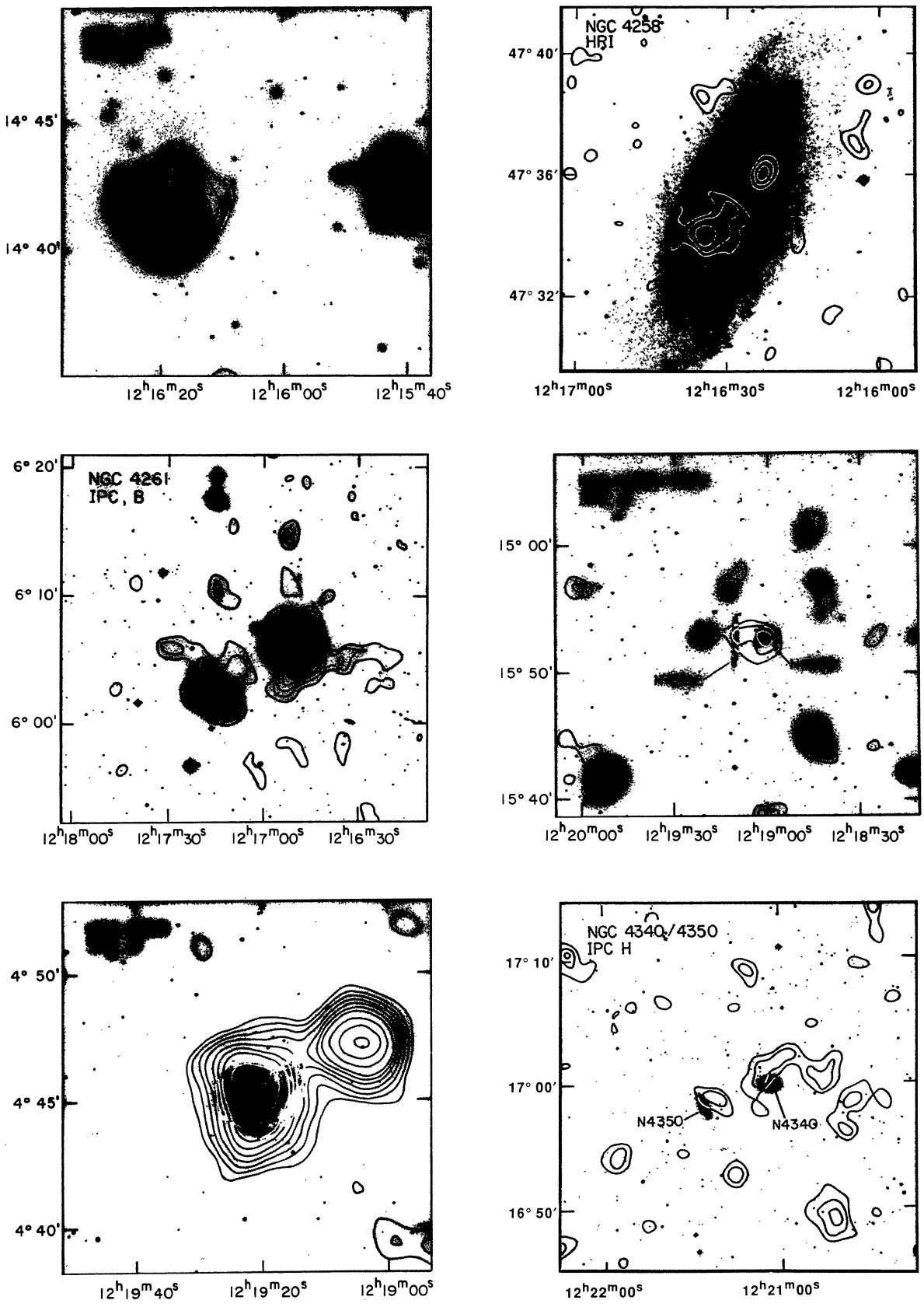

FIG. 7—*Continued*

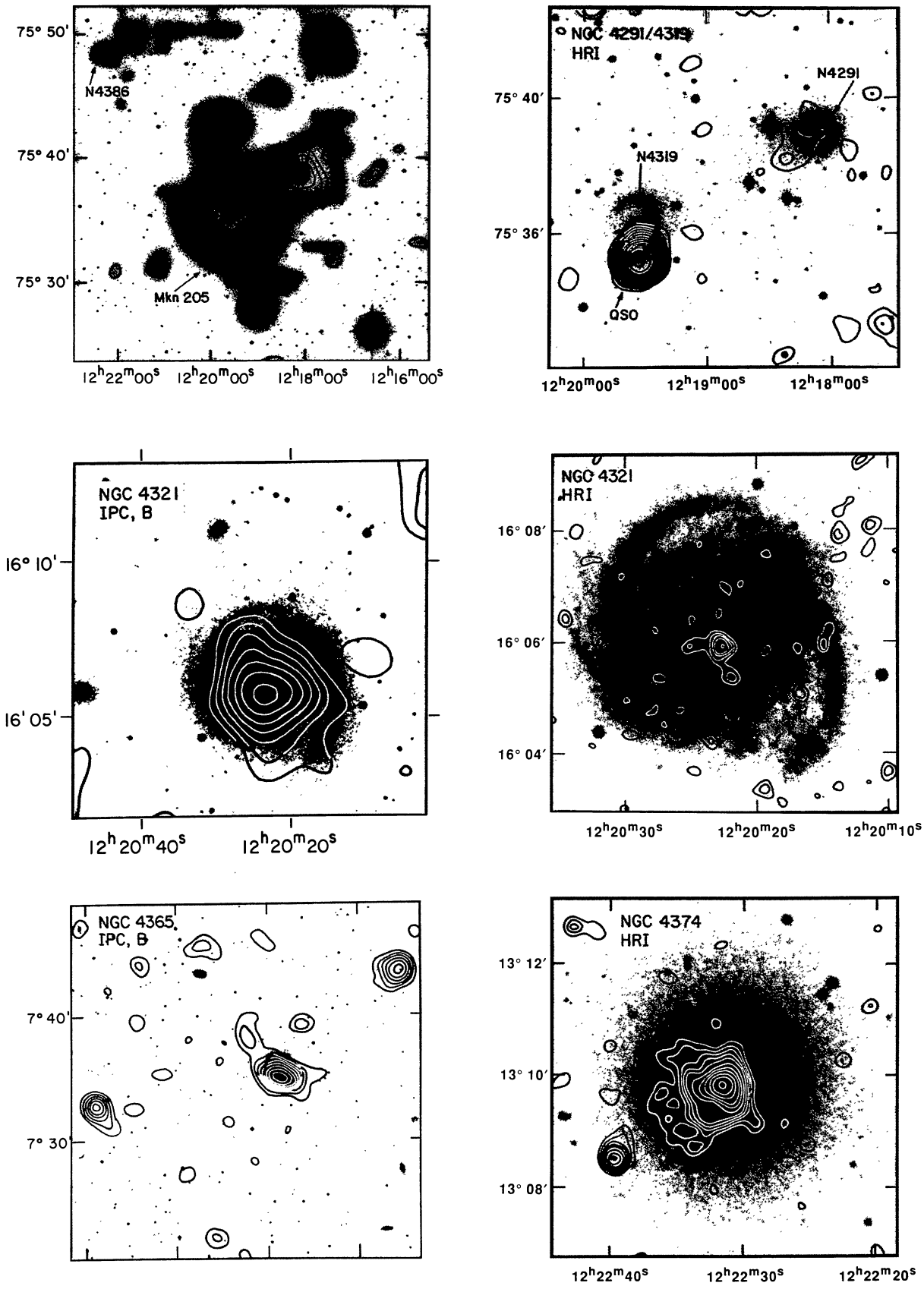

FIG. 7—*Continued*

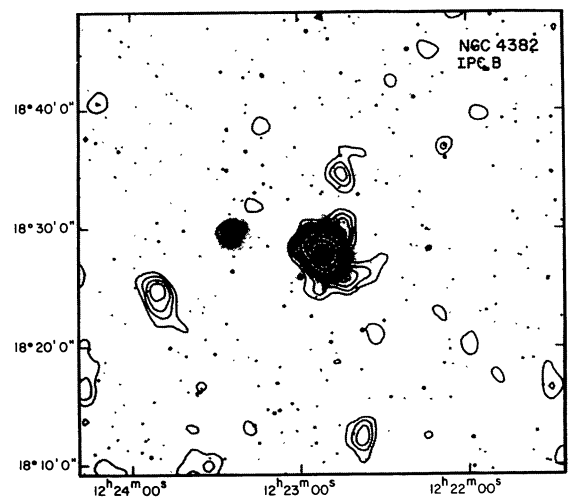

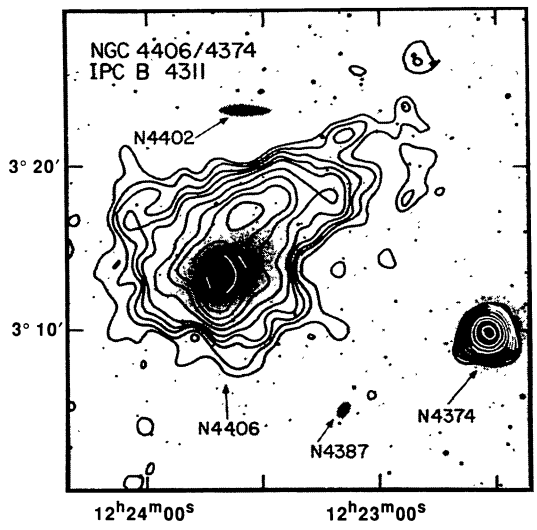

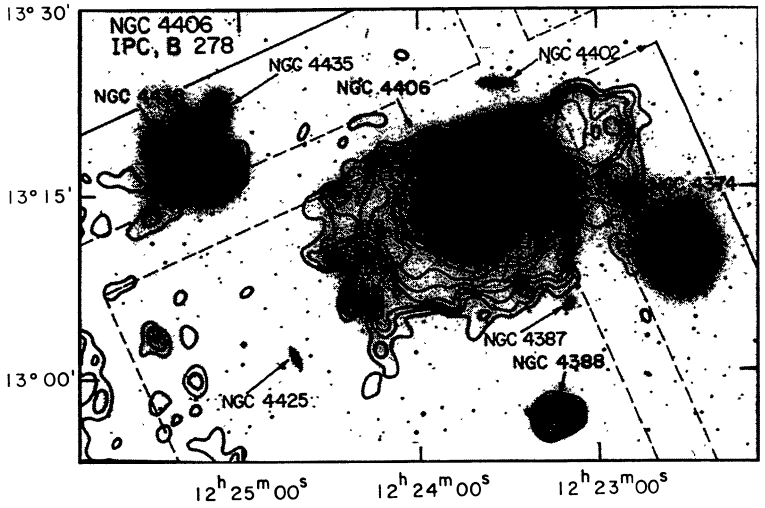

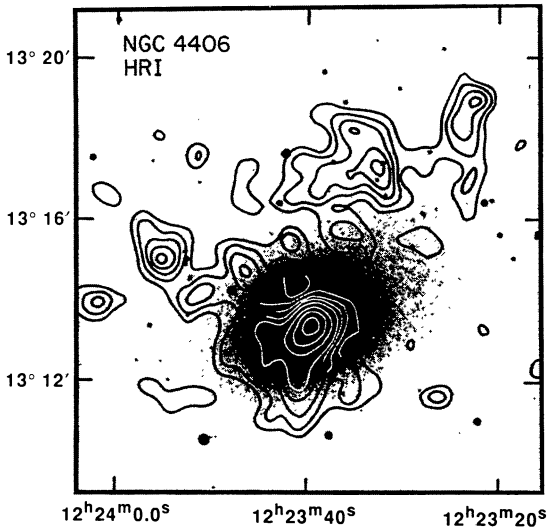

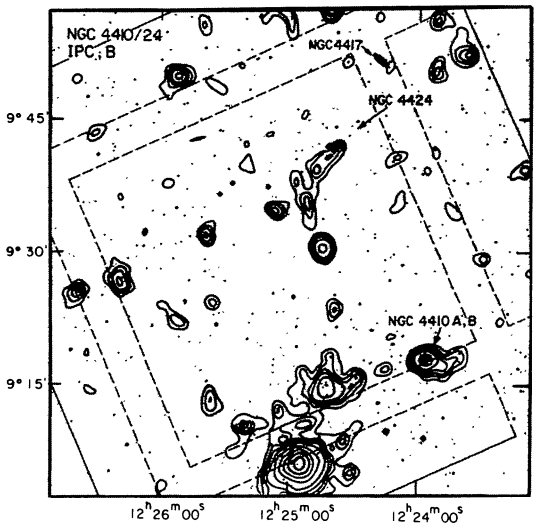

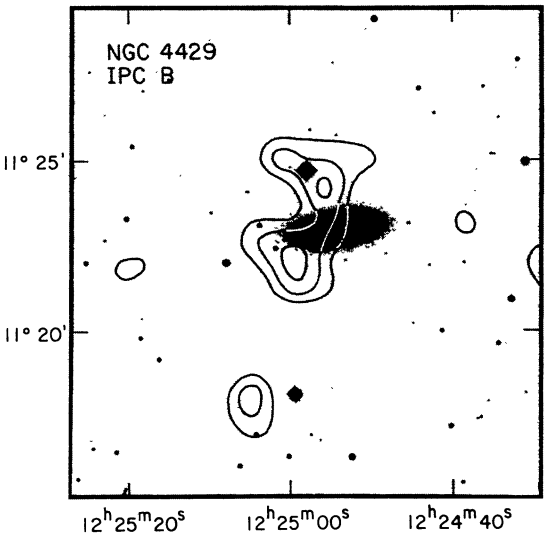

FIG. 7—*Continued*

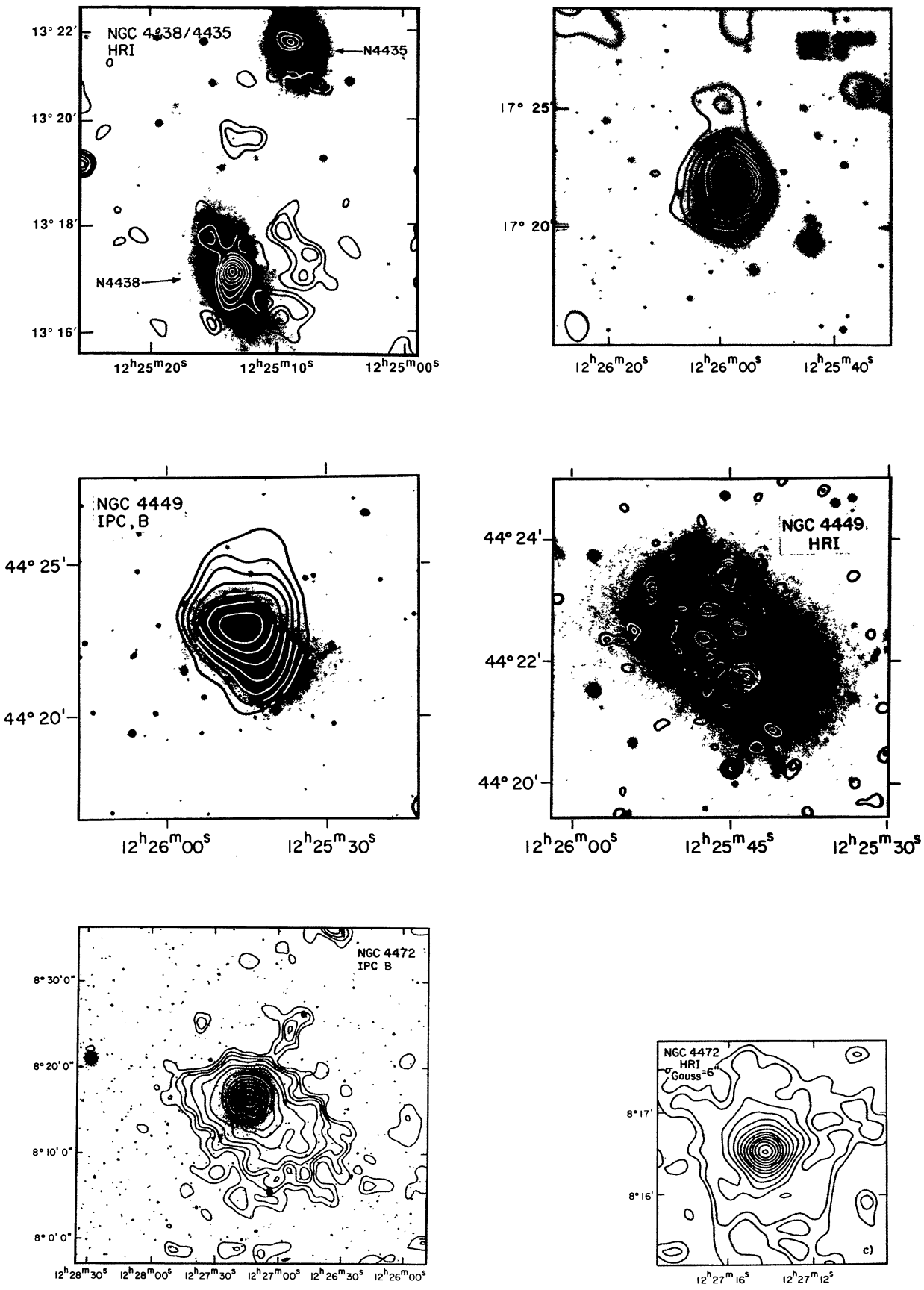

FIG. 7—*Continued*

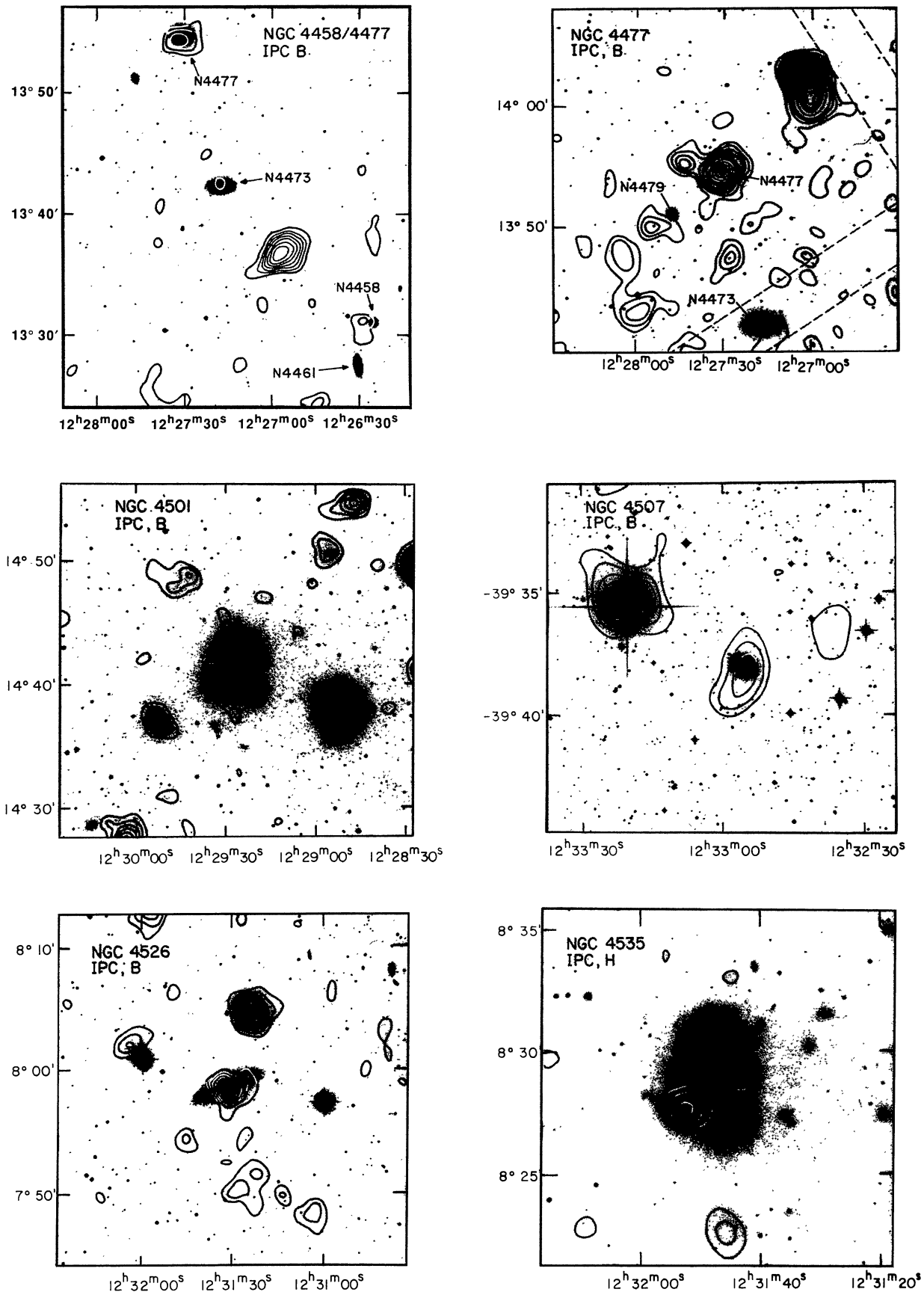

FIG. 7—*Continued*

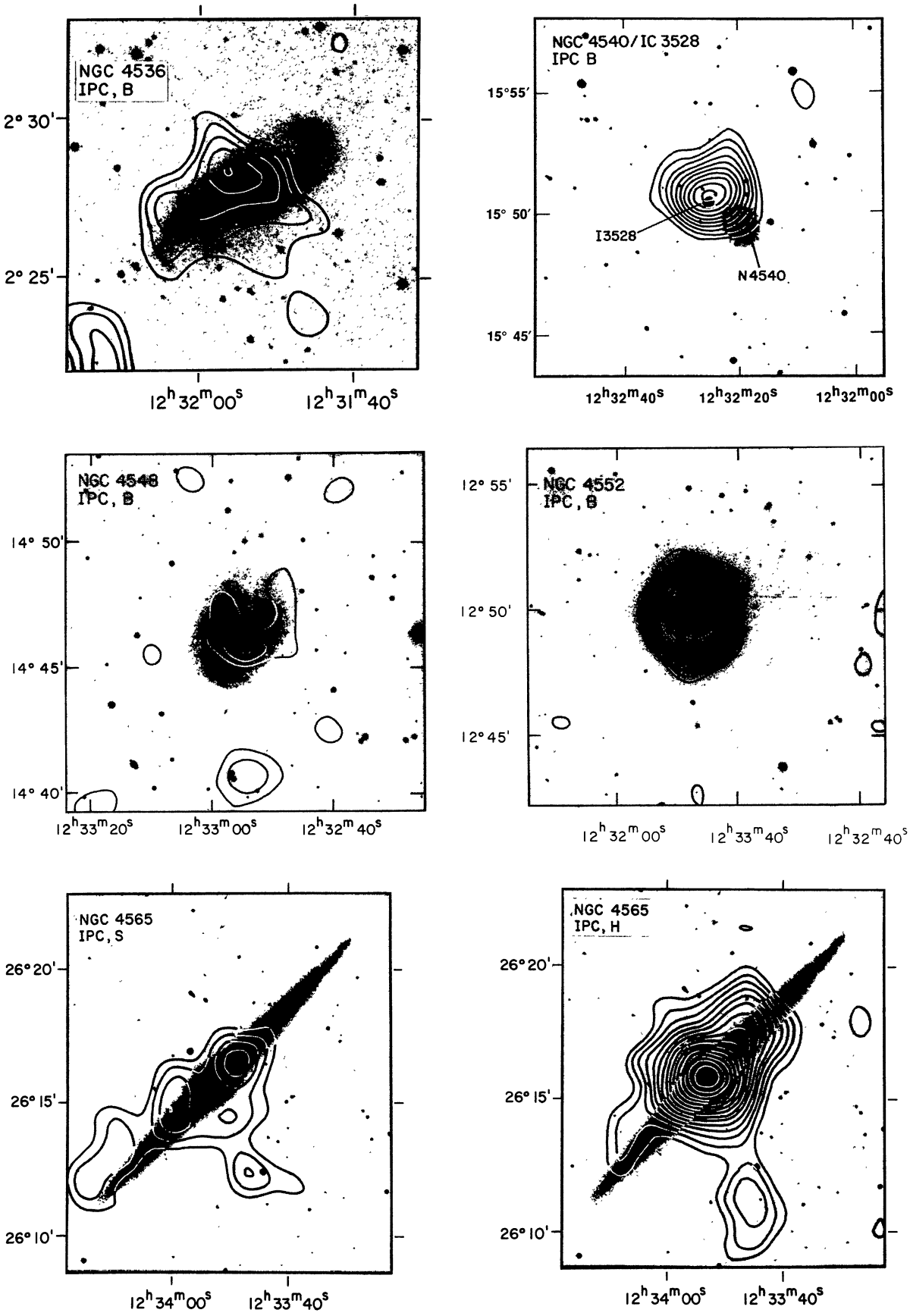

FIG. 7—*Continued*

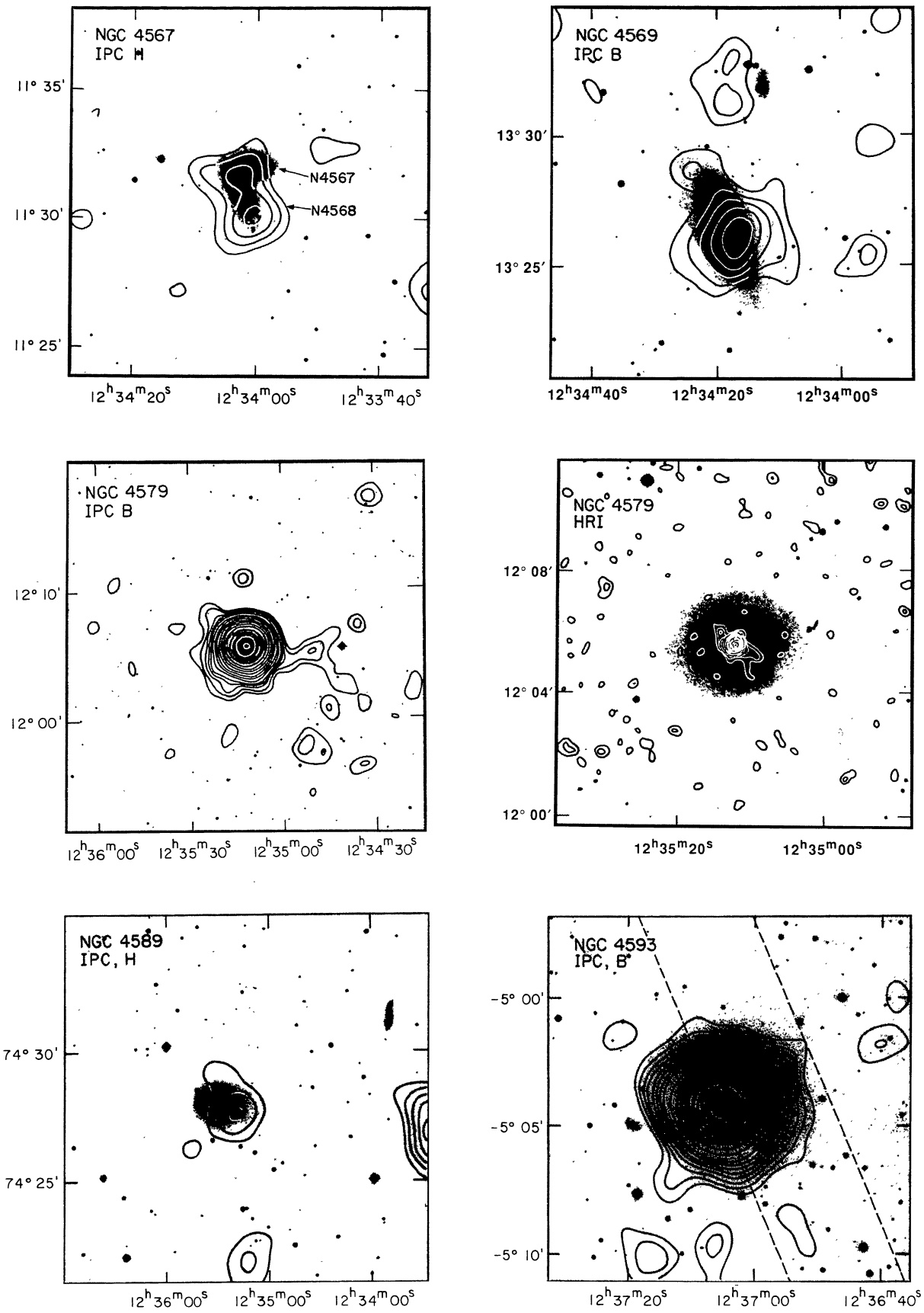

FIG. 7—*Continued*

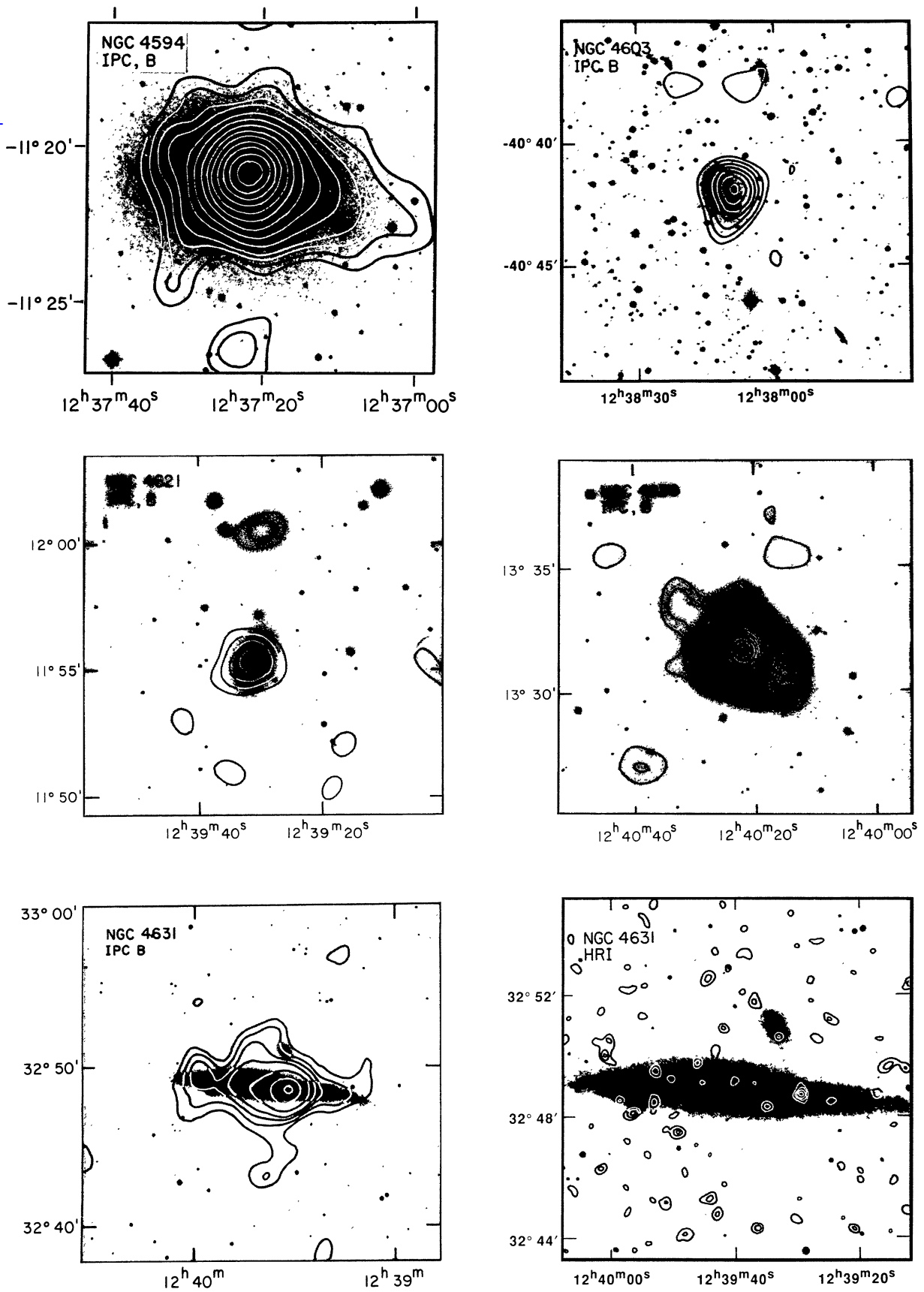

FIG. 7—*Continued*

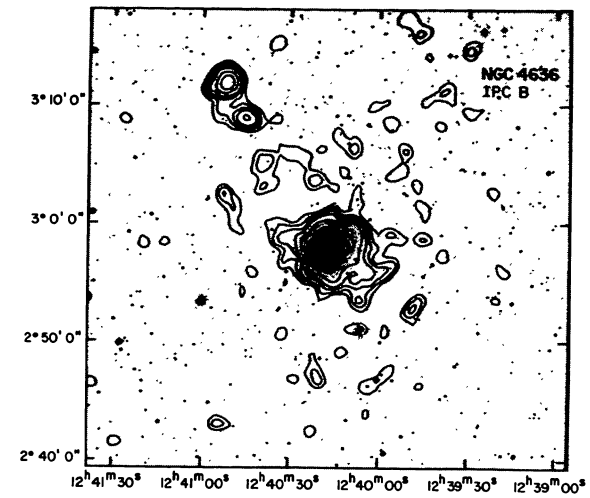

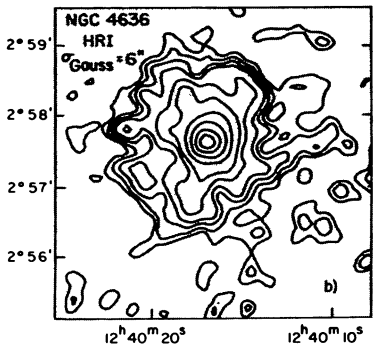

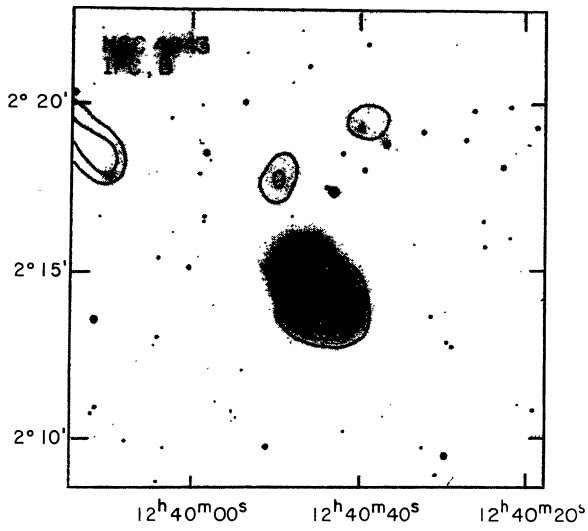

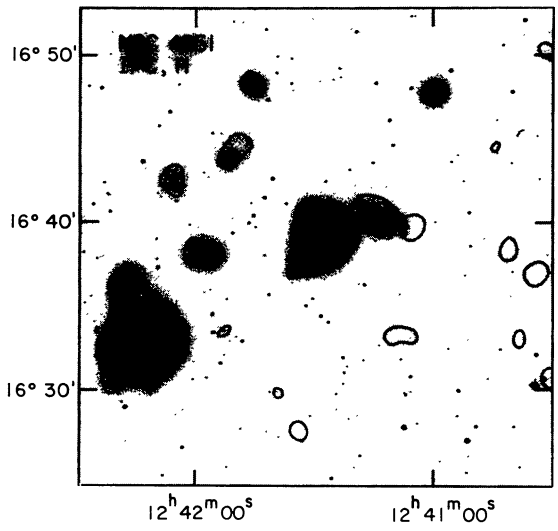

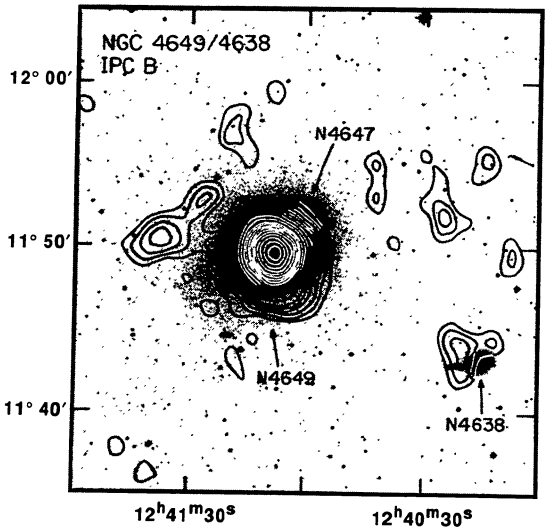

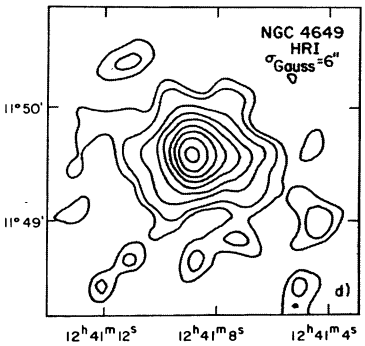

FIG. 7—*Continued*

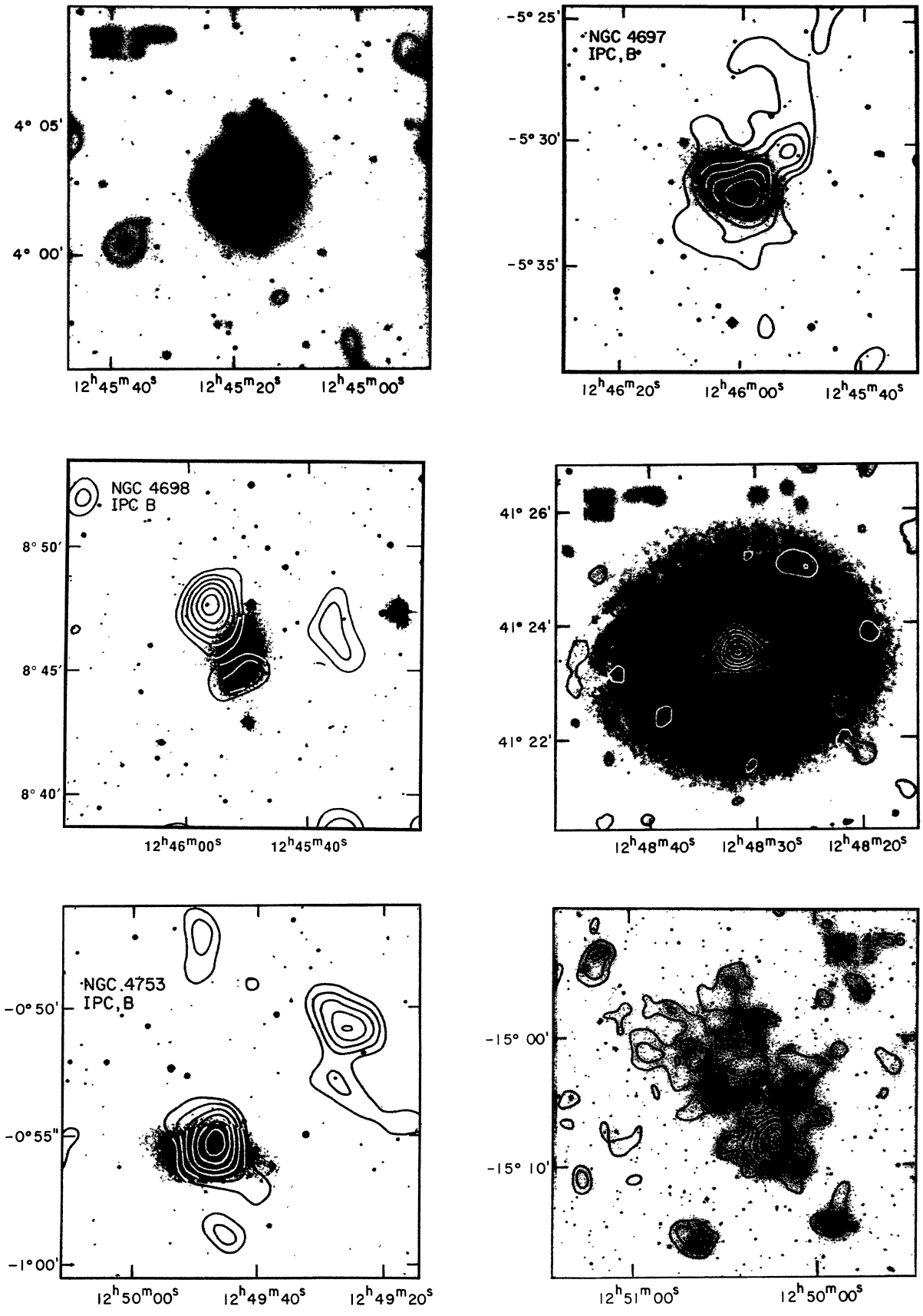

FIG. 7—*Continued*

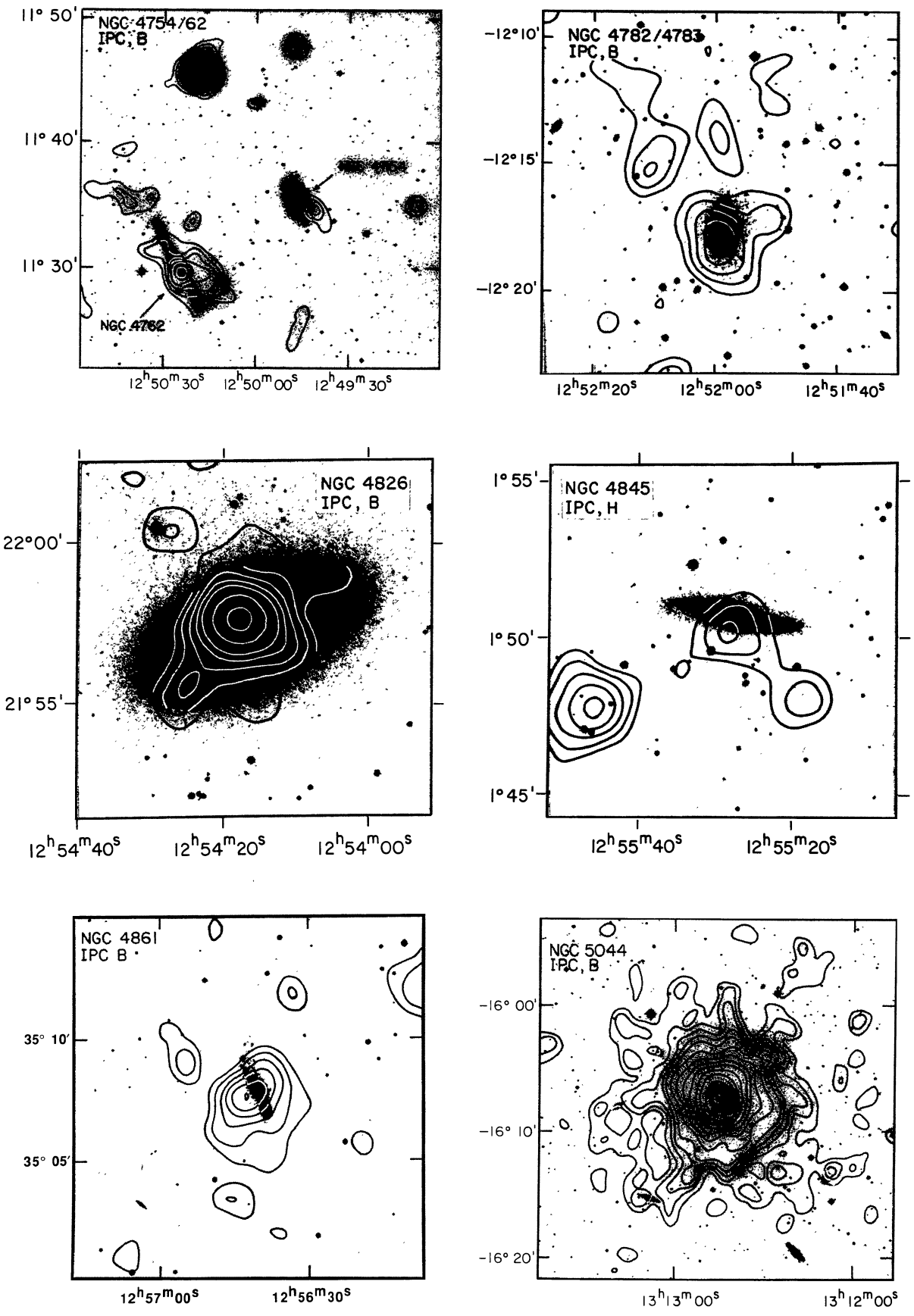

FIG. 7—*Continued*

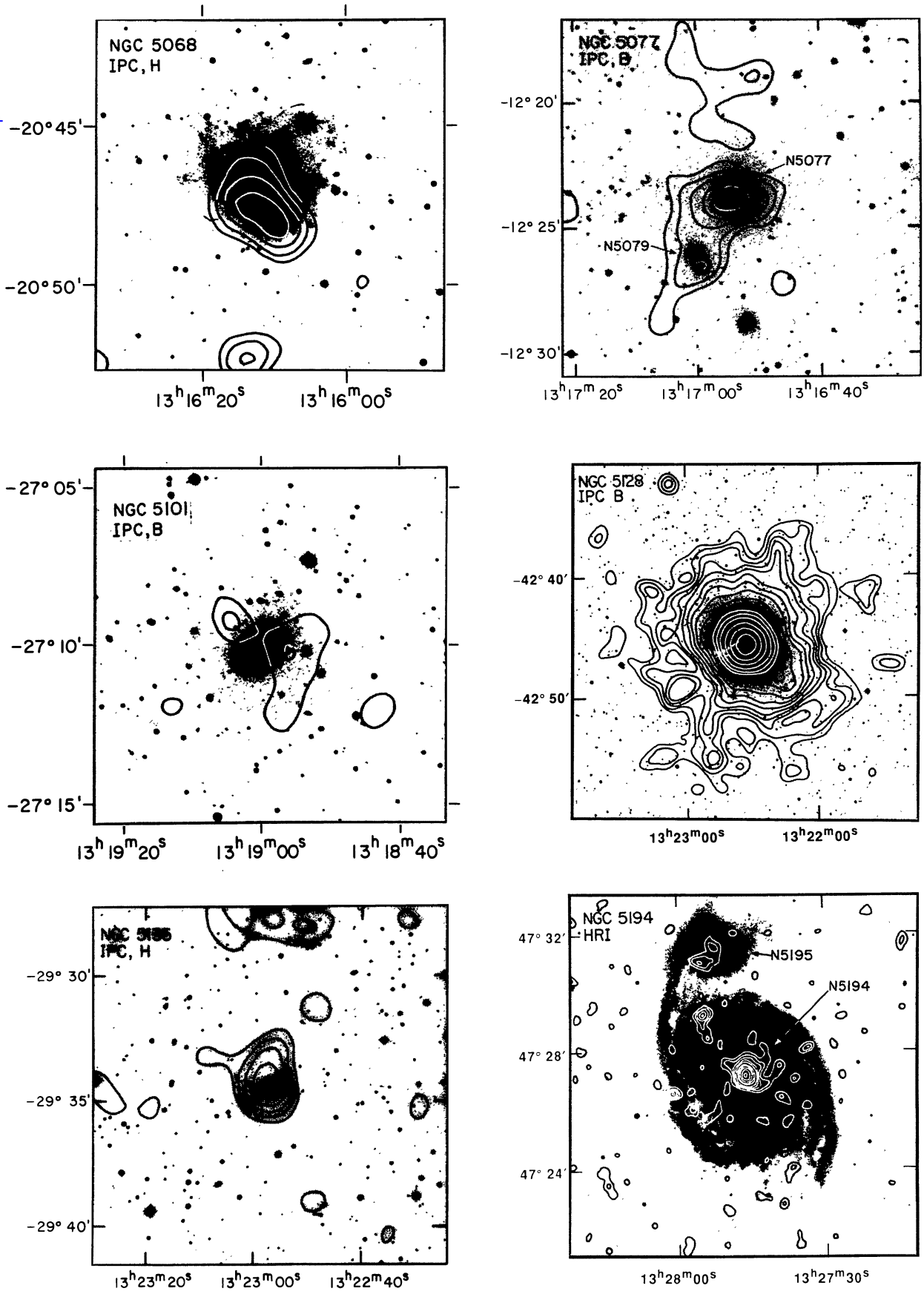

FIG. 7—*Continued*

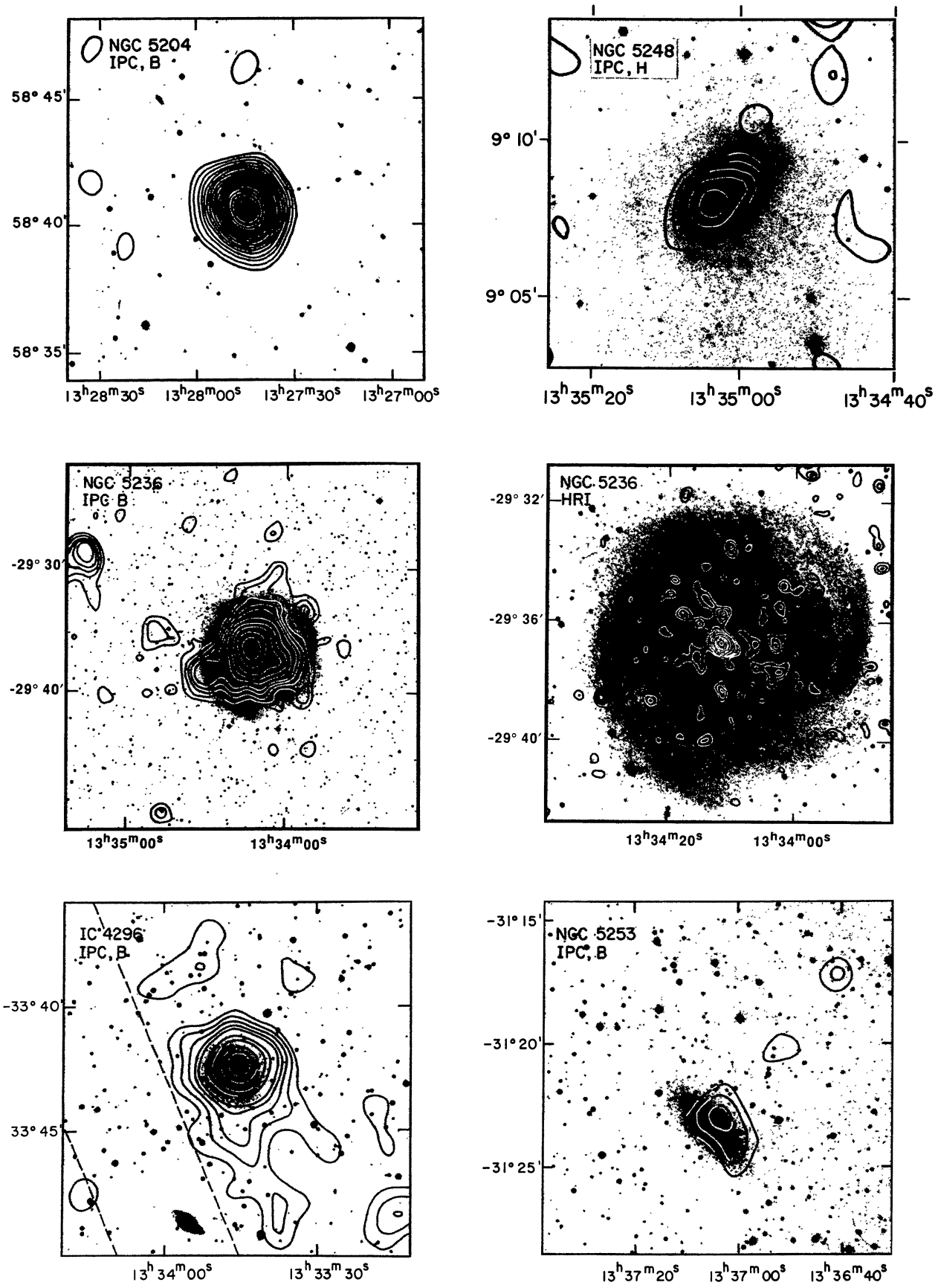

FIG. 7—*Continued*

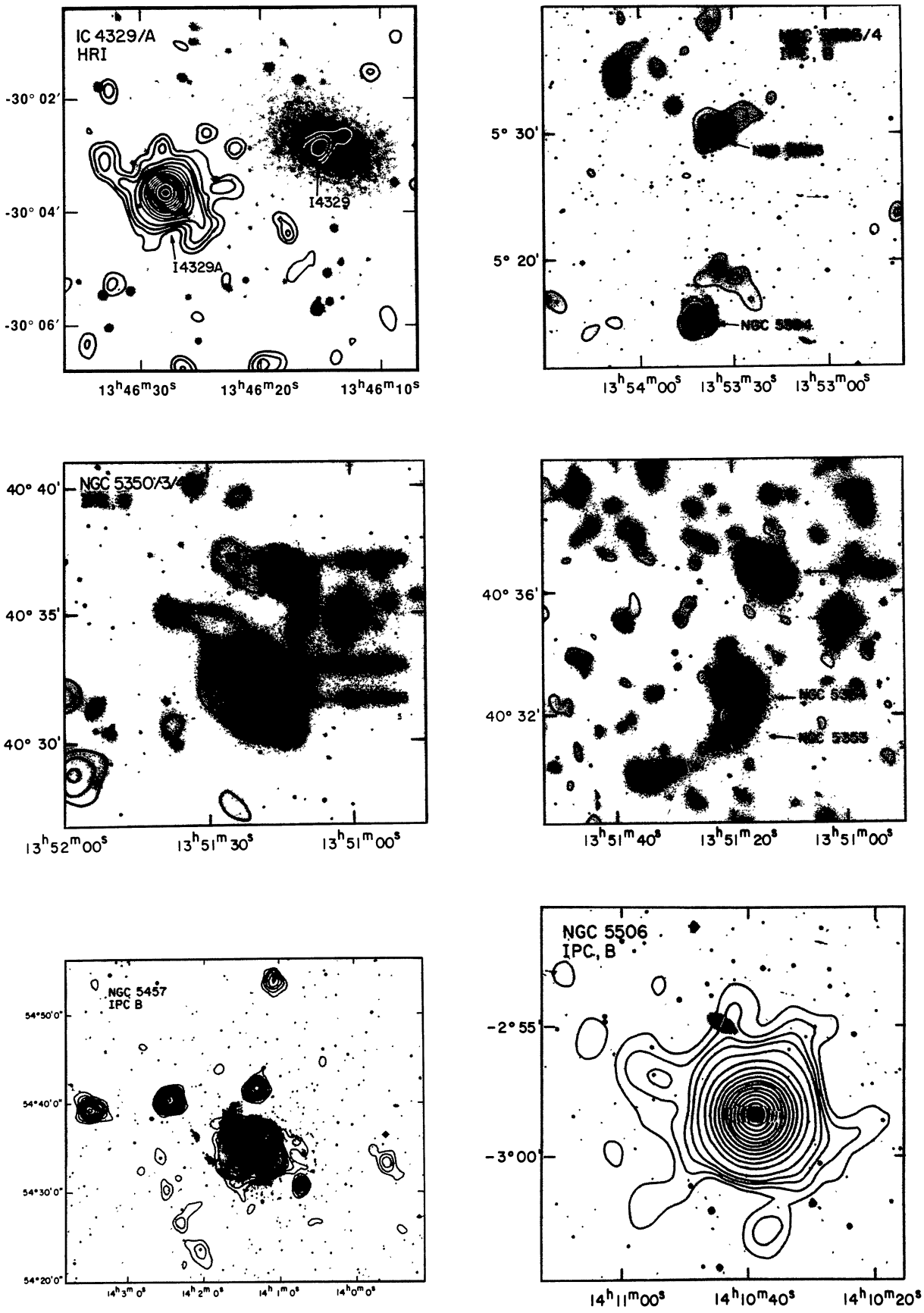

FIG. 7—*Continued*

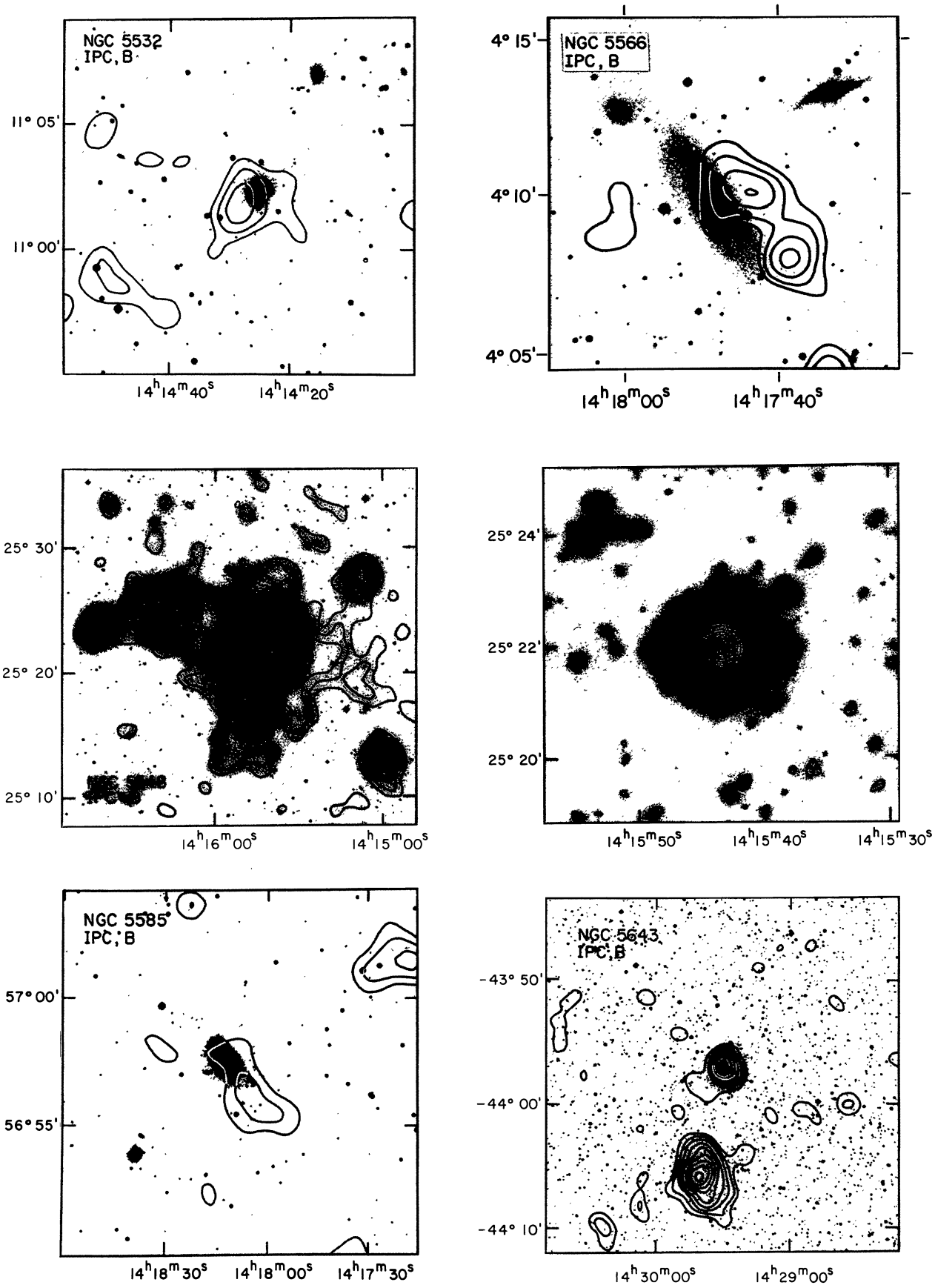

FIG. 7—*Continued*

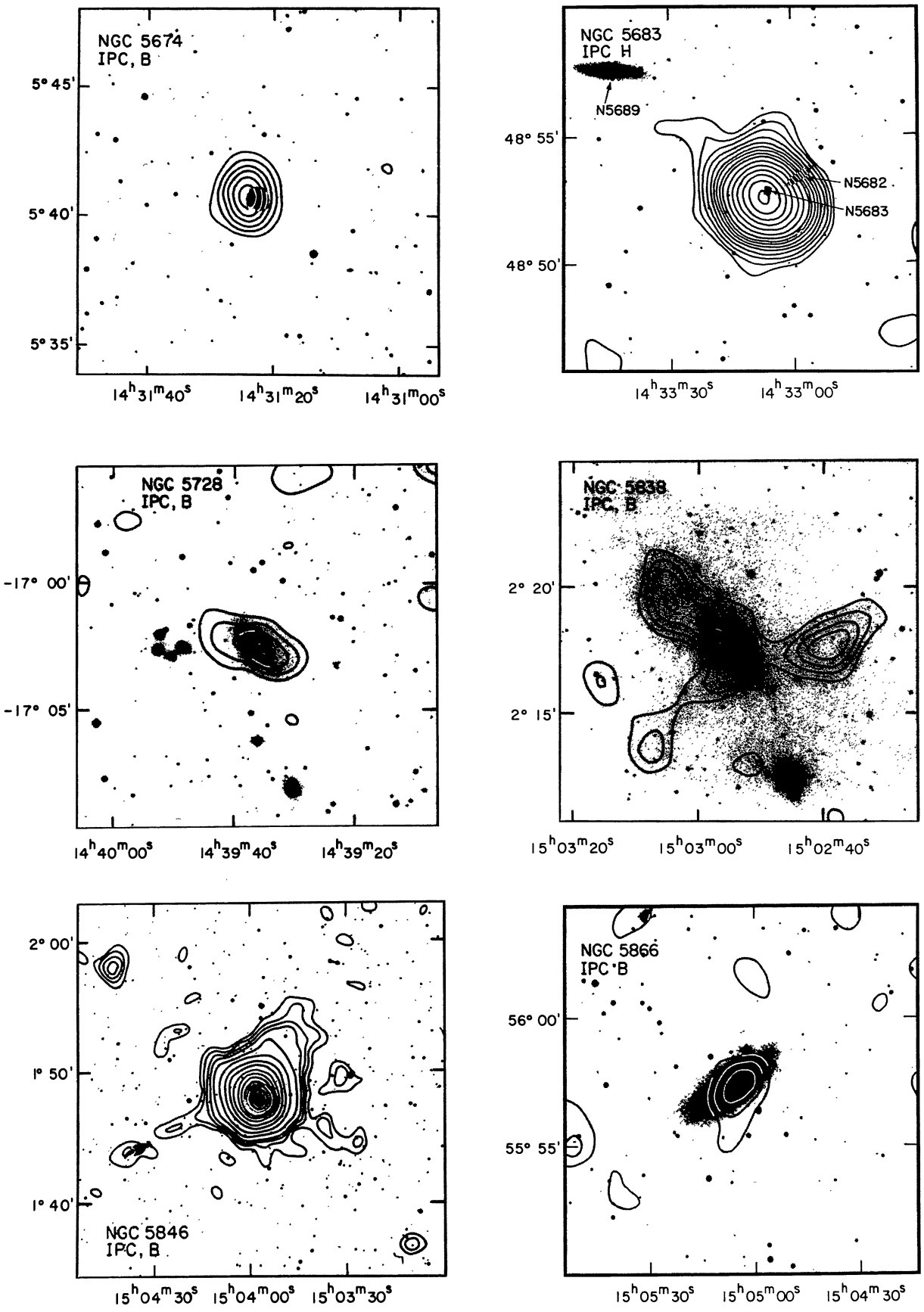

FIG. 7—*Continued*

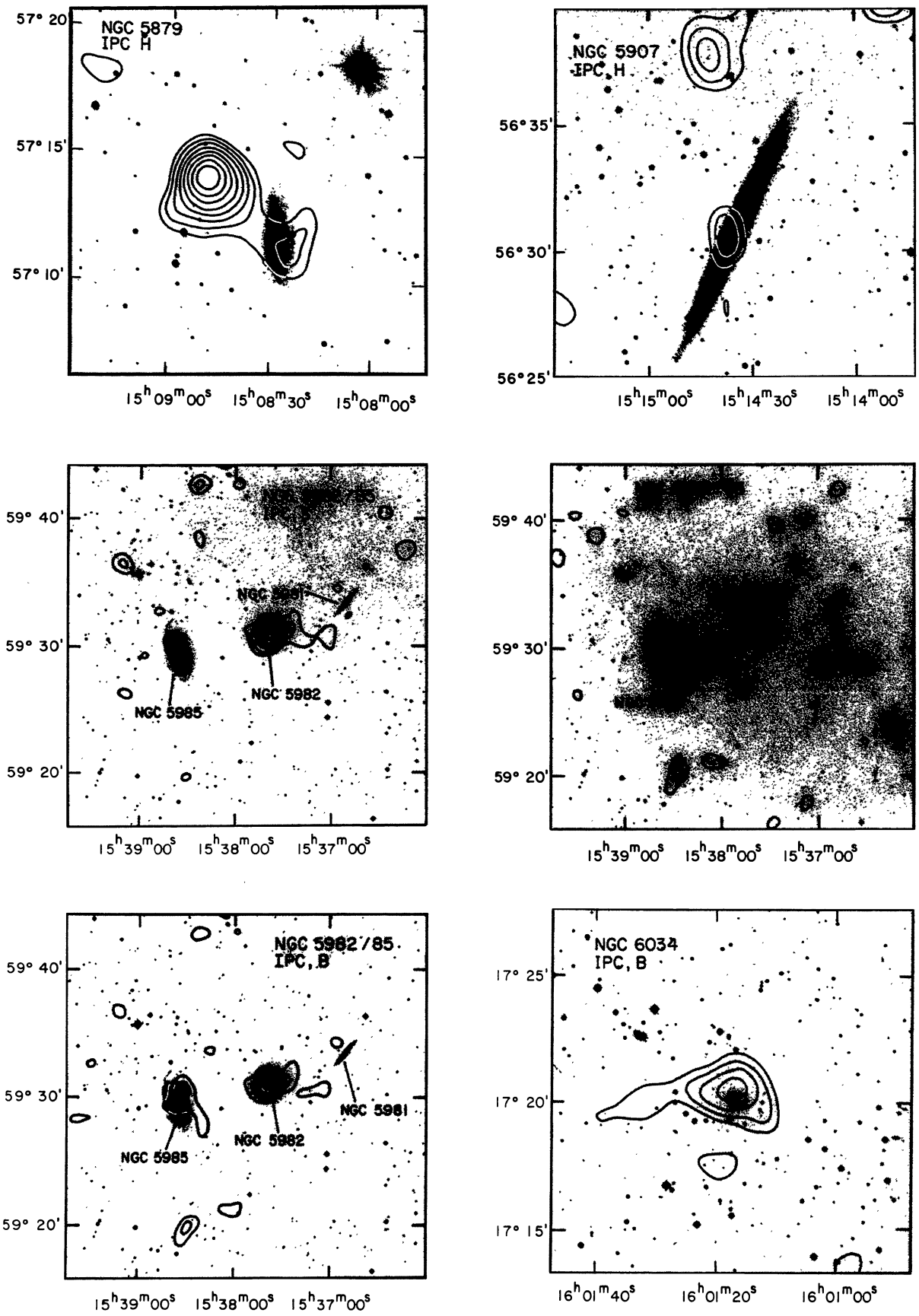

FIG. 7—*Continued*

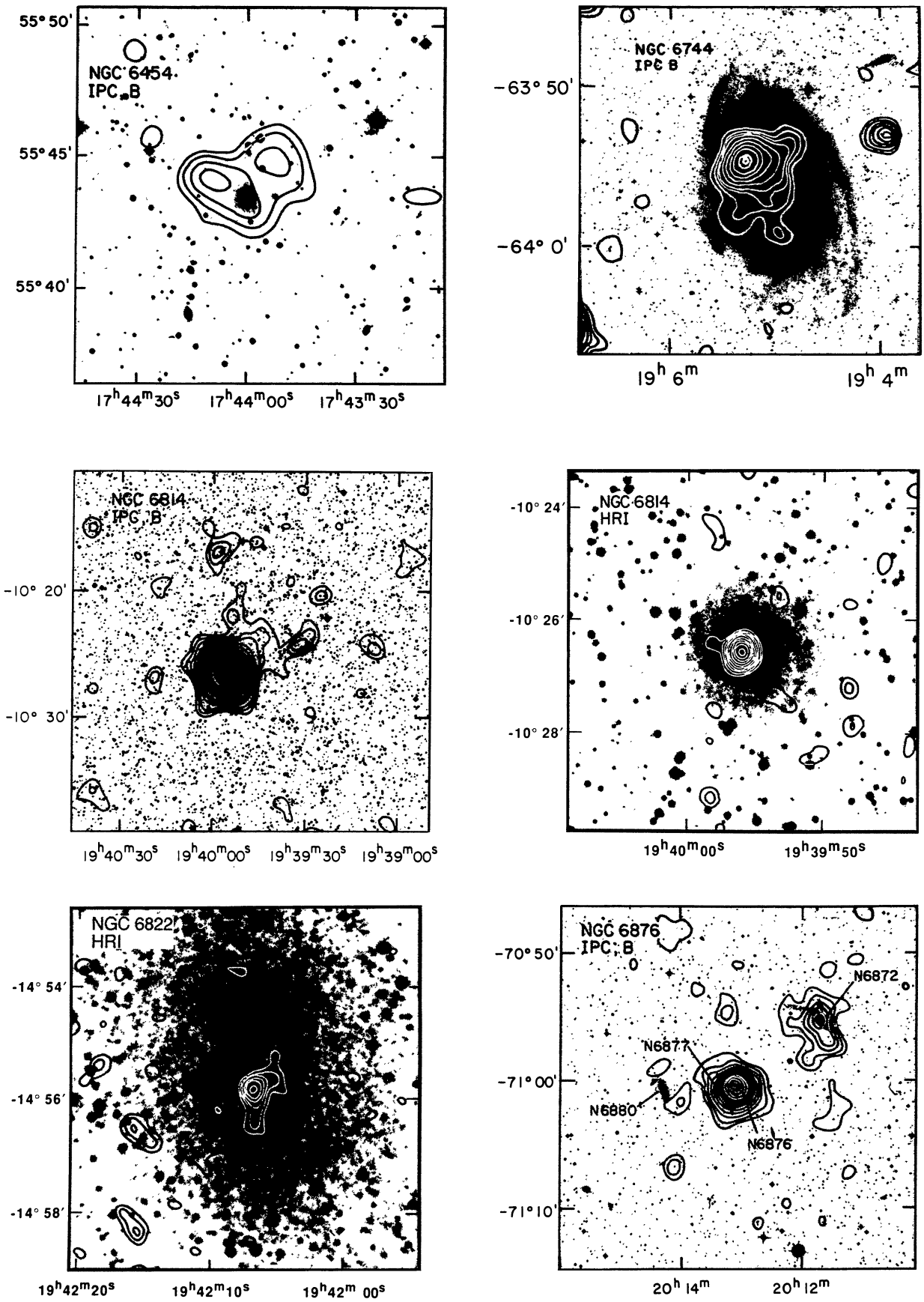

FIG. 7—*Continued*

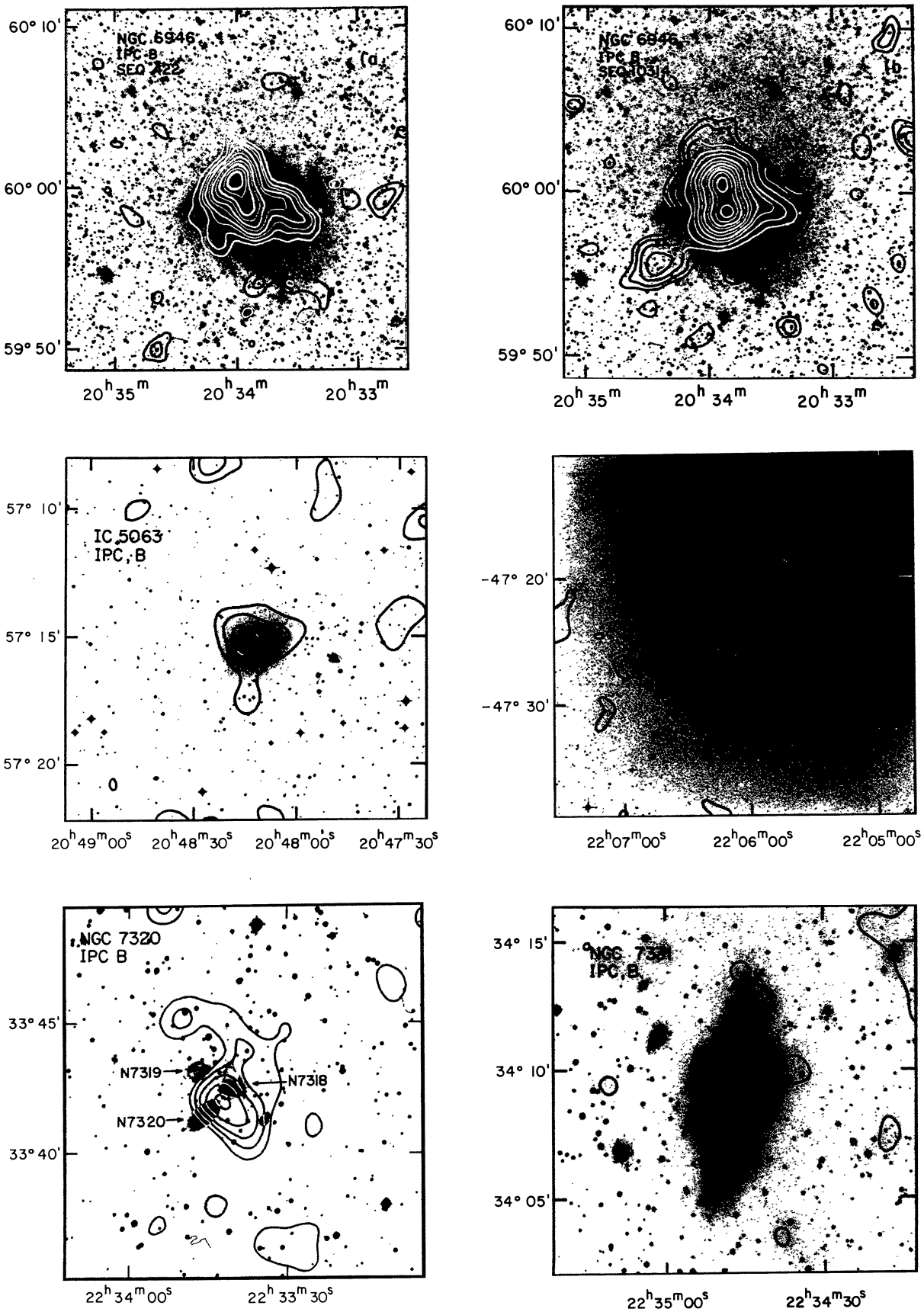

FIG. 7—*Continued*

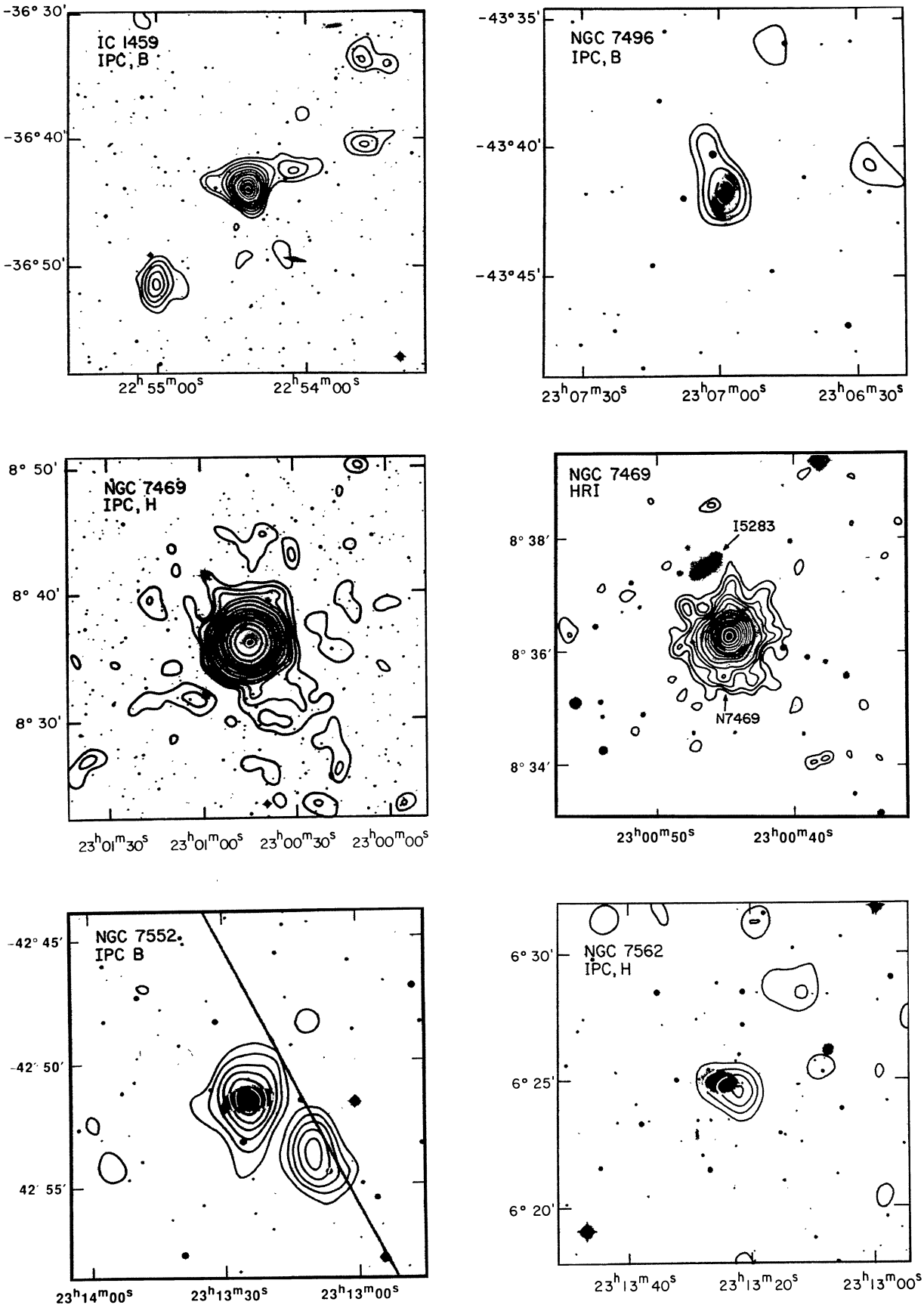

FIG. 7—*Continued*

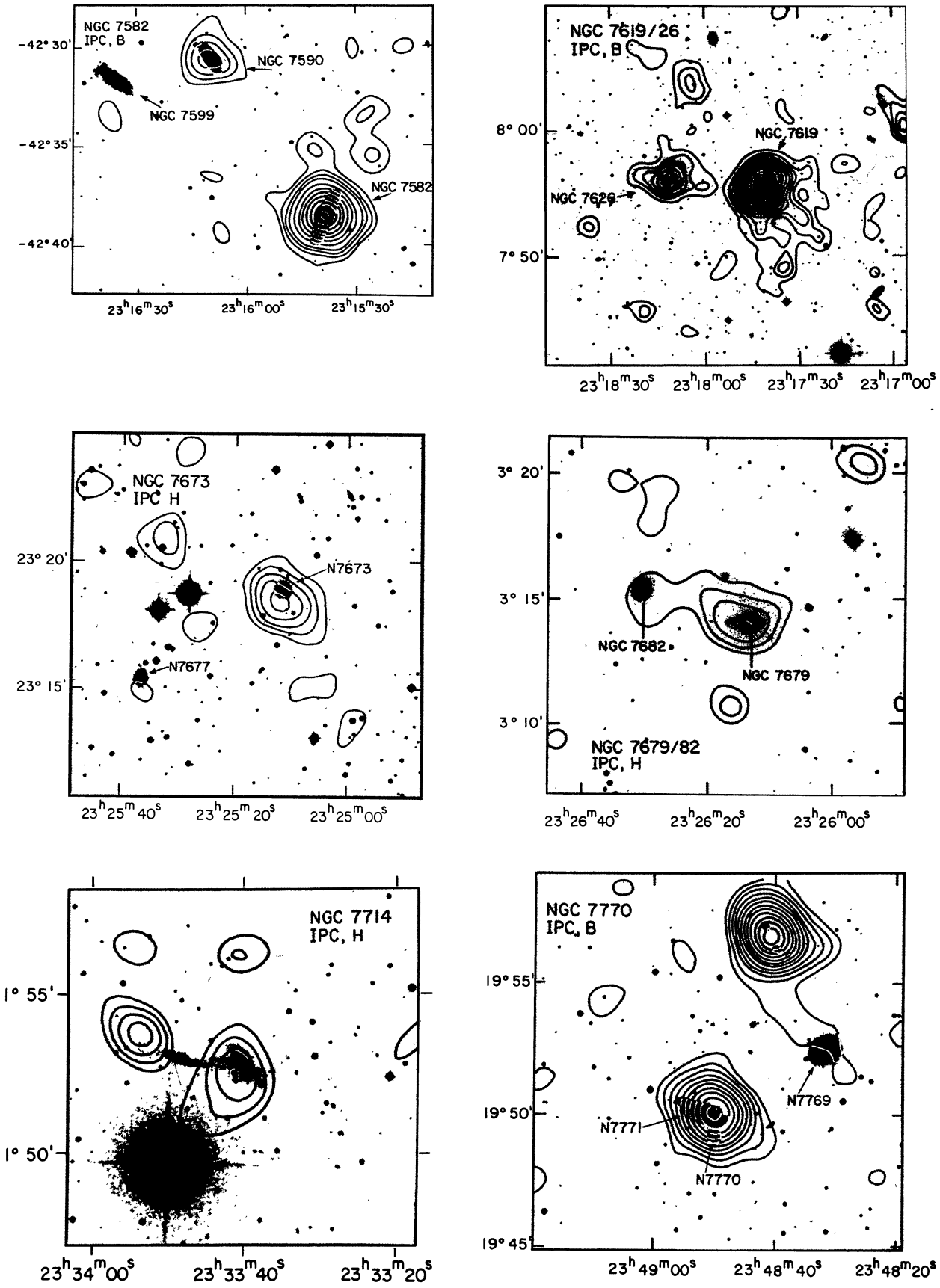

FIG. 7—*Continued*

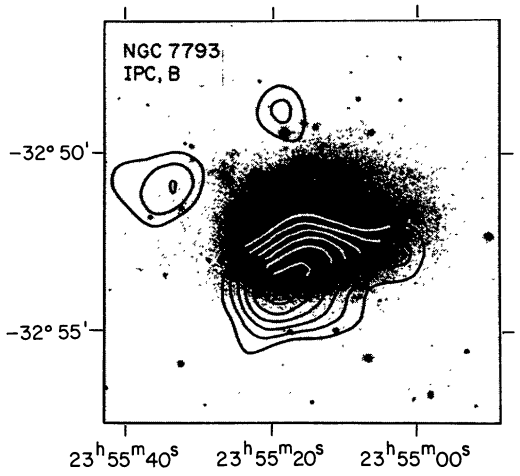

FIG. 7—*Continued*

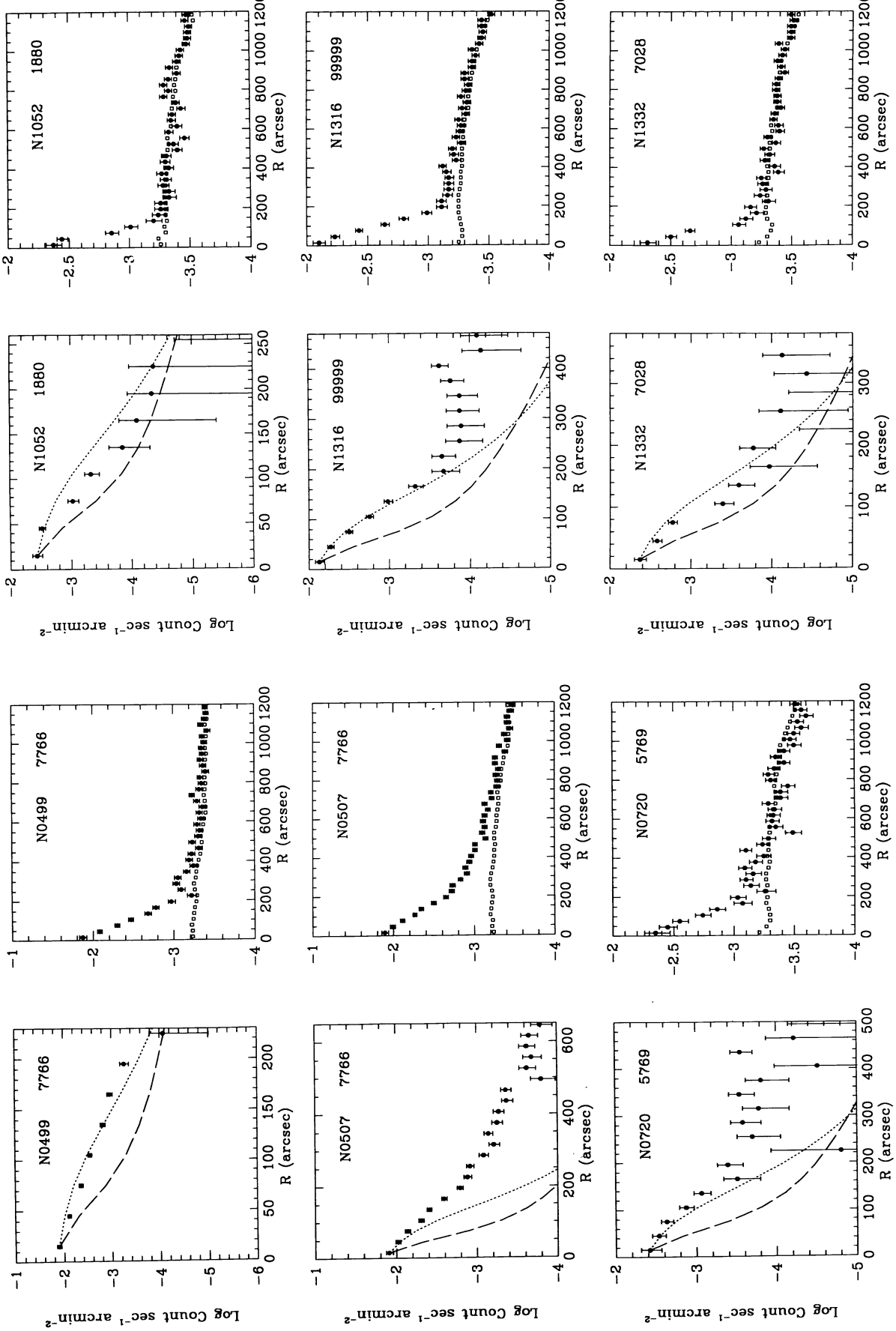

FIG. 8.—Radial profiles of the X-ray surface brightness of "normal" E and S0 galaxies observed with the IPC and detected with more than 100 net counts. The galaxy name and the sequence number are given in each plot. In the case of profiles obtained from merged observations, we use "99999" as a sequence number. For each galaxy we show the radial profile of the observed image with that of the renormalized background template (*right*) and the background-subtracted profile compared with the instrumental PRF (*left*). We show two representative IPC PRFs, which bracket the range observed (dotted line for 0.3 keV, dashed line for 4.5 keV; Mauche & Gorenstein 1986).

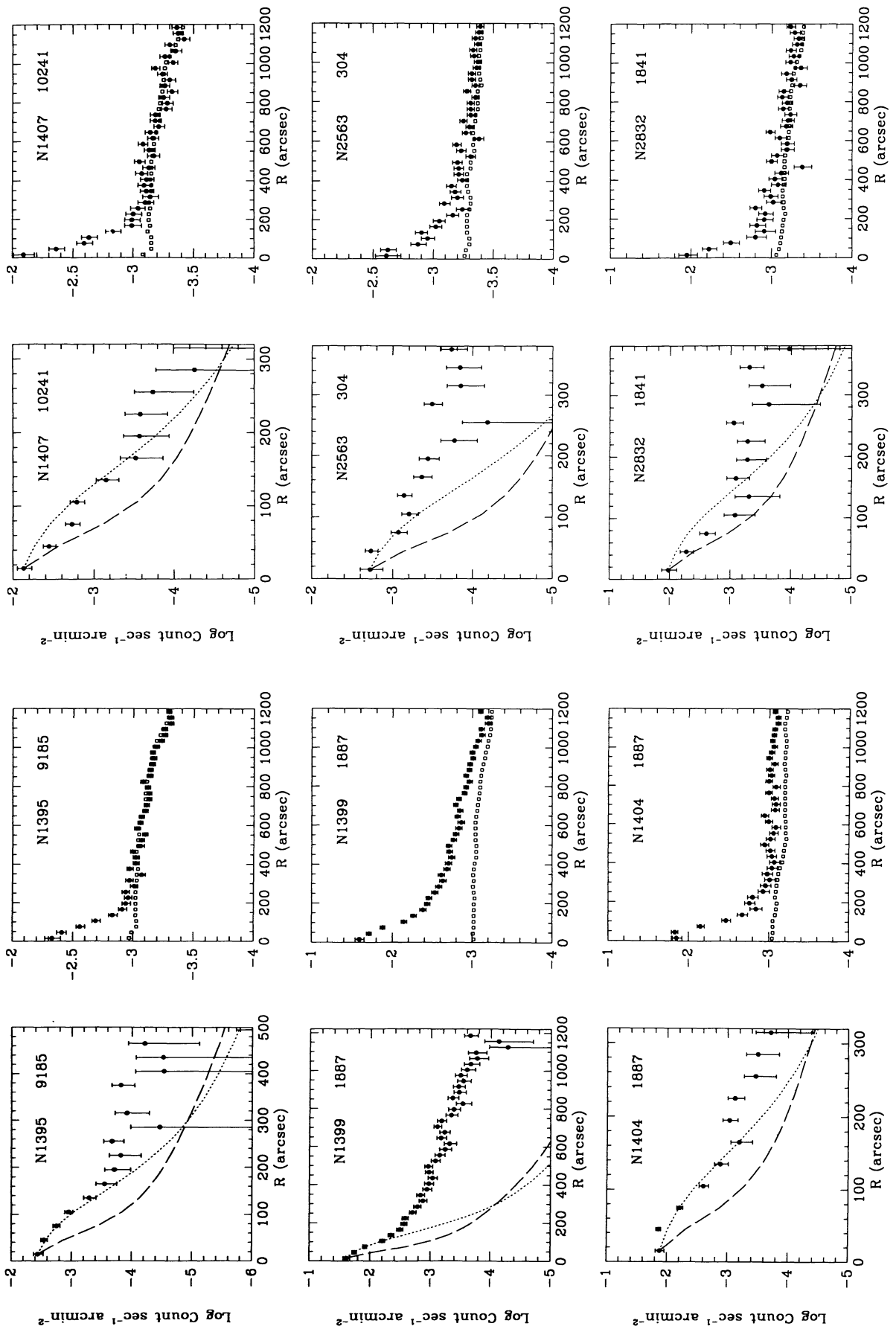

FIG. 8—*Continued*

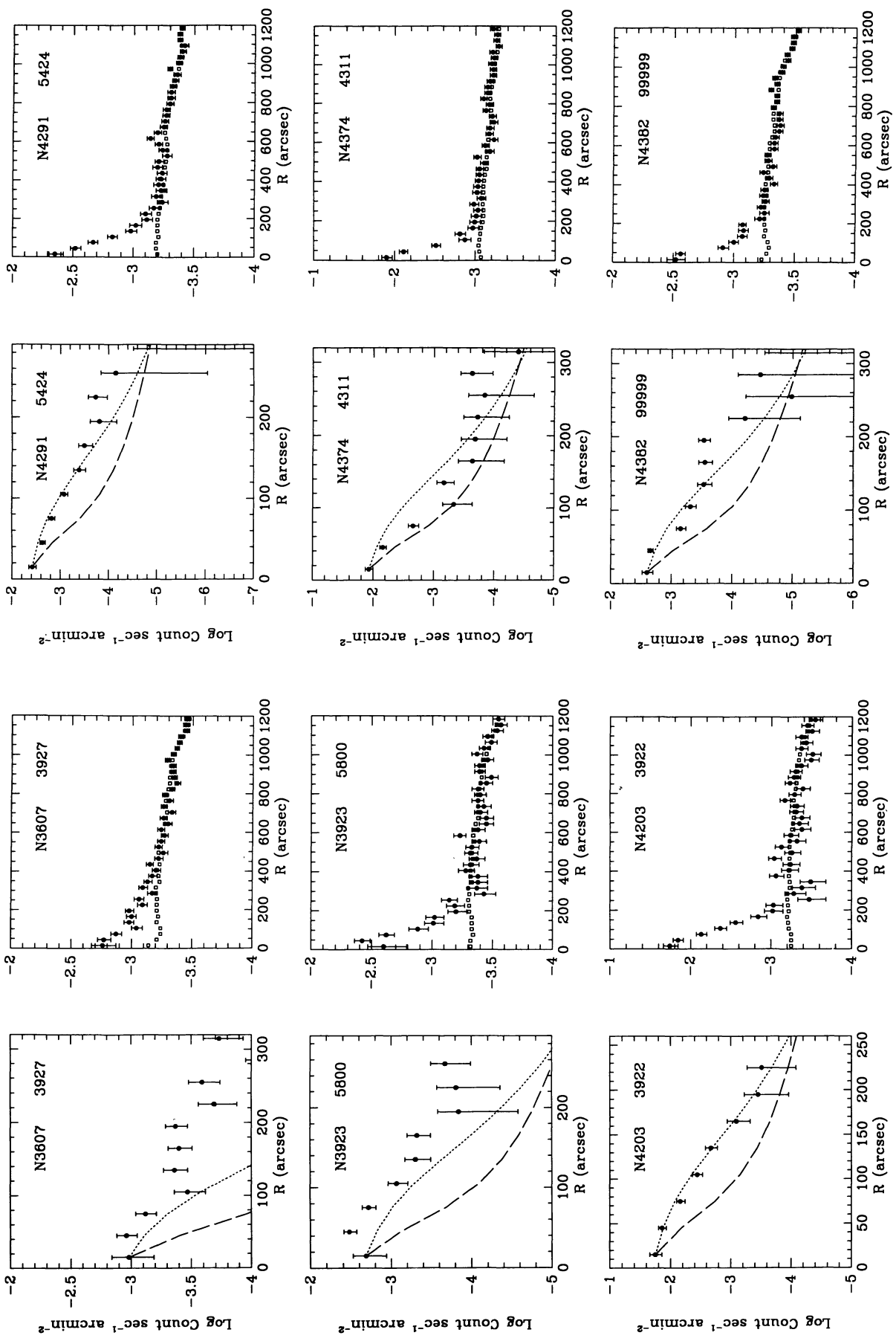

FIG. 8—*Continued*

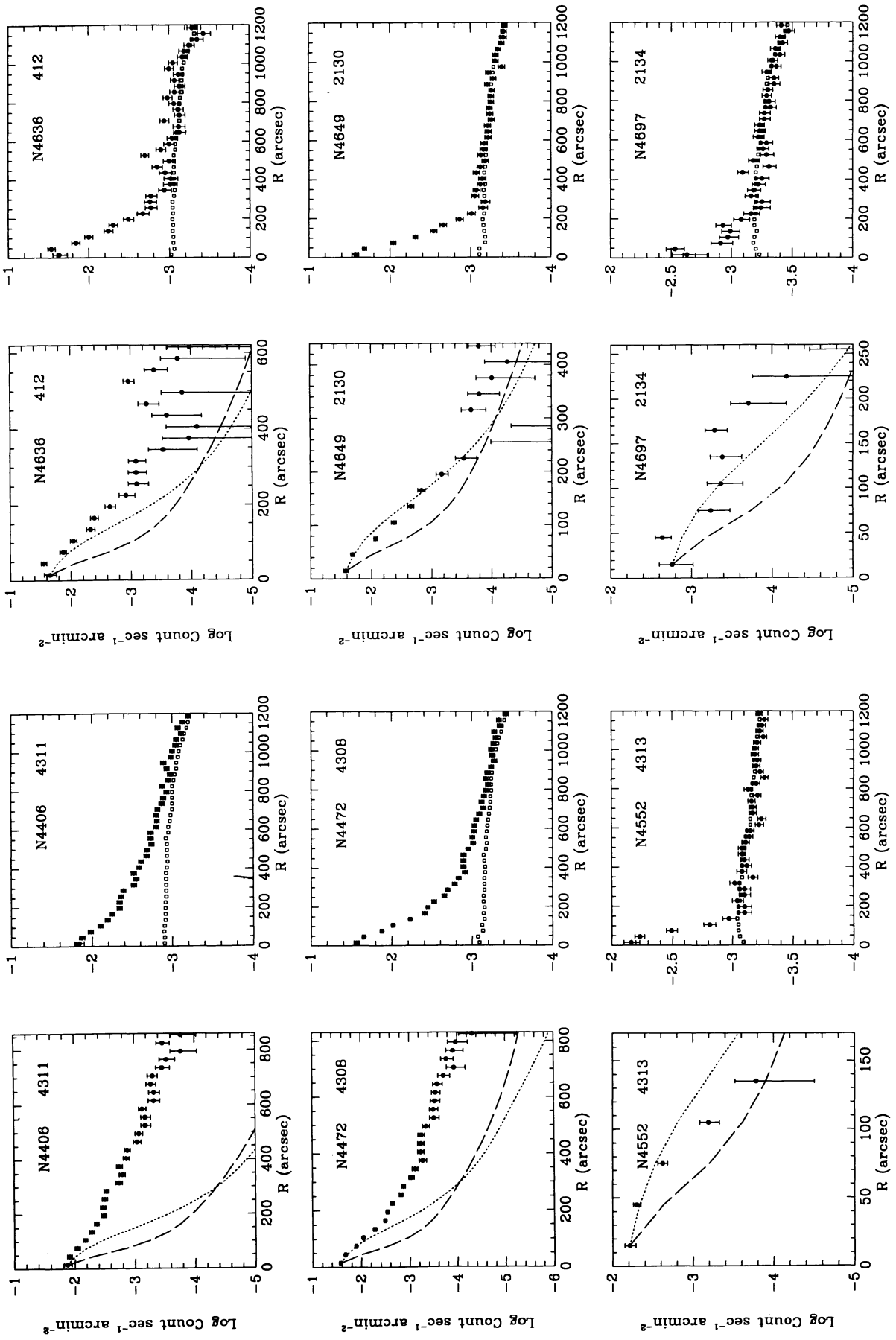

FIG. 8—*Continued*

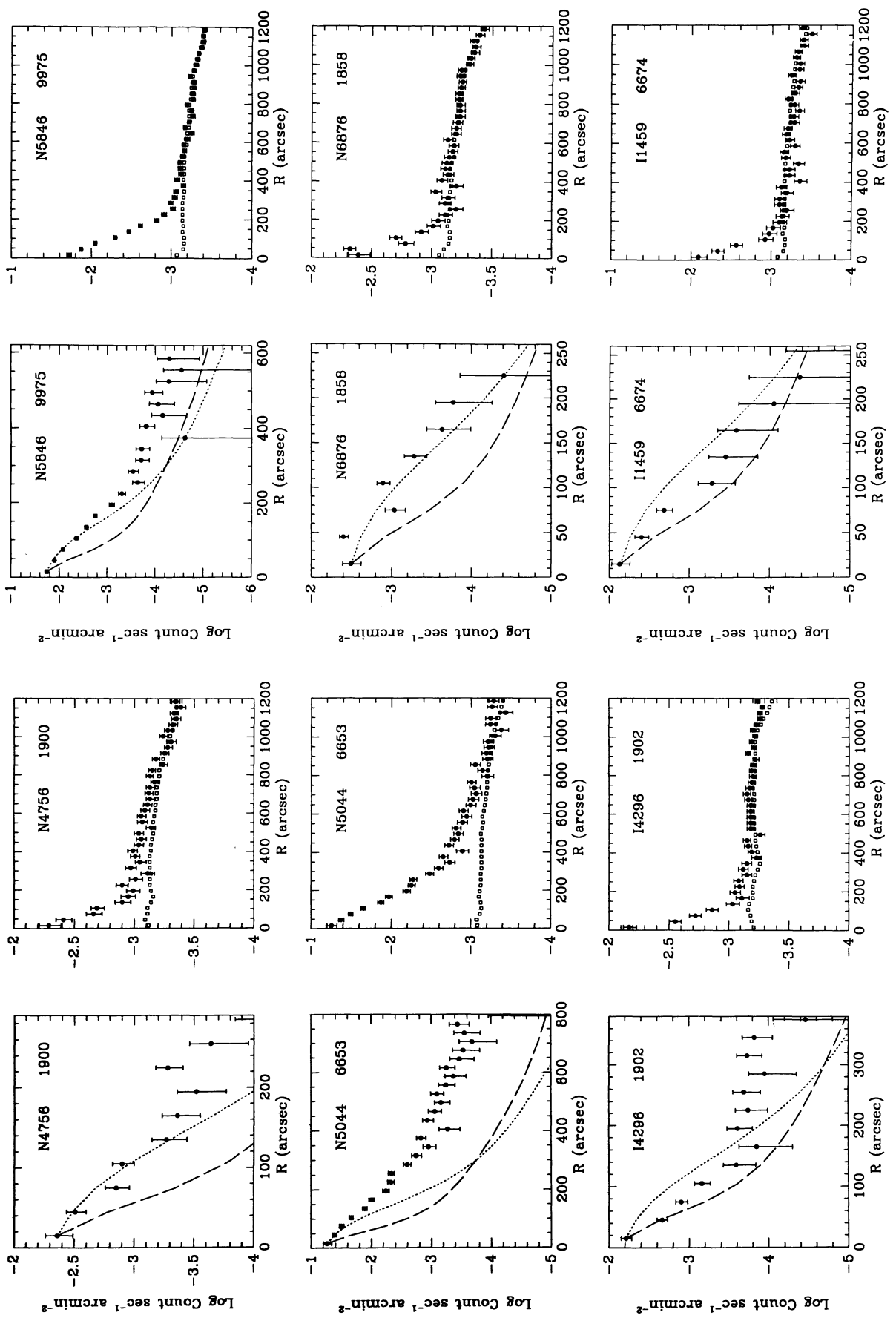

FIG. 8—*Continued*

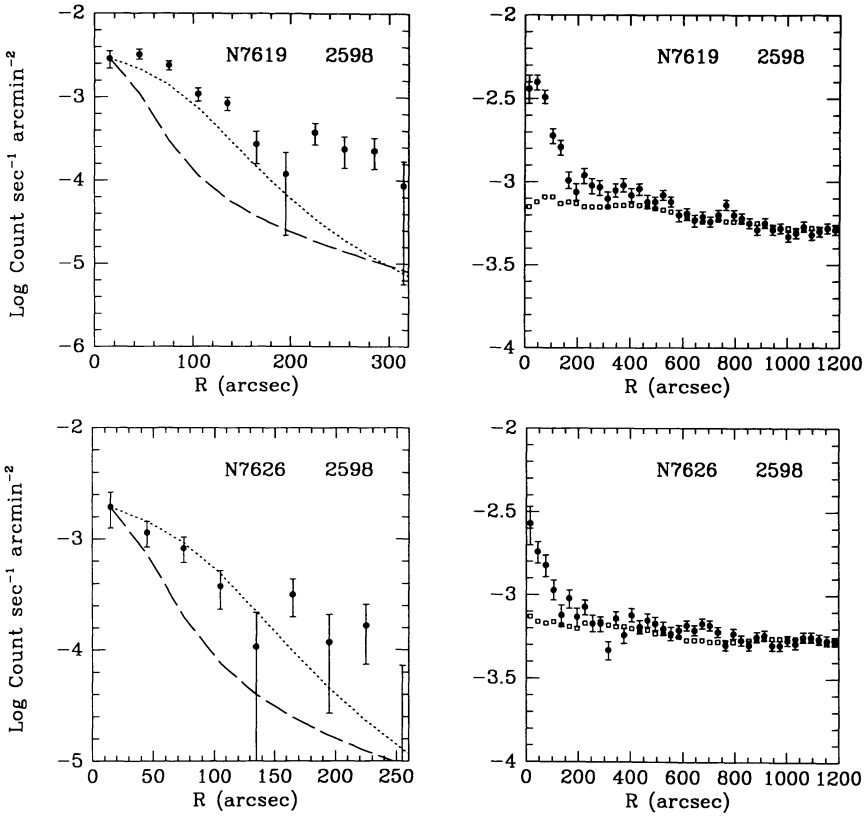

FIG. 8—*Continued*

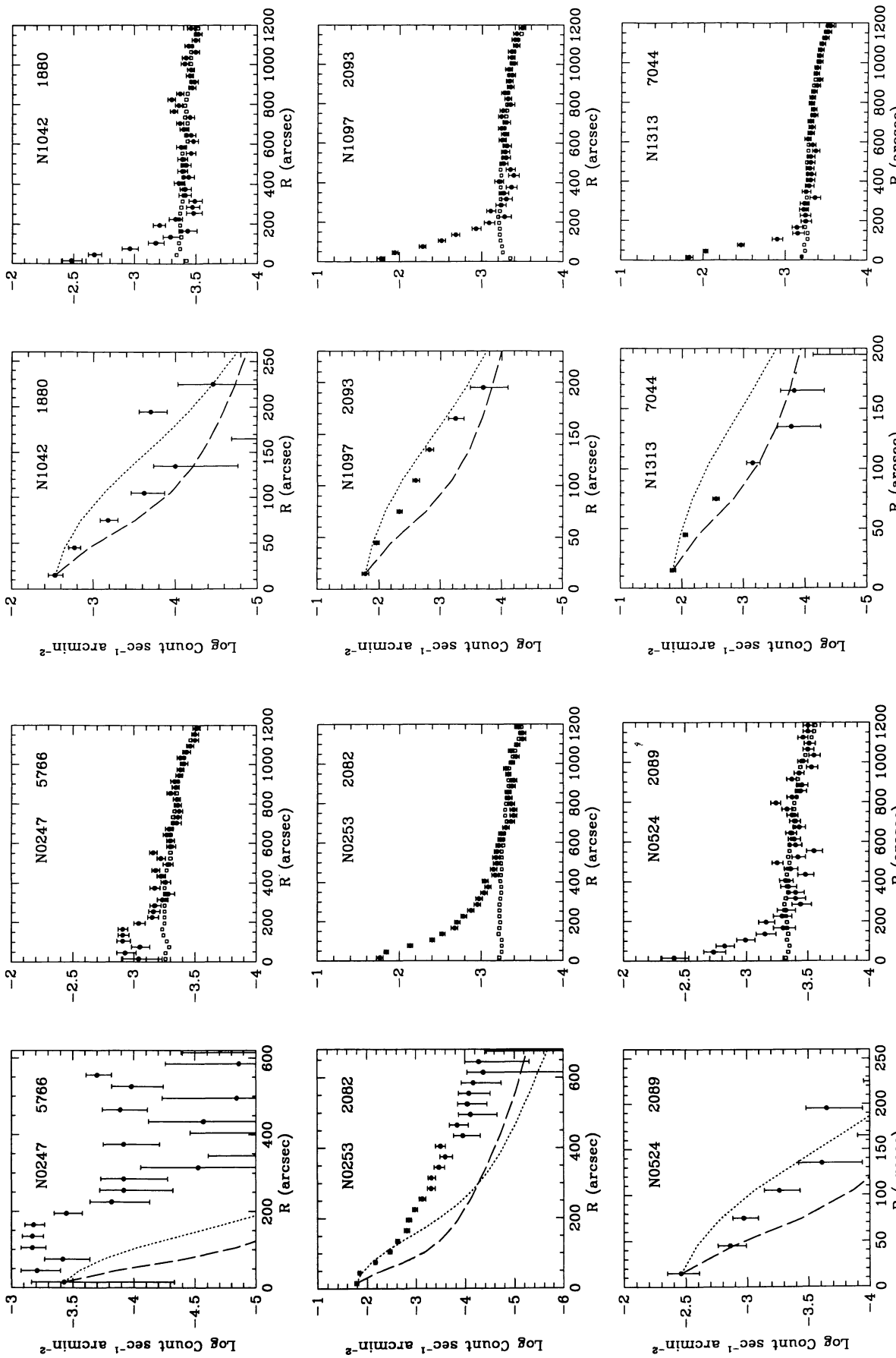

FIG. 9.—Radial profiles of the X-ray surface brightness of "normal" S and Irr galaxies observed with the IPC and detected with more than 100 net counts. The galaxy name and the sequence number are given in each plot. In the case of profiles obtained from merged observations, we use "99999" as a sequence number. For each galaxy we show the radial profile of the observed image with that of the renormalized background template (*right*) and the background-subtracted profile compared with the instrumental PRF (*left*). We show two representative IPC PRFs, which bracket the range observed (dotted line for 0.3 keV, dashed line for 4.5 keV; Mauche & Gorenstein 1986).

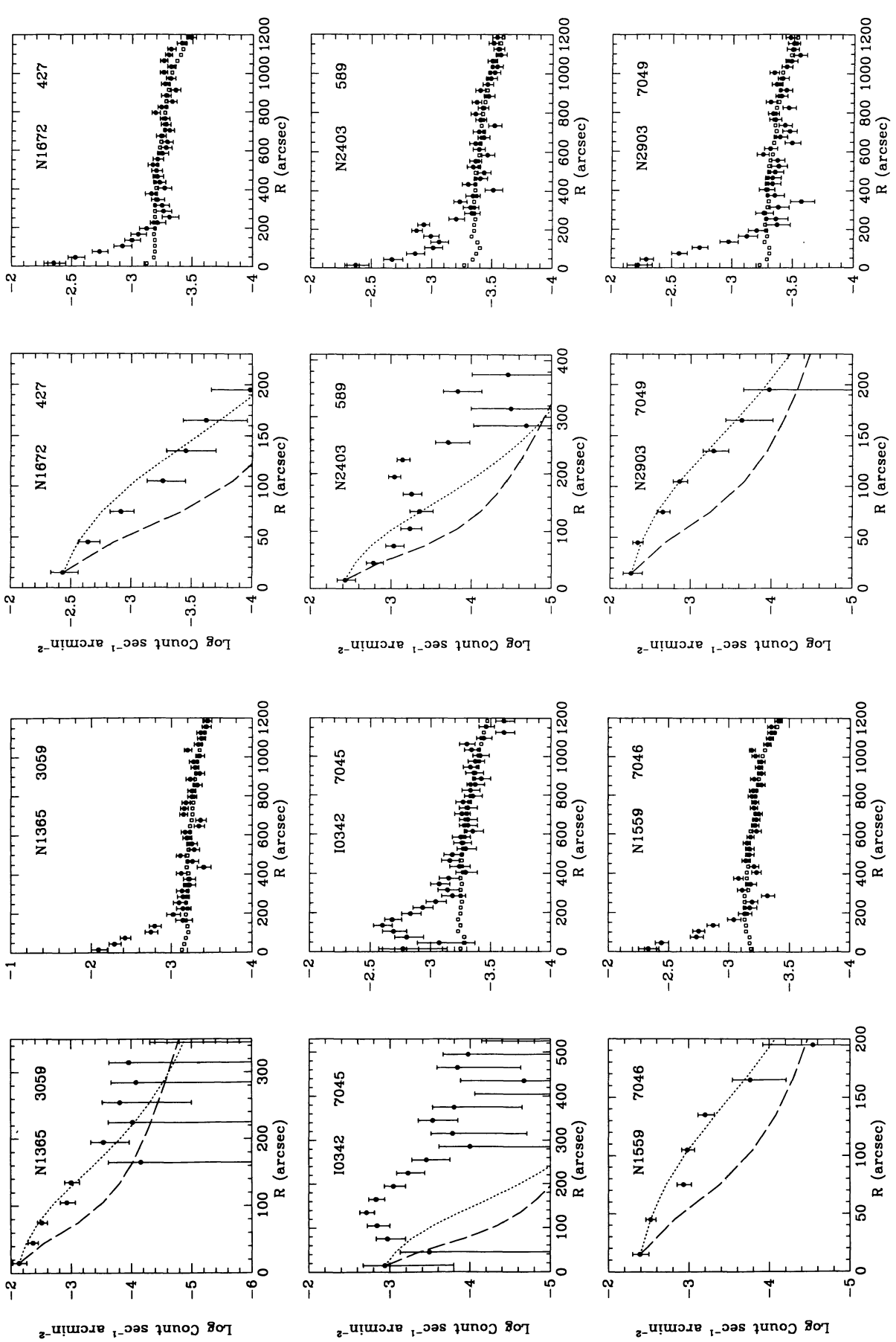

FIG. 9—*Continued*

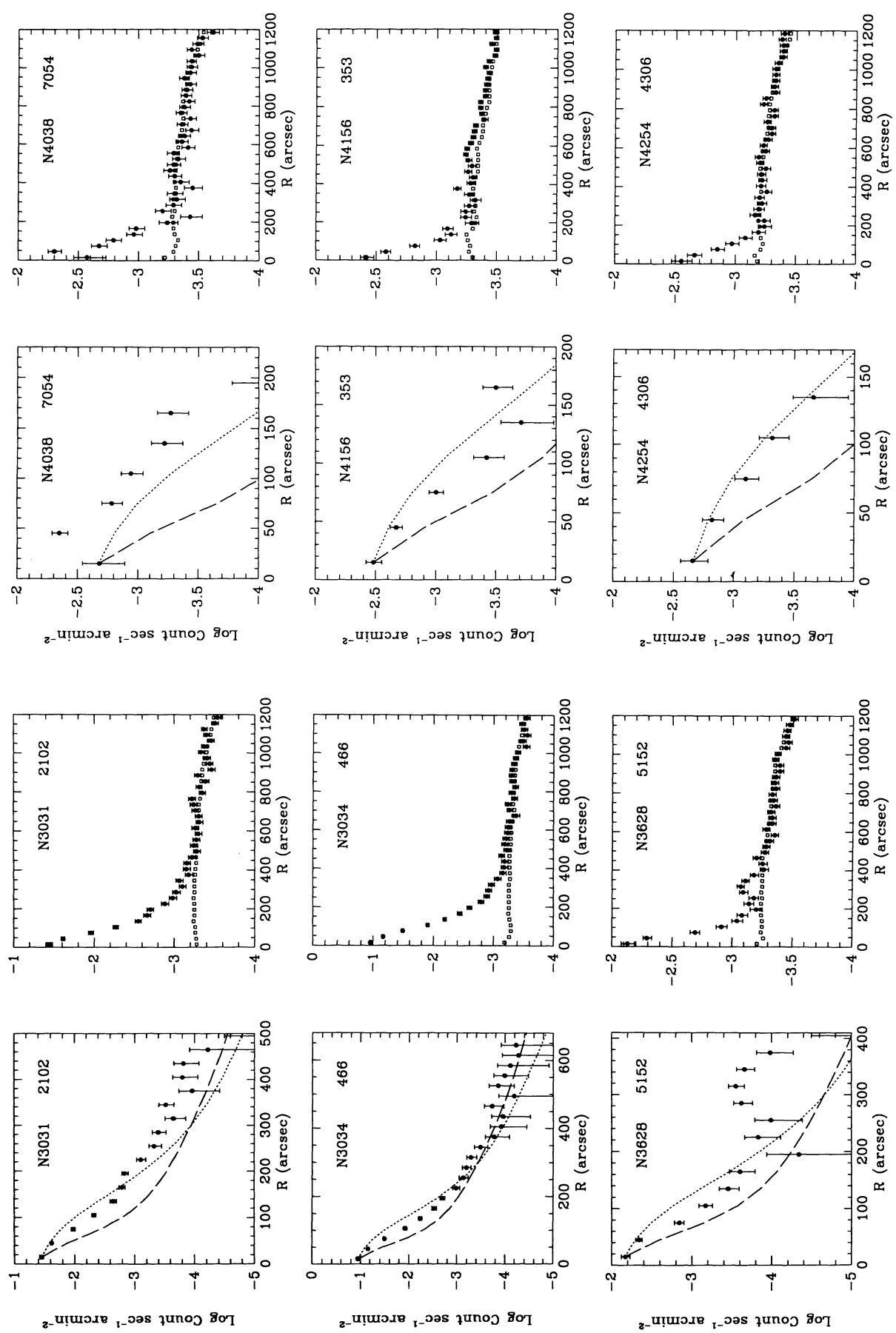

FIG. 9—*Continued*

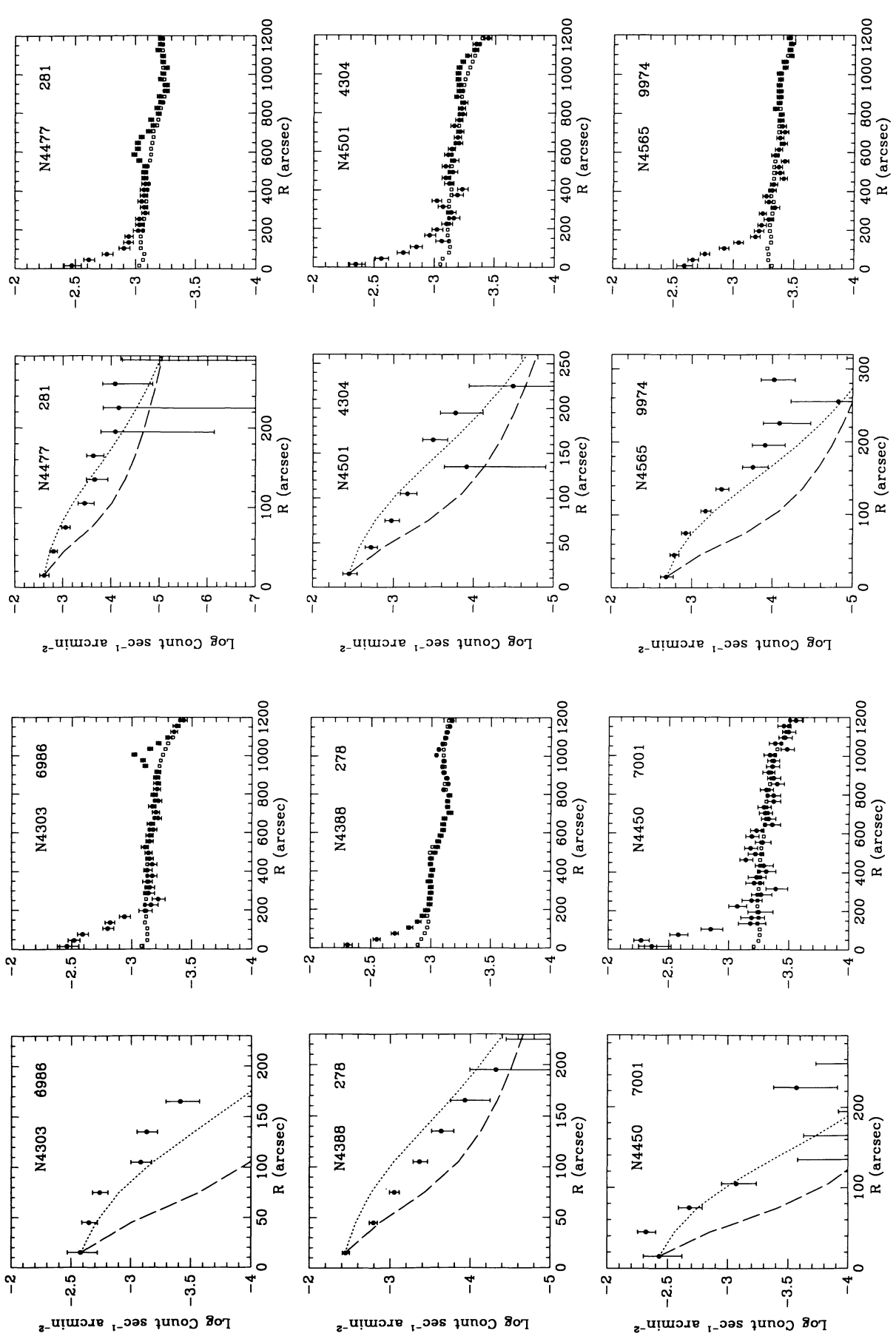

FIG. 9—*Continued*

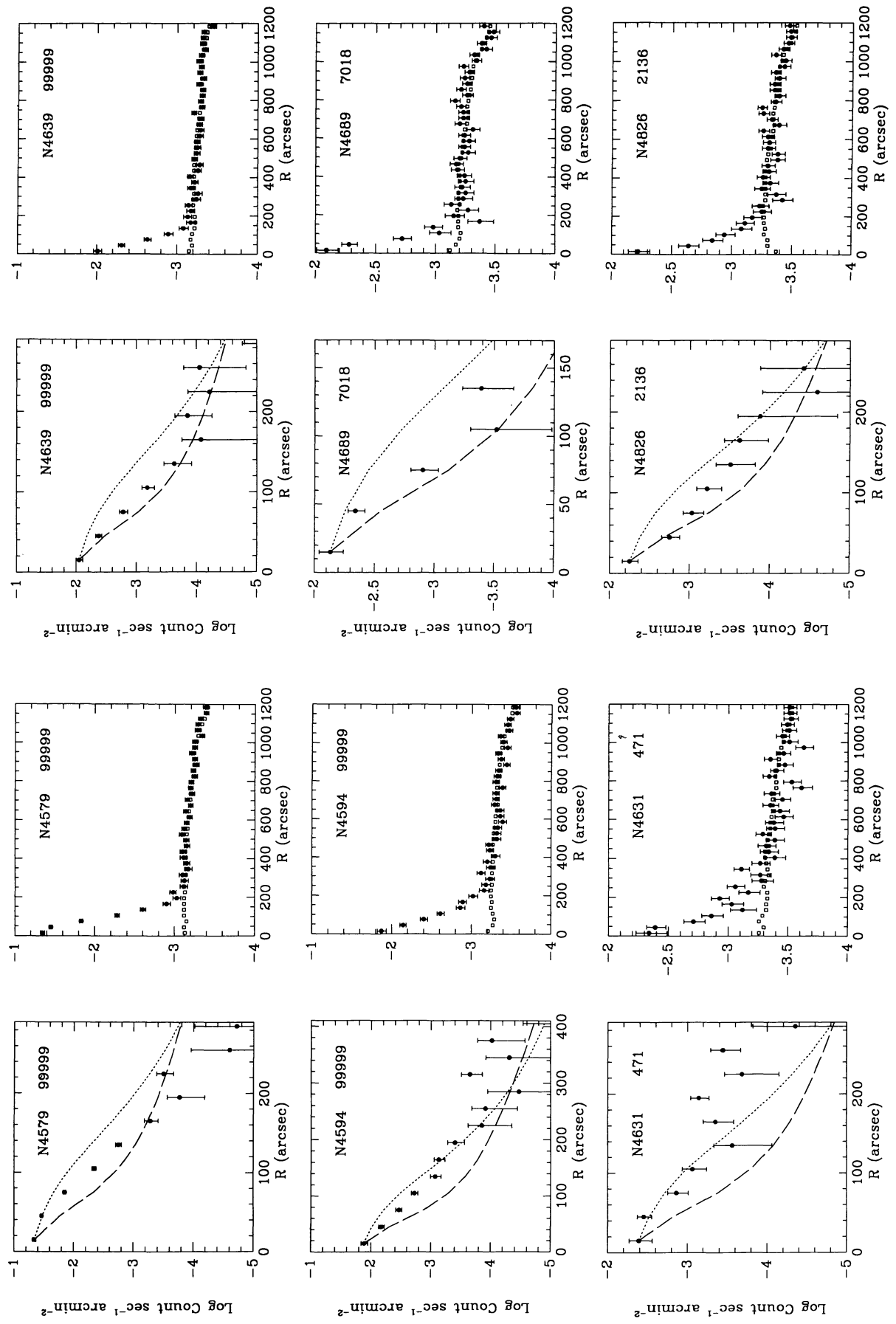

FIG. 9—*Continued*

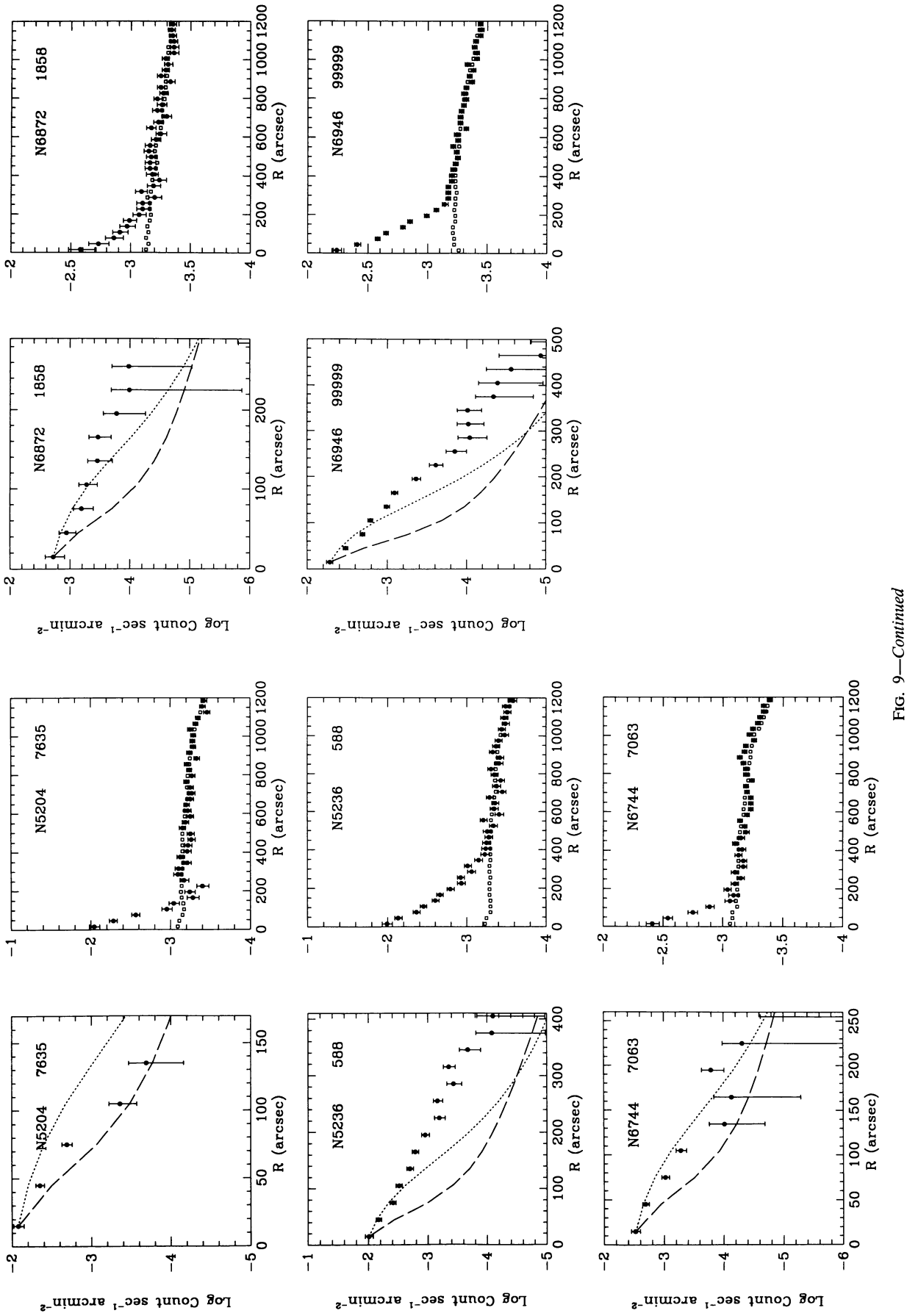

FIG. 9—*Continued*

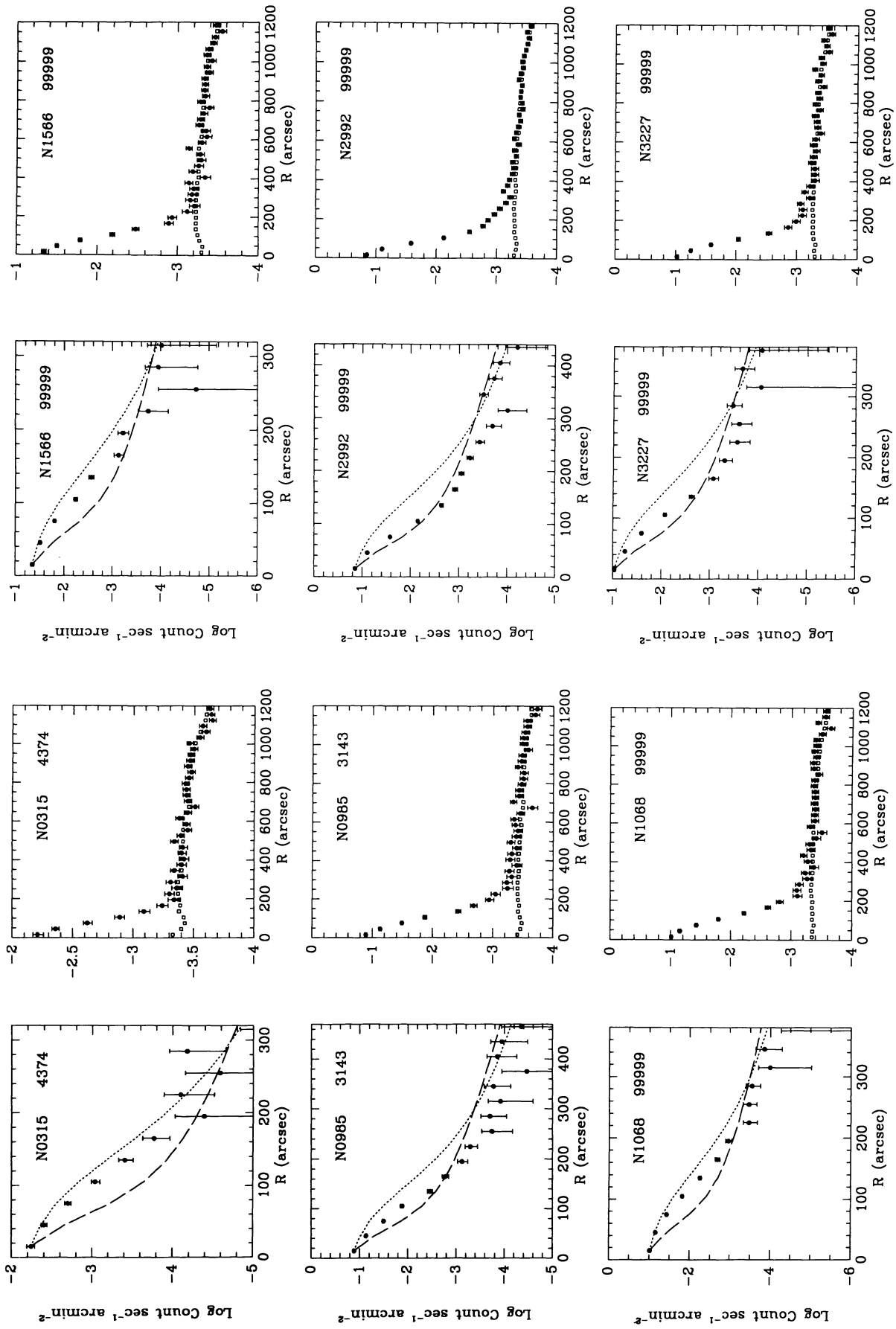

FIG. 10.—Radial profiles of the X-ray surface brightness of AGN galaxies observed with the IPC and detected with more than 100 net counts. The galaxy name and the sequence number are given in each plot. In the case of profiles obtained from merged observations, we use "99999" as a sequence number. For each galaxy we show the radial profile of the observed image with that of the renormalized background template (*right*) and the background subtracted profile compared with the instrumental PRF (*left*). We show two representative IPC PRFs, which bracket the range observed (dotted line for 0.3 keV, dashed line for 4.5 keV; Mauche & Gorenstein 1986).

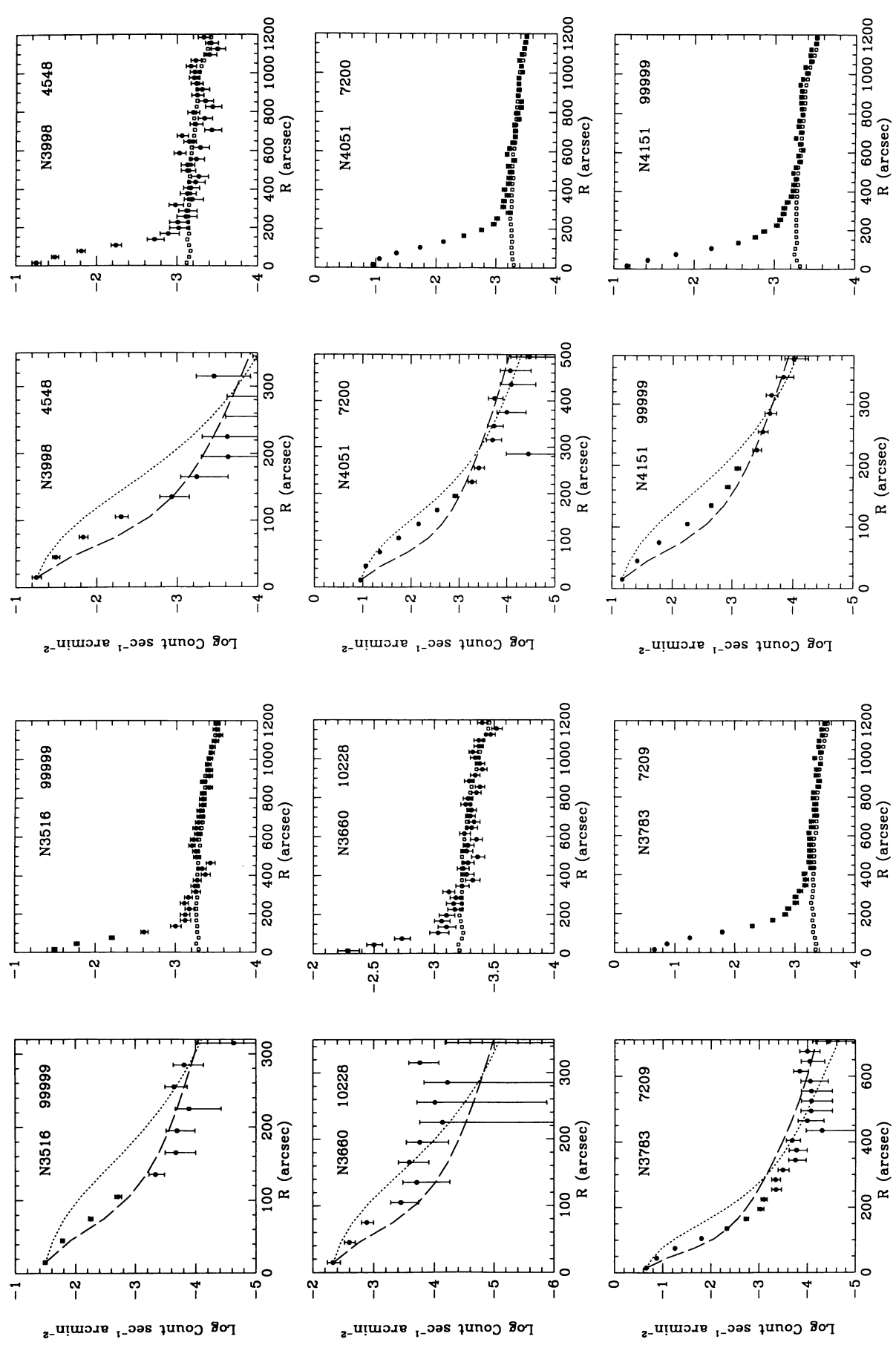

FIG. 10—*Continued*

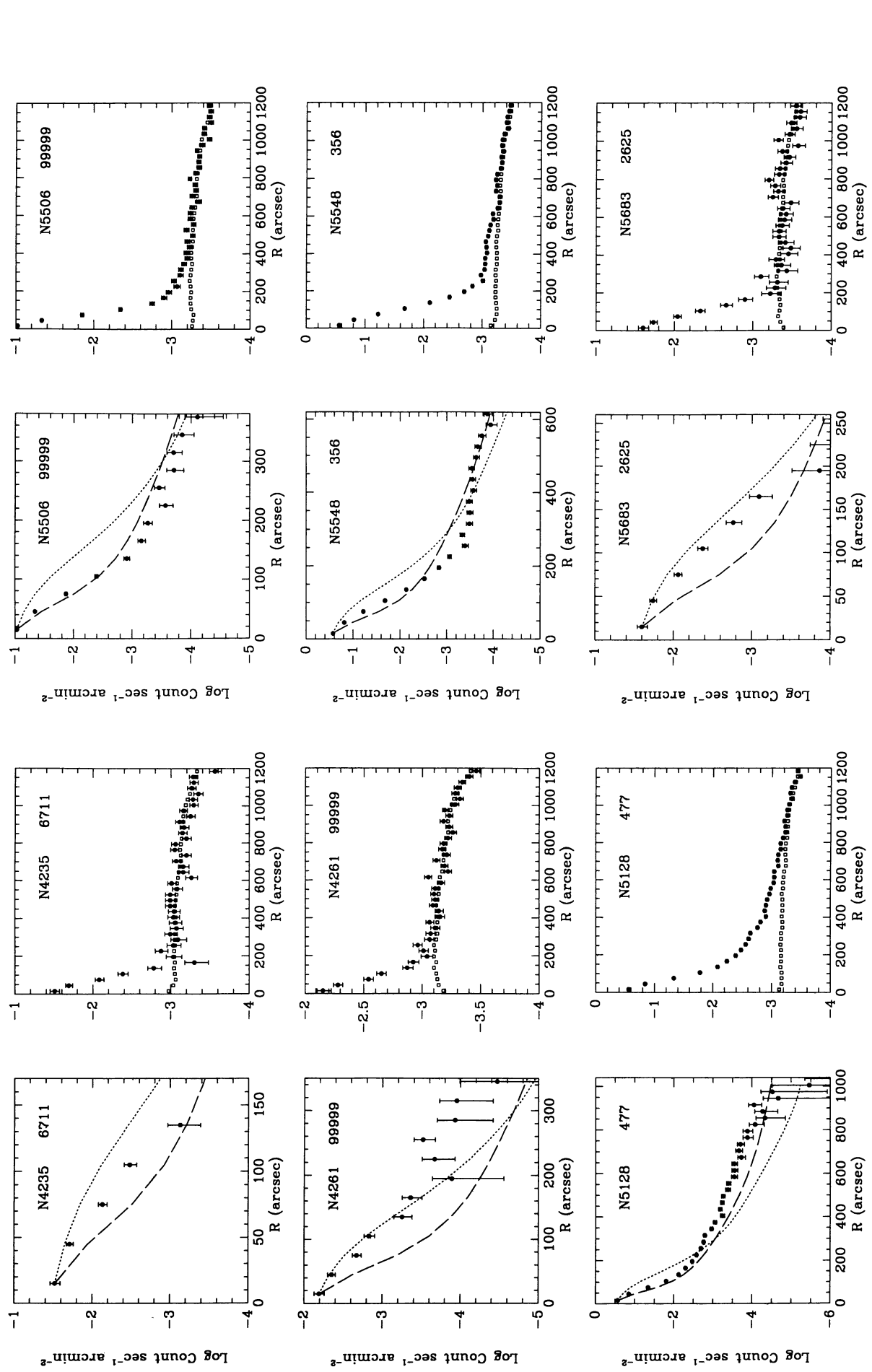

FIG. 10—*Continued*

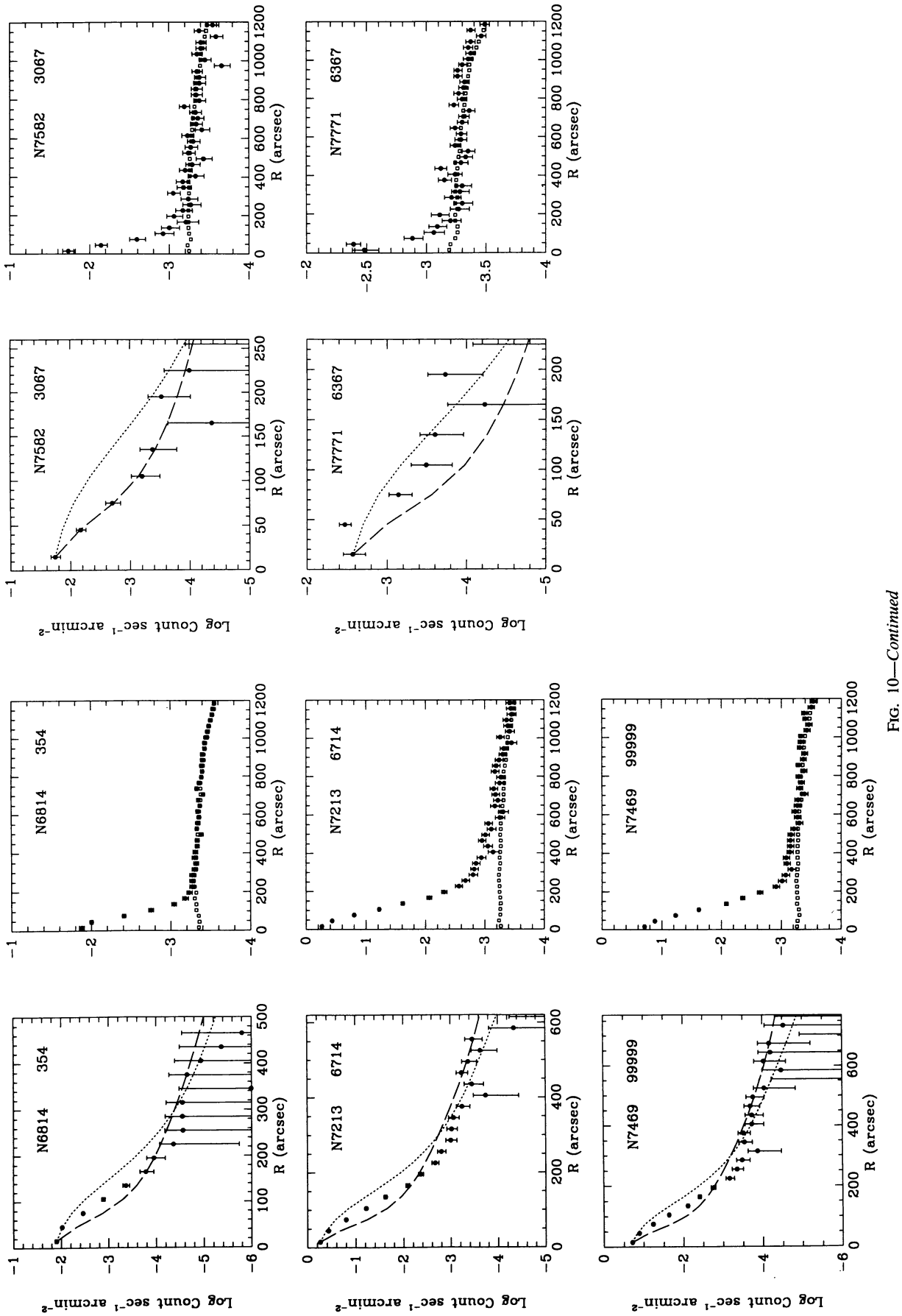

FIG. 10—*Continued*

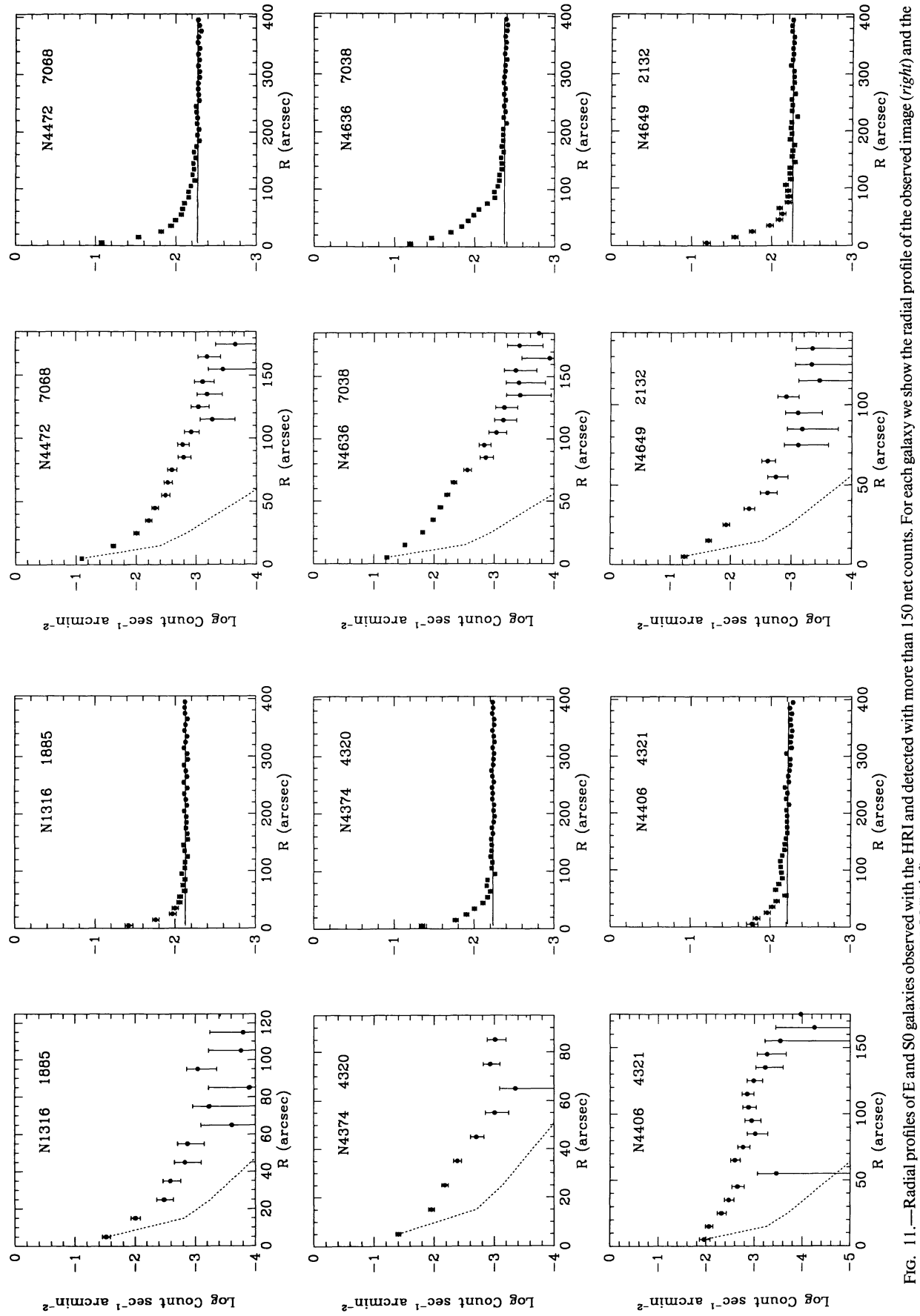

FIG. 11.—Radial profiles of E and S0 galaxies observed with the HRI and detected with more than 150 net counts. For each galaxy we show the radial profile of the observed image (*right*) and the background-subtracted profile compared with the HRI PRF (*left*).

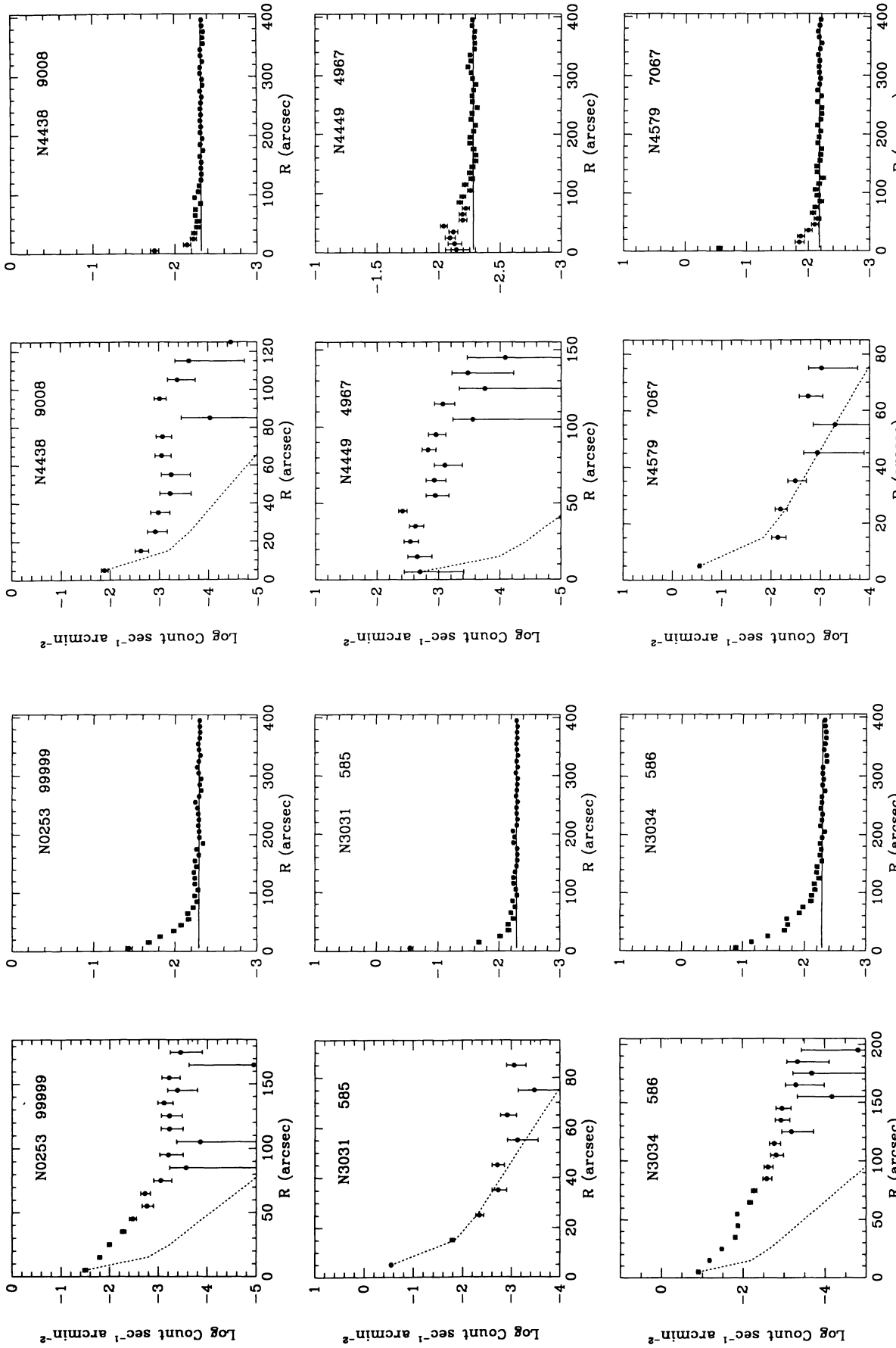

FIG. 12.—Radial profiles of S and Irr galaxies observed with the HRI and detected with more than 150 net counts. For each galaxy we show the radial profile of the observed image (*right*) and the background-subtracted profile compared with the HRI PRF (*left*).

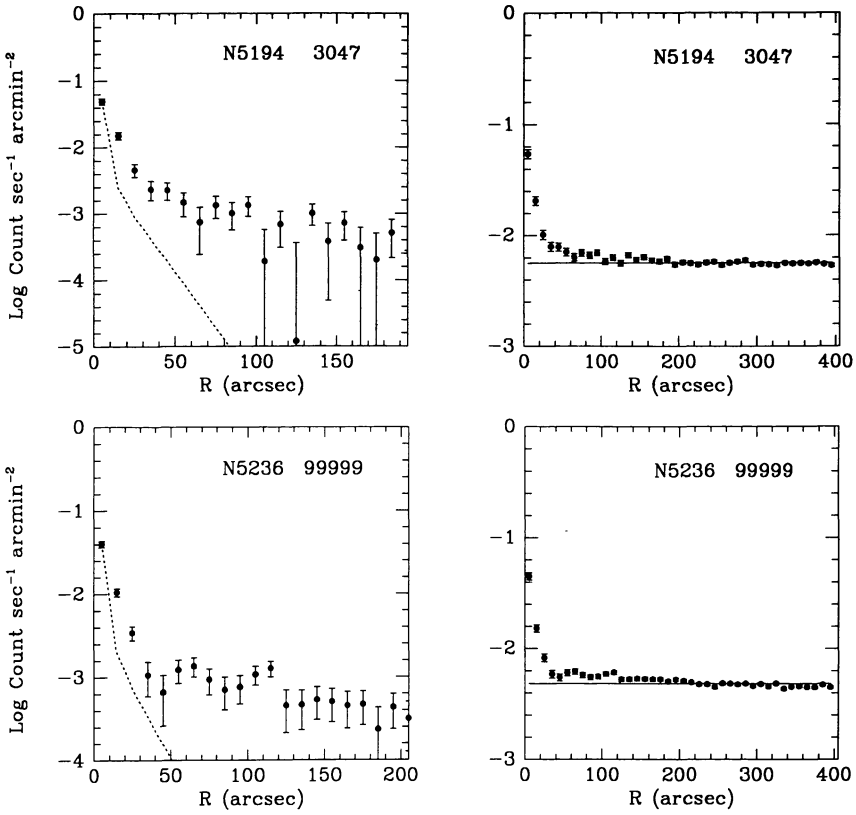

FIG. 12—*Continued*

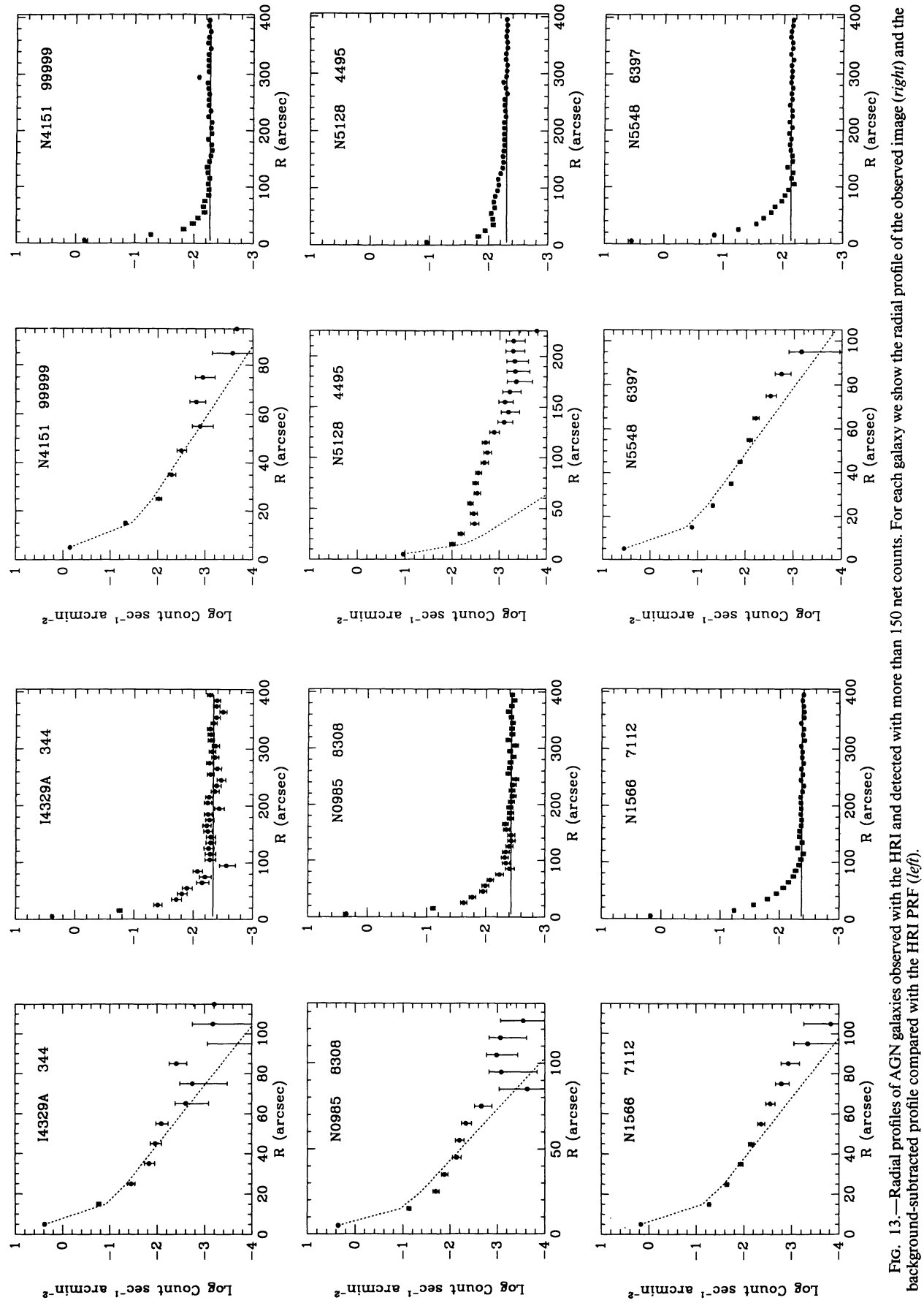

FIG. 13.—Radial profiles of AGN galaxies observed with the HRI and detected with more than 150 net counts. For each galaxy we show the radial profile of the observed image (*right*) and the background-subtracted profile compared with the HRI PRF (*left*).

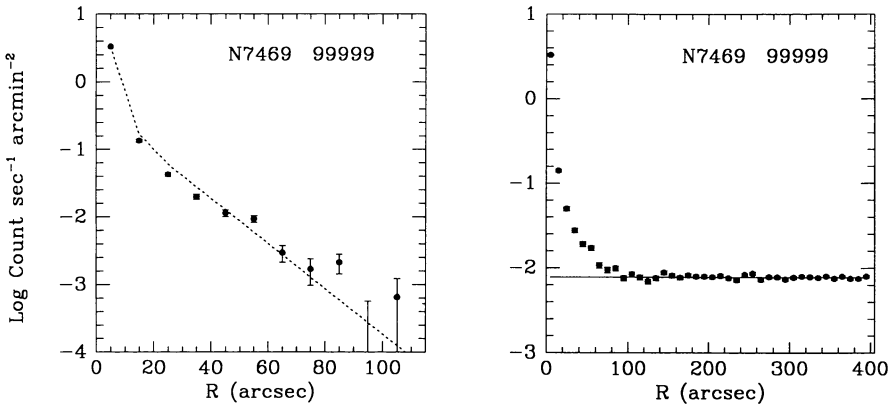

FIG. 13—*Continued*

TABLE 1

OBSERVATIONS

Name		RA (1950)	DEC (1950)	N_H (cm^{-2})	Inst.	Sequence number	start year	start day	Exp. (second)	Offaxis (arcmin)
N0125		00 26 16	02 33 42	2.8E+20	I	6643	80	194	1591.0	6.2
N0127		00 26 37	02 35 48	2.8E+20	I	6643	80	194	1591.0	0.9
N0128		00 26 41	02 35 17	2.8E+20	I	6643	80	194	1591.0	0.3
N0130		00 26 44	02 35 42	2.8E+20	I	6643	80	194	1591.0	1.1
N0205		00 37 38	41 24 53	6.9E+20	H	2730	79	15	23317.0	0.3
N0216		00 38 57	-21 19 12	1.5E+20	I	9977	81	16	1297.1	21.1
N0227		00 40 04	-01 48 17	2.9E+20	I	5393	80	171	9482.5	29.1
N0247		00 44 40	-21 02 00	1.5E+20	I	5766	79	342	10225.0	0.5
N0253		00 45 08	-25 33 42	1.3E+20	I	2082	79	182	7762.6	0.6
N0253		00 45 08	-25 33 42	1.3E+20	H	583	79	186	26896.0	0.1
N0253		00 45 08	-25 33 42	1.3E+20	H	2084	79	189	9956.0	0.1
N0255		00 45 16	-11 44 30	2.2E+20	I	3023	79	181	1919.3	27.6
N0309		00 54 13	-10 11 18	3.7E+20	I	8992	81	7	5019.0	12.8
N0315	AGN	00 55 05	30 04 54	5.8E+20	I	463	79	7	2023.0	0.2
N0315	AGN	00 55 05	30 04 54	5.8E+20	I	4374	79	213	17433.8	0.2
N0315	AGN	00 55 05	30 04 54	5.8E+20	H	6331	80	5	19710.0	0.2
I1613		01 02 13	01 51 00	2.8E+20	I	2086	79	202	6876.7	0.2
I1613		01 02 13	01 51 00	2.8E+20	H	2087	80	16	3139.0	6.5
N0449		01 13 19	32 49 30	5.6E+20	I	6703	80	11	1988.2	0.1
N0495		01 20 07	33 12 42	5.3E+20	I	7766	80	208	9193.4	12.2
N0499		01 20 22	33 12 00	5.3E+20	I	7766	80	208	9193.4	11.0
N0507		01 20 50	32 59 42	5.3E+20	I	7766	80	208	9193.4	5.6
N0520		01 22 00	03 31 53	3.2E+20	I	2088	79	24	4511.6	0.1
N0521		01 22 00	01 28 12	3.2E+20	I	153	79	179	1049.9	14.6
N0524		01 22 10	09 16 42	4.9E+20	I	2089	79	192	5754.6	0.6
N0523		01 22 30	33 46 42	5.1E+20	I	4199	79	210	3652.9	0.8
N0533		01 22 56	01 30 17	3.2E+20	I	153	79	179	1049.9	28.7
N0578		01 28 05	-22 55 30	1.1E+20	I	424	79	201	2651.9	0.0
N0584		01 28 50	-07 07 35	3.4E+20	I	5768	81	28	3555.9	0.3
N0596		01 30 22	-07 17 17	3.2E+20	I	7951	81	28	9466.4	12.4
N0596		01 30 22	-07 17 17	3.4E+20	I	5768	81	28	3555.9	25.0
N0598		01 31 03	30 23 53	6.3E+20	I	2090	79	212	19810.9	0.4
N0598		01 31 03	30 23 53	6.3E+20	H	2724	79	217	39077.0	0.7
N0598		01 31 03	30 23 53	6.3E+20	I	2091	80	11	13091.5	0.4
N0598		01 31 03	30 23 53	6.3E+20	H	7577	80	14	25580.0	5.0
N0598		01 31 03	30 23 53	6.3E+20	H	9907	80	215	20567.0	6.6
N0613		01 31 59	-29 40 17	1.7E+20	I	3556	79	13	1970.6	21.1
N0615		01 32 35	-07 35 47	3.2E+20	I	7951	81	28	9466.4	28.2
N0625		01 32 55	-41 41 24	1.7E+20	I	5257	80	182	1697.1	0.2
N0628		01 34 01	15 31 36	4.8E+20	H	7599	80	5	37604.0	0.2
N0628		01 34 01	15 31 36	4.8E+20	I	7042	80	10	6650.7	0.2
N0670		01 44 37	27 38 05	7.2E+20	I	7756	80	205	6096.2	30.2
I1727		01 44 40	27 05 06	7.2E+20	I	7756	80	205	6096.2	3.3
N0672		01 45 05	27 11 06	7.2E+20	I	7756	80	205	6096.2	5.1
N0720		01 50 34	-13 59 05	1.4E+20	I	5769	80	22	4477.1	0.0
N0772		01 56 35	18 46 00	6.2E+20	I	464	79	201	858.6	0.0
N0871		02 14 27	14 19 00	7.9E+20	I	6339	80	214	5396.1	0.7
N0877		02 15 16	14 18 53	7.9E+20	I	6339	80	214	5396.1	12.6
N0936		02 25 05	-01 22 42	2.7E+20	I	5118	80	17	6421.2	9.8
N0936		02 25 05	-01 22 42	2.7E+20	I	5771	80	218	5632.3	0.3
N0941		02 25 55	-01 22 30	2.7E+20	I	5118	80	17	6421.2	8.2
N0941		02 25 55	-01 22 30	2.7E+20	I	5771	80	218	5632.3	12.7
N0945		02 26 10	-10 45 36	2.5E+20	I	10223	81	7	7492.3	0.0
N0984		02 31 52	23 12 26	9.0E+20	I	4544	80	45	1385.2	0.8
N0985	AGN	02 32 11	-09 00 18	3.0E+20	I	3143	79	201	3302.8	0.3
N0985	AGN	02 32 11	-09 00 18	3.0E+20	H	8308	80	220	5962.0	0.3
N1035		02 37 01	-08 20 47	2.9E+20	I	1880	80	17	10928.3	24.6
N1042		02 37 56	-08 38 47	2.9E+20	I	1880	80	17	10928.3	13.8
N1044		02 38 24	08 31 24	7.4E+20	H	9171	80	214	5857.0	0.5
N1052		02 38 37	-08 28 06	2.9E+20	I	1880	80	17	10928.3	1.0
N1068	AGN	02 40 07	-00 13 30	3.1E+20	I	1927	79	203	1456.4	0.5
N1068	AGN	02 40 07	-00 13 30	3.1E+20	I	1928	80	19	2488.9	0.5
N1058		02 40 23	37 07 48	6.3E+20	I	1773	79	213	1565.2	38.4
N1073		02 41 05	01 09 53	3.7E+20	I	2092	79	203	4719.6	0.3

TABLE 1—*Continued*

Name		RA (1950)	DEC (1950)	N_H (cm^{-2})	Inst.	Sequence number	start year	start day	Exp. (second)	Offaxis (arcmin)
N1079		02 41 35	29 12 53	1.7E+20	I	1823	79	30	533.9	38.9
N1087		02 43 52	-00 42 30	3.9E+20	I	9138	81	4	1352.4	15.2
N1090		02 44 01	-00 27 23	3.9E+20	I	9138	81	4	1352.4	0.3
N1097		02 44 11	-30 29 06	1.9E+20	I	2093	79	30	5314.9	1.5
N1167		02 58 35	35 00 12	9.9E+20	I	4545	80	52	1871.3	0.3
N1172		02 59 16	-15 01 47	4.6E+20	I	9183	80	223	5555.8	0.5
N1201		03 01 58	-26 15 53	1.5E+20	I	10116	81	16	1405.8	0.0
N1218	AGN	03 05 49	03 55 12	9.9E+20	I	9146	81	27	1467.7	0.1
N1297		03 16 59	-19 17 00	2.8E+20	I	2094	79	229	6284.6	18.4
N1300		03 17 25	-19 35 30	2.8E+20	I	2094	79	229	6284.6	1.8
N1300		03 17 25	-19 35 30	2.8E+20	H	2095	80	28	7055.0	1.9
N1313		03 17 39	-66 40 42	3.5E+20	I	7044	80	2	7775.1	0.1
N1316		03 20 47	-37 23 06	2.0E+20	I	1883	79	190	3311.1	2.3
N1316		03 20 47	-37 23 06	2.0E+20	I	1884	79	228	4840.9	2.3
N1316		03 20 47	-37 23 06	2.0E+20	H	1885	80	28	23274.0	2.1
N1316		03 20 47	-37 23 06	2.0E+20	I	10571	81	40	3855.3	0.2
N1317		03 20 51	-37 16 53	2.0E+20	I	1883	79	190	3311.1	8.4
N1317		03 20 51	-37 16 53	2.0E+20	I	1884	79	228	4840.9	8.4
N1317		03 20 51	-37 16 53	2.0E+20	H	1885	80	28	23274.0	8.3
N1317		03 20 51	-37 16 53	2.0E+20	I	10571	81	40	3855.3	6.2
N1325		03 22 13	-21 43 05	2.2E+20	I	7028	80	20	12498.6	28.7
N1332		03 24 04	-21 30 30	2.2E+20	I	7028	80	20	12498.6	0.0
N1337		03 25 40	-08 33 42	4.7E+20	I	4974	80	237	2357.7	26.8
N1345		03 27 06	-17 58 00	4.1E+20	I	8404	81	57	10582.1	27.9
N1350		03 29 10	-33 47 54	1.2E+20	I	5776	80	18	2723.4	3.0
N1353		03 29 49	-20 59 17	2.5E+20	I	7424	80	223	1393.2	19.6
N1358		03 31 11	-05 15 23	4.3E+20	I	5250	80	239	968.7	0.0
N1358		03 31 11	-05 15 23	4.3E+20	I	6369	80	239	6700.4	9.4
N1365		03 31 42	-36 18 17	1.4E+20	I	3058	79	229	772.2	1.2
N1365		03 31 42	-36 18 17	1.4E+20	I	3059	80	228	2921.6	1.2
N1365		03 31 42	-36 18 17	1.4E+20	I	4129	80	229	3312.7	29.7
N1374		03 33 21	-35 23 30	1.3E+20	I	5777	80	24	1585.0	20.7
N1379		03 34 08	-35 36 17	1.3E+20	I	5777	80	24	1585.0	28.2
N1379		03 34 08	-35 36 17	1.4E+20	I	1887	80	18	3657.9	32.7
N1379		03 34 08	-35 36 17	1.4E+20	I	4128	80	229	1046.6	23.8
N1380		03 34 31	-35 08 23	1.3E+20	I	5777	80	24	1585.0	0.2
N1381		03 34 36	-35 27 30	1.3E+20	I	5777	80	24	1585.0	19.1
N1381		03 34 36	-35 27 30	1.4E+20	I	1887	80	18	3657.9	27.4
N1381		03 34 36	-35 27 30	1.4E+20	I	4128	80	229	1046.6	27.2
N1386		03 34 52	-36 09 53	1.4E+20	I	4128	80	229	1046.6	20.5
N1386		03 34 52	-36 09 53	1.4E+20	I	4129	80	229	3312.7	10.7
N1387		03 35 02	-35 40 12	1.4E+20	I	1887	80	18	3657.9	22.7
N1387		03 35 02	-35 40 12	1.4E+20	I	4128	80	229	1046.6	13.5
N1387		03 35 02	-35 40 12	1.4E+20	I	4129	80	229	3312.7	30.5
N1389		03 35 17	-35 54 30	1.4E+20	I	1887	80	18	3657.9	28.4
N1389		03 35 17	-35 54 30	1.4E+20	I	4128	80	229	1046.6	5.2
N1389		03 35 17	-35 54 30	1.4E+20	I	4129	80	229	3312.7	20.6
N1385		03 35 20	-24 39 54	1.3E+20	I	4084	80	229	1342.2	32.7
N1395		03 36 19	-23 11 23	1.7E+20	I	9185	81	64	13922.2	0.6
N1399		03 36 35	-35 36 42	1.4E+20	I	1887	80	18	3657.9	4.6
N1399		03 36 35	-35 36 42	1.4E+20	I	4128	80	229	1046.6	18.8
N1398		03 36 45	-26 29 53	9.7E+19	I	2096	79	30	8481.7	1.3
N1398		03 36 45	-26 29 53	9.7E+19	I	2097	81	12	5331.0	1.3
N1404		03 36 57	-35 45 17	1.4E+20	I	1887	80	18	3657.9	12.4
N1404		03 36 57	-35 45 17	1.4E+20	I	4128	80	229	1046.6	17.2
N1400		03 37 15	-18 50 54	5.5E+20	I	10241	81	57	4230.8	11.7
N1407		03 37 57	-18 44 24	5.5E+20	I	10241	81	57	4230.8	0.2
N1421		03 40 09	-13 38 54	4.1E+20	I	9130	80	223	2192.0	0.2
N1425		03 40 10	-30 03 17	8.9E+19	I	3450	79	27	1045.6	18.3
I0342		03 41 57	67 56 24	3.0E+21	I	7045	80	228	2059.2	0.1
N1497		03 59 07	22 59 49	1.0E+21	I	4546	80	61	1539.7	0.3
N1510		04 01 54	-43 33 00	1.9E+20	I	5258	80	201	1984.7	0.0
N1512		04 02 16	-43 29 12	1.9E+20	I	5258	80	201	1984.7	5.5
N1533		04 08 50	-56 15 00	2.4E+20	I	7030	80	49	10378.5	0.6

TABLE 1—*Continued*

Name		RA (1950)	DEC (1950)	N_H (cm^{-2})	Inst.	Sequence number	start year	start day	Exp. (second)	Offaxis (arcmin)
N1536		04 09 57	-56 36 54	2.4E+20	I	7030	80	49	10378.5	24.0
N1553		04 15 05	-55 54 12	2.0E+20	I	5726	80	3	738.7	17.2
N1559		04 17 01	-62 54 17	3.4E+20	I	7046	80	104	8378.3	0.1
N1566	AGN	04 18 53	-55 03 24	1.9E+20	I	1938	79	210	2529.0	0.9
N1566	AGN	04 18 53	-55 03 24	1.9E+20	I	1937	79	263	2603.1	0.9
N1566	AGN	04 18 53	-55 03 24	1.9E+20	H	7112	79	365	16430.0	0.6
N1574		04 20 59	-57 05 24	2.2E+20	I	5782	80	3	1461.7	0.1
N1569		04 26 05	64 44 24	2.2E+21	I	414	79	57	2847.2	0.7
N1569		04 26 05	64 44 24	2.2E+21	H	2700	79	77	2314.0	0.5
N1600		04 29 12	-05 11 30	4.3E+20	I	6667	80	237	1730.1	0.6
N1614		04 31 36	-08 40 54	6.1E+20	I	6706	80	65	1344.7	0.1
N1625		04 34 35	-03 24 12	4.5E+20	I	7895	80	237	2580.3	11.9
N1672		04 44 58	-59 19 36	2.2E+20	I	427	80	104	5800.7	0.7
N1784		05 03 07	-11 56 24	7.8E+20	I	10225	81	51	14314.0	0.2
N1947		05 26 11	-63 48 00	3.5E+20	I	7276	80	197	1334.8	2.0
N1961		05 36 34	69 21 17	8.3E+20	I	9460	80	271	10236.7	9.8
N2196		06 10 04	-21 47 47	7.6E+20	I	10306	81	60	9533.2	22.5
N2314		07 03 54	75 24 23	4.6E+20	I	8955	80	271	4197.1	1.0
U3691		07 05 06	15 15 00	9.9E+20	I	5156	79	295	11842.1	0.9
N2276		07 10 31	85 50 54	5.8E+20	I	6645	80	64	1939.7	6.6
N2300		07 15 47	85 48 35	5.8E+20	I	6645	80	64	1939.7	2.6
N2366		07 23 37	69 19 06	3.8E+20	I	2098	79	278	3453.6	0.4
N2403		07 32 03	65 42 42	4.0E+20	I	589	79	98	5988.3	0.1
N2403		07 32 03	65 42 42	4.0E+20	H	584	79	108	27813.0	0.1
N2403		07 32 03	65 42 42	4.0E+20	I	5227	79	291	1833.7	23.0
N2403		07 32 03	65 42 42	4.0E+20	I	5226	79	291	4411.7	20.1
N2444		07 43 30	39 09 18	5.6E+20	I	3148	79	99	2250.2	1.3
N2441		07 46 20	73 09 23	3.3E+20	I	6842	80	70	2420.3	14.4
N2525		08 03 15	-11 17 06	9.0E+20	I	10226	81	94	3028.9	0.0
N2562		08 17 28	21 17 24	4.4E+20	I	304	79	295	8858.5	13.5
N2563		08 17 40	21 13 36	4.4E+20	I	304	79	295	8858.5	8.8
N2551		08 19 13	73 34 35	2.7E+20	I	2261	79	278	1531.3	17.7
N2613		08 31 11	-22 48 00	7.9E+20	I	10722	81	105	9647.5	0.2
N2608		08 32 15	28 38 47	4.0E+20	I	5155	79	298	11673.0	0.0
N2642		08 38 14	-03 56 35	3.2E+20	I	10227	81	114	3009.9	0.0
N2629		08 41 55	73 10 06	2.4E+20	I	8361	80	121	2595.1	0.3
N2646		08 45 00	73 38 54	2.4E+20	I	8361	80	121	2595.1	31.7
N2683		08 49 35	33 36 30	2.8E+20	I	3921	79	297	959.4	0.2
N2685		08 51 41	58 55 30	4.2E+20	I	415	79	283	2016.6	0.1
N2694		08 53 24	51 31 24	2.2E+20	I	8362	80	121	1859.4	1.9
N2693		08 53 25	51 32 17	2.2E+20	I	8362	80	121	1859.4	1.4
N2713		08 54 44	03 06 48	3.9E+20	I	306	79	300	1056.4	18.1
N2713		08 54 44	03 06 48	3.9E+20	I	6118	80	131	4925.2	18.1
N2716		08 54 59	03 17 00	3.9E+20	I	306	79	300	1056.4	7.5
N2716		08 54 59	03 17 00	3.9E+20	I	6118	80	131	4925.2	7.5
N2763		09 04 29	-15 17 53	6.0E+20	I	5789	79	317	5746.2	0.2
N2773		09 06 58	07 23 06	4.0E+20	I	457	79	142	3414.0	17.2
N2773		09 06 58	07 23 06	4.0E+20	I	7048	80	130	6080.1	13.7
N2775		09 07 41	07 14 30	4.0E+20	I	457	79	142	3414.0	4.5
N2775		09 07 41	07 14 30	4.0E+20	I	7048	80	130	6080.1	0.0
N2777		09 08 02	07 24 42	4.0E+20	I	457	79	142	3414.0	9.7
N2777		09 08 02	07 24 42	4.0E+20	I	7048	80	130	6080.1	11.4
N2782		09 10 54	40 19 17	1.7E+20	I	1941	79	293	1850.4	0.3
N2835		09 15 37	-22 08 48	8.3E+20	I	5790	80	158	5905.5	0.5
N2831		09 16 43	33 57 18	1.7E+20	I	1841	79	297	1550.6	2.8
N2832		09 16 45	33 57 35	1.7E+20	I	1841	79	297	1550.6	2.5
N2848		09 17 49	-16 18 47	5.1E+20	I	5791	80	125	6587.3	10.0
N2841		09 18 35	51 11 18	1.4E+20	I	2099	79	120	4907.7	0.4
N2859		09 21 15	34 43 42	1.5E+20	I	2101	79	298	7427.4	0.5
N2903		09 29 20	21 43 12	3.3E+20	I	7049	80	137	4369.1	0.2
N2903		09 29 20	21 43 12	3.4E+20	I	5229	80	136	991.0	20.2
N2911		09 31 05	10 22 36	3.3E+20	I	3293	79	142	1550.3	0.6
N2914		09 31 21	10 19 54	3.3E+20	I	3293	79	142	1550.3	4.3
N2955		09 38 15	36 06 35	1.3E+20	I	7720	80	136	4464.6	17.2

TABLE 1—*Continued*

Name		RA (1950)	DEC (1950)	N_H (cm^{-2})	Inst.	Sequence number	start year	start day	Exp. (second)	Offaxis (arcmin)
N2974		09 40 02	-03 28 06	3.7E+20	I	7655	80	128	4767.7	1.1
N2976		09 43 10	68 08 53	4.6E+20	I	3035	79	117	1269.3	28.6
N2992	AGN	09 43 18	-14 05 41	5.2E+20	H	441	78	326	1085.0	4.4
N2992	AGN	09 43 18	-14 05 41	5.2E+20	H	1117	78	327	54.0	4.0
N2992	AGN	09 43 18	-14 05 41	5.2E+20	I	3060	79	316	1462.4	0.4
N2992	AGN	09 43 18	-14 05 41	5.2E+20	I	3061	79	336	1526.9	0.4
N2992	AGN	09 43 18	-14 05 41	5.2E+20	I	6376	80	157	7704.9	0.3
N2993		09 43 23	-14 08 06	5.2E+20	H	441	78	326	1085.0	6.0
N2993		09 43 23	-14 08 06	5.2E+20	H	1117	78	327	54.0	6.3
N2993		09 43 23	-14 08 06	5.2E+20	I	3060	79	316	1462.4	2.6
N2993		09 43 23	-14 08 06	5.2E+20	I	3061	79	336	1526.9	2.6
N2993		09 43 23	-14 08 06	5.2E+20	I	6376	80	157	7704.9	2.8
N3031		09 51 30	69 18 17	4.1E+20	I	2102	79	117	6515.2	0.6
N3031		09 51 30	69 18 17	4.1E+20	H	585	79	123	29284.0	0.1
N3031		09 51 30	69 18 17	4.3E+20	I	466	79	98	4449.8	36.6
N3034		09 51 41	69 54 54	4.1E+20	I	2102	79	117	6515.2	36.9
N3034		09 51 41	69 54 54	4.3E+20	I	466	79	98	4449.8	0.1
N3034		09 51 41	69 54 54	4.3E+20	H	586	79	123	12880.0	0.1
N3067		09 55 26	32 36 30	1.7E+20	I	2712	79	145	1595.3	11.8
N3078		09 56 08	-26 41 12	5.2E+20	I	10242	80	364	5476.8	0.0
N3081		09 57 11	-22 35 05	4.5E+20	I	5251	80	167	1640.6	0.0
N3065		09 57 35	72 24 36	3.4E+20	I	3470	79	117	904.8	3.5
N3066		09 57 51	72 21 54	3.4E+20	I	3470	79	117	904.8	1.1
N3079		09 58 35	55 55 24	8.4E+19	I	423	79	119	845.7	0.1
N3079		09 58 35	55 55 24	8.4E+19	H	4628	79	319	15256.0	14.0
N3077		09 59 22	68 58 30	3.7E+20	I	2105	79	277	8152.7	0.5
N3115		10 02 44	-07 28 30	4.5E+20	I	3920	79	316	2065.0	0.0
N3125		10 04 18	-29 41 30	6.2E+20	I	430	79	168	1779.6	2.4
N3145		10 07 43	-12 11 18	6.1E+20	I	9696	80	356	4589.0	22.8
N3156		10 10 06	03 22 42	2.6E+20	I	6681	79	341	2068.9	22.9
N3166		10 11 10	03 40 30	2.6E+20	I	6681	79	341	2068.9	1.1
N3169		10 11 38	03 43 12	2.6E+20	I	6681	79	341	2068.9	8.6
N3175		10 12 24	-28 37 12	5.7E+20	I	5407	80	167	1858.7	26.1
N3184		10 15 17	41 40 00	1.4E+20	H	2893	79	123	1401.0	0.2
N3222		10 19 50	20 08 24	2.2E+20	I	1945	79	140	2165.9	13.5
N3222		10 19 50	20 08 24	2.2E+20	I	1946	80	135	2310.1	13.5
N3222		10 19 50	20 08 24	2.4E+20	I	7793	80	131	1462.4	20.1
N3227	AGN	10 20 47	20 07 05	2.2E+20	I	1945	79	140	2165.9	0.1
N3227	AGN	10 20 47	20 07 05	2.2E+20	I	1946	80	135	2310.1	0.1
N3227	AGN	10 20 47	20 07 05	2.4E+20	I	7793	80	131	1462.4	25.1
I2574		10 24 40	68 40 06	2.1E+20	I	7050	80	111	6144.1	0.0
N3258		10 26 38	-35 21 00	6.4E+20	I	1896	79	171	2366.2	0.2
N3268		10 27 46	-35 04 11	6.4E+20	I	1896	79	171	2366.2	21.9
N3271		10 28 12	-35 06 11	6.4E+20	I	1896	79	171	2366.2	24.3
N3281		10 29 36	-34 36 00	6.5E+20	I	9220	80	364	921.8	0.0
N3277		10 30 08	28 46 12	1.9E+20	I	2644	79	143	1938.7	26.6
N3310		10 35 39	53 45 54	1.1E+20	I	467	79	118	1389.2	0.1
N3346		10 40 59	15 08 06	2.9E+20	I	10093	80	346	4907.3	1.8
N3351		10 41 19	11 58 05	2.9E+20	I	497	80	145	4310.3	27.7
N3353		10 42 17	56 13 36	6.2E+19	I	6371	80	145	3296.9	0.0
N3367		10 43 56	14 00 48	2.9E+20	I	5793	80	147	6112.1	26.9
N3368		10 44 08	12 05 05	2.8E+20	I	2109	80	148	3614.9	12.7
N3377		10 45 03	14 15 00	2.9E+20	I	5793	80	147	6112.1	6.5
N3379		10 45 11	12 50 47	2.8E+20	I	2110	79	342	1088.5	0.3
N3384		10 45 38	12 53 42	2.8E+20	I	2110	79	342	1088.5	6.9
N3389		10 45 50	12 47 54	2.8E+20	I	2110	79	342	1088.5	9.8
N3395		10 47 02	33 14 41	2.0E+20	I	3936	80	138	5422.2	17.6
N3430		10 49 25	33 12 53	2.0E+20	I	3936	80	138	5422.2	13.3
N3430		10 49 25	33 12 53	2.0E+20	I	6675	80	152	1227.8	0.4
N3445		10 51 34	57 15 18	6.1E+19	I	7764	80	145	1288.4	1.0
N3448		10 51 40	54 34 30	8.6E+19	I	416	79	118	1787.9	0.1
N3455		10 51 52	17 33 05	2.4E+20	I	7757	80	346	5921.5	1.0
N3458		10 52 58	57 23 00	6.1E+19	I	7764	80	145	1288.4	14.7
N3489		10 57 41	14 10 11	1.9E+20	I	5796	80	349	2017.1	0.2

TABLE 1—*Continued*

Name		RA (1950)	DEC (1950)	N_H (cm^{-2})	Inst.	Sequence number	start year	start day	Exp. (second)	Offaxis (arcmin)
N3504		11 00 29	28 14 30	1.9E+20	I	4047	79	341	2514.3	0.5
N3512		11 01 20	28 18 17	1.9E+20	I	4047	79	341	2514.3	11.7
N3516	AGN	11 03 23	72 50 24	3.0E+20	I	1948	79	117	3105.4	0.4
N3516	AGN	11 03 23	72 50 24	3.0E+20	I	1947	79	278	3948.3	0.4
N3585		11 10 50	-26 28 47	5.3E+20	I	7034	80	161	9965.9	2.0
N3593		11 12 00	13 05 24	1.8E+20	I	5797	79	353	4823.0	0.2
N3605		11 14 08	18 17 36	1.5E+20	I	3927	79	341	16041.8	2.7
N3607		11 14 17	18 19 42	1.5E+20	I	3927	79	341	16041.8	0.3
N3608		11 14 21	18 25 36	1.5E+20	I	3927	79	341	16041.8	6.2
N3628		11 17 40	13 52 05	2.0E+20	I	5152	79	339	12680.4	0.0
N3660	AGN	11 21 06	-08 24 00	3.8E+20	I	10228	80	355	5606.3	0.2
N3675		11 23 25	43 51 42	2.3E+20	I	5231	79	325	8318.7	26.0
N3690		11 25 42	58 50 00	1.2E+20	H	442	78	323	3780.0	2.3
N3718		11 29 50	53 20 42	1.1E+20	I	2654	79	119	1100.7	7.7
N3718		11 29 50	53 20 42	1.1E+20	H	1897	79	150	4546.0	3.6
N3729		11 31 04	53 24 00	1.1E+20	I	2654	79	119	1100.7	15.9
N3729		11 31 04	53 24 00	1.1E+20	H	1897	79	150	4546.0	12.7
N3735		11 33 06	70 48 35	1.4E+20	I	4601	79	317	3154.2	23.7
N3735		11 33 06	70 48 35	1.4E+20	I	9157	80	363	6026.8	22.7
N3783	AGN	11 36 33	-37 27 42	9.3E+20	I	7209	80	1	7442.2	0.9
N3801		11 37 41	18 00 24	2.1E+20	I	6644	79	340	2073.7	20.2
N3818		11 39 24	-05 52 42	3.5E+20	I	5799	80	354	1742.5	0.3
N3884		11 43 36	20 41 04	2.6E+20	I	5190	79	352	2439.3	27.6
N3887		11 44 33	-16 34 35	3.4E+20	I	10229	81	5	7310.7	0.2
N3888		11 44 55	56 14 53	1.0E+20	I	6101	79	324	5996.7	14.5
N3893		11 46 01	48 59 24	2.2E+20	I	7759	80	154	3949.3	0.5
N3894		11 46 10	59 41 42	1.7E+20	I	4949	79	324	2828.1	0.1
N3896		11 46 18	48 57 12	2.2E+20	I	7759	80	154	3949.3	3.4
N3898		11 46 36	56 21 47	1.0E+20	I	6101	79	324	5996.7	27.8
N3923		11 48 30	-28 31 42	6.4E+20	I	5800	80	363	4464.6	0.0
N3991		11 54 55	32 36 48	1.7E+20	I	443	79	141	1528.9	2.0
N3990		11 55 01	55 44 18	1.2E+20	I	4548	79	325	1282.0	2.8
N3994		11 55 01	32 33 18	1.7E+20	I	443	79	141	1528.9	1.7
N3995		11 55 10	32 34 17	1.7E+20	I	443	79	141	1528.9	2.4
N3998	AGN	11 55 20	55 44 05	1.2E+20	I	4548	79	325	1282.0	0.2
I0749		11 56 00	43 00 48	1.4E+20	I	7760	80	131	4388.3	2.9
I0750		11 56 17	43 00 06	1.4E+20	I	7760	80	131	4388.3	1.5
N4036		11 58 54	62 10 30	2.1E+20	I	7593	80	161	2102.0	0.2
N4038		11 59 19	-18 35 05	4.1E+20	I	469	79	172	1740.0	0.5
N4038		11 59 19	-18 35 05	4.1E+20	I	7054	80	166	5213.2	0.6
N4041		11 59 39	62 25 00	2.1E+20	I	7593	80	161	2102.0	15.6
N4045		12 00 09	02 15 30	1.8E+20	I	2601	79	171	10359.0	26.4
N4051	AGN	12 00 37	44 48 42	1.3E+20	I	7200	79	346	8796.6	0.8
N4104		12 04 05	28 27 00	1.7E+20	I	4258	79	143	4175.8	30.4
N4105		12 04 06	-29 28 53	5.7E+20	I	5801	80	364	6560.9	0.0
N4145		12 07 30	40 09 41	2.1E+20	I	353	79	138	19928.5	30.2
N4145		12 07 30	40 09 41	2.1E+20	I	352	79	346	6901.0	30.2
N4151	AGN	12 08 00	39 40 54	2.1E+20	I	353	79	138	19928.5	0.9
N4151	AGN	12 08 00	39 40 54	2.1E+20	H	340	79	151	10037.0	0.0
N4151	AGN	12 08 00	39 40 54	2.1E+20	I	352	79	346	6901.0	0.9
N4151	AGN	12 08 00	39 40 54	2.1E+20	H	6395	80	141	9381.0	0.1
N4156		12 08 17	39 44 54	2.1E+20	I	353	79	138	19928.5	6.0
N4156		12 08 17	39 44 54	2.1E+20	H	340	79	151	10037.0	5.2
N4156		12 08 17	39 44 54	2.1E+20	I	352	79	346	6901.0	6.0
N4156		12 08 17	39 44 54	2.1E+20	H	6395	80	141	9381.0	5.0
N4168	VIR	12 09 44	13 29 00	2.6E+20	I	6974	79	340	5108.6	0.0
N4168	VIR	12 09 44	13 29 00	2.6E+20	I	6975	80	176	823.7	0.0
N4178	VIR	12 10 14	11 08 48	1.9E+20	I	4055	79	355	1280.3	27.3
N4178	VIR	12 10 14	11 08 48	2.0E+20	I	6976	79	350	2615.4	0.2
N4178	VIR	12 10 14	11 08 48	2.0E+20	I	6977	80	177	4640.4	0.2
N4190		12 11 13	36 54 35	1.7E+20	I	7816	80	144	3008.5	12.7
N4190		12 11 13	36 54 35	1.7E+20	I	7817	80	177	3708.6	12.7
N4189	VIR	12 11 14	13 42 12	2.6E+20	I	6974	79	340	5108.6	25.6
N4189	VIR	12 11 14	13 42 12	2.6E+20	I	6975	80	176	823.7	25.6

TABLE 1—*Continued*

Name		RA (1950)	DEC (1950)	N_H (cm^{-2})	Inst.	Sequence number	start year	start day	Exp. (second)	Offaxis (arcmin)
N4192	VIR	12 11 15	15 10 48	2.7E+20	I	6978	79	350	6504.6	0.0
N4192	VIR	12 11 15	15 10 48	2.7E+20	I	6979	80	177	7365.0	0.0
N4203		12 12 34	33 28 42	1.2E+20	I	3922	80	178	1543.6	0.0
N4206	VIR	12 12 44	13 18 12	2.8E+20	I	4303	79	340	8710.9	8.3
N4212	VIR	12 13 07	14 10 48	2.7E+20	I	5341	80	346	1795.4	21.9
N4212	VIR	12 13 07	14 10 48	2.8E+20	I	6982	79	339	6305.6	0.2
N4214		12 13 08	36 36 30	1.7E+20	I	7816	80	144	3008.5	22.1
N4214		12 13 08	36 36 30	1.7E+20	H	2897	80	174	2188.0	0.6
N4214		12 13 08	36 36 30	1.7E+20	I	7817	80	177	3708.6	22.1
N4216	VIR	12 13 21	13 25 23	2.8E+20	I	4303	79	340	8710.9	3.3
N4215		12 13 22	06 41 00	1.5E+20	I	10119	80	346	1994.8	0.2
N4224		12 14 01	07 44 24	1.6E+20	I	6711	80	176	2132.8	18.5
N4236		12 14 22	69 45 00	1.8E+20	I	5803	80	145	13484.8	0.3
N4233		12 14 35	07 54 05	1.6E+20	I	6711	80	176	2132.8	26.1
N4235	AGN	12 14 37	07 28 06	1.5E+20	I	6711	80	176	2132.8	0.3
N4244		12 15 00	38 05 11	1.9E+20	I	5153	79	346	13735.1	0.2
N4245		12 15 05	29 52 54	1.7E+20	I	6712	79	350	2440.5	14.6
N4246		12 15 25	07 27 54	1.5E+20	I	6711	80	176	2132.8	12.1
N4251		12 15 36	28 27 06	1.8E+20	I	7036	80	179	10103.0	0.2
N4254	VIR	12 16 17	14 41 42	2.8E+20	I	4306	80	177	10781.0	0.3
N4258		12 16 29	47 35 00	1.2E+20	H	10756	78	326	1478.0	0.1
N4260		12 16 49	06 22 36	1.6E+20	I	2672	79	181	2148.8	16.5
N4260		12 16 49	06 22 36	1.6E+20	I	6309	80	347	6905.9	15.6
N4261	AGN	12 16 50	06 06 05	1.6E+20	I	2672	79	181	2148.8	0.0
N4261	AGN	12 16 50	06 06 05	1.6E+20	I	6309	80	347	6905.9	1.2
N4267	VIR	12 17 13	13 04 35	2.8E+20	I	6984	79	351	5051.2	0.2
N4270		12 17 17	05 44 30	1.6E+20	I	2672	79	181	2148.8	22.6
N4270		12 17 17	05 44 30	1.6E+20	I	6309	80	347	6905.9	23.7
N4274		12 17 20	29 53 17	1.7E+20	I	6712	79	350	2440.5	26.0
N4273		12 17 23	05 37 17	1.6E+20	I	2672	79	181	2148.8	30.0
N4273		12 17 23	05 37 17	1.6E+20	I	6309	80	347	6905.9	31.1
N4281		12 17 49	05 39 54	1.6E+20	I	2672	79	181	2148.8	30.0
N4281		12 17 49	05 39 54	1.6E+20	I	6309	80	347	6905.9	31.2
N4291		12 18 07	75 38 47	2.9E+20	H	559	78	326	5902.0	6.4
N4291		12 18 07	75 38 47	2.9E+20	I	5424	80	111	13112.9	6.4
N4291		12 18 07	75 38 47	3.2E+20	I	5233	79	324	2896.3	18.6
N4298	VIR	12 19 00	14 53 05	2.7E+20	I	4305	79	351	14919.0	1.5
N4303		12 19 22	04 45 05	1.7E+20	I	3267	79	178	1375.5	16.6
N4303		12 19 22	04 45 05	1.7E+20	I	6986	80	176	10425.6	0.3
N4319		12 19 34	75 35 54	2.9E+20	I	5424	80	111	13112.9	1.0
N4319		12 19 34	75 35 54	3.2E+20	I	5233	79	324	2896.3	18.4
N4321	VIR	12 20 23	16 06 00	2.4E+20	H	2892	79	158	3942.0	0.2
N4321	VIR	12 20 23	16 06 00	2.4E+20	I	4300	79	168	857.9	1.9
N4321	VIR	12 20 23	16 06 00	2.4E+20	I	4301	79	178	1914.4	1.9
N4321	VIR	12 20 23	16 06 00	2.4E+20	H	4968	79	344	13183.0	1.7
N4321	VIR	12 20 23	16 06 00	2.4E+20	H	8968	80	181	23210.0	1.7
N4340	VIR	12 21 04	17 00 00	2.5E+20	I	6988	81	10	10654.9	2.5
N4342	VIR	12 21 07	07 20 00	1.6E+20	I	6992	79	349	4854.0	19.7
N4342	VIR	12 21 07	07 20 00	1.6E+20	I	6993	80	178	4753.6	19.7
N4350	VIR	12 21 26	16 58 17	2.5E+20	I	6988	81	10	10654.9	3.0
N4351	VIR	12 21 29	12 28 54	2.6E+20	I	6990	79	350	1581.4	0.0
N4365	VIR	12 21 56	07 35 42	1.6E+20	I	6992	79	349	4854.0	0.2
N4365	VIR	12 21 56	07 35 42	1.6E+20	I	6993	80	178	4753.6	0.2
N4386		12 22 22	75 48 17	2.9E+20	I	5424	80	111	13112.9	17.1
N4386		12 22 22	75 48 17	3.2E+20	I	5233	79	324	2896.3	6.1
N4374	VIR	12 22 31	13 09 48	2.6E+20	I	278	78	355	34963.8	23.8
N4374	VIR	12 22 31	13 09 48	2.6E+20	H	4320	79	188	41229.0	0.3
N4374	VIR	12 22 31	13 09 48	2.7E+20	I	4311	79	183	4558.2	17.8
N4378		12 22 45	05 12 06	1.7E+20	I	9155	80	347	5293.6	0.5
N4382	VIR	12 22 53	18 28 00	2.7E+20	I	2121	79	180	8148.0	0.0
N4382	VIR	12 22 53	18 28 00	2.7E+20	I	6994	80	179	10361.5	0.2
N4383	VIR	12 22 54	16 44 47	2.5E+20	I	6988	81	10	10655.0	27.9
N4387	VIR	12 23 09	13 05 18	2.6E+20	I	278	78	355	34963.8	13.5
N4387	VIR	12 23 09	13 05 18	2.6E+20	I	7590	80	190	1577.6	32.4

TABLE 1—*Continued*

Name		RA (1950)	DEC (1950)	N_H (cm^{-2})	Inst.	Sequence number	start year	start day	Exp. (second)	Offaxis (arcmin)
N4387	VIR	12 23 09	13 05 18	2.7E+20	I	4311	79	183	4558.2	11.8
N4385		12 23 12	00 50 54	1.9E+20	I	4049	79	354	823.3	1.8
N4388	VIR	12 23 14	12 56 17	2.6E+20	I	278	78	355	34963.8	11.8
N4388	VIR	12 23 14	12 56 17	2.7E+20	I	4311	79	183	4558.2	19.0
N4394	VIR	12 23 25	18 29 23	2.7E+20	I	2121	79	180	8148.0	7.7
N4394	VIR	12 23 25	18 29 23	2.7E+20	I	6994	80	179	10361.5	7.9
N4406	VIR	12 23 40	13 13 23	2.6E+20	I	278	78	355	34963.8	14.2
N4406	VIR	12 23 40	13 13 23	2.6E+20	I	7590	80	190	1577.6	22.9
N4406	VIR	12 23 40	13 13 23	2.7E+20	I	4311	79	183	4558.2	0.8
N4406	VIR	12 23 40	13 13 23	2.7E+20	H	4321	79	186	25430.0	0.8
N4410		12 23 56	09 17 48	1.8E+20	I	280	78	358	46778.1	19.8
N4414		12 23 57	31 29 53	1.5E+20	I	542	78	353	5028.5	29.7
N4417	VIR	12 24 18	09 51 42	1.8E+20	I	280	78	358	46778.1	23.9
N4417	VIR	12 24 18	09 51 42	1.8E+20	H	2891	80	174	1550.0	11.4
N4424	VIR	12 24 40	09 41 47	1.8E+20	I	280	78	358	46778.1	12.7
N4424	VIR	12 24 40	09 41 47	1.8E+20	H	2891	80	174	1550.0	0.5
N4425	VIR	12 24 42	13 00 42	2.6E+20	I	278	78	355	34963.8	10.3
N4425	VIR	12 24 42	13 00 42	2.6E+20	I	7590	80	190	1577.6	18.1
N4425	VIR	12 24 42	13 00 42	2.7E+20	I	4311	79	183	4558.2	19.7
N4429	VIR	12 24 54	11 23 06	2.3E+20	I	6999	81	10	5460.6	0.2
N4435	VIR	12 25 08	13 21 23	2.6E+20	I	278	78	355	34963.8	27.0
N4435	VIR	12 25 08	13 21 23	2.6E+20	I	7590	80	190	1577.6	4.4
N4435	VIR	12 25 08	13 21 23	2.6E+20	H	9008	81	14	50308.0	4.5
N4435	VIR	12 25 08	13 21 23	2.7E+20	I	4311	79	183	4558.2	22.2
N4438	VIR	12 25 14	13 17 06	2.6E+20	I	278	78	355	34963.8	24.8
N4438	VIR	12 25 14	13 17 06	2.6E+20	I	7590	80	190	1577.6	0.2
N4438	VIR	12 25 14	13 17 06	2.6E+20	H	9008	81	14	50308.0	0.1
N4438	VIR	12 25 14	13 17 06	2.7E+20	I	4311	79	183	4558.2	22.6
N4449		12 25 47	44 22 17	1.4E+20	I	2123	79	167	1612.3	0.3
N4449		12 25 47	44 22 17	1.4E+20	H	4967	79	344	31862.0	1.2
N4450	VIR	12 25 59	17 21 42	2.4E+20	I	7001	79	353	3256.0	0.2
N4458	VIR	12 26 25	13 31 06	2.6E+20	I	7590	80	190	1577.6	22.4
N4458	VIR	12 26 25	13 31 06	2.6E+20	I	7003	81	11	5068.5	16.4
N4459	VIR	12 26 29	14 15 18	2.6E+20	I	7003	81	11	5068.5	38.1
N4459	VIR	12 26 29	14 15 18	2.7E+20	I	281	78	356	14695.0	26.9
N4459	VIR	12 26 29	14 15 18	2.7E+20	I	2124	79	181	4388.1	0.3
N4461	VIR	12 26 31	13 27 42	2.6E+20	I	7590	80	190	1577.6	21.7
N4461	VIR	12 26 31	13 27 42	2.6E+20	I	7003	81	11	5068.5	17.3
N4464	VIR	12 26 49	08 26 06	1.6E+20	I	4308	79	183	7672.2	11.6
N4467	VIR	12 26 57	08 16 12	1.6E+20	I	4308	79	183	7672.2	3.7
N4467	VIR	12 26 57	08 16 12	1.6E+20	H	7068	79	365	32153.0	4.3
N4472	VIR	12 27 14	08 16 42	1.6E+20	I	4308	79	183	7672.2	0.8
N4472	VIR	12 27 14	08 16 42	1.6E+20	I	4052	79	354	1657.9	35.3
N4472	VIR	12 27 14	08 16 42	1.6E+20	H	7068	79	365	32153.0	0.1
N4472	VIR	12 27 14	08 16 42	1.6E+20	I	5721	81	6	27849.3	41.2
N4473	VIR	12 27 17	13 42 24	2.6E+20	I	7003	81	11	5068.5	3.2
N4473	VIR	12 27 17	13 42 24	2.7E+20	I	281	78	356	14695.0	20.5
N4473	VIR	12 27 17	13 42 24	2.7E+20	I	2124	79	181	4388.1	34.6
N4474	VIR	12 27 22	14 20 42	2.7E+20	I	281	78	356	14695.0	22.7
N4474	VIR	12 27 22	14 20 42	2.7E+20	I	2124	79	181	4388.1	14.1
N4477	VIR	12 27 31	13 54 42	2.6E+20	I	7003	81	11	5068.5	15.3
N4477	VIR	12 27 31	13 54 42	2.7E+20	I	281	78	356	14695.0	8.8
N4477	VIR	12 27 31	13 54 42	2.7E+20	I	2124	79	181	4388.1	25.3
N4479	VIR	12 27 46	13 51 12	2.6E+20	I	7003	81	11	5068.5	12.9
N4479	VIR	12 27 46	13 51 12	2.7E+20	I	281	78	356	14695.0	9.4
N4492	VIR	12 28 27	08 21 18	1.6E+20	I	4308	79	183	7672.2	19.3
N4501	VIR	12 29 28	14 41 42	2.5E+20	I	4304	80	178	10272.0	1.0
N4503	VIR	12 29 34	11 27 12	2.3E+20	I	279	78	359	20344.0	12.1
N4519	VIR	12 30 58	08 55 47	1.6E+20	I	4310	80	177	9673.0	30.3
N4519	VIR	12 30 58	08 55 47	1.7E+20	I	7445	80	171	1865.6	21.9
N4522	VIR	12 31 08	09 27 00	1.7E+20	I	7445	80	171	1865.6	10.4
N4526	VIR	12 31 31	07 58 30	1.6E+20	I	4309	79	190	8388.8	0.5
N4526	VIR	12 31 31	07 58 30	1.6E+20	I	4310	80	177	9673.0	29.8
N4527		12 31 35	02 55 42	1.9E+20	I	9134	80	196	3688.3	28.3

TABLE 1—*Continued*

Name		RA (1950)	DEC (1950)	N_H (cm^{-2})	Inst.	Sequence number	start year	start day	Exp. (second)	Offaxis (arcmin)
N4527		12 31 35	02 55 42	1.9E+20	I	9133	80	197	2076.5	0.0
N4535	VIR	12 31 48	08 28 36	1.6E+20	I	4310	80	177	9673.0	0.6
N4536		12 31 54	02 27 42	1.9E+20	I	9134	80	196	3688.3	0.3
N4536		12 31 54	02 27 42	1.9E+20	I	9133	80	197	2076.5	28.4
N4540	VIR	12 32 20	15 49 35	2.3E+20	I	7795	80	190	1728.8	25.0
I3528	AGN	12 32 25	15 50 30	2.3E+20	I	7795	80	190	1728.8	26.3
N4507		12 32 54	-39 38 00	7.1E+20	I	2664	80	9	809.3	0.0
N4548	VIR	12 32 55	14 46 24	2.4E+20	I	7007	79	348	5008.3	0.0
N4548	VIR	12 32 55	14 46 24	2.4E+20	I	7011	80	176	1423.1	27.5
N4550	VIR	12 32 59	12 29 47	2.5E+20	I	4313	79	182	8426.0	10.4
N4551	VIR	12 33 06	12 32 24	2.5E+20	I	4313	79	182	8426.0	7.6
N4552	VIR	12 33 08	12 50 00	2.5E+20	I	4313	79	182	8426.0	10.0
N4565		12 33 52	26 15 36	1.3E+20	I	9974	81	16	20694.6	7.0
N4564	VIR	12 33 55	11 42 54	2.4E+20	I	4317	79	182	5456.1	6.0
N4564	VIR	12 33 55	11 42 54	2.4E+20	H	2898	80	174	1624.0	0.3
N4564	VIR	12 33 55	11 42 54	2.5E+20	I	2126	79	178	1058.8	29.8
N4564	VIR	12 33 55	11 42 54	2.5E+20	I	4315	79	191	7290.0	29.0
N4567	VIR	12 34 01	11 32 00	2.4E+20	I	4317	79	182	5456.1	5.0
N4569	VIR	12 34 19	13 26 23	2.5E+20	I	4045	79	352	1948.1	0.6
N4569	VIR	12 34 19	13 26 23	2.5E+20	I	4314	79	353	3320.3	0.6
N4571	VIR	12 34 25	14 29 36	2.4E+20	I	7007	79	348	5008.3	27.5
N4571	VIR	12 34 25	14 29 36	2.4E+20	I	7011	80	176	1423.1	0.0
N4578	VIR	12 34 59	09 49 47	1.7E+20	I	10120	81	8	2248.4	0.0
N4579	VIR	12 35 12	12 05 35	2.5E+20	I	2126	79	178	1058.8	0.4
N4579	VIR	12 35 12	12 05 35	2.5E+20	I	4315	79	191	7290.0	0.6
N4579	VIR	12 35 12	12 05 35	2.5E+20	H	7067	79	365	9540.0	0.1
N4589		12 35 28	74 28 00	2.1E+20	I	10243	80	364	5722.9	0.1
N4593	AGN	12 37 05	-05 04 11	2.1E+20	I	6717	80	171	948.6	19.6
N4594		12 37 23	-11 21 00	3.8E+20	I	2127	79	178	5282.2	0.0
N4594		12 37 23	-11 21 00	3.8E+20	I	2128	80	202	1207.4	0.0
N4597		12 37 38	-05 31 30	2.1E+20	I	6717	80	171	948.6	21.8
N4602		12 38 03	-04 52 00	2.1E+20	I	6717	80	171	948.6	20.3
N4603		12 38 11	-40 42 05	7.7E+20	I	6054	80	11	12295.4	9.4
N4603		12 38 11	-40 42 05	7.7E+20	I	6055	80	12	14814.4	29.2
N4621	VIR	12 39 31	11 55 12	2.4E+20	I	2130	79	179	6160.6	23.8
N4621	VIR	12 39 31	11 55 12	2.5E+20	I	2129	80	193	6250.1	0.5
N4631		12 39 41	32 48 47	1.3E+20	I	471	78	354	3047.6	0.2
N4631		12 39 41	32 48 47	1.3E+20	H	4367	79	185	9191.0	0.1
N4638	VIR	12 40 16	11 42 54	2.4E+20	I	2130	79	179	6160.6	14.1
N4638	VIR	12 40 16	11 42 54	2.5E+20	I	2129	80	193	6250.1	16.7
N4636		12 40 17	02 57 42	1.9E+20	I	412	79	179	1383.9	0.3
N4636		12 40 17	02 57 42	1.9E+20	H	7038	80	12	31764.0	0.0
N4639	VIR	12 40 21	13 31 53	2.3E+20	I	7013	80	179	5145.1	8.7
N4639	VIR	12 40 21	13 31 53	2.3E+20	I	7014	80	180	4430.6	8.7
N4643		12 40 48	02 15 06	1.8E+20	I	2133	79	178	4151.5	0.3
N4647	VIR	12 41 01	11 51 12	2.4E+20	I	2130	79	179	6160.6	1.7
N4647	VIR	12 41 01	11 51 12	2.4E+20	H	2132	80	192	16925.0	1.7
N4647	VIR	12 41 01	11 51 12	2.5E+20	I	2129	80	193	6250.1	22.8
N4649	VIR	12 41 09	11 49 30	2.4E+20	I	2130	79	179	6160.6	0.9
N4649	VIR	12 41 09	11 49 30	2.4E+20	H	2132	80	192	16925.0	0.9
N4649	VIR	12 41 09	11 49 30	2.5E+20	I	2129	80	193	6250.1	25.1
N4651	VIR	12 41 13	16 40 05	2.0E+20	I	3241	79	180	3814.1	3.7
N4645		12 41 25	-41 28 42	7.7E+20	I	6056	80	212	11986.1	13.0
N4654	VIR	12 41 26	13 24 00	2.3E+20	I	7013	80	179	5145.1	8.9
N4654	VIR	12 41 26	13 24 00	2.3E+20	I	7014	80	180	4430.6	8.9
N4656		12 41 32	32 26 30	1.3E+20	I	471	78	354	3047.6	32.4
N4660	VIR	12 42 01	11 27 36	2.4E+20	I	2130	79	179	6160.6	26.1
N4665		12 42 33	03 19 47	1.9E+20	I	7016	80	178	5763.1	0.3
N4665		12 42 33	03 19 47	1.9E+20	I	7017	80	347	6408.1	0.3
N4689	VIR	12 45 15	14 02 05	2.2E+20	I	7018	80	180	4297.1	0.2
N4698	VIR	12 45 52	08 45 35	1.8E+20	I	7022	80	178	5580.6	0.2
N4698	VIR	12 45 52	08 45 35	1.8E+20	I	7023	80	179	4712.6	0.2
N4697		12 46 01	-05 31 42	2.0E+20	I	2134	79	178	4957.4	0.7
N4697		12 46 01	-05 31 42	2.1E+20	I	4004	79	201	3484.6	14.2

TABLE 1—*Continued*

Name		RA (1950)	DEC (1950)	N_H (cm^{-2})	Inst.	Sequence number	start year	start day	Exp. (second)	Offaxis (arcmin)
N4736		12 48 32	41 23 36	1.4E+20	H	2699	79	345	1840.0	0.4
N4754	VIR	12 49 47	11 35 05	2.2E+20	I	7024	79	353	6561.0	5.3
N4754	VIR	12 49 47	11 35 05	2.2E+20	I	7025	80	179	5681.7	5.3
N4753		12 49 48	-00 55 42	1.6E+20	I	7039	80	198	12092.6	0.0
N4756		12 50 15	-15 08 36	3.5E+20	I	1900	79	8	5511.3	4.3
N4762	VIR	12 50 25	11 30 06	2.2E+20	I	7024	79	353	6561.0	5.3
N4762	VIR	12 50 25	11 30 06	2.2E+20	I	7025	80	179	5681.7	5.3
N4782		12 51 59	-12 18 06	3.5E+20	I	444	79	178	1422.2	0.3
N4798		12 52 34	27 41 00	9.7E+19	I	3917	79	183	3187.8	16.6
N4808		12 53 17	04 34 24	2.1E+20	I	5375	80	346	1904.5	19.8
I3896		12 53 51	-05 04 35	2.1E+20	I	544	79	7	3046.0	26.8
I3896		12 53 51	-05 04 35	2.1E+20	I	4645	80	196	25094.9	26.8
N4826		12 54 17	21 57 05	2.4E+20	I	3176	79	181	1540.8	21.4
N4826		12 54 17	21 57 05	2.6E+20	I	2136	79	181	4867.4	0.1
N4845		12 55 28	01 50 47	1.7E+20	I	9156	80	198	4789.7	0.5
N4861		12 56 40	35 07 54	1.1E+20	I	445	78	352	2604.7	0.2
N4880		12 57 40	12 45 05	2.2E+20	I	5990	79	352	3126.5	11.3
N4926		12 59 29	27 53 36	9.0E+19	I	1790	79	6	6381.4	28.5
N4939		13 01 38	-10 04 24	3.3E+20	I	3968	79	205	950.6	22.9
I4182		13 03 30	37 52 30	1.0E+20	H	2895	79	345	3035.0	0.5
N5033		13 11 08	36 51 47	1.0E+20	I	5128	80	180	6215.5	35.4
N5037		13 12 22	-16 19 36	5.0E+20	I	6653	80	12	1389.6	13.1
N5044		13 12 44	-16 07 18	5.0E+20	I	6653	80	12	1389.6	1.0
N5049		13 13 19	-16 08 00	5.0E+20	I	6653	80	12	1389.6	7.7
N5054		13 14 19	-16 22 06	5.0E+20	I	6653	80	12	1389.6	26.2
N5068		13 16 13	-20 46 35	7.9E+20	I	5807	80	204	4265.4	0.2
N5077		13 16 53	-12 23 42	3.1E+20	I	10244	81	32	6140.5	0.3
N5079		13 16 59	-12 26 12	3.1E+20	I	10244	81	32	6140.5	3.1
N5084		13 17 34	-21 33 54	8.0E+20	I	8996	80	363	3938.3	30.9
N5088		13 17 42	-12 18 47	3.1E+20	I	10244	81	32	6140.5	13.1
N5101		13 19 01	-27 10 06	5.0E+20	I	2138	79	8	4144.2	1.0
N5102		13 19 07	-36 22 06	4.7E+20	I	7040	80	10	1896.0	0.2
N5128	AGN	13 22 32	-42 45 30	8.3E+20	I	477	79	35	12473.0	0.6
N5128	AGN	13 22 32	-42 45 30	8.3E+20	H	4495	79	216	31472.0	0.0
N5128	AGN	13 22 32	-42 45 30	8.4E+20	H	475	79	15	16421.0	9.5
N5128	AGN	13 22 32	-42 45 30	8.4E+20	I	4493	79	214	14803.1	9.5
N5135		13 22 56	-29 34 17	4.6E+20	I	5255	80	9	2266.4	0.2
N5150		13 24 50	-29 18 12	4.6E+20	I	5255	80	9	2266.4	29.7
N5204		13 27 44	58 40 42	1.6E+20	I	7635	80	159	6975.4	0.3
N5194		13 27 46	47 27 17	1.3E+20	H	3047	79	345	22884.0	0.1
N5195		13 27 53	47 31 47	1.3E+20	H	3047	79	345	22884.0	4.7
I4296		13 33 47	-33 42 24	4.3E+20	I	1902	80	207	10592.7	13.3
N5236		13 34 10	-29 36 47	4.2E+20	I	588	79	212	5708.1	0.0
N5236		13 34 10	-29 36 47	4.2E+20	H	587	80	15	24188.0	0.0
N5236		13 34 10	-29 36 47	4.2E+20	H	10447	81	44	19644.0	0.0
N5248		13 35 03	09 08 30	2.1E+20	I	9136	81	28	3639.6	0.2
N5253		13 37 05	-31 23 23	4.0E+20	H	2889	79	219	2197.0	0.2
N5253		13 37 05	-31 23 23	4.0E+20	I	7061	80	363	6092.7	0.2
N5253		13 37 05	-31 23 23	4.0E+20	H	10315	81	45	21686.0	0.2
N5302		13 45 58	-30 15 54	4.3E+20	I	7822	80	205	4788.7	19.0
I4329		13 46 14	-30 02 47	4.3E+20	H	344	79	218	2363.0	0.5
I4329		13 46 14	-30 02 47	4.3E+20	I	7822	80	205	4788.7	22.5
I4329A	AGN	13 46 28	-30 03 42	4.3E+20	H	344	79	218	2363.0	3.5
I4329A	AGN	13 46 28	-30 03 42	4.3E+20	I	7822	80	205	4788.7	25.1
N5322		13 47 35	60 26 23	1.8E+20	I	10245	80	358	5851.0	0.1
N5313		13 47 37	40 14 00	9.2E+19	I	3935	79	347	5194.6	4.8
N5318		13 48 18	33 57 00	1.2E+20	I	4549	79	348	2125.3	1.1
N5326		13 48 42	39 49 12	9.2E+19	I	3935	79	347	5194.6	30.1
N5326		13 48 42	39 49 12	9.6E+19	I	3933	79	347	4378.1	10.7
N5350		13 51 14	40 36 42	1.1E+20	I	3932	79	347	3217.6	4.5
N5350		13 51 14	40 36 42	1.1E+20	H	8929	80	181	9648.0	5.0
N5354		13 51 20	40 32 30	1.1E+20	H	8929	80	181	9648.0	0.7
N5353		13 51 21	40 31 30	1.1E+20	I	3932	79	347	3217.6	4.5
N5353		13 51 21	40 31 30	1.1E+20	H	8929	80	181	9648.0	0.4

TABLE 1—*Continued*

Name		RA (1950)	DEC (1950)	N_H (cm^{-2})	Inst.	Sequence number	start year	start day	Exp. (second)	Offaxis (arcmin)
N5371		13 53 33	40 42 24	1.1E+20	I	3932	79	347	3217.6	23.4
N5363		13 53 37	05 30 00	2.1E+20	I	7277	81	4	1582.3	0.2
N5364		13 53 42	05 15 36	2.1E+20	I	7277	81	4	1582.3	14.5
N5410		13 58 48	41 13 00	1.2E+20	I	3151	79	167	1820.4	0.8
N5457		14 01 28	54 35 35	1.2E+20	I	2140	79	6	10383.4	0.5
N5457		14 01 28	54 35 35	1.2E+20	I	2141	79	167	6074.6	0.5
N5457		14 01 28	54 35 35	1.2E+20	H	2899	79	365	2740.0	0.5
N5473		14 02 59	55 07 54	1.3E+20	I	8337	80	356	3368.6	22.4
N5474		14 03 15	53 54 00	1.2E+20	I	7636	80	155	6628.2	0.3
N5477		14 03 47	54 42 06	1.2E+20	I	2140	79	6	10383.4	20.8
N5477		14 03 47	54 42 06	1.2E+20	I	2141	79	167	6074.6	20.8
N5485		14 05 27	55 14 11	1.3E+20	I	8337	80	356	3368.6	0.4
N5506	AGN	14 10 38	-02 58 30	3.8E+20	I	3062	79	202	2257.1	1.1
N5506	AGN	14 10 38	-02 58 30	3.8E+20	I	3063	79	211	1901.4	1.1
N5506	AGN	14 10 38	-02 58 30	3.8E+20	I	7204	80	194	6454.3	0.0
N5506	AGN	14 10 38	-02 58 30	3.8E+20	I	9502	81	5	2942.3	0.0
I0989		14 12 18	03 21 00	2.4E+20	I	4550	80	17	1486.2	0.8
N5532		14 14 25	11 02 18	1.9E+20	I	1905	79	24	3229.4	6.4
N5548	AGN	14 15 43	25 22 00	1.7E+20	I	356	79	180	22397.2	0.2
N5548	AGN	14 15 43	25 22 00	1.7E+20	H	6397	80	181	14288.0	0.2
N5548	AGN	14 15 43	25 22 00	1.7E+20	H	8315	80	182	11363.0	10.0
N5566		14 17 49	04 09 41	2.3E+20	I	2143	80	18	4901.6	0.6
N5566		14 17 49	04 09 41	2.4E+20	I	6685	80	17	2543.2	21.9
N5585		14 18 12	56 57 30	1.4E+20	I	7637	80	154	6197.9	0.0
N5574		14 18 25	03 28 00	2.4E+20	I	6685	80	17	2543.2	20.9
N5576		14 18 33	03 29 53	2.4E+20	I	6685	80	17	2543.2	19.9
N5645		14 28 10	07 29 47	2.0E+20	I	3300	79	191	1909.4	9.8
I1024		14 28 55	03 13 48	2.6E+20	I	4551	80	23	1929.1	0.0
N5643		14 29 28	-43 57 12	1.1E+21	I	5252	80	23	1541.2	0.0
N5674		14 31 21	05 39 35	2.4E+20	I	6361	80	36	5286.0	0.9
N5682		14 32 58	48 53 24	2.3E+20	I	2625	80	3	2113.9	1.9
N5683	AGN	14 33 06	48 52 54	2.3E+20	I	2625	80	3	2113.9	0.9
N5689		14 33 44	48 57 35	2.3E+20	I	2625	80	3	2113.9	8.4
N5728		14 39 37	-17 02 17	7.4E+20	I	5256	80	48	1493.7	0.2
N5838		15 02 54	02 17 36	4.1E+20	I	10456	81	52	16108.1	0.0
N5838		15 02 54	02 17 36	4.2E+20	I	9975	81	26	14344.0	33.8
N5846		15 03 56	01 47 47	4.1E+20	I	10456	81	52	16108.1	33.6
N5846		15 03 56	01 47 47	4.2E+20	I	9975	81	26	14344.0	0.5
N5850		15 04 35	01 44 12	4.2E+20	I	9975	81	26	14344.0	9.9
N5866		15 05 07	55 57 17	1.5E+20	I	2144	79	6	2051.4	0.3
N5879		15 08 29	57 11 23	1.5E+20	I	9143	80	357	2481.0	0.0
N5907		15 14 37	56 30 23	1.4E+20	I	7062	80	2	3855.0	0.1
N5898		15 15 17	-23 55 00	8.8E+20	I	1997	79	57	1742.2	17.4
N5898		15 15 17	-23 55 00	8.8E+20	I	1998	79	215	1966.5	17.4
N5898		15 15 17	-23 55 00	8.8E+20	I	9647	81	39	2569.2	18.0
N5898		15 15 17	-23 55 00	8.8E+20	I	7493	81	41	2352.4	18.0
N5903		15 15 40	-23 53 05	8.8E+20	I	1997	79	57	1742.2	21.6
N5903		15 15 40	-23 53 05	8.8E+20	I	1998	79	215	1966.5	21.6
N5903		15 15 40	-23 53 05	8.8E+20	I	9647	81	39	2569.2	22.3
N5903		15 15 40	-23 53 05	8.8E+20	I	7493	81	41	2352.4	22.3
N5936		15 27 39	13 09 36	3.4E+20	I	803	79	27	2236.7	21.7
N5981		15 36 51	59 33 12	1.8E+20	I	6646	80	2	1975.9	17.3
N5982		15 37 38	59 31 06	1.8E+20	I	6646	80	2	1975.9	13.0
N5985		15 38 36	59 29 36	1.8E+20	I	6646	80	2	1975.9	9.9
N6027		15 57 00	20 54 12	3.9E+20	I	462	79	36	1163.1	5.2
N6034		16 01 10	17 20 07	3.4E+20	I	3923	79	225	1541.5	1.4
N6052		16 03 01	20 40 30	3.9E+20	I	411	79	242	827.6	0.2
N6146		16 23 34	40 59 24	9.4E+19	I	4547	80	200	1123.2	1.4
N6314		17 10 33	23 19 48	4.7E+20	I	4933	80	71	1932.3	18.2
N6300		17 12 18	-62 45 47	7.6E+20	I	6373	80	72	3113.0	0.1
N6454		17 44 00	55 43 00	3.8E+20	I	421	79	205	990.6	0.1
N6503		17 49 58	70 09 30	4.0E+20	I	2720	79	203	1810.7	9.9
N6503		17 49 58	70 09 30	4.1E+20	I	8846	80	148	828.7	6.9
N6503		17 49 58	70 09 30	4.2E+20	I	8888	80	150	375.8	29.5

TABLE 1—*Continued*

Name		RA (1950)	DEC (1950)	N_H (cm^{-2})	Inst.	Sequence number	start year	start day	Exp. (second)	Offaxis (arcmin)
N6621		18 13 09	68 20 54	5.3E+20	I	8885	80	148	1028.9	22.5
N6643		18 21 14	74 32 42	6.2E+20	I	3092	79	168	1367.3	22.2
N6643		18 21 14	74 32 42	6.2E+20	I	7696	80	197	19603.5	22.3
N6654		18 25 13	73 09 12	5.8E+20	I	5193	80	96	2022.1	32.6
N6744		19 05 02	-63 56 17	6.1E+20	I	7063	80	270	20546.1	1.8
N6814	AGN	19 39 55	-10 26 36	9.6E+20	I	354	79	102	26650.1	0.5
N6814	AGN	19 39 55	-10 26 36	9.6E+20	H	345	79	111	2641.0	0.5
N6822		19 42 07	-14 55 42	9.0E+20	H	2729	79	304	33386.0	2.9
N6872		20 11 40	-70 55 30	5.2E+20	I	1858	79	278	6609.4	8.8
N6876		20 13 05	-71 01 00	5.2E+20	I	1858	79	278	6609.4	0.0
N6877		20 13 21	-71 00 36	5.2E+20	I	1858	79	278	6609.4	1.4
N6880		20 14 16	-71 01 00	5.2E+20	I	1858	79	278	6609.4	5.8
N6890		20 14 50	-44 57 24	4.5E+20	I	5253	79	300	1567.5	0.2
N6946		20 33 48	59 59 00	2.0E+21	I	422	79	145	4879.5	0.1
N6946		20 33 48	59 59 00	2.0E+21	I	10314	80	345	20871.7	0.1
N6946		20 33 48	59 59 00	2.0E+21	I	10597	81	27	7444.1	0.1
N6951		20 36 37	65 55 54	1.5E+21	I	9137	81	27	1203.1	0.1
N6962		20 44 45	00 08 00	5.8E+20	I	10691	81	114	5186.8	2.3
N6963		20 44 46	00 17 54	5.8E+20	I	10691	81	114	5186.8	7.9
N6964		20 44 50	00 06 48	5.8E+20	I	10691	81	114	5186.8	3.2
I5063		20 48 12	-57 15 11	4.8E+20	I	5254	80	123	2087.1	0.1
N7213	AGN	22 06 12	-47 25 00	1.9E+20	I	6714	80	136	1648.8	0.2
N7213	AGN	22 06 12	-47 25 00	2.0E+20	I	2236	79	295	1331.7	19.4
N7236		22 12 18	13 36 06	4.9E+20	H	1913	79	151	6828.0	3.0
N7237		22 12 20	13 35 30	4.9E+20	H	1913	79	151	6828.0	3.5
N7314		22 33 00	-26 18 30	2.0E+20	H	1160	79	151	2217.0	13.9
N7320		22 33 45	33 41 24	7.5E+20	I	7827	80	363	2879.7	0.9
N7320		22 33 45	33 41 24	7.6E+20	I	9145	80	364	1207.8	30.9
N7331		22 34 47	34 09 30	7.5E+20	I	7827	80	363	2879.7	31.7
N7331		22 34 47	34 09 30	7.6E+20	I	9145	80	364	1207.8	0.0
N7332		22 35 01	23 32 17	4.5E+20	I	10122	80	363	1729.9	0.2
N7339		22 35 23	23 31 30	4.5E+20	I	10122	80	363	1729.9	5.3
N7343		22 36 19	33 48 30	7.6E+20	I	9145	80	364	1207.8	28.3
I1459		22 54 23	-36 43 47	1.2E+20	I	6674	80	157	3277.3	0.2
I5269		22 54 57	-36 17 42	1.2E+20	I	6674	80	157	3277.4	27.0
N7469	AGN	23 00 44	08 36 17	4.7E+20	H	3168	79	151	2290.0	0.6
N7469	AGN	23 00 44	08 36 17	4.7E+20	I	1977	80	171	1938.6	0.2
N7469	AGN	23 00 44	08 36 17	4.7E+20	I	1978	80	355	1991.0	0.2
N7469	AGN	23 00 44	08 36 17	4.7E+20	H	10218	81	6	12450.0	0.1
I5283		23 00 46	08 37 24	4.7E+20	H	3168	79	151	2290.0	1.7
I5283		23 00 46	08 37 24	4.7E+20	H	10218	81	6	12450.0	1.2
N7496		23 06 59	-43 42 00	2.0E+20	I	435	79	141	2390.2	0.2
N7552		23 13 25	-42 51 30	1.9E+20	I	5259	79	324	2056.5	0.2
N7552		23 13 25	-42 51 30	1.9E+20	I	7582	80	138	1651.6	12.8
N7552		23 13 25	-42 51 30	1.9E+20	I	1874	80	157	1899.3	27.0
N7552		23 13 25	-42 51 30	2.0E+20	I	3066	79	325	1528.2	29.4
N7552		23 13 25	-42 51 30	2.0E+20	I	3067	80	136	2106.1	29.4
N7562		23 13 25	06 24 54	5.7E+20	I	8364	80	153	3382.4	1.0
N7582	AGN	23 15 38	-42 38 42	1.8E+20	I	6218	80	157	1899.4	23.5
N7582	AGN	23 15 38	-42 38 42	1.9E+20	I	5259	79	324	2056.5	27.7
N7582	AGN	23 15 38	-42 38 42	1.9E+20	I	7582	80	138	1651.6	24.6
N7582	AGN	23 15 38	-42 38 42	1.9E+20	I	6385	80	158	9767.8	25.4
N7582	AGN	23 15 38	-42 38 42	2.0E+20	I	3066	79	325	1528.2	1.8
N7582	AGN	23 15 38	-42 38 42	2.0E+20	I	3067	80	136	2106.1	1.8
N7590		23 16 11	-42 30 42	1.8E+20	I	6218	80	157	1899.4	14.7
N7590		23 16 11	-42 30 42	1.9E+20	I	6385	80	158	9767.8	15.4
N7590		23 16 11	-42 30 42	2.0E+20	I	3066	79	325	1528.2	8.5
N7590		23 16 11	-42 30 42	2.0E+20	I	3067	80	136	2106.1	8.5
N7599		23 16 36	-42 31 47	1.8E+20	I	6218	80	157	1899.4	16.4
N7599		23 16 36	-42 31 47	1.9E+20	I	6385	80	158	9767.8	13.5
N7599		23 16 36	-42 31 47	2.0E+20	I	3066	79	325	1528.2	10.9
N7599		23 16 36	-42 31 47	2.0E+20	I	3067	80	136	2106.1	10.9
N7611		23 17 04	07 47 24	5.0E+20	I	2598	80	354	8757.0	9.8
N7617		23 17 37	07 53 30	5.0E+20	I	2598	80	354	8757.0	7.9

TABLE 1—*Continued*

Name		RA (1950)	DEC (1950)	N_H (cm^{-2})	Inst.	Sequence number	start year	start day	Exp. (second)	Offaxis (arcmin)
N7619		23 17 43	07 56 00	5.0E+20	I	2598	80	354	8757.0	10.2
N7623		23 17 58	08 07 24	5.0E+20	I	2598	80	354	8757.0	22.0
N7626		23 18 10	07 56 35	5.0E+20	I	2598	80	354	8757.0	12.7
N7673		23 25 12	23 18 54	4.4E+20	I	10201	80	362	4498.6	0.2
N7677		23 25 36	23 15 18	4.4E+20	I	10201	80	362	4498.6	6.8
N7679		23 26 14	03 14 11	4.9E+20	I	9153	81	7	890.2	0.5
N7682		23 26 30	03 15 30	4.9E+20	I	9153	81	7	890.2	4.7
N7714		23 33 40	01 52 42	4.9E+20	I	4043	79	354	2613.7	0.4
N7769		23 48 31	19 52 17	4.3E+20	I	6367	80	10	5642.0	5.0
N7770		23 48 49	19 49 06	4.3E+20	I	6367	80	10	5642.0	0.5
N7771	AGN	23 48 52	19 50 00	4.3E+20	I	6367	80	10	5642.0	1.5
N7793		23 55 15	-32 52 05	1.1E+20	I	2146	79	145	1849.7	1.2

TABLE 3A

X-RAY DATA FOR ELLIPTICAL AND S0 GALAXIES

Name	Seq	B (mag)	Type (T)	X-ray Position RA	X-ray Position Dec	R (')	Counts	Error	Rate (10^{-3} sec^{-1})	Fx (10^{-13} cgs)	D (Mpc)	Log Lx (erg s^{-1})
N0127	I 6643	14.68	-2				< 24.54		< 15.43	< 4.27	80.0	<41.51
N0128	I 6643	12.63	-2				< 24.02		< 15.09	< 4.17	82.6	<41.53
N0130	I 6643	14.78	-3				< 25.07		< 15.75	< 4.36	88.9	<41.62
N0205	H 2730	8.60	-3				< 378.99		< 16.25	< 17.88	0.7	<38.02
N0221		8.79	-6			a					0.7	37.73
N0315	H 6331	12.20	-3	00 55 05.7	30 04 57	60	71.58	21.9	3.63	3.84	99.9	41.66
N0315	I99999	12.20	-3			b	620.61	34.7	31.90	9.69	99.9	42.06
N0499	I 7766	12.64	-3	01 20 24	33 12 02	210	919.25	36.3	99.99	30.01	88.6	42.45
N0507	I 7766	11.76	-2	01 20 51	32 59 38	630	2877.64	71.2	313.01	93.95	99.3	43.04
N0533	I 153	12.75	-5	01 22 56	01 29 59	270	117.48	18.0	111.90	31.42	107.9	42.64
N0584	I 5768	11.20	-2				< 36.34		< 10.22	< 2.89	37.6	<40.69
N0596	I 7951	11.88	-5				< 81.95		< 8.66	< 2.44	38.2	<40.63
N0720	I 5769	11.15	-5	01 50 34	-13 58 52	480	294.17	27.7	65.71	17.02	32.6	41.34
N0984	I 4544	14.70	-2				< 19.24		< 13.89	< 4.54	87.5	<41.62
N1044	H 9171	14.00	-3				< 7.40		< 1.26	< 1.41	122.5	<41.40
N1052	I 1880	11.53	-3	02 38 37	-08 28 01	240	207.66	22.1	19.00	5.28	28.6	40.71
N1167	I 4545	12.79	-3				< 17.09		< 9.13	< 3.03	99.9	<41.56
N1172	I 9183	13.00	-2				< 30.11		< 5.42	< 1.59	29.4	<40.22
N1201	I10116	11.56	-2				< 30.79		< 21.90	< 5.70	32.5	<40.86
N1316	H 1885	9.32	-2	03 20 47.2	-37 23 07	120	329.71	50.5	14.12	11.62	27.2	41.01
N1316	I99999	9.32	-2			b	894.83	44.8	74.52	19.86	27.2	41.25
N1332	I 7028	11.29	-2	03 24 04	-21 30 28	360	311.59	30.4	24.93	6.72	28.4	40.81
N1387	I99999	11.83	-2			b	108.33	22.2	24.85	6.43	27.2	40.76
N1389	I99999	12.39	-2			b	< 43.88		< 10.07	< 2.60	27.2	<40.36
N1395	I 9185	11.18	-5	03 36 20	-23 11 14	480	589.32	56.6	42.33	11.14	32.1	41.14
N1399	I 1887	10.79	-5	03 36 35	-35 36 56	1200	3251.98	93.0	889.03	229.42	27.2	42.31
N1404	I 1887	11.06	-5	03 36 56	-35 45 18	300	470.91	28.4	128.74	33.22	27.2	41.47
N1400	I10241	12.08	-3				< 69.87		< 16.51	< 4.98	8.0	<39.58
N1407	I10241	10.93	-5	03 37 55	-18 44 09	300	198.79	21.0	46.99	14.18	34.7	41.31
N1497	I 4546	14.20	-2				< 9.49		< 6.16	< 2.06	122.6	<41.57
N1510	I 5258	13.24	-6				< 31.37		< 15.81	< 4.20	16.6	<40.14
N1553	I 5726	10.36	-2	04 15 08	-55 54 43	270	39.87	9.1	53.97	14.36	21.5	40.90
N1574	I 5782	11.13	-2				< 38.07		< 26.05	< 7.01	21.5	<40.59
N1600 c	I 6667	12.01	-5	04 29 17	-05 11 56	300	54.66	11.7	31.59	9.19	90.3	41.95
N1947	I 7276	11.75	-2				< 20.89		< 15.65	< 4.45	19.4	<40.30
N2314	I 8955	12.83	-5				< 43.11		< 10.27	< 3.01	84.6	<41.41
N2300	I 6645	11.99	-5	07 15 37	85 48 40	240	69.07	10.7	35.61	10.85	49.8	41.51
N2444	I 3148	13.43	-2				< 38.48		< 17.10	< 5.17	84.6	<41.65
N2562	I 304	13.37	-1				< 93.38		< 10.54	< 3.07	102.4	<41.59
N2563	I 304	12.92	-2	08 17 42	21 13 57	360	365.17	31.8	41.22	12.00	96.1	42.12
N2629	I 8361	13.30	-2				< 21.00		< 8.09	< 2.20	80.8	<41.24
N2685	I 415	11.85	-2				< 24.54		< 12.17	< 3.53	26.0	<40.46
N2694	I 8362	14.96	-5				< 24.67		< 13.27	< 3.56	107.5	<41.69
N2693	I 8362	12.70	-5				< 23.56		< 12.67	< 3.40	103.7	<41.64
N2716	I99999	12.90	-1			b	< 31.24		< 5.22	< 1.50	73.7	<40.99
N2832	I 1841	12.39	-5	09 16 44	33 57 31	360	134.47	16.2	86.72	22.85	142.3	42.74
N2859	I 2101	11.75	-2				< 34.21		< 4.61	< 1.20	40.8	<40.38
N2911	I 3293	12.53	-2				< 20.63		< 13.31	< 3.76	69.2	<41.33
N2974	I 7655	11.68	-5	09 40 03	-03 28 26	240	55.46	13.1	11.63	3.32	45.8	40.92
N3078	I10242	11.92	-5	09 56 09	-26 40 58	210	78.87	13.5	14.40	4.30	53.7	41.17
N3065	I 3470	12.81	-2	09 57 34	72 25 16	120	25.17	5.9	27.82	7.88	50.3	41.38
N3115	I 3920	9.89	-2				< 45.39		< 21.98	< 6.41	10.8	<39.95
N3222	I99999	13.39	-2			b	< 42.76		< 9.55	< 2.58	117.2	<41.63
N3258 c	I 1896	12.48	-5	10 26 45	-35 21 00	180	53.73	10.4	22.71	7.02	60.3	41.48
N3377	I 5793	11.10	-5				< 30.08		< 4.92	< 1.36	13.0	<39.44
N3379	I 2110	10.33	-5				< 26.04		< 23.92	< 6.62	13.0	<40.13
N3384	I 2110	10.70	-2				< 14.82		< 13.61	< 3.76	13.0	<39.88
N3458	I 7764	13.15	-2				< 20.83		< 16.17	< 3.92	47.4	<41.02
N3516	I99999	12.34	-2			b	779.48	32.9	110.51	30.80	62.5	42.16
N3585 c	I 7034	10.81	-3	11 10 55	-26 28 59	150	54.15	11.7	5.43	1.63	34.7	40.37
N3607	I 3927	11.08	-2	11 14 16	18 19 25	300	382.48	32.5	23.84	6.19	32.0	40.88
N3608	I 3927	11.88	-5	11 14 19	18 26 00	180	115.31	19.8	7.19	1.87	37.6	40.50
N3818	I 5799	12.79	-5				< 29.78		< 17.09	< 4.86	40.3	<40.98
N3894 c	I 4949	12.90	-5	11 46 09	59 42 01	210	53.09	11.3	18.77	4.93	74.7	41.52

TABLE 3A—*Continued*

Name	Seq	B (mag)	Type (T)	X-ray Position RA	X-ray Position Dec	R (")	Counts	Error	Rate (10^{-3} sec^{-1})	Fx (10^{-13} cgs)	D (Mpc)	Log Lx (erg s^{-1})
N3923	I 5800	10.79	-3	11 48 30	-28 31 24	270	158.30	17.2	35.46	10.96	41.5	41.35
N3990	I 4548	13.11	-3				< 15.00		< 11.70	< 2.98	27.3	<40.42
N3998	I 4548	11.50	-2	11 55 22	55 43 51	330	300.95	19.7	234.75	59.88	34.7	41.94
N4105	I 5801	11.76	-2	12 04 10	-29 28 00	240	77.48	16.6	11.81	3.58	43.6	40.91
N4168	I99999	12.21	-5			b	48.89	12.2	8.24	2.26	27.0	40.29
N4203	I 3922	11.62	-2	12 12 32	33 28 43	240	189.97	15.4	123.07	31.42	15.6	40.96
N4215	I10119	13.04	-2				< 15.59		< 7.81	< 2.04	56.4	<40.89
N4251	I 7036	11.62	-2				< 46.44		< 4.60	< 1.22	15.6	<39.55
N4261	I99999	11.38	-5			b	456.33	32.7	50.40	13.18	56.4	41.70
N4267	I 6984	11.78	-2				< 40.57		< 8.03	< 2.23	27.0	<40.29
N4291	H 559	12.26	-5	12 18 07.0	75 38 46	70	42.13	13.6	8.31	7.46	47.2	41.30
N4291	I 5424	12.26	-5	12 18 02	75 38 40	270	389.29	30.3	29.69	8.24	47.2	41.34
N4340	I 6988	11.93	-2				< 92.74		< 8.70	< 2.37	27.0	<40.32
N4350	I 6988	11.88	-2				< 64.30		< 6.04	< 1.64	27.0	<40.16
N4365	I99999	10.60	-5			b	109.55	14.9	11.40	2.99	27.0	40.42
N4386	I99999	12.53	-2			b	< 57.87		< 3.61	< 1.01	45.2	<40.39
N4374	H 4320	10.23	-5	12 22 31.5	13 09 48	90	734.04	49.7	17.80	15.59	27.0	41.13
N4374	I99999	10.23	-5			b	2364.83	100.5	59.84	16.43	27.0	41.16
N4382	I99999	10.10	-2			b	403.84	32.2	21.82	6.02	27.0	40.72
N4387	I 4311	12.75	-5				< 64.33		< 14.11	< 3.89	27.0	<40.53
N4406	H 4321	10.02	-3	12 23 39.5	13 13 22	170	742.18	69.3	29.19	25.78	27.0	41.35
N4406	I 4311	10.02	-3	12 23 41	13 13 11	840	3292.21	79.9	722.25	198.81	27.0	42.24
N4417	H 2891	12.07	-2				< 25.33		< 16.34	< 13.13	27.0	<41.06
N4425	I 278	12.79	-2				< 260.48		< 7.45	< 2.05	27.0	<40.25
N4435	H 9008	11.72	-2				< 143.67		< 2.86	< 2.50	27.0	<40.34
N4435	I99999	11.72	-2			b	< 504.69		< 13.81	< 3.80	27.0	<40.52
N4458	I 7003	12.70	-5	12 26 28	13 30 36	90	35.28	10.0	6.96	1.91	27.0	40.22
N4459	I 2124	11.49	-2				< 45.64		< 10.40	< 2.87	27.0	<40.40
N4467	H 7068	15.18	-5				< 22.94		< 0.71	< 0.56	27.0	<39.69
N4472	H 7068	9.32	-3	12 27 14.2	08 16 32	180	1681.68	82.1	52.30	40.87	27.0	41.55
N4472	I 4308	9.32	-3	12 27 13	08 16 25	810	3829.83	82.0	499.18	130.89	27.0	42.06
N4473 c	I99999	11.07	-5			b	129.32	32.8	13.68	3.76	27.0	40.52
N4474	I 2124	12.70	-2				< 31.68		< 7.22	< 1.99	27.0	<40.24
N4479	I99999	13.21	-2			b	< 102.26		< 5.17	< 1.43	27.0	<40.10
N4526	I99999	10.59	-2			b	108.22	24.6	5.99	1.57	27.0	40.14
N4507	I 2664	12.80	-1				< 21.48		< 26.54	< 8.35	72.5	<41.72
N4550	I 4313	12.33	-3				< 56.41		< 6.70	< 1.83	27.0	<40.20
N4551	I 4313	12.65	-5				< 85.47		< 10.14	< 2.77	27.0	<40.38
N4552	I 4313	10.80	-2	12 33 07	12 49 45	150	296.22	22.8	35.16	9.60	27.0	40.92
N4564	H 2898	11.87	-5				< 26.30		< 16.19	< 13.91	27.0	<41.08
N4564	I 4317	11.87	-5				< 35.98		< 6.59	< 1.79	27.0	<40.19
N4578	I10120	12.04	-2				< 23.72		< 10.55	< 2.78	27.0	<40.38
N4589	I10243	11.81	-5				< 35.05		< 6.12	< 1.65	48.2	<40.66
N4621	I 2129	10.67	-5				< 70.80		< 11.33	< 3.10	27.0	<40.43
N4638 c	I 2130	12.05	-2	12 40 21	11 44 11	150	43.18	12.6	7.01	1.91	27.0	40.22
N4636	H 7038	10.50	-3	12 40 17.1	02 57 36	180	1941.13	77.1	61.11	49.71	27.3	41.65
N4636	I 412	10.50	-3	12 40 17	02 57 44	600	567.84	30.8	410.33	108.94	27.3	41.99
N4649	H 2132	9.83	-2	12 41 09.0	11 49 32	140	584.30	47.3	34.52	29.66	27.0	41.41
N4649	I 2130	9.83	-2	12 41 08	11 49 37	420	1064.24	41.4	172.75	46.98	27.0	41.61
N4645	I 6056	12.56	-5				< 45.04		< 3.76	< 1.20	74.6	<40.90
N4697	I99999	10.11	-5			b	176.39	23.9	20.89	5.58	37.4	40.97
N4754	I99999	11.41	-2			b	< 70.26		< 5.74	< 1.54	27.0	<40.13
N4753	I 7039	10.85	-2	12 49 47	-00 55 24	180	79.03	17.3	6.54	1.71	24.3	40.08
N4756	I 1900	13.28	-5	12 50 13	-15 08 01	270	235.82	22.2	42.79	12.16	88.4	42.06
N4762	I99999	11.26	-2			b	172.52	26.5	14.09	3.79	27.0	40.52
N4782	I 444	12.75	-5	12 51 59	-12 17 49	180	34.57	7.6	24.31	6.89	84.7	41.77
I3896	I 544	12.37	-5				< 66.76		< 21.92	< 5.87	48.5	<41.22
N4880	I 5990	12.57	-2				< 31.69		< 10.14	< 2.73	25.2	<40.32
N5044	I 6653	11.87	-5	13 12 44	-16 07 22	780	1473.78	44.7	1060.56	315.01	62.5	43.17
N5077	I10244	12.52	-5	13 16 54	-12 23 55	120	50.75	9.9	8.26	2.32	65.2	41.07
N5084	I 8996	11.95	-2	13 17 33	-21 34 01	180	91.43	19.2	23.22	7.46	42.4	41.21
N5102	I 7040	10.47	-2				< 22.25		< 11.73	< 3.44	5.6	<39.11
N5128	H99999	6.62	-2			b	3260.21	105.1	68.07	78.42	7.9	40.77
N5128	I 477	6.62	-2	13 22 33	-42 45 35	1020	15754.90	159.7	1263.12	407.61	7.9	41.48

TABLE 3A—*Continued*

Name	Seq	B (mag)	Type (T)	X-ray Position RA	Dec	R (")	Counts	Error	Rate (10^{-3} sec^{-1})	Fx (10^{-13} cgs)	D (Mpc)	Log Lx (erg s^{-1})
N5195	H 3047	10.50	-2	13 27 52.6	47 31 13	40	71.28	15.8	3.11	2.32	14.9	39.79
I4296	I 1902	11.43	-5	13 33 45	-33 42 16	360	469.40	40.2	44.31	12.86	78.4	41.98
I4329	H 344	12.48	-2				< 30.67		< 12.98	< 12.78	93.8	<42.13
N5322	I10245	10.91	-5				< 79.02		< 13.51	< 3.58	50.8	<41.04
N5318	I 4549	13.40	-2				< 17.75		< 8.35	< 2.14	95.7	<41.37
N5354	H 8929	12.19	-2				< 58.35		< 6.05	< 4.33	63.9	<41.33
N5353	H 8929	12.05	-3	13 51 19.5	40 31 45	30	38.25	9.2	3.96	2.84	60.8	41.10
N5353	I 3932	12.05	-3	13 51 19	40 32 00	150	73.70	11.4	22.91	5.79	60.8	41.41
N5363	I 7277	11.06	-2	13 53 36	05 29 59	210	23.73	7.7	15.00	4.02	36.0	40.79
N5485	I 8337	12.44	-2				< 46.98		< 13.95	< 3.59	52.7	<41.08
I0989	I 4550	14.00	-5				< 13.08		< 8.80	< 2.39	157.9	<41.85
N5532 c	I 1905	12.64	-2	14 14 27	11 01 59	180	36.43	10.8	11.28	2.99	154.6	41.93
N5576	I 6685	11.76	-5				< 24.88		< 9.78	< 2.65	42.4	<40.76
I1024	I 4551	13.90	-2				< 16.70		< 8.66	< 2.37	40.1	<40.66
N5838	I10456	11.72	-2	15 02 57	02 17 50	120	78.90	15.0	4.90	1.42	45.8	40.55
N5846	I 9975	11.13	-2	15 03 57	01 47 55	600	2544.01	75.3	177.36	51.38	45.8	42.11
N5866	I 2144	10.86	-2	15 05 06	55 57 17	90	15.95	5.0	7.78	2.02	24.6	40.17
N5982	I 6646	12.03	-5	15 37 38	59 31 05	150	38.22	9.4	19.35	5.12	69.1	41.47
N6027	I 462	14.23	-2				< 18.01		< 15.48	< 4.45	97.6	<41.71
N6034	I 3923	14.60	-5	16 01 17	17 20 29	240	29.72	9.4	19.28	5.46	209.5	42.46
N6146	I 4547	13.50	-2				< 20.82		< 18.54	< 4.64	183.2	<42.27
N6876	I 1858	12.45	-5	20 13 08	-71 00 45	240	205.58	21.2	31.10	9.29	73.4	41.78
N6880	I 1858	14.00	-1				< 74.20		< 11.23	< 3.35	75.2	<41.36
N6963	I10691	14.40	-5				< 32.06		< 6.18	< 1.88	89.1	<41.25
N6964	I10691	13.12	-5				< 30.74		< 5.93	< 1.80	79.0	<41.13
N7236	H 1913	14.08	-3				< 17.27		< 2.53	< 2.57	158.0	<41.89
N7237	H 1913	14.33	-3				< 23.54		< 3.45	< 3.50	158.3	<42.02
N7332	I10122	11.58	-2				< 18.65		< 10.78	< 3.15	29.3	<40.51
I1459	I 6674	10.96	-5	22 54 23	-36 43 57	240	105.65	14.9	32.24	8.23	32.1	41.01
N7562	I 8364	12.28	-5				< 41.13		< 12.16	< 3.69	72.0	<41.36
N7619	I 2598	12.17	-5	23 17 42	07 55 30	300	440.37	33.1	50.29	14.92	75.0	42.00
N7626	I 2598	12.17	-5	23 18 12	07 56 00	240	167.44	24.8	19.12	5.67	68.3	41.50

TABLE 3B

X-RAY DATA FOR SPIRAL AND IRREGULAR GALAXIES

Name	Seq	B (mag)	Type (T)	X-ray Position RA	X-ray Position Dec	R (")	Counts	Error	Rate (10^{-3} sec^{-1})	Fx (10^{-13} cgs)	D (Mpc)	Log Lx (erg s^{-1})
N0125	I 6643	12.88	0				< 18.78		< 11.80	< 4.28	104.9	<41.75
N0224		3.12	3			a					0.7	39.56
N0247	I 5766	8.88	5	00 44 28	-21 01 59	600	424.02	46.3	41.47	13.71	2.1	38.86
N0253	H99999	7.38	5			b	1184.58	80.8	32.14	34.98	3.0	39.58
N0253	I 2082	7.38	5	00 45 06	-25 33 43	660	1639.52	57.6	211.21	68.81	3.0	39.87
SMC		2.48	9			a					0.063	37.79
N0309	I 8992	12.07	5				< 38.01		< 7.57	< 2.87	109.5	<41.61
I1613	H 2087	9.75	10				< 502.53		< 160.09	<223.07	0.7	<39.12
I1613 c	I 2086	9.75	10	01 02 28	01 46 15	300	414.43	27.3	60.27	21.95	0.7	38.11
N0449	I 6703	14.65	5				< 23.22		< 11.68	< 4.77	97.8	<41.74
N0521	I 153	12.19	5				< 12.42		< 11.83	< 4.39	97.5	<41.70
N0520	I 2088	12.09	0				< 37.17		< 8.24	< 3.06	44.7	<40.86
N0524	I 2089	11.62	0	01 22 10	09 16 29	240	101.20	15.4	17.59	7.01	51.6	41.35
N0523	I 4199	13.50	d				< 22.65		< 6.20	< 2.49	97.6	<41.45
N0578	I 424	11.04	5				< 28.81		< 10.87	< 3.46	31.3	<40.61
N0598	H99999	5.69	5			a				161.20	0.7	38.98
N0598	I99999	5.69	5			a				210.00	0.7	39.09
N0625	I 5257	11.91	0				< 14.39		< 8.48	< 2.84	6.3	<39.13
N0628	H 7599	9.41	5				< 467.89		< 12.44	< 20.63	15.6	<40.78
N0628	I 7042	9.41	5	01 34 03	15 31 57	300	56.90	16.5	8.56	3.39	15.6	39.99
I1727	I 7756	11.50	9				< 29.24		< 4.80	< 2.05	10.3	<39.42
N0672	I 7756	10.68	5				< 30.49		< 5.00	< 2.14	12.1	<39.57
N0772	I 464	10.33	3				< 12.45		< 14.51	< 6.04	52.4	<41.30
N0871	I 6339	13.50	5				< 31.08		< 5.76	< 2.51	73.4	<41.21
N0877	I 6339	12.06	5	02 15 13	14 18 03	120	29.37	7.8	5.44	2.37	76.8	41.22
N0936	I99999	11.19	0			b	145.83	27.4	12.10	4.35	27.2	40.59
N0941	I99999	12.56	6			b	< 499.03		< 41.40	< 14.90	32.8	<41.28
N0945	I10223	12.80	5				< 33.93		< 4.53	< 1.61	85.4	<41.15
N0985	H 8308	13.83	10	02 32 10.8	-09 00 26	130	1562.97	43.6	262.16	373.50	253.6	44.46
N0985	I 3143	13.83	10	02 32 11	-09 00 19	450	1802.01	45.0	545.60	200.75	253.6	44.19
N1042	I 1880	11.14	5	02 37 58	-08 37 33	240	173.17	23.4	15.85	5.78	26.8	40.70
N1068	I99999	9.03	3			b	2203.67	49.1	558.55	206.50	23.1	42.12
N1073 c	I 2092	11.20	5	02 41 04	01 08 59	210	47.29	11.3	10.02	3.82	24.4	40.43
N1087	I 9138	11.13	5				< 25.12		< 18.58	< 7.13	30.5	<40.90
N1090	I 9138	12.03	5				< 15.12		< 11.18	< 4.29	56.1	<41.21
N1097	I 2093	9.75	4	02 44 09	-30 29 04	210	470.89	24.3	88.60	30.30	23.3	41.29
N1218	I 9146	13.43	0	03 05 49	03 55 00	210	83.80	10.4	57.10	25.84	169.4	42.95
N1300	H 2095	10.43	3				< 116.77		< 16.55	< 23.06	30.2	<41.40
N1300	I 2094	10.43	3	03 17 25	-19 35 00	120	28.60	7.7	4.55	1.65	30.2	40.26
N1313	I 7044	8.93	5	03 17 42	-66 40 12	180	390.48	22.7	50.22	18.91	5.9	39.90
N1317	H 1885	12.04	1				< 115.54		< 4.96	< 6.21	27.2	<40.74
N1317	I99999	12.04	1			b	< 92.86		< 7.73	< 2.66	27.2	<40.37
N1350	I 5776	11.02	1				< 40.52		< 14.88	< 4.77	27.2	<40.63
N1358	I99999	12.95	1			b	27.61	8.5	3.60	1.40	76.7	40.99
N1365	I99999	9.45	3			b	192.36	19.8	52.08	17.12	27.2	41.18
N1380	I 5777	11.10	0	03 34 30	-35 08 20	210	33.54	9.0	21.16	6.84	27.2	40.78
N1386	I 4129	11.08	1	03 34 48	-36 09 43	180	60.50	12.1	18.26	5.97	27.2	40.72
N1398	I99999	10.04	2			b	159.87	18.9	11.57	3.60	25.9	40.46
N1421 c	I 9130	11.14	5	03 40 07	-13 40 59	270	36.42	10.8	16.61	6.41	41.0	41.11
I0342	I 7045	7.86	6	03 41 35	67 56 19	510	165.75	20.6	80.49	49.27	6.3	40.37
N1512	I 5258	10.77	3				< 21.54		< 10.86	< 3.71	15.3	<40.02
N1533	I 7030	11.65	0	04 08 45	-56 14 38	240	80.95	18.9	7.80	2.76	21.5	40.18
N1559	I 7046	10.44	5	04 16 59	-62 54 03	180	219.21	19.7	26.16	9.80	23.0	40.79
N1566	H 7112	9.79	5	04 18 53.2	-55 03 21	110	2934.22	60.8	178.59	219.62	21.5	42.08
N1566	I99999	9.79	5			b	1246.34	38.5	242.85	82.68	21.5	41.66
N1569	H 2700	11.08	9				< 18.76		< 8.11	< 27.80	2.6	<39.35
N1569	I 414	11.08	9	04 26 05	64 44 32	210	99.33	11.9	34.89	19.31	2.6	39.19
N1614	I 6706	13.15	5	04 31 35	-08 40 53	180	21.08	6.8	15.68	6.50	91.1	41.81
N1625	I 7895	12.32	4				< 18.23		< 7.07	< 2.77	91.7	<41.45
N1672	I 427	10.40	3	04 44 55	-59 19 59	210	127.05	16.5	21.90	7.65	23.3	40.70
N1784	I10225	11.82	4				< 86.17		< 6.02	< 2.62	46.1	<40.82
LMC		0.36	9			a					0.055	38.82
N1961	I 9460	10.91	3	05 36 39	69 20 59	180	64.41	15.4	6.29	2.77	84.8	41.38
U3691	I 5156	13.30	6				< 91.08		< 7.69	< 3.48	46.0	<40.95

TABLE 3B—*Continued*

Name	Seq	B (mag)	Type (T)	X-ray Position RA	X-ray Position Dec	R (″)	Counts	Error	Rate (10^{-3} sec^{-1})	Fx (10^{-13} cgs)	D (Mpc)	Log Lx (erg s^{-1})
N2276	I 6645	11.53	5				< 32.10		< 16.55	< 6.82	59.1	<41.45
N2366	I 2098	11.03	9				< 21.63		< 6.26	< 2.39	4.7	<38.80
N2403	H 584	8.29	5	07 31 36.6	65 42 20	100	147.06	24.1	7.60	11.89	6.8	39.82
N2403	I99999	8.29	5			b	515.82	38.5	49.60	19.12	6.8	40.02
N2441	I 6842	12.55	5				< 21.70		< 8.97	< 3.34	79.9	<41.41
N2525	I10226	11.31	5				< 19.44		< 6.42	< 2.86	33.9	<40.59
N2608 c	I 5155	12.25	4	08 32 16	28 39 10	120	34.84	11.2	2.98	1.15	49.8	40.53
N2642	I10227	11.88	3				< 28.05		< 9.32	< 3.47	88.1	<41.51
N2683	I 3921	9.34	3				< 21.69		< 22.61	< 8.24	9.2	<39.92
N2763	I 5789	12.12	5				< 31.32		< 5.45	< 2.26	41.3	<40.66
N2773	I99999	14.70	5			b	63.78	13.4	6.72	2.59	112.6	41.59
N2775	I99999	11.10	1			b	103.65	15.1	10.92	4.22	27.3	40.58
N2777	I99999	14.10	2			b	< 40.02		< 4.22	< 1.63	35.0	<40.38
N2782	I 1941	11.50	1				< 29.56		< 15.97	< 5.40	59.9	<41.37
N2835 c	I 5790	10.25	5	09 15 35	-22 08 00	150	27.32	9.1	4.63	2.03	17.4	39.87
N2848	I 5791	12.00	5				< 34.06		< 5.17	< 2.08	44.5	<40.69
N2841	I 2099	9.24	3	09 18 36	51 11 35	180	70.64	12.1	14.39	4.71	19.3	40.32
N2903	I 7049	8.91	5	09 29 20	21 43 31	210	167.93	16.0	38.44	14.34	10.1	40.24
N2914	I 3293	13.59	2				< 16.71		< 10.78	< 4.03	68.3	<41.35
N2992	H99999	11.61	1			b	80.48	10.5	70.66	120.19	49.0	42.54
N2992	I99999	11.61	1			b	5444.70	78.1	509.13	204.80	49.0	42.77
N2993	H99999	12.40	2			b	< 6.71		< 5.89	< 10.02	49.0	<41.46
N3031	H 585	7.01	3	09 51 26.9	69 18 08	90	1095.40	46.7	37.41	58.94	2.2	39.53
N3031	I 2102	7.01	3	09 51 26	69 18 08	480	1564.56	47.9	240.14	92.92	2.2	39.73
N3034	H 586	9.21	0	09 51 42.0	69 54 51	200	1506.48	63.0	116.96	187.14	8.4	41.20
N3034	I 466	9.21	0	09 51 42	69 55 00	660	2686.29	59.8	603.69	235.45	8.4	41.30
N3067	I 2712	11.76	3				< 23.48		< 14.72	< 4.94	38.9	<40.95
N3081	I 5251	12.50	1	09 57 10	-22 35 18	180	33.91	7.6	20.67	8.09	52.2	41.42
N3066	I 3470	13.19	4				< 19.72		< 21.80	< 8.19	52.1	<41.42
N3079	I 423	10.31	5				< 31.57		< 37.33	< 11.47	32.8	<41.17
N3079	H 4628	10.31	5	09 58 36.0	55 55 38	60	91.91	20.1	6.02	5.91	32.8	40.88
N3077	I 2105	10.57	0				< 66.52		< 8.16	< 3.10	3.4	<38.63
N3125	I 430	12.88	0				< 28.88		< 16.23	< 6.76	22.5	<40.61
N3166	I 6681	10.65	1	10 11 13	03 40 39	150	17.54	5.7	8.48	3.04	35.4	40.66
N3169	I 6681	10.56	3				< 23.74		< 11.48	< 4.12	31.7	<40.70
N3175	I 5407	11.61	5				< 27.63		< 14.86	< 6.10	23.9	<40.62
N3184	H 2893	10.14	5				< 59.28		< 42.32	< 47.16	14.0	<41.04
N3227	I99999	10.92	3			b	2382.74	56.4	401.25	140.34	33.1	42.26
I2574	I 7050	10.45	9	10 25 01	68 43 37	90	25.63	8.0	4.17	1.44	4.3	38.50
N3281	I 9220	11.96	1				< 15.84		< 17.18	< 7.22	70.2	<41.63
N3310	I 467	10.84	4	10 35 39	53 46 06	150	48.00	7.9	34.55	10.92	30.1	41.07
N3346	I10093	11.86	5				< 26.83		< 5.47	< 1.99	36.0	<40.49
N3351	I 497	9.88	3				< 92.30		< 21.41	< 7.80	13.0	<40.20
N3353	I 6371	13.20	3	10 42 16	56 13 23	90	19.14	6.0	5.81	1.73	27.0	40.18
N3368	I 2109	9.49	2				< 54.93		< 15.20	< 5.51	13.0	<40.05
N3389	I 2110	11.85	5				< 20.39		< 18.73	< 6.79	36.2	<41.03
N3395	I 3936	11.94	5	10 47 04	33 14 55	180	58.55	14.1	10.80	3.72	44.0	40.94
N3430	I99999	11.68	4			b	< 55.53		< 8.35	< 2.87	42.9	<40.80
N3445	I 7764	12.49	5				< 14.39		< 11.17	< 3.33	52.1	<41.03
N3448	I 416	12.15	0	10 51 42	54 34 30	120	22.13	6.2	12.38	3.81	39.4	40.85
N3455	I 7757	12.37	5				< 44.11		< 7.45	< 2.63	32.9	<40.53
N3489	I 5796	11.13	0				< 27.17		< 13.47	< 4.60	10.3	<39.77
N3504	I 4047	11.25	3	11 00 27	28 14 21	150	29.62	7.4	11.78	4.03	42.6	40.94
N3512	I 4047	12.69	5				< 27.36		< 10.88	< 3.72	40.2	<40.86
N3593	I 5797	10.78	1	11 11 57	13 05 14	120	33.69	8.3	6.99	2.37	8.8	39.34
N3628	I 5152	9.49	4	11 17 40	13 51 42	390	604.15	39.5	47.64	16.41	12.4	40.48
N3660	I10228	14.00	4	11 21 01	-08 23 20	330	154.65	21.7	27.59	10.55	78.6	41.89
N3690	H 442	11.66	9	11 25 42.0	58 50 29	30	17.01	5.7	4.52	4.80	71.5	41.47
N3718	H 1897	10.44	1				< 82.49		< 18.14	< 18.71	27.3	<41.22
N3718	I 2654	10.44	1				< 30.15		< 27.39	< 8.69	27.3	<40.89
N3729	H 1897	11.58	1				< 43.78		< 9.63	< 9.93	27.3	<40.95
N3729	I 2654	11.58	1				< 12.35		< 11.22	< 3.57	27.3	<40.50
N3783	I 7209	12.68	1	11 36 33	-37 27 44	690	6912.50	91.6	928.82	416.29	61.9	43.28
N3884	I 5190	13.50	1	11 43 37	20 40 24	210	80.44	16.8	32.98	11.81	145.5	42.48

TABLE 3B—*Continued*

Name	Seq	B (mag)	Type (T)	X-ray Position RA	X-ray Position Dec	R (")	Counts	Error	Rate (10^{-3} sec^{-1})	Fx (10^{-13} cgs)	D (Mpc)	Log Lx (erg s^{-1})
N3887	I10229	10.99	3				< 46.07		< 6.30	< 2.36	31.0	<40.43
N3888	I 6101	12.72	5				< 34.21		< 5.70	< 1.79	60.3	<40.89
N3893	I 7759	10.65	5				< 33.10		< 8.38	< 2.92	27.3	<40.42
N3896	I 7759	13.70	0				< 22.65		< 5.74	< 1.99	28.8	<40.30
N3991	I 443	12.86	10	11 54 56	32 36 29	210	21.82	7.1	14.27	4.82	71.9	41.47
N3994	I 443	12.97	5				< 15.36		< 10.04	< 3.39	72.0	<41.32
N3995	I 443	12.19	5				< 15.18		< 9.93	< 3.35	75.6	<41.36
I0749	I 7760	12.44	5				< 24.37		< 5.55	< 1.82	27.3	<40.21
I0750	I 7760	12.09	3				< 24.92		< 5.68	< 1.86	27.3	<40.22
N4036	I 7593	11.56	0				< 24.95		< 11.87	< 4.10	39.5	<40.88
N4038	I99999	10.82	5			b	255.20	20.3	36.70	14.16	41.0	41.45
N4041	I 7593	11.34	5				< 35.28		< 16.79	< 5.79	36.5	<40.97
N4051	I 7200	10.56	4	12 00 37	44 48 38	480	5999.93	83.5	682.07	220.45	27.3	42.29
N4151	H99999	10.53	2			b	1729.18	49.6	89.05	113.10	32.6	42.16
N4151	I99999	10.53	2			b	7524.15	93.2	280.44	97.00	32.6	42.09
N4156	H99999	13.55	3			b	57.72	9.7	2.97	3.78	142.4	41.96
N4156	I99999	13.55	3			b	416.36	28.5	15.52	5.37	142.4	42.11
N4178	I99999	11.26	5			b	< 69.86		< 8.18	< 2.79	27.0	<40.39
N4190	I99999	12.84	9			b	118.26	15.0	17.61	5.92	4.5	39.16
N4192	I99999	9.85	3			b	51.25	13.7	3.70	1.33	27.0	40.06
N4206	I 4303	12.80	4				< 48.75		< 5.60	< 2.03	27.0	<40.25
N4212	I 6982	11.44	5	12 13 07	14 10 00	90	33.30	7.3	5.28	1.91	27.0	40.22
N4214	H 2897	10.03	9				< 73.69		< 33.68	< 39.96	5.6	<40.18
N4216	I 4303	9.76	3	12 13 20	13 24 59	90	27.32	8.2	3.14	1.14	27.0	40.00
N4224	I 6711	12.04	1				< 25.03		< 11.74	< 3.90	56.4	<41.17
N4236 c	I 5803	9.35	7	12 14 14	69 44 30	e	44.06	13.0	3.27	1.02	3.5	38.17
N4235	I 6711	12.00	1	12 14 27	38 00 19	150	260.74	17.3	122.25	40.61	56.4	42.19
N4244 c	I 5153	9.73	6	12 14 36	07 28 15	120	88.71	15.1	6.46	2.20	5.0	38.82
N4245	I 6712	12.25	1				< 21.14		< 8.66	< 2.91	15.6	<39.93
N4246	I 6711	13.03	5				< 22.73		< 10.66	< 3.54	82.1	<41.46
N4254	I 4306	10.11	5	12 16 19	14 41 28	150	135.75	16.3	12.59	4.56	27.0	40.60
N4258	H10756	8.04	3	12 16 30.0	47 35 00	e	44.61	11.4	43.06	45.66	10.9	40.81
N4260	I 2672	12.30	1				< 37.78		< 17.58	< 5.86	56.4	<41.35
N4298	I 4305	11.61	5	12 19 06	14 52 59	240	91.54	23.7	6.14	2.22	27.0	40.29
N4303	I99999	9.86	5			b	330.75	25.9	28.03	9.42	24.4	40.83
N4321	H99999	9.79	5			b	244.46	41.1	6.06	8.04	27.0	40.85
N4321	I99999	9.79	5			b	66.14	11.0	23.86	8.43	27.0	40.87
N4351	I 6990	12.47	2				< 16.97		< 10.73	< 3.86	27.0	<40.53
N4378 c	I 9155	12.28	1	12 22 47	05 11 44	180	51.54	13.5	9.74	3.28	56.4	41.10
N4385	I 4049	12.60	4				< 17.95		< 21.80	< 7.43	53.8	<41.41
N4388	I 278	10.65	2	12 23 16	12 56 10	210	643.82	51.9	18.41	6.60	27.0	40.76
N4394	I99999	11.28	3			b	< 73.49		< 3.97	< 1.43	27.0	<40.10
N4424	H 2891	11.50	1				< 27.88		< 17.99	< 21.74	27.0	<41.28
N4424 c	I 280	11.50	1	12 24 39	09 41 47	90	60.48	19.5	1.29	0.44	27.0	39.58
N4429 c	I 6999	11.15	0	12 24 53	11 23 05	210	49.93	14.1	9.14	3.20	27.0	40.45
N4438	I99999	9.97	3			b	100.24	21.6	16.34	5.89	27.0	40.71
N4438	H 9008	9.97	3	12 25 14.0	13 17 07	120	454.26	59.6	9.03	12.29	27.0	41.03
N4449	H 4967	9.65	9	12 25 46.0	44 22 17	150	565.00	62.9	17.73	19.76	4.8	39.74
N4449	I 2123	9.65	9	12 25 45	44 23 06	180	62.77	9.3	38.93	12.72	4.8	39.54
N4450	I 7001	10.31	2	12 25 58	17 21 47	270	105.80	15.0	32.49	11.48	27.0	41.00
N4461	I 7003	12.09	1				< 48.49		< 9.57	< 3.44	27.0	<40.48
N4464	I 4308	13.31	0				< 102.76		< 13.39	< 4.48	27.0	<40.59
N4477	I99999	11.24	0			b	473.32	45.3	19.60	7.07	27.0	40.79
N4501	I 4304	9.77	4	12 29 27	14 41 56	240	217.70	24.8	21.19	7.53	27.0	40.82
N4503	I 279	12.22	1				< 74.31		< 3.65	< 1.29	27.0	<40.05
N4522	I 7445	11.97	4				< 34.10		< 18.28	< 6.16	27.0	<40.73
N4527	I 9133	10.30	3				< 33.53		< 16.15	< 5.52	21.7	<40.49
N4535	I 4310	10.12	5				< 80.60		< 8.33	< 2.79	27.0	<40.39
N4536	I 9134	10.44	5	12 31 57	02 28 00	210	63.87	12.9	17.32	5.90	21.4	40.51
I3528	I 7795	15.40	3	12 32 24	15 50 47	180	130.22	17.8	75.33	26.49	282.7	43.40
N4548	I99999	10.43	3			b	< 88.34		< 13.74	< 4.85	27.0	<40.63
N4565	I 9974	9.06	3	12 33 52	26 15 51	300	501.26	38.5	24.22	7.85	15.6	40.36
N4567	I 4317	11.67	5	12 34 02	11 31 30	210	72.34	16.2	13.26	4.68	27.0	40.61
N4569	I99999	9.39	2			b	88.91	15.6	16.88	6.00	27.0	40.72

TABLE 3B—*Continued*

Name		Seq	B (mag)	Type (T)	X-ray Position RA	Dec	R (")	Counts	Error	Rate (10^{-3} sec^{-1})	Fx (10^{-13} cgs)	D (Mpc)	Log Lx (erg s^{-1})
N4571		I 7011	11.49	5				< 13.75		< 9.66	< 3.41	27.0	<40.47
N4579		H 7067	10.01	2	12 35 12.1	12 05 34	80	341.73	26.6	35.82	48.12	27.0	41.62
N4579		I99999	10.01	2			b	1838.72	47.3	220.24	78.64	27.0	41.84
N4594		I99999	8.40	2			b	496.30	31.1	76.48	29.24	32.1	41.56
N4603		I 6054	11.43	5	12 38 09	-40 41 51	120	62.66	13.2	5.10	2.21	74.6	41.17
N4631		H 4367	8.98	5				< 146.56		< 15.95	< 17.35	11.1	<40.41
N4631		I 471	8.98	5	12 39 32	32 48 15	270	130.37	15.0	42.78	13.81	11.1	40.31
N4639		I99999	11.57	3			b	353.72	29.3	36.94	12.95	27.0	41.05
N4643	c	I 2133	11.55	0	12 40 45	02 13 59	90	28.72	6.9	6.92	2.35	41.3	40.68
N4647		H 2132	11.66	5				< 96.74		< 5.72	< 7.58	27.0	<40.82
N4651		I 3241	10.95	5				< 38.03		< 9.97	< 3.43	27.0	<40.48
N4654		I99999	10.68	5			b	< 86.34		< 9.02	< 3.16	27.0	<40.44
N4665		I99999	11.43	0			b	< 110.41		< 9.07	< 3.10	28.8	<40.49
N4689		I 7018	11.22	5	12 45 17	14 02 41	150	108.52	12.8	25.25	8.77	27.0	40.88
N4698	c	I99999	11.15	1			b	72.53	17.0	7.05	2.38	27.0	40.32
N4736		H 2699	8.38	2	12 48 31.7	41 23 31	60	33.71	7.9	18.32	20.42	6.9	40.07
N4826		I 2136	8.62	2	12 54 16	21 57 33	270	106.93	16.5	21.97	7.89	6.6	39.61
N4845		I 9156	11.07	1				< 36.04		< 7.52	< 2.52	25.1	<40.28
N4861		I 445	12.48	9	12 56 40	35 07 49	300	60.80	12.5	23.34	7.42	28.6	40.86
I4182		H 2895	11.70	9				< 63.40		< 20.89	< 20.89	7.1	<40.10
N5033		I 5128	10.11	4	13 11 08	36 51 47	270	1536.30	72.1	247.17	77.37	30.1	41.92
N5037		I 6653	11.90	2				< 23.77		< 17.10	< 6.84	46.6	<41.25
N5068		I 5807	10.15	5				< 62.47		< 14.65	< 6.37	10.8	<39.95
N5079		I10244	13.80	4				< 38.57		< 6.28	< 2.32	64.5	<41.06
N5088		I10244	12.45	5				< 36.70		< 5.98	< 2.21	39.4	<40.61
N5101		I 2138	11.48	1				< 61.22		< 14.77	< 5.90	44.0	<41.14
N5135		I 5255	11.91	3	13 22 54	-29 34 24	120	19.30	5.9	8.52	3.35	85.7	41.47
N5204		I 7635	11.29	7	13 27 44	58 40 42	150	200.56	17.3	28.75	9.58	7.7	39.83
N5194		H 3047	8.57	4	13 27 46.4	47 27 12	190	717.59	70.6	31.36	34.12	12.4	40.80
N5236		H99999	8.08	5			b	1296.20	93.1	29.57	46.95	7.6	40.51
N5236		I 588	8.08	5	13 34 13	-29 36 24	390	750.32	33.7	131.45	50.98	7.6	40.55
N5248		I 9136	10.42	4	13 35 03	09 08 08	120	33.34	8.1	9.16	3.17	36.5	40.70
N5253		H99999	10.98	0			b	< 75.24		< 3.15	< 4.92	5.1	<39.19
N5253		I 7061	10.98	0	13 37 03	-31 23 00	150	34.33	10.4	5.63	2.17	5.1	38.83
I4329A		H 344	13.37	0	13 46 27.9	-30 03 44	90	730.32	28.5	309.06	494.50	99.4	43.77
N5313		I 3935	12.69	3				< 35.52		< 6.84	< 2.12	60.8	<40.97
N5326		I 3933	12.94	1				< 28.19		< 6.44	< 2.01	60.8	<40.95
N5350		H 8929	11.84	4				< 66.59		< 6.90	< 7.12	60.8	<41.50
N5350		I 3932	11.84	4				< 33.56		< 10.43	< 3.30	60.8	<41.16
N5364		I 7277	10.64	5				< 34.73		< 21.95	< 7.59	41.0	<41.18
N5410		I 3151	14.00	5				< 20.50		< 11.26	< 3.62	85.4	<41.50
N5457		H 2899	7.89	5			a					8.7	
N5457		I99999	7.89	5			a				19.35	8.7	40.24
N5474		I 7636	11.01	6				< 36.16		< 5.45	< 1.74	9.6	<39.28
N5477		I 2140	13.90	9				< 68.96		< 6.64	< 2.13	10.3	<39.43
N5506		I99999	13.60	1			b	3967.86	69.5	292.72	111.83	46.1	42.45
N5548		I 356	12.90	1	14 15 43	25 22 07	600	24300.95	168.2	1085.00	365.19	109.8	43.72
N5548		H99999	12.90	1			b	10182.28	108.4	396.95	470.98	109.8	43.83
N5566	c	I 2143	10.35	1	14 17 39	04 08 29	180	40.02	11.5	8.16	2.87	42.4	40.79
N5585		I 7637	10.94	7				< 59.60		< 9.62	< 3.16	11.2	<39.68
N5645		I 3300	12.35	5				< 24.36		< 12.76	< 4.40	39.9	<40.92
N5643		I 5252	10.19	5	14 29 29	-43 56 53	150	35.02	7.6	22.72	10.46	27.2	40.97
N5674		I 6361	13.70	3	14 31 24	05 40 50	150	37.65	10.0	7.12	2.52	158.0	41.88
N5683		I 2625	15.17	0	14 33 07	48 52 43	240	298.44	18.7	141.18	49.62	243.1	43.55
N5689		I 2625	12.44	1				< 21.40		< 10.12	< 3.56	57.2	<41.14
N5728		I 5256	11.27	3	14 39 36	-17 02 37	150	18.96	5.8	12.69	5.46	67.8	41.48
N5850		I 9975	11.20	3	15 04 38	01 43 44	90	33.72	10.5	2.35	0.91	45.8	40.36
N5879		I 9143	11.11	3				< 29.23		< 11.78	< 3.90	27.0	<40.53
N5907		I 7062	10.28	5				< 35.24		< 9.14	< 2.99	23.9	<40.31
N5985		I 6646	11.01	3				< 49.36		< 24.98	< 8.49	63.0	<41.61
N6052		I 411	13.21	5				< 22.42		< 27.09	< 10.40	99.4	<42.09
N6300		I 6373	9.96	3				< 37.01		< 11.89	< 5.14	23.0	<40.51
N6454	c	I 421	14.50	5	17 44 00	55 44 00	180	27.97	6.6	28.24	10.78	190.4	42.67
N6503		I99999	10.15	5			b	< 42.68		< 14.16	< 5.46	9.8	<39.80

TABLE 3B—*Continued*

Name	Seq	B (mag)	Type (T)	X-ray Position RA	Dec	R (")	Counts	Error	Rate (10^{-3} sec^{-1})	Fx (10^{-13} cgs)	D (Mpc)	Log Lx (erg s^{-1})
N6744	I 7063	8.63	4	19 5 17	-63 54 57	240	355.06	33.9	17.28	7.17	16.7	40.38
N6814	H 345	11.37	4	19 39 56.0	-10 26 32	60	66.45	10.4	25.16	52.14	36.6	41.92
N6814	I 354	11.37	4	19 39 56	-10 26 32	480	1641.64	64.9	61.60	27.72	36.6	41.65
N6822	H 2729	8.90	10	19 42 07.0	-14 55 49	60	140.72	32.0	4.21	8.56	0.7	37.70
N6872	I 1858	11.52	3	20 11 43	-70 55 14	270	142.09	22.8	21.50	8.66	90.5	41.93
N6890	I 5253	12.35	2				< 15.87		< 10.13	< 3.96	51.1	<41.09
N6946	I99999	8.84	5			b	1980.91	76.9	59.67	32.05	8.8	40.47
N6951	I 9137	11.31	3				< 14.07		< 11.70	< 5.81	38.7	<41.02
N6962	I10691	12.22	2				< 38.25		< 7.37	< 3.03	86.4	<41.43
I5063	I 5254	13.14	0				< 46.44		< 22.25	< 8.82	65.3	<41.65
N7213	I 6714	10.72	1	22 06 09	-47 24 35	600	4498.19	69.1	2728.14	932.75	35.4	43.15
N7314	H 1160	11.11	5				< 18.69		< 8.43	< 10.54	29.4	<41.04
N7320	I 7827	12.55	7	22 33 43	33 42 07	270	57.77	13.3	20.06	8.64	22.2	40.71
N7331	I 9145	9.14	3	22 34 47	34 08 59	180	24.61	6.4	20.38	8.81	23.0	40.75
N7339	I10122	12.20	4				< 29.73		< 17.18	< 6.74	31.0	<40.89
N7469	H99999	11.95	2			b	5632.75	82.7	382.14	629.20	97.0	43.85
N7469	I99999	11.95	2			b	3881.26	69.4	987.71	390.08	97.0	43.64
I5283	H99999	14.25	6			b	< 19.90		< 1.35	< 2.22	100.1	<41.43
N7496	I 435	11.41	5				< 30.96		< 12.95	< 4.45	32.3	<40.74
N7552	I99999	10.99	4			b	94.95	13.8	25.60	8.74	31.3	41.01
N7582	I99999	10.60	2			b	434.04	32.5	32.39	11.09	28.3	41.03
N7590	I99999	11.59	5			b	126.71	21.0	8.28	2.83	27.8	40.42
N7599	I99999	11.36	5			b	92.52	20.5	6.05	2.07	32.5	40.42
N7611	I 2598	12.99	0				< 84.28		< 9.62	< 3.85	65.1	<41.29
N7673	I10201	12.66	5	23 25 12	23 18 54	150	32.05	9.1	7.12	2.78	69.6	41.21
N7677	I10201	13.90	4				< 42.41		< 9.43	< 3.68	72.6	<41.37
N7679	I 9153	12.79	5	23 26 15	03 13 44	270	23.97	7.1	26.93	10.72	101.7	42.12
N7682	I 9153	14.10	2				< 26.42		< 29.68	< 11.82	101.5	<42.16
N7714	I 4043	13.00	3	23 33 40	01 52 39	90	18.50	5.4	7.08	2.82	59.3	41.07
N7769	I 6367	12.44	4				< 44.68		< 7.92	< 3.09	84.6	<41.42
N7771	I 6367	12.51	1	23 48 49	19 49 55	210	104.74	14.9	18.56	7.24	85.7	41.80
N7793	I 2146	9.25	7	23 55 18	-32 53 38	150	39.55	7.7	21.38	6.81	2.8	38.81

[a] X-ray data are from Fabbiano 1989 for LMC, SMC, M31, and M32; Trinchieri et al. 1988 for M33; and Trinchieri et al. 1990 for M101.
[b] Multiple observations (sequence numbers are 99999). Individual data are in Table 4.
[c] X-ray source may not be associated with galaxy.
[d] N523: no morphological type available (peculiar galaxy).
[e] See Table 8 for descriptions of source regions.

TABLE 4

MULTIPLE OBSERVATIONS

Name		Seq	Exp. (sec)	X-ray Position RA	Dec	R (")	Rate (10^{-3} sec^{-1})	Error	Variable
N0253	H	583	26896.0	00 45 06.4	-25 33 51	180	31.08	2.59	
N0253	H	2084	9956.0	00 45 06.0	-25 33 44	180	35.01	4.38	
N0315	I	463	2023.0	00 55 04	30 04 36	150	17.61	3.71	?
N0315	I	4374	17433.8	00 55 06	30 05 00	300	33.55	1.94	
N0936	I	5118	6421.2	02 25 14	-01 22 00	330	14.67	3.42	
N0936	I	5771	5632.3	02 25 06	-01 22 16	300	9.16	2.91	
N0941	I	5118	6421.2				<76.61		
N0941	I	5771	5632.3				< 5.99		
N1068	I	1927	1456.4	02 40 07	-00 13 29	360	548.68	20.26	
N1068	I	1928	2488.9	02 40 07	-00 13 24	360	564.33	15.75	
N1316	I	1883	3311.1	03 20 49	-37 22 42	450	82.39	7.04	
N1316	I	1884	4840.9	03 20 47	-37 22 51	450	72.51	5.64	
N1316	I	10571	3855.3	03 20 46	-37 23 07	450	70.29	6.98	
N1317	I	1883	3311.1				< 6.63		
N1317	I	1884	4840.9				<13.33		
N1317	I	10571	3855.3				<11.01		
N1358	I	5250	968.7	03 31 10	-05 16 00	60	5.94	2.89	
N1358	I	6369	6700.5	03 31 13	-05 15 00	90	3.26	1.20	
N1365	I	3058	772.2	03 31 43	-36 18 08	240	53.57	10.23	
N1365	I	3059	2921.6	03 31 44	-36 18 25	330	51.68	6.23	
N1387	I	4128	1046.6	03 35 05	-35 41 00	180	17.36	7.15	
N1387	I	4129	3312.8	03 35 00	-35 40 34	210	27.45	6.31	
N1389	I	4128	1046.6				<14.24		
N1389	I	4129	3312.8				<13.62		
N1398	I	2096	8481.7	03 36 46	-26 30 16	150	10.50	1.60	
N1398	I	2097	5331.0	03 36 45	-26 29 22	210	13.29	2.48	
N1566	I	1937	2603.1	04 18 54	-55 03 16	300	295.63	11.37	yes
N1566	I	1938	2529.0	04 18 53	-55 03 12	300	188.53	9.73	
N2403	I	589	5988.3	07 32 06	65 42 33	390	46.37	4.19	
N2403	I	5226	4411.7	07 32 09	65 42 54	390	53.99	6.64	
N2716	I	306	1056.4				<13.52		
N2716	I	6118	4925.2				< 5.64		
N2773	I	457	3414.0	09 07 05	07 22 59	120	7.93	2.29	
N2773	I	7048	6080.1	09 07 05	07 22 59	150	6.04	1.80	
N2775	I	457	3414.0	09 07 39	07 14 30	150	6.76	2.22	
N2775	I	7048	6080.1	09 07 40	07 14 29	180	13.25	2.14	
N2777	I	457	3414.0				< 6.46		
N2777	I	7048	6080.1				< 4.90		
N2992	H	441	1085.0	09 43 17.9	-14 05 45	80	66.98	9.31	yes
N2992	H	1117	54.0	09 43 17.8	-14 06 00	30	144.63	51.85	
N2992	I	3060	1462.4	09 43 18	-14 05 42	240	263.29	14.29	
N2992	I	3061	1526.9	09 43 18	-14 05 45	270	247.97	13.49	
N2992	I	6376	7704.9	09 43 17	-14 05 35	420	607.54	9.40	

TABLE 4—*Continued*

Name	Seq		Exp. (sec)	X-ray Position RA	Dec	R (")	Rate (10^{-3} sec^{-1})	Error	Variable
N2993	H	441	1085.0				< 7.48		
N2993	H	1117	54.0				<65.50		
N3222	I	1945	2165.9				<15.17		
N3222	I	1946	2310.1				< 9.67		
N3227	I	1945	2165.9	10 20 46	20 07 20	360	148.59	9.65	yes
N3227	I	1946	2310.1	10 20 46	20 07 14	360	637.30	17.49	
N3227	I	7793	1462.4	10 20 46	20 07 20	240	402.39	22.74	
N3430	I	3936	5422.2				< 8.34		
N3430	I	6675	1227.8				<17.88		
N3516	I	1947	3948.3	11 03 25	72 50 15	300	158.57	7.19	yes
N3516	I	1948	3105.4	11 03 21	72 50 39	300	49.40	5.35	
N4038	I	469	1740.0	11 59 20	-18 34 40	270	43.24	6.55	
N4038	I	7054	5213.3	11 59 20	-18 35 50	210	34.52	3.22	
N4151	H	340	10037.0	12 08 00.9	39 41 05	80	87.96	3.38	
N4151	H	6395	9381.0	12 08 00.7	39 41 04	80	83.64	3.64	
N4151	I	352	6901.0	12 08 02	39 41 01	360	277.02	6.87	
N4151	I	353	19928.5	12 08 01	39 41 13	360	281.63	4.02	
N4156	H	340	10037.0	12 08 17.9	39 45 04	20	2.00	0.59	
N4156	H	6395	9381.0	12 08 18.1	39 45 03	20	4.02	0.83	
N4156	I	352	6901.0	12 08 20	39 44 42	180	11.70	1.99	
N4156	I	353	19928.5	12 08 18	39 45 16	180	16.84	1.25	
N4168	I	6974	5108.6	12 09 39	13 28 59	180	8.98	2.19	
N4168	I	6975	823.7	12 09 43	13 28 59	180	3.04	4.69	
N4178	I	4055	1280.3				<23.46		
N4178	I	6976	2615.4				<11.41		
N4178	I	6977	4640.4				< 8.98		
N4190	I	7816	3008.5	12 11 15	36 54 33	120	17.86	3.19	
N4190	I	7817	3708.6	12 11 14	36 54 29	150	17.41	3.12	
N4192	I	6978	6504.6	12 11 14	15 10 59	150	4.86	1.66	
N4192	I	6979	7365.0	12 11 14	15 10 59	120	2.67	1.14	
N4261	I	2672	2148.8	12 16 50	06 06 10	330	59.14	7.77	
N4261	I	6309	6905.9	12 16 50	06 06 25	330	47.68	4.07	
N4303	I	3267	1375.5	12 19 22	04 45 22	210	34.28	7.41	
N4303	I	6986	10425.6	12 19 20	04 45 09	210	27.21	2.29	
N4321	H	2892	3942.0	12 20 23.2	16 06 01	80	13.08	3.43	
N4321	H	4968	13183.0	12 20 23.0	16 06 01	80	6.90	1.70	
N4321	H	8968	23210.0	12 20 22.7	16 05 56	80	4.39	1.39	
N4321	I	4300	857.9	12 20 23	16 05 49	150	17.91	5.94	
N4321	I	4301	1914.4	12 20 23	16 05 49	210	26.52	5.12	
N4365	I	6992	4854.0	12 21 56	07 35 13	120	10.38	2.00	
N4365	I	6993	4753.6	12 21 55	07 35 30	150	12.45	2.40	
N4374	I	278	34963.8	12 22 31	13 09 44	300	58.06	2.73	
N4374	I	4311	4558.3	12 22 31	13 09 54	300	73.13	6.97	
N4382	I	2121	8148.0	12 22 54	18 28 02	300	21.69	2.80	
N4382	I	6994	10361.5	12 22 51	18 28 02	240	21.92	2.20	

TABLE 4—*Continued*

Name	Seq	Exp. (sec)	X-ray Position RA	Dec	R (")	Rate (10^{-3} sec^{-1})	Error	Variable
N4386	I 5233	2896.3				< 6.45		
N4386	I 5424	13112.9				< 4.18		
N4394	I 2121	8148.0				< 5.85		
N4394	I 6994	10361.5				< 4.73		
N4435	I 278	34963.8				<14.48		
N4435	I 7590	1577.7				<15.94		
N4438	I 4311	4558.3	12 25 12	13 17 47	180	17.81	4.11	
N4438	I 7590	1577.7	12 25 12	13 17 06	210	12.04	6.78	
N4473	I 2124	4388.1	12 27 16	13 42 23	210	27.25	6.80	
N4473	I 7003	5068.5	12 27 16	13 42 23	180	9.81	14.00	
N4477	I 281	14695.0	12 27 31	13 54 52	270	19.21	2.48	
N4477	I 2124	4388.1	12 27 29	13 54 31	210	29.21	4.96	
N4477	I 7003	5068.5	12 27 31	13 54 20	150	12.42	3.11	
N4479	I 281	14695.0				< 8.95		
N4479	I 7003	5068.5				< 7.78		
N4526	I 4309	8388.8	12 31 32	07 58 23	180	7.04	1.75	
N4526	I 4310	9673.0	12 31 29	07 58 30	120	5.09	2.04	
N4548	I 7007	5008.3				<12.67		
N4548	I 7011	1423.1				<30.82		
N4569	I 4045	1948.1	12 34 15	13 26 29	210	16.12	4.83	
N4569	I 4314	3320.3	12 34 15	13 26 29	210	17.32	3.73	
N4579	I 2126	1058.8	12 35 12	12 05 44	270	231.32	16.15	
N4579	I 4315	7290.0	12 35 11	12 05 41	270	218.63	6.05	
N4594	I 2127	5282.2	12 37 23	-11 20 40	390	73.28	5.15	
N4594	I 2128	1207.4	12 37 23	-11 20 48	390	90.45	12.51	
N4639	I 7013	5145.1	12 40 22	13 31 51	270	38.76	4.22	
N4639	I 7014	4430.6	12 40 22	13 31 37	270	34.83	4.42	
N4654	I 7013	5145.1				<11.07		
N4654	I 7014	4430.6				<11.03		
N4665	I 7016	5763.1				<10.50		
N4665	I 7017	6408.1				<11.55		
N4697	I 2134	4957.4	12 45 58	-05 32 00	240	21.54	3.29	
N4697	I 4004	3484.6	12 45 59	-05 31 41	300	19.99	5.06	
N4698	I 7022	5580.6	12 45 52	08 46 59	180	5.91	2.24	
N4698	I 7023	4712.6	12 45 52	08 46 59	180	8.40	2.46	
N4754	I 7024	6561.0				< 5.96		
N4754	I 7025	5681.7				< 8.76		
N4762	I 7024	6561.0	12 50 24	11 30 03	240	11.08	2.79	
N4762	I 7025	5681.7	12 50 23	11 29 59	270	17.57	3.37	
N5128	H 475	16421.0	13 22 31.9	-42 45 28	120	74.25	3.02	
N5128	H 4495	31472.0	13 22 31.8	-42 45 35	220	64.85	3.00	

TABLE 4—*Continued*

Name	Seq		Exp. (sec)	X-ray Position RA	Dec	R (")	Rate (10^{-3} sec^{-1})	Error	Variable
N5236	H	587	24188.0	13 34 11.9	-29 36 43	200	27.67	2.82	
N5236	H	10447	19644.0	13 34 11.0	-29 36 38	200	31.92	3.37	
N5253	H	2889	2197.0				<11.05		
N5253	H	10315	21686.0				< 3.30		
N5506	I	3062	2257.1	14 10 39	-02 58 17	360	236.50	11.43	?
N5506	I	3063	1901.4	14 10 39	-02 58 23	360	325.27	14.31	
N5506	I	7204	6454.3	14 10 37	-02 58 20	360	296.15	7.47	
N5506	I	9502	2942.3	14 10 40	-02 58 22	360	307.29	11.32	
N5548	H	6397	14288.0	14 15 43.4	25 22 00	100	411.67	5.78	
N5548	H	8315	11363.0	14 15 43.3	25 22 01	100	378.45	6.20	
N6503	I	2720	1810.7				<23.27		
N6503	I	8846	828.7				<13.53		
N6503	I	8888	375.8				<29.26		
N6946	I	422	4879.5	20 34 00	60 00 58	480	58.14	5.86	
N6946	I	10314	20871.7	20 33 55	60 00 34	480	61.68	2.88	*
N6946	I	10597	7444.1	20 33 59	60 00 28	480	55.06	5.17	
N7469	H	3168	2290.0	23 00 44.6	08 36 16	110	761.66	18.78	?
N7469	H	10218	12450.0	23 00 44.7	08 36 16	110	312.33	5.69	
N7469	I	1977	1938.6	23 00 45	08 36 17	750	915.20	23.68	
N7469	I	1978	1991.0	23 00 44	08 36 14	720	1058.31	26.12	
I5283	H	3168	2290.0				< 4.15		
I5283	H	10218	12450.0				< 1.64		
N7552	I	5259	2056.5	23 13 25	-42 51 03	180	24.39	4.81	
N7552	I	7582	1651.6	23 13 24	-42 51 12	180	27.13	5.86	
N7582	I	3066	1528.2	23 15 37	-42 38 32	210	54.47	7.20	yes
N7582	I	3067	2106.1	23 15 39	-42 38 32	240	48.99	6.08	
N7582	I	6385	9767.8	23 15 41	-42 38 43	180	25.33	2.84	
N7590	I	3066	1528.2	23 16 12	-42 30 39	180	10.35	4.49	
N7590	I	3067	2106.1	23 16 12	-42 30 39	180	11.61	3.84	
N7590	I	6218	1899.4	23 16 10	-42 30 41	180	17.21	8.19	
N7590	I	6385	9767.8	23 16 11	-42 30 49	210	7.09	1.66	
N7599	I	3066	1528.2	23 16 36	-42 31 47	180	5.21	5.97	
N7599	I	3067	2106.1	23 16 36	-42 31 47	180	-0.14	6.29	
N7599	I	6218	1899.4	23 16 35	-42 31 48	180	11.39	7.73	
N7599	I	6385	9767.8	23 16 40	-42 32 14	180	7.79	1.72	

* N6946: IPC 10314 contains SN 1980K (Canizares et al. 1982).

TABLE 5

X-RAY DATA FOR MARGINALLY DETECTED SOURCES

NAME	SEQUENCE		B (mag)	TYPE (T)	X-RAY POSITION R.A.	X-RAY POSITION Decl.	R	COUNTS	ERROR	RATE (10^{-3} s^{-1})	F_x (10^{-13} cgs)	D (Mpc)	log L_x (erg s^{-1})
A. Elliptical and S0 Galaxies													
N1574	I	5782	11.13	−2	04 20 57	−57 05 23	210″	18.40	6.6	12.59	3.39	21.5	40.27
N4435	H	9008	11.72	−2	12 25 08.0	13 21 23	40	54.75	19.8	1.09	0.95	27.0	39.92
N4459	I	2124	11.49	−2	12 26 26	14 15 19	120	20.36	8.4	4.64	1.28	27.0	40.05
N4507	I	2664	12.80	−1	12 32 54	−39 38 00	120	9.86	3.9	12.18	3.83	72.5	41.38
N4589	I	10243	11.81	−5	12 35 17	74 27 40	90	14.48	6.9	2.53	0.68	48.2	40.28
N4621	I	2129	10.67	−5	12 39 30	11 55 31	180	32.85	12.6	5.26	1.44	27.0	40.10
I4329	H	344	12.48	−2	13 46 15.0	−30 02 54	40	13.29	5.5	5.63	5.54	93.8	41.77
N7562	I	8364	12.28	−5	23 13 23	06 24 29	150	19.08	7.3	5.64	1.71	72.0	41.03
B. Spiral and Irregular Galaxies													
N0628	H	7599	9.41	5	01 33 58.0	15 31 52	40	37.02	16.8	0.98	1.27	15.6	39.57
N1087	I	9138	11.13	5	02 43 52	−00 43 00	120	8.07	3.7	7.76	2.98	30.5	40.52
N1784	I	10225	11.82	4	05 03 07	−11 55 29	150	40.77	15.1	2.85	1.24	46.1	40.50
N2683	I	3921	9.34	3	08 49 35	33 37 45	120	9.32	4.1	9.71	3.54	9.2	39.55
N2777	I	457	14.10	2	09 08 01	07 24 30	90	8.90	4.2	2.93	1.13	35.0	40.22
N2782	I	1941	11.50	1	09 10 52	40 19 40	120	13.97	5.2	7.55	2.55	59.9	41.04
N3079	I	423	10.31	5	09 58 34	55 55 24	180	15.41	5.4	18.22	5.60	32.8	40.86
N3077	I	2105	10.57	0	09 59 23	68 58 29	150	32.85	11.2	4.03	1.53	3.4	38.33
N3125	I	430	12.88	0	10 04 17	−29 41 30	120	13.88	5.0	7.80	3.25	22.5	40.29
N3169	I	6681	10.56	3	10 11 40	03 42 59	90	9.68	3.9	5.21	1.87	31.7	40.35
N3351	I	497	9.88	3	10 41 16	11 57 34	180	21.90	8.5	9.86	3.59	13.0	39.86
N3368	I	2109	9.49	2	10 44 09	12 04 44	180	21.44	8.3	7.03	2.55	13.0	39.71
N3718	H	1897	10.44	1	11 29 50.0	53 20 42	40	9.53	4.1	2.10	2.16	27.3	40.28
N3718	I	2654	10.44	1	11 29 49	53 20 59	120	13.72	4.6	13.68	4.34	27.3	40.59
N3887	I	10229	10.99	3	11 44 33	−16 34 30	120	21.88	8.1	2.99	1.12	31.0	40.11
N3893	I	7759	10.65	5	11 46 00	49 00 00	90	16.13	5.7	4.08	1.42	27.3	40.10
N4535	I	4310	10.12	5	12 31 46	08 28 35	180	32.88	15.9	3.40	1.14	27.0	40.00
N4548	I	7007	10.43	3	12 32 54	14 45 30	180	28.34	11.7	5.66	2.00	27.0	40.24
N4651	I	3241	10.95	5	12 41 15	16 40 13	150	15.98	7.3	4.19	1.44	27.0	40.10
N5068	I	5807	10.15	5	13 16 13	−20 47 50	210	30.72	10.6	7.20	3.13	10.8	39.64
N5079	I	10244	13.80	4	13 17 00	−12 26 39	90	18.45	6.7	3.00	1.11	64.5	40.74
N5101	I	2138	11.48	1	13 19 00	−27 10 00	180	28.50	10.9	6.88	2.75	44.0	40.80
N5350	I	3932	11.84	4	13 51 20	40 37 00	120	14.12	6.5	4.39	1.39	60.8	40.79
N5364	I	7277	10.64	5	13 53 41	05 15 35	120	13.26	4.8	10.53	3.64	41.0	40.86
N5585	I	7637	10.94	7	14 18 04	56 55 59	150	27.71	10.6	4.47	1.47	11.2	39.34
N5985	I	6646	11.01	3	15 38 34	59 30 19	150	21.28	7.6	12.04	4.09	63.0	41.29
I5063	I	5254	13.14	0	20 48 15	−57 16 59	210	21.89	8.2	10.49	4.16	65.3	41.33
N7496	I	435	11.41	5	23 06 58	−43 42 00	90	15.37	5.2	6.43	2.21	32.3	40.44
N7769	I	6367	12.44	4	23 48 32	19 53 00	120	19.13	7.7	3.59	1.40	84.6	41.08

TABLE 6

X-RAY DATA FOR SOURCES PARTLY HIDDEN BY THE IPC RIBS
ELLIPTICAL AND S0 GALAXIES

Name		Seq	B (mag)	Type (T)	X-ray Position RA	Dec	R (")	Counts	Error	Rate (10^{-3} sec^{-1})	Fx (10^{-13} cgs)	D (Mpc)	Log Lx (erg s^{-1})
N0227		I 5393	13.35	-5				< 27.48		< 5.94	< 1.65	103.1	<41.32
N0596	a	I 5768	11.88	-5				< 15.17		< 7.36	< 2.08	38.2	<40.56
N1297		I 2094	12.61	-5				< 18.30		< 4.14	< 1.14	29.4	<40.07
N1374		I 5777	12.30	-5				< 14.74		< 14.06	< 3.61	27.2	<40.50
N1379		I 1887	12.07	-5				< 20.77		< 13.45	< 3.47	27.2	<40.49
N1379		I 4128	12.07	-5				< 11.91		< 18.44	< 4.77	27.2	<40.63
N1379		I 5777	12.07	-5				< 11.78		< 15.22	< 3.90	27.2	<40.54
N1381		I 1887	12.34	-2				< 13.08		< 6.89	< 1.78	27.2	<40.20
N1381		I 4128	12.34	-2				< 15.59		< 28.48	< 7.36	27.2	<40.81
N1381		I 5777	12.34	-2				< 14.85		< 13.45	< 3.45	27.2	<40.48
N1387	a	I 1887	11.83	-2				< 31.77		< 13.77	< 3.55	27.2	<40.50
N1389	a	I 1887	12.39	-2				< 36.65		< 20.26	< 5.23	27.2	<40.67
N1399	a	I 4128	10.79	-5	03 36 34	-35 36 43	480	362.26	21.9	490.02	126.73	27.2	42.05
N1404	a	I 4128	11.06	-5	03 36 55	-35 45 23	270	114.89	12.4	147.36	38.11	27.2	41.53
N2646		I 8361	12.85	-2				< 32.51		< 29.09	< 7.91	82.3	<41.81
N3156		I 6681	13.00	-5				< 18.41		< 14.44	< 3.97	29.9	<40.63
N3222	a	I 7793	13.39	-2				< 8.14		< 8.24	< 2.24	117.2	<41.57
N3801		I 6644	12.68	-2				< 14.62		< 10.49	< 2.81	73.6	<41.26
N4104		I 4258	13.70	-2	12 04 10	28 26 49	300	129.37	14.1	70.38	18.53	171.5	42.81
N4233		I 6711	12.97	-2				< 45.19		< 38.68	< 10.09	56.4	<41.58
N4270		I 2672	13.17	-2				< 19.73		< 14.75	< 3.86	56.4	<41.17
N4270		I 6309	13.17	-2				< 26.88		< 6.47	< 1.69	56.4	<40.81
N4281		I 2672	12.26	-2				< 9.39		< 9.40	< 2.46	56.4	<40.97
N4281		I 6309	12.26	-2				<104.42		< 34.06	< 8.91	56.4	<41.53
N4291	a	I 5233	12.26	-5	12 18 18	75 39 02	270	35.86	8.9	17.15	4.82	47.2	41.11
N4342		I 6992	13.54	-5				< 58.99		< 17.91	< 4.69	27.0	<40.61
N4342		I 6993	13.54	-5				< 57.33		< 17.76	< 4.65	27.0	<40.61
N4383		I 6988	12.98	-2				< 75.76		< 13.89	< 3.78	27.0	<40.52
N4387	a	I 278	12.75	-5				<194.24		< 6.74	< 1.85	27.0	<40.21
N4387	a	I 7590	12.75	-5				< 21.81		< 33.76	< 9.28	27.0	<40.91
N4406	a	I 278	10.02	-3	12 23 40	13 12 57	840	17998.79	187.7	635.68	174.49	27.0	42.18
N4406	a	I 7590	10.02	-3	12 23 38	13 13 23	540	370.63	26.2	386.91	106.41	27.0	41.97
N4417		I 280	12.07	-2				<115.82		< 4.20	< 1.11	27.0	<39.99
N4425	a	I 4311	12.79	-2				< 58.34		< 18.64	< 5.13	27.0	<40.65
N4425	a	I 7590	12.79	-2				< 16.12		< 14.30	< 3.93	27.0	<40.54
N4435	a	I 4311	11.72	-2				< 64.05		< 22.28	< 6.13	27.0	<40.73
N4458	a	I 7590	12.70	-5				< 24.78		< 24.96	< 6.86	27.0	<40.78
N4459	a	I 281	11.49	-2				< 75.37		< 9.72	< 2.68	27.0	<40.37
N4459	a	I 7003	11.49	-2				< 23.39		< 15.98	< 4.39	27.0	<40.58
N4472	a	I 4052	9.32	-3	12 27 14	08 16 52	390	164.44	14.7	287.58	75.34	27.0	41.82
N4472	a	I 5721	9.32	-3	12 27 34	08 16 34	420	457.37	34.0	59.09	15.48	27.0	41.13
N4473	a	I 281	11.07	-5				<181.69		< 18.59	< 5.12	27.0	<40.65
N4474	a	I 281	12.70	-2				< 44.42		< 4.87	< 1.34	27.0	<40.07
N4564	a	I 2126	11.87	-5				< 11.30		< 22.79	< 6.23	27.0	<40.74
N4564	a	I 4315	11.87	-5				< 60.87		< 17.23	< 4.71	27.0	<40.61
N4621	a	I 2130	10.67	-5				< 50.79		< 13.82	< 3.76	27.0	<40.52
N4638	a	I 2129	12.05	-2				< 52.17		< 11.10	< 3.03	27.0	<40.42
N4649	a	I 2129	9.83	-2	12 41 09	11 49 53	420	698.96	33.1	195.22	53.32	27.0	41.67
N4660		I 2130	11.87	-5				< 62.06		< 18.43	< 5.01	27.0	<40.64
N4798		I 3917	13.87	-3				< 31.46		< 13.16	< 3.30	164.5	<42.03
I3896	a	I 4645	12.37	-5				< 50.21		< 3.76	< 1.01	48.5	<40.45
N4926		I 1790	13.69	-3				< 28.19		< 8.83	< 2.20	162.8	<41.84
N5128	b	I 4493	6.62	-2								7.9	
N5302		I 7822	12.71	-1				< 19.19		< 5.73	< 1.67	75.6	<41.06
N5473		I 8337	12.36	-2				< 37.35		< 17.75	< 4.57	53.0	<41.19
N5574		I 6685	13.25	-2				< 22.48		< 13.42	< 3.64	46.1	<40.97
N5838	a	I 9975	11.72	-2	15 02 54	02 17 35	180	75.93	13.5	13.87	4.02	45.8	41.00
N5846	a	I10456	11.13	-2	15 03 56	01 48 10	600	940.98	46.3	147.47	42.62	45.8	42.03
N5898		I 1997	12.41	-2				< 45.41		< 35.46	< 11.56	52.4	<41.58
N5898		I 1998	12.41	-2				< 29.16		< 20.17	< 6.58	52.4	<41.33
N5898		I 7493	12.41	-2				< 39.12		< 23.01	< 7.50	52.4	<41.39

TABLE 6—*Continued*

Name	Seq	B (mag)	Type (T)	X-ray Position RA	Dec	R (")	Counts	Error	Rate (10^{-3} sec^{-1})	Fx (10^{-13} cgs)	D (Mpc)	Log Lx (erg s^{-1})
N5898	I 9647	12.41	-2				< 17.11		< 9.21	< 3.00	52.4	<40.99
N5903	I 1997	12.35	-3				< 40.65		< 36.03	< 11.74	57.7	<41.67
N5903	I 1998	12.35	-3				< 60.15		< 47.22	< 15.39	57.7	<41.79
N5903	I 7493	12.35	-3				< 43.70		< 29.32	< 9.56	57.7	<41.58
N5903	I 9647	12.35	-3				< 55.55		< 34.13	< 11.13	57.7	<41.65
I5269	I 6674	13.57	-2				< 17.48		< 10.10	< 2.58	43.2	<40.76
N7623	I 2598	13.05	-1				< 40.51		< 7.26	< 2.15	74.7	<41.16

SPIRAL AND IRREGULAR GALAXIES

Name	Seq	B (mag)	Type (T)	X-ray Position RA	Dec	R (")	Counts	Error	Rate (10^{-3} sec^{-1})	Fx (10^{-13} cgs)	D (Mpc)	Log Lx (erg s^{-1})
N0216	I 9977	13.29	0				< 11.69		< 13.74	< 4.53	30.7	<40.71
N0255	I 3023	12.03	5				< 16.88		< 16.96	< 5.92	32.1	<40.86
N0613	I 3556	10.19	3				< 26.71		< 20.57	< 6.89	28.1	<40.81
N0615	I 7951	11.39	3				< 36.19		< 7.61	< 2.83	37.1	<40.67
N0670	I 7756	12.19	3				< 19.78		< 7.10	< 3.04	74.3	<41.30
N1035	I 1880	12.42	5				< 29.59		< 4.72	< 1.72	24.1	<40.08
N1058	I 1773	11.60	5				< 11.20		< 25.17	< 10.51	14.6	<40.43
N1079	I 1823	12.22	1				< 7.04		< 47.23	< 15.89	27.2	<41.15
N1325	I 7028	11.34	3				< 41.52		< 6.84	< 2.39	28.4	<40.36
N1337	I 4974	11.50	5				< 37.49		< 29.36	< 11.59	24.1	<40.91
N1345	I 8404	13.85	5				< 43.81		< 8.12	< 3.14	29.1	<40.50
N1353	I 7424	11.67	4				< 8.05		< 8.42	< 2.99	28.6	<40.47
N1365 a	I 4129	9.45	3	03 31 44	-36 19 16	150	33.45	7.4	21.34	6.98	27.2	40.79
N1386 a	I 4128	11.08	1				< 21.24		< 29.92	< 9.80	27.2	<40.94
N1385	I 4084	11.21	5				< 14.94		< 27.78	< 9.00	28.1	<40.93
N1425	I 3450	10.77	5				< 10.16		< 13.69	< 4.23	28.0	<40.60
N1536	I 7030	12.70	5				< 29.12		< 4.72	< 1.67	21.5	<39.97
N2196	I10306	11.25	2	06 10 03	-21 47 20	180	45.82	12.2	7.69	3.32	46.3	40.93
N2403 a	I 5227	8.29	5	07 31 40	65 42 16	390	47.88	11.2	41.68	16.05	6.8	39.95
N2551	I 2261	12.31	2				< 14.10		< 12.68	< 4.57	54.8	<41.22
N2613	I10722	9.60	3				< 43.37		< 4.50	< 1.96	35.2	<40.46
N2713	I 306	11.87	4				< 10.50		< 13.91	< 5.34	80.2	<41.61
N2713	I 6118	11.87	4				< 34.98		< 9.94	< 3.82	80.2	<41.47
N2903 a	I 5229	8.91	5	09 29 19	21 43 12	180	15.76	4.8	23.63	8.86	10.1	40.03
N2955	I 7720	12.90	5				< 24.60		< 7.39	< 2.40	145.8	<41.79
N2976	I 3035	10.25	7				< 29.18		< 46.61	< 18.32	3.4	<39.40
N3031 b	I 466	7.01	3								2.2	
N3034 b	I 2102	9.21	0								8.4	
N3145	I 9696	11.73	4				< 28.62		< 10.09	< 4.20	76.0	<41.46
N3277	I 2644	12.31	1				< 21.45		< 20.37	< 6.97	40.2	<41.13
N3367	I 5793	11.74	5	10 43 54	14 00 42	150	40.65	8.5	12.77	4.65	70.1	41.44
N3675	I 5231	10.12	3				< 6.60		< 1.45	< 0.50	20.6	<39.40
N3735	I 4601	11.62	5				< 15.91		< 8.40	< 2.74	65.9	<41.15
N3735	I 9157	11.62	5				< 33.08		< 8.83	< 2.88	65.9	<41.18
N3898	I 6101	10.96	1				< 33.12		< 10.75	< 3.37	35.2	<40.70
N4045	I 2601	12.26	4				< 32.70		< 5.88	< 2.00	50.6	<40.79
N4145	I 352	11.12	5				< 38.65		< 5.60	< 1.94	33.3	<40.41
N4145	I 353	11.12	5				< 40.26		< 2.02	< 0.70	33.3	<39.97
N4189	I 6974	12.20	5				< 28.16		< 9.82	< 3.52	27.0	<40.49
N4189	I 6975	12.20	5				< 6.72		< 14.53	< 5.21	27.0	<40.66
N4212 a	I 5341	11.44	5				< 13.55		< 11.71	< 4.22	27.0	<40.57
N4214	I 7816	10.03	9	12 13 08	36 36 30	120	26.12	6.2	13.73	4.62	5.6	39.24
N4214	I 7817	10.03	9	12 13 08	36 36 30	90	5.23	3.9	2.23	0.75	5.6	38.45
N4260 a	I 6309	12.30	1				< 52.82		< 9.91	< 3.31	56.4	<41.10
N4274	I 6712	10.35	1				< 15.05		< 11.09	< 3.72	15.6	<40.03
N4273	I 2672	11.94	5				< 12.66		< 12.65	< 4.22	56.4	<41.21
N4273	I 6309	11.94	5				< 26.99		< 8.78	< 2.93	56.4	<41.05
N4388 a	I 4311	10.65	2				< 24.72		< 7.75	< 2.79	27.0	<40.39
N4410	I 280	14.40		12 23 55	09 18 09	210	299.52	33.0	9.38	3.18	157.1	41.97
N4414	I 542	10.48	5				< 37.97		< 16.22	< 5.35	15.6	<40.19
N4438 a	I 278	9.97	3	12 25 13	13 17 21	300	1062.13	52.0	53.01	19.01	27.0	41.22

TABLE 6—*Continued*

Name		Seq	B (mag)	Type (T)	X-ray Position RA	Dec	R (")	Counts	Error	Rate (10^{-3} sec^{-1})	Fx (10^{-13} cgs)	D (Mpc)	Log Lx (erg s^{-1})
N4461	a	I 7590	12.09	1				< 16.04		< 15.79	< 5.68	27.0	<40.70
N4492		I 4308	12.95	1				< 57.13		< 10.75	< 3.60	27.0	<40.50
N4519		I 4310	11.94	5				< 33.26		< 7.59	< 2.54	27.0	<40.35
N4519		I 7445	11.94	5				< 23.68		< 19.89	< 6.71	27.0	<40.77
N4527	a	I 9134	10.30	3				< 34.34		< 18.68	< 6.37	21.7	<40.56
N4536	a	I 9133	10.44	5				< 17.06		< 16.45	< 5.62	21.4	<40.49
N4571	a	I 7007	11.49	5				< 26.48		< 10.21	< 3.61	27.0	<40.50
N4593		I 6717	11.15	3	12 37 05	-05 04 10	300	534.68	23.7	825.09	285.69	63.5	43.14
N4597		I 6717	12.05	5				< 10.00		< 16.53	< 5.73	27.3	<40.71
N4602		I 6717	11.65	5				< 19.76		< 31.07	< 10.76	60.9	<41.68
N4603	a	I 6055	11.43	5				< 25.01		< 3.49	< 1.51	74.6	<41.00
N4656		I 471	10.45	10				< 21.13		< 16.64	< 5.37	11.6	<39.94
N4808		I 5375	11.99	5				< 22.62		< 17.60	< 6.08	33.6	<40.91
N4826	a	I 3176	8.62	2				< 28.14		< 28.20	< 10.00	6.6	<39.72
N4939		I 3968	11.05	4				< 20.20		< 34.96	< 13.06	71.2	<41.90
N5054		I 6653	10.75	3				< 12.19		< 15.96	< 6.39	43.9	<41.17
N5150		I 5255	12.72	3				< 27.55		< 25.74	< 10.12	90.9	<42.00
I4329A		I 7822	13.37	0	13 46 29	-30 03 22	420	4134.24	66.3	1539.05	600.24	99.4	43.85
N5326	a	I 3935	12.94	1				< 29.23		< 12.24	< 3.80	60.8	<41.23
N5371		I 3932	10.81	3				< 43.93		< 22.41	< 7.09	60.8	<41.50
N5477	a	I 2141	13.90	9				< 75.28		< 18.71	< 6.01	10.3	<39.88
N5566	a	I 6685	10.35	1				< 18.56		< 11.44	< 4.04	42.4	<40.94
N5936		I 803	12.70	5				< 15.29		< 10.74	< 4.03	88.2	<41.57
N5981		I 6646	13.90	5				< 35.91		< 24.74	< 8.41	62.8	<41.60
N6314		I 4933	13.15	1				< 13.95		< 10.04	< 3.97	140.2	<41.97
N6621		I 8885	13.36	3				< 11.33		< 17.70	< 7.17	133.7	<42.19
N6643		I 3092	11.07	5				< 16.86		< 19.73	< 8.22	41.0	<41.22
N6643		I 7696	11.07	5				<114.75		< 9.38	< 3.91	41.0	<40.90
N6654		I 5193	11.90	0				< 20.68		< 24.57	< 10.09	47.4	<41.43
N7213	a	I 2236	10.72	1	22 06 06	-47 24 31	420	1173.80	35.5	1235.19	425.15	35.4	42.80
N7320	b	I 9145	12.55	7								22.2	
N7331	b	I 7827	9.14	3								23.0	
N7343		I 9145	13.70	4				< 12.26		< 20.34	< 8.80	30.7	<41.00
N7552	a	I 1874	10.99	4				< 49.24		< 48.78	< 16.67	31.3	<41.29
N7552	a	I 3066	10.99	4	23 13 25	-42 51 30	120	19.37	5.0	26.64	9.13	31.3	41.03
N7552	a	I 3067	10.99	4	23 13 25	-42 51 30	150	17.57	5.2	17.53	6.01	31.3	40.85
N7582	a	I 5259	10.60	2	23 15 37	-42 38 42	180	40.87	8.2	38.33	13.10	28.3	41.10
N7582	a	I 6218	10.60	2				< 26.90		< 23.50	< 7.99	28.3	<40.88
N7582	a	I 7582	10.60	2	23 15 38	-42 39 05	150	30.08	6.3	31.47	10.74	28.3	41.01

[a] Unobscured data are in Tables 3A and 3B.
[b] Flux was not estimated (see Tables 3A and 3B).

TABLE 7

GALAXIES CONFUSED WITH NEARBY EXTENDED OR STRONG SOURCES

Name	Sequence	Nearby Source	Detection
N0495	7766	N0499	No
N2831	1841	N2832	No
N2993	3060	N2992	Yes
N2993	3061	N2992	Yes
N2993	6376	N2992	Yes
N3268	1896	cluster	
N3271	1896	cluster	
N3605	3927	N3607	No
N4319	5233	QSO	No
N4319	5424	QSO	No
N4467	4308	N4472	No
N4540	7795	I3528	No
N4647	2129	N4649	No
N4647	2130	N4649	No
N5049	6653	N5044	
I4329	7822	I4329A	No
N5682	2625	N5683	
N6877	1858	N6876	No
N7617	2598	N7619	No
N7770	6367	N7771	No

TABLE 8A

SEPARATE COMPONENTS OF THE X-RAY EMISSION

NAME	X-RAY POSITION R.A.	X-RAY POSITION Decl.	SEQUENCE	TYPE (T)	R	RATE (10^{-3} s^{-1})	ERROR	F_x (10^{-13} cgs)	D (Mpc)	log L_x (ergs s^{-1})
N0247 1	00^h 44^m 22^s	−21° 00′ 02″	I5766	5	180″	11.29	1.68	3.73	2.1	38.29
2	00 44 35	−21 03 58			180	13.32	1.68	4.40		38.37
3	00 44 36	−20 53 08			150	6.01	1.39	1.99		38.02
N1313 1	03 17 42	−66 40 13	I7044	5	180	50.22	2.92	18.91	5.9	39.90
2[a]	03 17 45	−66 47 03			180	36.16	2.72	13.61		...
N3628 1	11 17 40	13 51 42	I5152	4	240	31.94	2.17	11.00	12.4	40.31
2	11 18 01	13 50 59			180	12.16	1.56	4.19		39.89
N4236 1	12 14 15	69 44 30	I5803	7	90	1.25	0.66	0.43	3.5	37.80
2	12 14 45	69 40 00			90	2.03	0.72	0.69		38.01
N2403 1[a]	07 30 19.5	65 46 59	H584	5	50	10.63	0.87	16.62		...
3	07 31 36.6	65 42 20			60	5.29	0.87	8.26	6.8	39.66
4	07 31 54.6	65 46 09			30	1.25	0.43	1.95		39.03
5	07 32 12.6	65 46 18			30	0.91	0.42	1.43		38.90
N4258 1	12 16 23.2	47 36 00	H10756	3	30	7.90	2.98	8.37	10.9	40.08
2	12 16 35.0	47 34 01			100	35.16	7.98	37.29		40.72
N4449 1	12 25 43.2	44 21 45	H4967	9	30	2.59	0.46	2.89	4.8	38.90
2	12 25 44.3	44 22 35			30	2.20	0.45	2.45		38.83
3	12 25 44.7	44 20 15			40	1.72	0.53	1.92		38.72
4	12 25 44.9	44 23 25			40	3.53	0.58	3.94		39.04

[a] These sources are not likely to belong to these galaxies and are not included in the fluxes given in Table 3.

TABLE 8B

REFERENCES TO PREVIOUS WORK

Name	Reference
I0342	FT
N0224	Trinchieri & Fabbiano 1991
N0253	Fabbiano & Trinchieri 1984; Fabbiano 1988b
N0598	Trinchieri, Fabbiano & Peres 1988
N2403	IPC fluxes are in FT, HRI fluxes are in Table 7A
N3031	Fabbiano 1988a
N4631	FT
N5457	Trinchieri, Fabbiano, & Romaine 1990
N6946	FT

TABLE 9

EXTENT PARAMETERS FOR SOURCES WITH MORE THAN 100 COUNTS IN IPC OBSERVATIONS ELLIPTICAL AND S0 GALAXIES

Name		Seq	Type (T)	S/N	R (")	C(90)/C(180)	Error	σ (0.3 keV)	σ (4.5 keV)
N0499		7766	-3	25.3	210	0.557	0.020	73.7 (68.1 - 79.7)	85.6 (81.1 - 90.5)
N0507		7766	-2	40.4	630	0.438	0.015	121.8 (113.2 - 131.4)	127.1 (119.5 - 136.5)
N0720		5769	-5	10.6	480	0.547	0.048	76.6 (63.5 - 92.5)	88.0 (77.3 - 101.3)
N1052		1880	-3	9.4	240	0.763	0.052	30.0 (< 32.5)	47.7 (30.5 - 56.0)
N1316		1883	-2	11.7	450	0.492	0.040	95.1 (81.3 - 113.7)	103.7 (91.8 - 120.0)
N1316		1884	-2	12.9	450	0.597	0.037	63.0 (53.7 - 72.8)	76.9 (69.8 - 84.9)
N1316		10571	-2	10.1	450	0.675	0.043	44.4 (30.8 - 54.2)	62.7 (54.7 - 70.2)
N1332		7028	-2	10.3	360	0.768	0.042	30.0 (< 30.0)	46.8 (31.9 - 53.2)
N1395		9185	-5	10.4	480	0.573	0.036	69.2 (60.0 - 79.7)	82.0 (74.5 - 90.5)
N1399		1887	-5	37.1	1200	0.532	0.019	81.3 (75.4 - 87.6)	91.8 (87.1 - 97.0)
N1404		1887	-5	16.6	300	0.752	0.029	30.0 (< 30.1)	49.2 (43.9 - 53.8)
N1407		10241	-5	9.4	300	0.574	0.050	68.9 (56.2 - 83.9)	81.7 (71.6 - 93.9)
N2563		304	-2	11.5	360	0.429	0.045	127.4 (102.7 - 170.0)	132.5 (110.4 - 172.2)
N2832		1841	-5	8.3	360	0.675	0.073	44.4 (< 61.8)	62.7 (49.7 - 75.9)
N3607		3927	-2	11.8	300	0.428	0.046	128.0 (102.7 - 172.5)	133.2 (110.4 - 174.6)
N3923		5800	-3	9.2	270	0.588	0.054	65.3 (51.8 - 80.6)	78.7 (68.4 - 91.3)
N4203		3922	-2	12.3	240	0.632	0.040	54.2 (45.1 - 64.3)	70.2 (63.2 - 77.9)
N4291		5424	-5	12.9	270	0.609	0.038	60.0 (50.7 - 69.7)	74.5 (67.5 - 82.4)
N4374		4311	-5	10.5	300	0.789	0.047	30.0 (< 30.0)	41.2 (< 50.6)
N4374	a	278	-5	21.3	300	0.667	0.021	46.3 (40.7 - 50.9)	64.1 (60.4 - 67.7)
N4382		2121	-2	7.8	300	0.578	0.066	67.9 (51.4 - 87.9)	80.9 (68.1 - 97.3)
N4382		6994	-2	10.0	240	0.581	0.050	67.1 (54.5 - 81.6)	80.2 (70.4 - 92.0)
N4406		4311	-3	41.2	840	0.399	0.018	152.9 (135.7 - 173.8)	155.8 (140.7 - 175.8)
N4472		4308	-3	46.7	810	0.521	0.012	84.9 (80.9 - 88.9)	94.7 (91.5 - 98.1)
N4552		4313	-2	13.0	150	0.848	0.039	30.0 (< 30.0)	30.0 (< 32.3)
N4636		412	-3	18.5	600	0.528	0.028	82.6 (73.9 - 92.1)	92.8 (85.9 - 101.0)
N4649		2130	-2	25.7	420	0.663	0.017	47.2 (43.1 - 50.9)	64.8 (61.8 - 67.7)
N4697		2134	-5	6.6	240	0.484	0.072	98.3 (73.9 - 140.0)	106.5 (85.9 - 144.3)
N4756		1900	-5	10.6	270	0.522	0.050	84.5 (69.5 - 103.6)	94.4 (82.2 - 111.2)
N5044		6653	-5	33.0	780	0.471	0.018	104.1 (96.3 - 113.2)	111.6 (104.7 - 119.5)
I1459		6674	-5	7.1	240	0.749	0.068	30.0 (< 42.8)	49.6 (30.2 - 61.6)
N5846		9975	-2	33.8	600	0.565	0.012	71.4 (68.1 - 74.8)	83.8 (81.1 - 86.6)
N6876		1858	-5	9.7	240	0.558	0.048	73.4 (60.8 - 88.6)	85.4 (75.1 - 97.8)
I4296		1902	-5	11.7	360	0.694	0.048	38.6 (< 50.9)	59.3 (50.6 - 67.7)
N7619		2598	-5	13.3	300	0.580	0.038	67.3 (57.7 - 78.1)	80.4 (72.8 - 89.3)
N7626		2598	-5	6.7	240	0.572	0.077	69.5 (50.2 - 94.0)	82.2 (67.2 - 102.6)

SPIRAL AND IRREGULAR GALAXIES

Name		Seq	Type (T)	S/N	R (")	C(90)/C(180)	Error	σ (0.3 keV)	σ (4.5 keV)
I0342-1		7045	6	6.7	210	0.574	0.070	68.9 (51.4 - 90.7)	81.7 (68.1 - 99.7)
I0342-2		7045	6	3.2	150	0.989	0.179	30.0 (< 30.0)	30.0 (< 31.9)
I0342-3		7045	6	6.2	210	0.572	0.082	69.5 (49.1 - 95.9)	82.2 (66.3 - 104.4)
N0247-1		5766	5	6.7	180	0.771	0.088	30.0 (< 42.2)	46.3 (< 61.3)
N0247-2		5766	5	7.9	180	0.624	0.068	56.2 (39.3 - 73.9)	71.6 (59.6 - 85.9)
N0247-3		5766	5	4.3	150	0.769	0.132	30.0 (< 53.0)	46.7 (< 69.3)
N0253		2082	5	28.5	660	0.597	0.017	63.0 (58.7 - 67.3)	76.9 (73.5 - 80.4)
N0524		2089	0	6.6	240	0.667	0.079	46.3 (< 65.3)	64.1 (50.0 - 78.7)
N1042		1880	5	7.4	240	0.845	0.079	30.0 (< 30.0)	30.0 (< 47.2)
N1097		2093	4	19.4	210	0.663	0.025	47.2 (40.7 - 52.8)	64.8 (60.4 - 69.1)
N1313		7044	5	17.2	180	0.875	0.027	30.0 (< 30.0)	30.0 (< 30.0)
N1365		3059	3	8.3	330	0.659	0.055	48.1 (31.7 - 61.3)	65.5 (55.4 - 75.5)
N1559		7046	5	11.1	180	0.553	0.046	74.8 (62.5 - 89.6)	86.6 (76.5 - 98.8)
N1672		427	3	7.7	210	0.638	0.066	52.8 (34.8 - 69.5)	69.1 (57.3 - 82.2)
N2403	b	589	5	11.1	390	0.480	0.054	100.0 (80.6 - 129.3)	108.0 (91.3 - 134.5)
N2403	b	5226	5	8.1	390	0.532	0.085	81.3 (58.0 - 116.5)	91.8 (72.9 - 122.4)
N2903		7049	5	10.5	210	0.635	0.047	53.5 (42.5 - 65.3)	69.6 (61.5 - 78.7)
N3031		2102	3	32.7	480	0.701	0.014	35.9 (31.4 - 41.0)	57.9 (55.2 - 60.6)
N3034		466	0	45.0	660	0.737	0.010	30.0 (< 30.0)	51.4 (49.9 - 53.0)

TABLE 9—*Continued*

Name	Seq	Type (T)	S/N	R (")	C(90)/C(180)	Error	σ (0.3 keV)	σ (4.5 keV)
N3628-1	5152	4	14.7	240	0.716	0.033	31.2 (< 42.2)	55.1 (49.6 - 61.3)
N3628-2	5152	4	7.8	180	0.709	0.072	33.1 (< 53.0)	56.4 (43.9 - 69.3)
N4038	7054	5	10.7	210	0.551	0.045	75.4 (63.3 - 90.0)	87.1 (77.1 - 99.1)
N4156	353	3	13.5	180	0.737	0.039	30.0 (< 37.1)	51.4 (45.2 - 58.5)
N4254	4306	5	8.3	150	0.665	0.063	46.8 (< 61.8)	64.4 (52.9 - 75.9)
N4303	6986	5	11.9	210	0.525	0.040	83.5 (71.4 - 97.9)	93.6 (83.8 - 106.2)
N4388	278	2	12.4	210	0.671	0.042	45.4 (31.9 - 55.0)	63.4 (55.6 - 70.7)
N4450	7001	2	7.1	270	0.787	0.069	30.0 (< 30.8)	42.0 (< 54.7)
N4477	281	0	7.8	270	0.623	0.062	56.5 (41.6 - 72.5)	71.8 (60.9 - 84.7)
N4501	4304	4	8.8	240	0.620	0.055	57.2 (44.4 - 71.4)	72.4 (62.7 - 83.8)
N4565	9974	3	13.0	300	0.550	0.035	75.7 (66.0 - 86.9)	87.3 (79.4 - 96.4)
N4579	2126	2	14.3	270	0.844	0.027	30.0 (< 30.0)	30.0 (< 30.2)
N4579	4315	2	36.1	270	0.797	0.012	30.0 (< 30.0)	37.7 (32.3 - 42.7)
N4594	2127	2	14.2	390	0.638	0.031	52.8 (45.8 - 60.5)	69.1 (63.8 - 74.9)
N4594	2128	2	7.2	390	0.594	0.063	63.8 (48.5 - 81.6)	77.5 (65.8 - 92.0)
N4631	471	5	8.7	270	0.627	0.068	55.5 (38.2 - 73.1)	71.1 (59.1 - 85.2)
N4639	7013	3	9.2	270	0.787	0.050	30.0 (< 30.0)	42.0 (< 51.4)
N4639	7014	3	7.9	270	0.826	0.063	30.0 (< 30.0)	30.0 (< 47.7)
N4689	7018	5	8.5	150	0.820	0.058	30.0 (< 30.0)	30.0 (< 47.8)
N4826	2136	2	6.5	270	0.620	0.071	57.2 (39.7 - 76.0)	72.4 (59.8 - 87.5)
N5204	7635	7	11.6	150	0.864	0.042	30.0 (< 30.0)	30.0 (< 30.0)
N5236	588	5	22.3	390	0.459	0.024	110.0 (98.7 - 123.6)	116.8 (106.9 - 128.8)
N6744	7063	4	10.5	240	0.715	0.050	31.4 (< 46.8)	55.2 (47.4 - 64.4)
N6872	1858	3	6.2	270	0.446	0.074	117.1 (85.2 - 190.0)	122.9 (95.0 - 190.0)
N6946	422	5	9.9	480	0.508	0.045	89.3 (74.8 - 108.0)	98.5 (86.6 - 115.0)
N6946	10314	5	21.4	480	0.442	0.019	119.4 (109.0 - 131.4)	124.9 (115.9 - 136.5)
N6946	10597	5	10.6	480	0.496	0.033	93.6 (82.2 - 108.0)	102.3 (92.6 - 115.0)

AGNs

Name		Seq	Type (T)	S/N	R (")	C(90)/C(180)	Error	σ (0.3 keV)	σ (4.5 keV)
N0315		4374	-3	17.3	300	0.699	0.026	36.7 (< 44.9)	58.3 (53.4 - 63.1)
N0985		3143	10	40.1	450	0.785	0.010	30.0 (< 30.0)	42.7 (38.7 - 45.4)
N1068		1927	3	27.0	360	0.745	0.016	30.0 (< 30.0)	50.1 (48.0 - 52.7)
N1068		1928	3	35.8	360	0.715	0.013	31.4 (< 35.6)	55.2 (52.9 - 57.7)
N1566		1937	5	26.0	300	0.753	0.017	30.0 (< 30.0)	49.1 (46.5 - 51.5)
N1566		1938	5	19.4	300	0.752	0.023	30.0 (< 30.0)	49.2 (45.4 - 52.7)
N2992		3060	1	18.4	240	0.877	0.020	30.0 (< 30.0)	30.0 (< 30.0)
N2992		3061	1	18.4	270	0.871	0.020	30.0 (< 30.0)	30.0 (< 30.0)
N2992		6376	1	64.7	420	0.859	0.006	30.0 (< 30.0)	30.0 (< 30.0)
N3227		1945	3	15.4	360	0.787	0.027	30.0 (< 30.0)	42.0 (30.7 - 48.1)
N3227		1946	3	36.5	360	0.815	0.011	30.0 (< 30.0)	30.5 (< 34.4)
N3227	a	7793	3	17.6	240	0.723	0.026	30.1 (< 37.4)	53.8 (49.6 - 58.7)
N3516		1947	-2	22.1	300	0.849	0.018	30.0 (< 30.0)	30.0 (< 30.0)
N3516		1948	-2	9.2	300	0.820	0.047	30.0 (< 30.0)	30.0 (< 45.9)
N3660		10228	4	7.1	330	0.721	0.070	30.3 (< 49.8)	54.1 (40.4 - 66.9)
N3783		7209	1	75.5	690	0.840	0.005	30.0 (< 30.0)	30.0 (< 30.0)
N3998		4548	-2	15.3	330	0.819	0.026	30.0 (< 30.0)	30.0 (< 39.6)
N4051		7200	4	71.9	480	0.726	0.006	30.0 (< 30.5)	53.2 (52.2 - 54.3)
N4151		352	2	40.3	360	0.798	0.010	30.0 (< 30.0)	37.2 (32.7 - 41.6)
N4151		353	2	70.0	360	0.808	0.006	30.0 (< 30.0)	32.7 (30.7 - 35.3)
N4235		6711	1	15.1	150	0.806	0.029	30.0 (< 30.0)	33.5 (< 45.0)
N4261		2672	-5	7.6	330	0.561	0.064	72.5 (56.0 - 93.2)	84.7 (71.5 - 102.0)
N4261		6309	-5	11.7	330	0.619	0.040	57.5 (48.1 - 67.6)	72.6 (65.5 - 80.6)
N5128		477	-2	103.5	1020	0.792	0.004	30.0 (< 30.0)	40.0 (38.2 - 41.6)
N5506		3062	1	20.7	360	0.863	0.018	30.0 (< 30.0)	30.0 (< 30.0)
N5506		3063	1	22.7	360	0.859	0.016	30.0 (< 30.0)	30.0 (< 30.0)
N5506		7204	1	39.7	360	0.864	0.009	30.0 (< 30.0)	30.0 (< 30.0)
N5506		9502	1	27.1	360	0.863	0.014	30.0 (< 30.0)	30.0 (< 30.0)
N5548		356	1	144.5	600	0.801	0.003	30.0 (< 30.0)	35.8 (34.4 - 37.2)

TABLE 9—*Continued*

Name	Seq	Type (T)	S/N	R (")	C(90)/C(180)	Error	σ (0.3 keV)	σ (4.5 keV)
N5683	2625	0	16.0	240	0.702	0.029	35.6 (< 44.9)	57.7 (52.3 - 63.1)
N6814	354	4	25.3	480	0.803	0.013	30.0 (< 30.0)	34.8 (30.3 - 40.8)
N7213	6714	1	65.1	600	0.772	0.007	30.0 (< 30.0)	46.1 (44.5 - 47.4)
N7469	1977	2	38.6	750	0.763	0.011	30.0 (< 30.0)	47.7 (45.7 - 49.2)
N7469	1978	2	40.5	720	0.750	0.010	30.0 (< 30.0)	49.5 (48.1 - 50.9)
N7582	3067	2	8.1	240	0.846	0.059	30.0 (< 30.0)	30.0 (< 42.0)
N7771	6367	1	7.0	210	0.767	0.079	30.0 (< 40.7)	47.0 (< 60.4)

NOTE.—I0342, N0247, N3628: for each source, see Table 8.
[a] Source is outside the IPC ribs.
[b] N2403: three sources are too close to estimate radial extents.

TABLE 10

EXTENT PARAMETERS FOR SOURCES WITH MORE THAN 150 COUNTS IN HRI OBSERVATIONS

Name	Sequence	Type (T)	S/N	*R*	C12	Error	σ	C36	Error	σ
Elliptical and S0 Galaxies										
N1316	1885	−2	6.5	120″	0.504	0.055	8.8 (7.7–10.3)	0.625	0.062	20.7 (18.4–23.2)
N4374	4320	−5	14.8	90	0.540	0.036	8.1 (7.4–8.8)	0.650	0.034	19.7 (18.5–21.0)
N4406	4321	−3	10.7	170	0.295	0.063	29.1 (>15.1)	0.563	0.058	23.2 (20.8–26.3)
N4472	7068	−3	20.5	180	0.525	0.026	8.4 (7.9–9.0)	0.620	0.022	20.9 (20.0–21.7)
N4636	7038	−3	25.2	180	0.399	0.025	12.3 (11.2–13.9)	0.523	0.017	25.3 (24.4–26.2)
N4649	2132	−2	12.4	140	0.456	0.039	10.1 (9.0–11.5)	0.707	0.036	17.7 (16.5–19.0)
Spiral and Irregular Galaxies										
N0253[a]	583	5	12.0	180	0.372	0.039	14.0 (11.8–18.0)	0.609	0.032	21.3 (20.1–22.6)
N0253[a]	2084	5	8.0	180	0.480	0.066	9.4 (8.0–11.6)	0.586	0.050	22.2 (20.3–24.6)
N3031[b]	585	3	23.5	90	0.853	0.014	2.9 (1.9–3.1)	0.901	0.019	8.8 (<10.7)
N3034[a]	586	0	23.9	200	0.382	0.026	13.3 (11.9–15.3)	0.561	0.018	23.3 (22.5–24.2)
N4438	9008	3	7.6	120	0.646	0.079	6.3 (5.2–7.6)	0.581	0.084	22.4 (19.2–26.8)
N4449-3	4967	9	3.3	40	0.968	0.234	1.0 (<5.1)	0.673	0.154	18.9 (<25.5)
N4449-4	4967	9	6.0	40	0.672	0.093	6.0 (4.7–7.4)	0.628	0.082	20.6 (17.6–24.1)
N4579	7067	2	12.9	80	0.927	0.022	1.0 (<1.0)	0.896	0.040	9.5 (<12.2)
N5194	3047	4	10.2	190	0.522	0.041	8.4 (7.6–9.4)	0.690	0.045	18.3 (16.8–19.9)
N5236	587	5	9.8	200	0.563	0.049	7.6 (6.8–8.6)	0.712	0.056	17.6 (15.7–19.5)
N5236	10447	5	9.5	200	0.557	0.048	7.8 (7.0–8.7)	0.833	0.072	13.2 (8.2–15.9)
AGNs										
I4329A	344	0	25.7	90	0.826	0.016	3.4 (3.0–3.8)	0.915	0.012	4.6 (<8.5)
N0985	8308	10	35.9	130	0.910	0.008	1.0 (<1.0)	0.919	0.008	3.0 (<6.5)
N1566	7112	5	48.3	110	0.901	0.006	1.0 (<1.0)	0.901	0.007	8.8 (7.6–9.7)
N4151	340	2	26.4	90	0.877	0.012	1.0 (<2.1)	0.932	0.014	3.0 (<8.5)
N4151	6395	2	22.7	90	0.777	0.017	4.5 (4.2–4.7)	0.932	0.018	3.0 (<8.2)
N5128	475	−2	24.6	120	0.684	0.018	5.8 (5.5–6.0)	0.815	0.017	14.0 (13.3–14.6)
N5128	4495	−2	21.6	220	0.784	0.025	4.4 (3.8–4.8)	0.631	0.025	20.4 (19.5–21.4)
N5548	6397	1	71.2	100	0.898	0.004	1.0 (<1.0)	0.922	0.004	3.0 (<3.0)
N5548	8315	1	61.0	100	0.691	0.008	5.7 (5.6–5.8)	0.923	0.005	3.0 (<3.0)
N7469	3168	2	40.6	110	0.910	0.007	1.0 (<1.0)	0.923	0.007	3.0 (<4.0)
N7469	10218	2	54.8	110	0.884	0.006	1.0 (<1.0)	0.917	0.006	3.0 (<6.5)

NOTE.—C12 = count (10″)/count (20″); C36 = count (30″)/count (60″).
[a] N253 and N3034 have extended gaseous emission (starburst galaxies).
[b] N3031: source at the center.

TABLE 11

NOTES ON INDIVIDUAL GALAXIES AND REFERENCES TO PREVIOUS WORK

Galaxy	Notes and References
I342	FT; separate sources
I1613	X-ray source is at the edge of the galaxy
I1727	VV 338
I2574	FT; X-ray source is at the edge of the galaxy
I3528	N4540 is inside the I3528 X-ray image
I4296	Close to the IPC ribs; Killeen et al. 1986
I5283	Arp 298
N205	M110
N221	M32
N224	M31; Van Speybroeck et al. 1979; Van Speybroeck & Betchold 1981; LVS; Fabbiano, Trinchieri, & Van Speybroeck 1987; Trinchieri & Fabbiano 1991; McKechnie et al. 1984 (*EXOSAT*)
N247	Separate sources; LVS
N253	Starburst galaxy with gaseous plumes; Van Speybroeck & Betchold 1981; LVS; Fabbiano & Trinchieri 1984; Fabbiano 1988a
N449	Mrk 1
N495	Inside the X-ray emission of NGC 499
N499	Nearby X-ray source (NGC 507)
N507	VV 207, Arp 229; nearby X-ray source (NGC 499)
N520	VV 231, Arp 157
N523	Arp 153
N533	Outside the IPC ribs; flux was estimated by unmasking the image
N598	M33; Long et al. 1981; LVS; Markert & Rallis 1983; Trinchieri, Fabbiano, & Peres 1988; Peres et al. 1989
N613	VV 824
N628	M74; FT
N672	VV 338
N720	TFC
N772	Arp 78
N877	Nearby X-ray sources
N936	The X-ray images of the two observations (IPC 5118, 5771) look different. There might be a nearby object flaring up.
N985	Mrk 1048, VV 285
N1042	X-ray centroid does not coincide with nucleus
N1068	3C 71, M77, Arp 37
N1073	X-ray centroid does not coincide with nucleus
N1097	Arp 77
N1201	A few X-ray sources are present close to the galaxy
N1218	UGC 2555, 3C 78
N1313	VV 436; a strong source is present to the south. This source was not included in the analysis; FT
N1316	Arp 154, For A
N1365	VV 825; Maccacaro et al. 1982
N1387	Outside the IPC ribs
N1395	Nulsen et al. 1984; TFC
N1398	X-ray centroid does not coincide with nucleus
N1399 and N1404	There is extended emission from intracluster medium; Killeen & Bicknell 1988a
N1400	X-ray source may be unrelated to the galaxy; nearby source (NGC 1407)
N1407	Dressel & Wilson 1985
N1421	X-ray image is extended in north-south direction. It might include other serendipitous sources.
N1559	FT
N1569	Arp 210
N1600	Unresolved extended source; in cluster; it might include contribution from the fainter neighbor galaxies.
N1614	Mrk 617, Arp 186
N1672	VV 826; FT
N1961	Arp 184; two sources are resolved in the hard band
N2196	Outside the IPC ribs.
N2276	Arp 25; nearby stellar source
N2300	Arp 114
N2363	Mrk 71
N2403	Separate sources; FT
N2444	Arp 143, VV117
N2563	Complex X-ray emission in field; in cluster; southern source may be not related to the galaxy
N2608	Arp 12; nearby strong source
N2685	Arp 336
N2782	Arp 215
N2831	Arp 315; inside the X-ray image of NGC 2832
N2903	FT
N2911–N2914	Arp 232 + Arp 137; X-ray source is between the two galaxies
N2992	Arp 245; Maccacaro et al. 1982
N2993	Arp 245; X-ray image confused with that of NGC 2992
N3031	M81; small Seyfert-like nucleus; Elvis & Van Speybroeck 1982; LVS; Fabbiano 1988b
N3034	M82, Arp 337, 3C 231; starburst galaxy with gaseous nuclear outflow; Van Speybroeck & Betchold 1981; Watson et al. 1984; Kronberg et al. 1985; Fabbiano 1988a; Schaaf et al. 1989
N3066	Mrk 133
N3077	Nearby stellar source
N3078	Nearby strong source
N3081	Nearby strong source
N3227	Arp 94, VV 209; The X-ray source is well centered on NGC 3227, but NGC 3226 is inside the X-ray emission
N3258 and N3260	X-ray image includes both galaxies; nearby extended source
N3310	Arp 217
N3351	M95
N3353	Mrk 35
N3367	Outside the IPC ribs
N3368	M96; X-ray source may be unrelated to the galaxy
N3379	M105
N3395	Arp 270, VV 246; The X-ray centroid coincides with NGC 3395, but NGC 3396 could also contribute to the X-ray emission
N3445	VV 14, Arp 24
N3448	Arp 205
N3605, 3607, 3608	In N3607 group; NGC 3605 and NGC 3608 are inside the X-ray image of NGC 3607; Biermann et al. 1982
N3628	Arp 317, VV 308; separate sources; absorbed starburst nucleus with possible outflow; Bregman & Glassgold 1982; Fabbiano, Heckman, & Keel 1990
N3660	Mrk 1291
N3690	Mrk 171, VV 118, Arp 299
N3718	Arp 214
N3884	Outside the IPC ribs
N3888	Mrk 188
N3894 N3895	X-ray emission includes both NGC 3894 and 3895 and extends to the south
N3994	VV 249
N3998	Dressel & Wilson 1985
N4038	N4038 + N4039 Antennae, VV 245, Arp 244; Fabbiano & Trinchieri 1983
N4104	Outside the IPC ribs
N4105	N4105 + N4106
N4151 and N4156	Nearby strong sources
N4168	Another close source which may not be related to the galaxy
N4190	VV 104
N4192	M98; several unrelated sources in the field

TABLE 11—*Continued*

Galaxy	Notes and References
N4236	A few faint sources are inside the optical image
N4244	A detected source is at the edge of the edge-on galaxy; Bregmann & Glassgold 1982
N4254	M99
N4258	M106
N4261	3C 270; nearby variable source
N4291	Nearby sources (Mrk 205 and another source)
N4298	N4298 + N4302
N4303	M61; nearby strong source
N4319	Confused with Mrk 205
N4321	M100; LVS; Palumbo et al. 1981
N4340, N4350	A few weak sources near the galaxies may not be associated with the galaxies
N4374	M84, 3C 272.1
N4382	M85; TFC
N4383	Mrk 769
N4385	Mrk 52
N4406	M86; Forman et al. 1979
N4410	Mrk 1325; partly hidden by the IPC ribs (N4410A + N4410B)
N4424	Extended emission near the galaxy
N4429	Nearby star possibly contributes to X-ray emission
N4435	VV 188, Arp 120
N4438	VV 188, Arp 120; Kotanyi et al. 1983
N4472	M49, Arp 134; TFC
N4501	M88; several unrelated sources in the field
N4507	Nearby stellar source
N4548	M91
N4552	M89
N4565	A few separate sources are present in the soft band; X-ray centroids in soft and hard bands do not coincide
N4567	N4567 + N4568, VV 219
N4569	M90, Arp 76
N4579	M58
N4593	Mrk 1330; partly hidden by the IPC ribs
N4594	Sombrero, M104
N4621	M59
N4631	Arp 281; FT
N4638	X-ray centroid does not coincide with nucleus
N4636	TFC
N4643	X-ray centroid does not coincide with nucleus
N4647	VV 206, Arp 116
N4649	M60, VV 206, Arp 116; TFC
N4651	Arp 189, VV 56; unrelated nearby sources
N4698	Two sources close to the galaxy; source to the north may be unrelated to the galaxy
N4736	M94
N4782	N4782 + N4783; VV 201, 3C 278
N4826	M64
N4861	Mrk 59, Arp 266
N5033	Flux was estimated by unmasking the image
N5068	X-ray centroid does not coincide with nucleus
N5077 and N5079	X-ray emission from both galaxies
N5084	Flux was estimated by unmasking the image
N5128	Cen A, Arp 153; Schreier et al. 1979; Feigelson et al. 1981
N5194	M51, VV 1, Arp 85; Palumbo et al. 1985
N5195	A dwarf companion of N5194; Palumbo et al. 1985
N5236	M83; Trinchieri et al. 1985; FT
N5350	Mrk 1485
N5353	The X-ray centroid coincides with NGC 5353 (HRI map), but NGC 5354 is inside the X-ray emission in the IPC observation; FT
N5410	VV256
N5457	M101, VV 344, Arp 26; LVS; McCammon & Sanders 1984; Trinchieri, Fabbiano, & Romaine 1990
N5506	Mrk 1376; Maccacaro et al. 1982
N5532	3C 296; X-ray centroid does not coincide with nucleus
N5548	Mrk 9027; complex field and several unrelated sources
N5566	Arp 286; two sources may be unrelated to the galaxy
N5674	X-ray centroid does not coincide with nucleus
N5683	Mrk 474
N5838	Nearby sources
N5846	Biermann & Kronberg 1983
N5866	M102
N5879	Nearby unrelated strong source
N6027	VV 115
N6052	Mrk 297, Arp 209, VV 86
N6300	VV 734
N6621	VV 247
N6744	FT
N6872	VV 297
N6946	Arp 29; IPC 10314 contains SN 1980K; Canizares et al. 1982; FT
N7237/6	3C 442, Arp 169
N7314	Arp 14
N7320	N7318 + N7319 + N7320, VV 288, Arp 319
N7469	Arp 298
N7496	VV 771
N7552	Variable nearby source; Maccacaro & Perola 1981
N7582	Maccacaro & Perola 1981; Maccacaro et al. 1982
N7590	Maccacaro & Perola 1981
N7619	Pegasus I cluster; Canizares et al. 1986
N7626	Pegasus I cluster; Canizares et al. 1986
N7673	Mrk 325
N7677	Mrk 326
N7679	Mrk 534, VV 329, Arp 216; nearby source NGC 7682
N7682	Nearby source NGC 7679
N7714	Mrk 538, VV 51, Arp 284; starburst galaxy; nearby source could be from the galaxy; Weedman et al. 1981
N7769	Mrk 9005
N7771	Mkn 9006
N7793	X-ray centroid does not coincide with nucleus

NOTE.—Other published X-ray fluxes of galaxies can be found in Long & Van Speybroeck 1983 (normal galaxies), Fabbiano, Trinchieri, & McDonald 1984 (S), Forman, Jones, & Tucker 1985 (E and S0), Canizares, Fabbiano, & Trinchieri 1987 (E and S0), Fabbiano, Feigelson, & Zamorani, 1982 (peculiar galaxies), Dressel & Wilson 1985 (E and S0 with radio core).